CONSTRUCTIVE MATHEMATICAL ANALYSIS

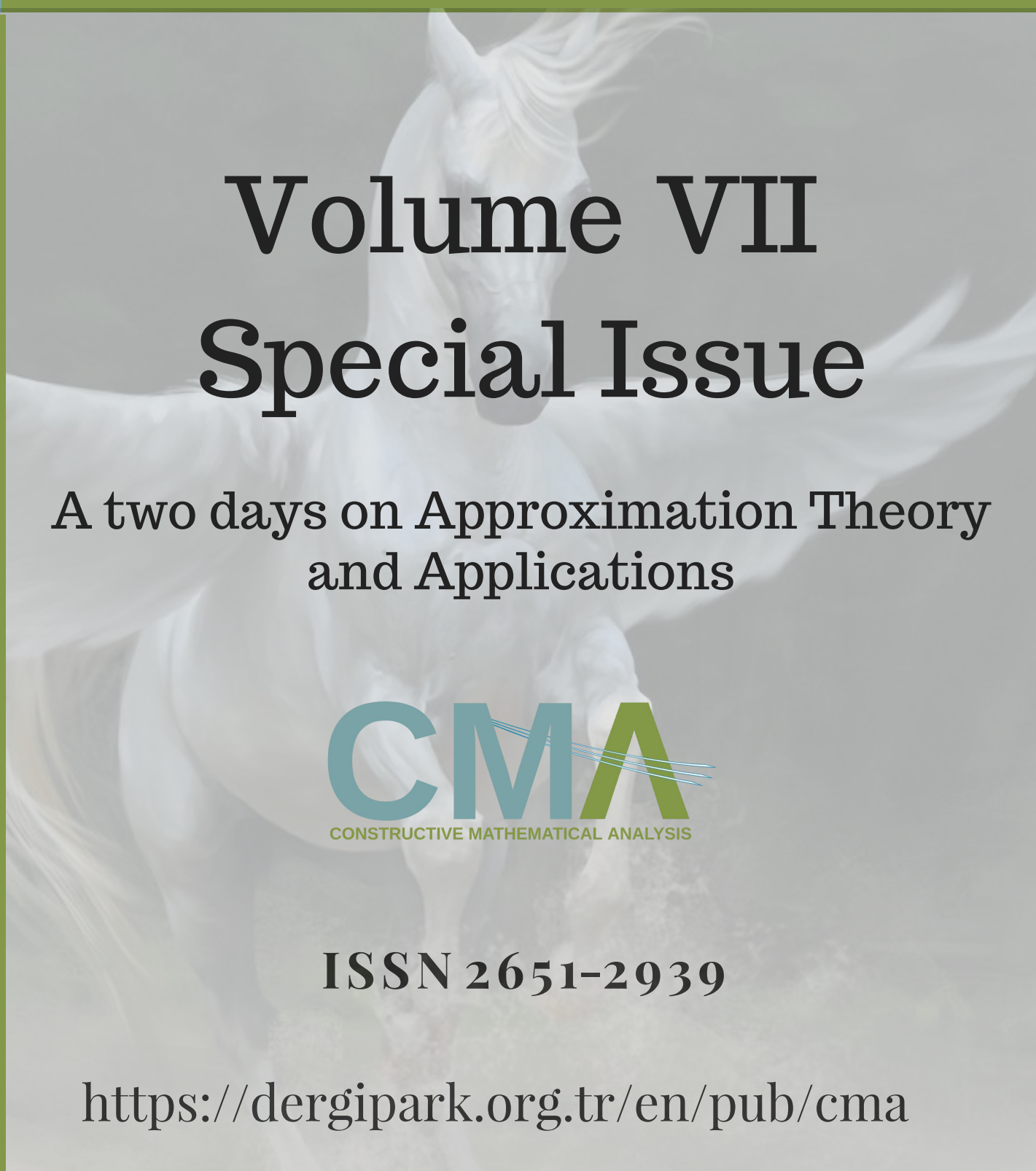

Volume VII
Special Issue

A two days on Approximation Theory and Applications

CMA
CONSTRUCTIVE MATHEMATICAL ANALYSIS

ISSN 2651-2939

https://dergipark.org.tr/en/pub/cma

VOLUME VII SPECIAL ISSUE
ISSN 2651-2939

2024
https://dergipark.org.tr/en/pub/cma

CONSTRUCTIVE MATHEMATICAL ANALYSIS

CMA
CONSTRUCTIVE MATHEMATICAL ANALYSIS

This special issue is dedicated to Prof. Dr. Paolo Emilio Ricci: on the occasion of his 80th birthday

Prof. Dr. Paolo Emilio Ricci

This special issue consists of the selected papers from "A two days on Approximation Theory and Applications"

The "A two days conference on Approximation Theory and Applications"

The "A two days conference on Approximation Theory and Applications" was held in Roma (Italy), at Istituto per le Applicazione del Calcolo "Mario Picone" (IAC) CNR on May 23th-24th, 2024, to congratulate Paolo Emilio Ricci whose research activity embraced various aspects of applied mathematics.The conference aimed to bring together researchers working in different fields of numerical analysis and mathematical modelling, with a special focus on special functions in approximation theory; operational methods; non-trigonometric Fourier analysis; polynomial and trigonometric approximation; quadrature formulas; Bell polynomials and applications to Laplace transform; Laguerre-type functions; numerical methods for integral equations; eigenvalue approximation; modeling of geometric shapes; fractional differential problems; classical numbers and polynomials in fractional context; approximation algorithms for biological models. This volume contains carefully selected papers, accepted after a rigorous peer-review process, according to the standard of the Constructive Mathematical Analysis (CMA) journal. The Organizing Committee is grateful to all the participants, including both those in person and others remotely, who contributed to the conference's success, attending with great interest, and sincere enthusiasm. Special thanks are due to the Prof. Tuncer Acar, Editor in Chief of Constructive Mathematical Analysis, for agreeing to publish this Special Issue. Finally, we thank all the anonymous referees for their insightful and accurate work.

Dedicated to Prof. Paolo Emilio Ricci: On the occasion of his 80th birthday

Paolo Emilio Ricci received his Doctoral degree (cum laude) under the supervision of Prof. Gaetano Fichera at Sapienza University of Rome. He was teaching and researching for forty years at the University of Rome and Catania. He was professor at the University Campus Bio-medico of Rome for several years. At present he is appointed at the Uninettuno International Telematic University in Rome, where he is a member of the Section of Mathematics "Luciano Modica". He presented his research at many conferences (Darmstadt, Moscow State University, Steklov Institute in St. Petersburg, I. Vekua Institute of Applied Mathematics in Tbilisi, Tel Aviv, Guangzhou, Rostock, Chemnitz, Budapest, Jaipur, etc.) and he is the author/coauthor of more than 280 scientific papers and author/editor of several books in the areas of pure and applied mathematics. In 2003 he received Laurea H.C. from I. Vekua Institute of Applied Mathematics, Tbilisi State University, Georgia; in 2015 he was awarded with the Prize of the Simon Stevin Institute for Geometry, Zandvoort, The Netherlands; in 2016 he received the Life-time achievement award and in 2022 the Golden Jubilee Award from Vijnana Parishad of India (Society for Applications of Mathematics), Bundelkhand University, Jhansi, U.P. India.

Special Issue Committee Members
Gabriella Bretti, Istituto per la Applicazioni del Calcolo (CNR), Italy
Clemente Cesarano, Uninettuno University, Italy
Gianluca Vinti, University of Perugia, Italy

Contents

CONSTRUCTIVE MATHEMATICAL ANALYSIS
7 (2024), No. SI, pp. 1-10
http://dergipark.org.tr/en/pub/cma
ISSN 2651 - 2939

Research Article

On discrete orthogonal U-Bernoulli Korobov-type polynomials

Dedicated to Professor Paolo Emilio Ricci, on occasion of his 80th birthday, with respect and friendship.

WILLIAM RAMÍREZ, URIELES ALEJANDRO, AND CLEMENTE CESARANO*

ABSTRACT. The primary objective of this paper is to introduce and examine the new class of discrete orthogonal polynomials called U–Bernoulli Korobov-type polynomials. Furthermore, we derive essential recurrence relations and explicit representations for this polynomial class. Most of the results are proven through the utilization of generating function methods. Lastly, we place particular emphasis on investigating the orthogonality relation associated with these polynomials.

Keywords: Bernoulli polynomials, U–Bernoulli Korobov, discrete orthogonal polynomials.

2020 Mathematics Subject Classification: 11B68, 11B83, 11B39, 05A19.

1. INTRODUCTION

The study of discrete Appell polynomials is significant in mathematics due to their special properties and wide range of applications. Analogous to continuous Appell polynomials, they feature a discrete shift operator as their primary differential operator. Moreover, they are closely related to orthogonal polynomials, such as Hermite and Chebyshev polynomials, which are vital in areas like approximation theory and quantum mechanics. Together, these polynomials contribute to the development of special functions that are applied across diverse fields, including mathematics, physics, engineering, and statistics (see, [7, 10, 17]).

In this context, let $f : \mathbb{Z} \to \mathbb{R}$ be any function of the natural numbers, and consider the discrete operator $\Delta f(x) = f(x+1) - f(x)$. This operator plays a crucial role in the definition and analysis of discrete Appell polynomials, further highlighting their importance in both theoretical and applied mathematics.

A discrete Appell sequence $\{p_n(x)\}_{n=0}^{\infty}$ is a sequence of polynomials such that (see, [6]):

$$\Delta p_k(x) = p_k(x+1) - p_k(x) = k p_{k-1}(x), \quad k \geq 1.$$

It is known that a Taylor series expansion can define Appell sequences (see, [1]):

$$A(z)e^{xz} = \sum_{n=0}^{\infty} P_n(x)\frac{z^n}{n!}, \tag{1.1}$$

where $A(z)$ is a function analytic at $z = 0$ with $A(0) \neq 0$; similarly, discrete Appell sequences can be defined by a Taylor generating expansion

Received: 19.06.2024; Accepted: 12.10.2024; Published Online: 16.12.2024
*Corresponding author: Clemente Cesarano; c.cesarano@uninettunouniversity.net
DOI: 10.33205/cma.1502670

$$A(z)(1+z)^x = \sum_{n=0}^{\infty} p_n(x)\frac{z^n}{n!}, \tag{1.2}$$

where $A(z)$ is a function analytic at $z = 0$ with $A(0) \neq 0$.

There is a substantial body of mathematical literature devoted to studying the families of Appell sequences. Typical examples include the trivial case $\{x^k\}_{k=0}^{\infty}$, whose generating function is given by (1.1) with $A(z) = 1$, and the Bernoulli polynomials, which were used by Euler in 1740 to sum $\sum_{n=1}^{\infty} 1/n^{2k}$. Their generating function is (1.1) with $A(z) = \frac{z}{e^z-1}$.

In the case of discrete Appell sequences, the trivial case, obtained from (1.2) with $A(t) = 1$, is the family $\{x^{\underline{k}}\}_{k=0}^{\infty}$, where

$$x^{\underline{k}} = x(x-1)\cdots(x-k+1) = \prod_{j=0}^{k-1}(x-j)$$

is the falling factorial (various notations have been used for these polynomials; here we follow [11] and [8, p. 47]). The discrete counterpart to the Bernoulli polynomials is the so-called Bernoulli polynomials of the second kind (see [3]), denoted by $b_k(x)$, which were independently introduced by Jordan [9] and Rey Pastor [16] in 1929. These polynomials, also known as Rey Pastor polynomials (see, [2]), are now defined by a generating function as in (1.1) via

$$\frac{z}{\log(1+z)}(1+z)^x = \sum_{k=0}^{\infty} b_k(x)\frac{z^k}{k!}.$$

We consider the discrete orthonormal polynomials $\{p(x)\}_{n\geq 0}$ corresponding to a positive measure with respect to a discrete weight $\omega(k)$ and satisfies the conditions

$$\sum_{k=0}^{\infty} p_n(k)p_m(k)\omega(k) = \delta_{m,n}, \tag{1.3}$$

where $\delta_{m,n}$ is the Kronecker delta (cf., [14, pp. 586]).

The moments μ_n of the discrete weight $\omega(k)$ in (1.3) are given by

$$\mu_n = \sum_{k=0}^{\infty} k^n\omega(k),\ n \geq 0.$$

In the special case when the discrete weight has the special form

$$\omega(k) = c(k)z^k, \quad z > 0,$$

which is the case for the Charlier polynomials $C_n(k;z)$ and the Meixner polynomials $M_n(k;\alpha;z)$ (see, [5, 13]), then

$$\mu_n(z) = \mu_n = \sum_{k=0}^{\infty} k^n c(k)z^k.$$

Considering the aforementioned context, the main objective of this work is to define and study the discrete U-Bernoulli Korobov-type polynomial. We study the algebraic and differential properties associated with this particular family of polynomials. Furthermore, we introduce an orthogonality relation that satisfies these polynomials.

2. Notation and background

Throughout this paper, let $\mathbb{N}, \mathbb{N}_0, \mathbb{Z}, \mathbb{R}$, and $\mathbb{C}$ denote, respectively, the set of all natural numbers, the set of all non-negative integers, the set of all integers, the set of all real numbers, and the set of all complex numbers.

The Korobov polynomials $K_n(x;\lambda)$ of the first kind are given by the generating function (cf., [12])

$$\frac{\lambda z}{(1+z)^{\lambda}-1}(1+z)^{x}=\sum_{n=0}^{\infty}K_n(x;\lambda)\frac{z^n}{n!}.$$

When $x=0$, $K_n(\lambda)=K_n(0,\lambda)$ are called the Korobov number.

In [4], L. Carlitz considered the degenerate Bernoulli polynomials which are given by the generating function to be

$$\frac{z}{(1+\lambda z)^{\frac{1}{\lambda}}-1}(1+\lambda z)^{\frac{x}{\lambda}}=\sum_{n=0}^{\infty}\mathscr{B}_n(x;\lambda)\frac{z^n}{n!}. \tag{2.4}$$

From (2.4), we have $\lim_{\lambda\to 0}\mathscr{B}_n(x;\lambda)=B_n(x), \qquad (n\geq 0)$.

Additionally, for $n\in\mathbb{N}_0$, we defined the new family U–Bernoulli polynomials $M_n(x)$ of degree n in the variable x by the power series expansion at 0 of the following generating function (see, [15]):

$$f(x;z)=\frac{z}{e^{-z}-1}e^{-xz}=\sum_{n=0}^{\infty}M_n(x)\frac{z^n}{n!}, \quad |z|<2\pi.$$

We have for the first few U–Bernoulli polynomials $M_n(x)$, that

$$M_0(x)=-1, \qquad M_3(x)=x^3-\frac{3}{2}x^2+\frac{1}{2}x,$$
$$M_1(x)=x-\frac{1}{2}, \qquad M_4(x)=-x^4+2x^3-x^2+\frac{1}{30},$$
$$M_2(x)=-x^2+x-\frac{1}{6}, \qquad M_5(x)=x^5-\frac{5}{2}x^4+\frac{5}{3}x^3-\frac{1}{6}x.$$

When $x=0$ in (2), the U-Bernoulli numbers are defined by the generating function

$$f(z)=\frac{z}{e^{-z}-1}=\sum_{n=0}^{\infty}M_n\frac{z^n}{n!}, \quad |z|<2\pi.$$

Some of these numbers are

$$M_0=-1; \quad M_1=-\frac{1}{2}; \quad M_2=-\frac{1}{6}; \quad M_3=0; \quad M_4=\frac{1}{30}; \quad M_5=0.$$

3. U–Bernoulli Korobov-type discrete polynomials

In this section, we introduce the U-Bernoulli Korobov-type discrete polynomials and derive several key results for these polynomials.

Definition 3.1. *The new family of U–Bernoulli Korobov-type discrete polynomials $\mathscr{P}_n(x)$ of degree n in $x\in\mathbb{N}$ are defined by the generating function*

$$\left(\frac{z}{e^{-z}-1}\right)(1+z)^{x}=\sum_{n=0}^{\infty}\mathscr{P}_n(x)\frac{z^n}{n!}, \quad |z|<2\pi. \tag{3.5}$$

The first six U–Bernoulli Korobov-type discrete polynomials $\mathscr{P}_n(x)$, are

$$\mathscr{P}_0(x) = -1, \qquad \mathscr{P}_3(x) = -x^3 + \frac{3}{2}x^2 - x,$$
$$\mathscr{P}_1(x) = -x - \frac{1}{2}, \qquad \mathscr{P}_4(x) = -x^4 + 4x^3 - 4x^2 + 3x + \frac{1}{30},$$
$$\mathscr{P}_2(x) = -x^2 - \frac{1}{6}, \qquad \mathscr{P}_5(x) = -x^5 + \frac{15}{2}x^4 - \frac{65}{3}x^3 + \frac{55}{2}x^2 - \frac{33}{6}x.$$

For $x = 0$ in (3.5) the U–Bernoulli Korobov-type discrete numbers $\mathscr{P}_n(0)$ are defined by the generating function

$$\frac{z}{e^{-z} - 1} = \sum_{n=0}^{\infty} \mathscr{P}_n \frac{z^n}{n!}, \quad |z| < 2\pi. \tag{3.6}$$

Some of these numbers are

$$\mathscr{P}_0 = -1; \quad \mathscr{P}_1 = -\frac{1}{2}; \quad \mathscr{P}_2 = -\frac{1}{6}; \quad \mathscr{P}_3 = 0; \quad \mathscr{P}_4 = \frac{1}{30}; \quad \mathscr{P}_5 = 0.$$

A consequence of (3.5) and (3.6) is the following proposition, which highlights several properties satisfied by this family of polynomials.

Proposition 3.1. *The U-Bernoulli Korobov-type discrete polynomials in the variable x, they satisfy the following relations*

(i) $$\mathscr{P}_n(x+y) = \sum_{k=0}^{n} \binom{n}{k} (y)_k \mathscr{P}_{n-k}(x),$$

(ii) $$\mathscr{P}_n(x) = \sum_{k=0}^{n-1} n \binom{n-1}{k} (x)_k + \sum_{k=0}^{n} \binom{n}{k} \mathscr{P}_k(x),$$

(iii) $$\sum_{k=0}^{n} \binom{n}{k} \mathscr{P}_k(x+y)\mathscr{P}_{n-k} = \sum_{k=0}^{n} \binom{n}{k} \mathscr{P}_{n-k}(x)\mathscr{P}_k(y),$$

(iv) $$\mathscr{P}_n(x) = \mathscr{P}_n + \sum_{k=0}^{n-1} \frac{n}{(k+1)} \binom{n-1}{k} (x)_{k+1} \mathscr{P}_{n-1-k},$$

(v) $$\mathscr{P}_n(x) = \sum_{k=0}^{\infty} \binom{x}{k} \frac{n!}{(n-k)!} \mathscr{P}_{n-k},$$

(vi) $$\mathscr{P}_n(x) = \mathscr{P}_n(x+1) - n\mathscr{P}_{n-1}(x).$$

Proof. (see (iii)). Let's consider the following expressions

$$\left(\frac{z}{e^{-z} - 1}\right)(1+z)^x = \sum_{n=0}^{\infty} \mathscr{P}_n(x) \frac{z^n}{n!} \tag{3.7}$$

and

$$\left(\frac{z}{e^{-z} - 1}\right)(1+z)^y = \sum_{n=0}^{\infty} \mathscr{P}_n(y) \frac{z^n}{n!}. \tag{3.8}$$

Of (3.7) and (3.8), we have

$$\left[\frac{z}{e^{-z}-1}\right]^2(1+z)^{x+y}=\left(\sum_{n=0}^{\infty}\mathscr{P}_n(x)\frac{z^n}{n!}\right)\left(\sum_{n=0}^{\infty}\mathscr{P}_n(y)\frac{z^n}{n!}\right)$$

$$\left(\sum_{n=0}^{\infty}\mathscr{P}_n\frac{z^n}{n!}\right)\left(\sum_{n=0}^{\infty}\mathscr{P}_n(x+y)\frac{z^n}{n!}\right)=\left(\sum_{n=0}^{\infty}\mathscr{P}_n(x)\frac{z^n}{n!}\right)\left(\sum_{n=0}^{\infty}\mathscr{P}_n(y)\frac{z^n}{n!}\right)$$

$$\sum_{n=0}^{\infty}\sum_{k=0}^{n}\binom{n}{k}\mathscr{P}_{n-k}\mathscr{P}_k(x+y)\frac{z^n}{n!}=\sum_{n=0}^{\infty}\sum_{k=0}^{n}\binom{n}{k}\mathscr{P}_{n-k}(x)\mathscr{P}_k(y)\frac{z^n}{n!}$$

$$\sum_{k=0}^{n}\binom{n}{k}\mathscr{P}_{n-k}\mathscr{P}_k(x+y)=\sum_{k=0}^{n}\binom{n}{k}\mathscr{P}_{n-k}(x)\mathscr{P}_k(y).$$

Therefore,

$$\sum_{k=0}^{n}\binom{n}{k}\left[\mathscr{P}_k(x+y)\mathscr{P}_{n-k}-\mathscr{P}_{n-k}(x)\,\mathscr{P}_k(y)\right]=0.$$

□

Theorem 3.1 (Differential expressions). *For $n\in\mathbb{N}$, let $\{\mathscr{P}_n(x)\}_{n\geq 0}$ be the sequences of U–Bernoulli Korobov-type discrete polynomials in the variable $x\in\mathbb{N}$, they satisfy the following relations*

(1)

$$(n-1)\mathscr{P}_n(x)-n\psi(x;z)\frac{\partial}{\partial x}\mathscr{P}_{n-1}(x)=0,$$

where

$$\psi(x;z)=\left[\frac{x}{(z+1)\log(z+1)}+\frac{e^{-z}}{(e^{-z}-1)\log(z+1)}\right],$$

(2)

$$\frac{\partial\mathscr{P}_n(x)}{\partial x}=\sum_{k=0}^{n-1}n\binom{n-1}{k}(-1)^k\frac{k!}{k+1}\mathscr{P}_{n-k-1}(x).$$

Proof. For the proof of (1). Consider the following equations

$$L(x;z)=\sum_{n=0}^{\infty}\mathscr{P}_n(x)\frac{z^n}{n!}, \tag{3.9}$$

$$L(x;z)=\frac{z}{e^{-z}-1}(1+z)^x. \tag{3.10}$$

Partially differentiating with respect to z in (3.9) and (3.10) , the result is

$$\frac{\partial L(x;z)}{\partial z}=\sum_{n=0}^{\infty}\mathscr{P}_n(x)\frac{nz^{n-1}}{n!}$$

and

$$\frac{\partial L(x;z)}{\partial z}=\frac{(1+z)^x}{e^{-z}-1}+\left[\frac{z(1+z)^x}{e^{-z}-1}\right]\frac{x}{1+z}+\left[\frac{z(1+z)^x}{e^{-z}-1}\right]\frac{e^{-z}}{e^{-z}-1}. \tag{3.11}$$

Partially differentiating with respect to x in (3.10) , we have

$$\frac{\partial L(x;z)}{\partial x}=\frac{z\log(z+1)(1+z)^x}{e^{-z}-1}.$$

Of (3.11), we have

$$0 = \frac{\partial L(x;z)}{\partial z} - \frac{(1+z)^x}{e^{-z}-1} - \left[\frac{z\log(z+1)(1+z)^x}{e^{-z}-1}\right]\frac{x}{(1+z)\log(z+1)}$$
$$- \left[\frac{z\log(z+1)(1+z)^x}{e^{-z}-1}\right]\frac{e^{-z}}{(e^{-z}-1)\log(z+1)}$$
$$0 = \frac{z\partial L(x;z)}{\partial z} - \left[\frac{zx}{(1+z)\log(z+1)} + \frac{ze^{-z}}{(e^{-z}-1)\log(z+1)}\right]\frac{\partial L(x;z)}{\partial x} - \frac{z(1+z)^x}{e^{-z}-1}$$
$$0 = \sum_{n=0}^{\infty}\mathscr{P}_n(x)\frac{nz^n}{n!} - \sum_{n=0}^{\infty}\left[\frac{x}{(1+z)\log(z+1)} + \frac{e^{-z}}{(e^{-z}-1)\log(z+1)}\right]\frac{\partial}{\partial x}\mathscr{P}_{n-1}(x)\frac{nz^n}{n!}$$
$$- \sum_{n=0}^{\infty}\mathscr{P}_n(x)\frac{z^n}{n!}$$
$$0 = (n-1)\mathscr{P}_n(x) - \left[\frac{x}{(1+z)\log(z+1)} + \frac{e^{-z}}{(e^{-z}-1)\log(z+1)}\right]n\frac{\partial}{\partial x}\mathscr{P}_{n-1}(x).$$

This completes the proof of (1).

For the proof of (2). Partially differentiating with respect to x in (3.1), we have

$$\left(\frac{z}{e^{-z}-1}\right)\frac{\partial}{\partial x}\left[(1+z)^x\right] = \sum_{n=0}^{\infty}\frac{\partial}{\partial x}\mathscr{P}_n(x)\frac{z^n}{n!}$$
$$\left(\sum_{n=0}^{\infty}\mathscr{P}_n(x)\frac{z^n}{n!}\right)\left(\sum_{n=0}^{\infty}\frac{(-1)^n}{n+1}z^{n+1}\right) = \sum_{n=0}^{\infty}\frac{\partial}{\partial x}\mathscr{P}_n(x)\frac{z^n}{n!}$$
$$\sum_{n=0}^{\infty}\sum_{k=0}^{n-1}\mathscr{P}_{n-1-k}(x)(-1)^k\binom{n-1}{k}\frac{k!}{(k+1)}n\frac{z^n}{n!} = \sum_{n=0}^{\infty}\frac{\partial}{\partial x}\mathscr{P}_n(x)\frac{z^n}{n!}.$$

Comparing the coefficients of $\frac{z^n}{n!}$ in both sides of the equation, the result is

$$\frac{\partial}{\partial x}\mathscr{P}_n(x) = \sum_{k=0}^{n-1}n\binom{n-1}{k}(-1)^k\frac{k!}{k+1}\mathscr{P}_{n-k-1}(x).$$

□

4. Orthogonality relation of the U-Bernoulli Korobov-type discrete polynomials

In this section, we will present a comprehensive demonstration of the orthogonality relationship associated with the U-Bernoulli Korobov-type discrete polynomials.

Theorem 4.2. *The U–Bernoulli Korobov-type discrete polynomials $\mathscr{P}_n(x)$, fulfill the following orthogonality relation*

$$\int_0^{\infty}\mathscr{P}_m(x)\;\mathscr{P}_n(x)\,d\mu(x) = (-1)^{n-1}\,m!\,n\,\delta_{m,n},$$

where

$$d\mu(x) = \omega(x,\lambda_1,\sigma_1)dx = \frac{(1-e^{\lambda_1})(1-e^{\sigma_1})\,e}{x!}dx,$$

with $x \in \mathbb{N}$, $z, v \in \mathbb{C}$, and $\lambda_1 \in \mathrm{Re}(z), \sigma_1 \in \mathrm{Re}(v)$.

Proof. Let's consider the following equality

$$L(x,z)=\left(\frac{z}{e^{-z}-1}\right)(1+z)^x=\sum_{n=0}^{\infty}\mathscr{P}_n(x)\frac{z^n}{n!},\qquad |z|<2\pi.$$

Then

$$\begin{aligned}L(x,z)&=\left(\frac{z}{e^{-z}-1}\right)(1+z)^x\\&=\sum_{n=0}^{\infty}\sum_{k=0}^{n}\binom{x}{k}\frac{\mathscr{P}_{n-k}}{(n-k)!}\,z^n\end{aligned}\tag{4.12}$$

$$L(x,z)=\sum_{n=0}^{\infty}L_n(x)z^n,\tag{4.13}$$

where we get

$$L_n(x)=\sum_{k=0}^{n}\binom{x}{n}\frac{\mathscr{P}_{n-k}}{(n-k)!}$$

$$L_n(x)=\sum_{k=0}^{n}\frac{1}{k!}\left(x(x-1)(x-2)\cdots(x-k+1)\right)\frac{\mathscr{P}_{n-k}}{(n-k)!}.\tag{4.14}$$

Note that (4.14) is a polynomial of degree n and $L_n(x)$, which coincides with the so-called U–Bernoulli Korobov-type discrete polynomial.

On the other hand, let

$$\begin{aligned}L(x,v)&=f(v)g(x,v)\\&=\left(\frac{v}{e^{-v}-1}\right)(1+v)^x\\&=\sum_{m=0}^{\infty}\sum_{k=0}^{m}\binom{x}{m}\frac{\mathscr{P}_{m-k}}{(m-k)!}\,v^m\end{aligned}\tag{4.15}$$

$$L(x,v)=\sum_{m=0}^{\infty}L_m(x)\,v^m,\tag{4.16}$$

where it is obtained

$$L_m(x)=\sum_{k=0}^{m}\binom{x}{m}\frac{\mathscr{P}_{m-k}}{(m-k)!}.$$

Considering the product of (4.12) and (4.15), we obtain

$$\begin{aligned}L(x,z)L(x,v)&=\left(\frac{z}{e^{-z}-1}\right)(1+z)^x\left(\frac{v}{e^{-v}-1}\right)(1+v)^x\\&=\left[\frac{zve^{z+v}}{(1-e^z)(1-e^v)}\right]\left[(1+z)^x(1+v)^x\right]\end{aligned}$$

then,

$$L(x,z)L(x,v)=\left[\frac{zve^{z+v}}{(1-e^z)(1-e^v)}\right]\left[(1+z)(1+v)\right]^x.$$

For any $k = x$, we have

$$(-1)^k L(x,z)L(x,v) = \left[\frac{zve^{z+v}}{(1-e^z)(1-e^v)}\right][(-1)(1+z)(1+v)]^k.$$

Then,

$$\begin{aligned}\sum_{k=0}^{\infty}\frac{(-1)^k L(x,z)L(x,v)}{k!} &= \frac{zve^{z+v}}{(1-e^z)(1-e^v)}\sum_{k=0}^{\infty}\frac{[-(1+z)(1+v)]^k}{k!}\\ &= \frac{zve^{z+v}}{(1-e^z)(1-e^v)}\,e^{-(1+z)(1+v)}\\ &= \left[\frac{zv\,e^{-1}}{(1-e^z)(1-e^v)}\right]e^{-zv}.\end{aligned}$$

Therefore,

$$\sum_{k=0}^{\infty}\frac{(-1)^k L(x,z)L(x,v)}{k!} = \sum_{n=0}^{\infty}\left[\frac{zv\,e^{-1}(-1)^n}{(1-e^z)(1-e^v)}\right]\frac{z^n v^n}{n!}, \tag{4.17}$$

from (4.13) and (4.16) on (4.17) left side we have

$$\sum_{k=0}^{\infty}\frac{(-1)^k L_m(k\,,z)L_n(k\,,v)}{k!} = \sum_{m\,,n=0}^{\infty}\sum_{k=0}^{\infty}L_m(k), L_n(k)\,\frac{(-1)^k}{k!}\,z^n v^m. \tag{4.18}$$

From (4.17) and (4.18) we get

$$\sum_{n=0}^{\infty}\left[\frac{zv\,e^{-1}(-1)^n}{(1-e^z)(1-e^v)}\right]\frac{z^n v^n}{n!} = \sum_{m\,,n=0}^{\infty}\sum_{k=0}^{\infty}L_m(k), L_n(k)\,\frac{(-1)^k}{k!}\,z^n v^m. \tag{4.19}$$

Which gives:

$$\begin{aligned}\sum_{n=0}^{\infty}\left[\frac{zv\,e^{-1}(-1)^n}{(1-e^z)(1-e^v)}\right]\frac{z^n v^n}{n!} &= \sum_{n=0}^{\infty}\left[\frac{e^{-1}(-1)^n}{(1-e^z)(1-e^v)}\right]\frac{z^{n+1}v^{n+1}}{n!}\\ &= \sum_{n=0}^{\infty}\left[\frac{e^{-1}(-1)^{n-1}}{(1-e^z)(1-e^v)}\right]\frac{nz^n v^n}{n!}.\end{aligned}$$

Therefore, in (4.19) we have

$$\sum_{n=0}^{\infty}\left[\frac{e^{-1}(-1)^{n-1}}{(1-e^z)(1-e^v)}\right]\frac{nz^n v^n}{n!} = \sum_{m\,,n=0}^{\infty}\sum_{k=0}^{\infty}L_m(k)L_n(k)\,\frac{(-1)^k}{k!}\,z^n v^m, \tag{4.20}$$

by comparing the coefficients in (4.20), one has

$$\sum_{k=0}^{\infty}L_m(x)\,L_n(x)\,\frac{(-1)^k}{k!} = \begin{cases}\dfrac{(-1)^{n-1}\,e^{-1}}{n!}\left[\dfrac{n}{(1-e^z)(1-e^v)}\right]; & \text{if } m = n.\\ 0; & \text{if } m \neq n.\end{cases} \tag{4.21}$$

In (4.21), we note that $\{L_n(x)\}_{n\geq 0}$, is a sequence of orthogonal polynomials with respect to the weight function $\dfrac{(-1)^k}{k!}$, $k = 0\,,1\,,2,\ldots$

Remark 4.1. *We define about (4.21) the functional $\mathscr{L}$ as follows:*

$$\mathscr{L}\left[L_m(x)L_n(x)\frac{(-1)^k}{k!}\right] = \frac{(-1)^{n-1}}{n!}\,e^{-1}\,\psi_n\,\delta_{m,n}, \tag{4.22}$$

where

$$\psi_n = \frac{n}{(1-e^z)(1-e^v)}.$$

Therefore (4.22) can be expressed in terms of the Riemann-Stieltjes integral as follows.

$$\int_0^\infty L_m(x)L_n(x)\,\frac{(-1)^k}{k!}\,dx = \frac{(-1)^{n-1}\,e^{-1}}{n!}\,\psi_n\,\delta_{m,n}. \tag{4.23}$$

In (4.13) and (4.16), we have that,

$$L(x,z) = \sum_{n=0}^{\infty} L_n(x)\,z^n \qquad \text{and} \qquad L(x,v) = \sum_{m=0}^{\infty} L_m(x)\,v^m.$$

Therefore,

$$L_n(x) = \frac{P_n(x)}{n!} \qquad \text{and} \qquad L_m(x) = \frac{P_m(x)}{m!}. \tag{4.24}$$

Of (4.24) and (4.23) we obtain

$$\int_0^\infty \frac{P_m(x)}{m!}\,\frac{P_n(x)}{n!}\,d\lambda = \frac{(-1)^{n-1}\,e^{-1}}{n!}\,\psi_n\,\delta_{m,n}, \tag{4.25}$$

where

$$d\,\lambda = \frac{(-1)^k}{k!}\,dx, \quad k = 0\,,1\,,2,\ldots$$

$$\int_0^\infty P_m(x)\,P_n(x)\,d\mu(x) = (-1)^{n-1}\,m!\psi_n\,\delta_{m,n}, \tag{4.26}$$

where $d\mu(x) = \dfrac{(-1)^x\,e}{x!}\,dx.$

□

References

[1] F. Avram, M.S. Taqqu: *Noncentral limit theorems and Appell polynomials,* Ann. Probab., **15** (1987), 767–775.
[2] J. Babini: *Polinomios generalizados de Bernoulli y sus correlativos,* Rev. Mat. Hisp.-Am., **10** (4) (1935), 23–25.
[3] L. Carlitz: *A note on Bernoulli and Euler polynomials of the second kind*, Scr. Math., **25** (1961), 323–330.
[4] L. Carlitz: *Degenerate Stirling, Beroulli and Eulerian numbers*, Utilitas Math., **15** (1979), 51–88.
[5] C. V. L. Charlier: *Über die darstellung willkurlicher funktionen,* Arkiv för Matematik, Astronomi och Fysik., **25** (3) (1970), 1–11.
[6] A.G. Asensi, E. Labarga, E. J.M. Ceniceros and J., Varona: *Boole-Dunklpolynomialsandgeneralizations,* Rev.RealAcad.Cienc.ExactasFis.Nat.Ser.A-Mat., **118** (2024), Article ID: 16.
[7] I. Gavrea, M. Ivan: *Approximation properties related to the Bell polynomials*, Constr. Math. Anal., **4** (2) (2021), 253–259.
[8] R.L. Graham, D.E. Knuth, O: *Patashnik, Concrete Mathematics,* A Foundation for Computer Science, 2nd ed., AddisonWesley, Reading, MA (1994).
[9] C. Jordan: *Sur les polynomes analogues aux polynomes de Bernoulli et sur des formules de sommation analogues à celle de MacLaurin-Euler,* Acta Szeged, **4** (1929), 130–150.
[10] V. Kostov: *The disconnectedness of certain sets defined after uni-variate polynomials,* Constr. Math. Anal., **5** (3) (2022), 119–133.

[11] D.E. Knuth: Two notes on notation, Am. Math. Mon., **99** (1992), 403–422.
[12] Korobov: *Special polynomials and their applications diophantine approximations*, Math. Notes, **2** (1996), 77–89.
[13] J. Meixner: *Orthogonale polynomsysteme mit einem besonderen Gestalt der erzeugenden funktion,* J. London Math. Soc., **9** (1934), 6–13.
[14] Y. Quintana, W. Ramírez and A. Urieles: *Euler matrices and their algebraic properties revisited,* Appl. Math. Inf. Sci., **14** (4) (2020), 583–596.
[15] W. Ramírez, D. Bedoya, A. Urieles, C. Cesarano and M. Ortega: *New U-Bernoulli, U-Euler and U-Genocchi Polynomials and Their Matrices,* Carpathian Math. Publ., **15** (2) (2023), 449–467.
[16] J. Rey Pastor: *Polinomios correlativos de los de Bernoulli*, Bol. Semin. Mat. Argent., **1** (3) (1929) 1–10.
[17] S. Zagorodnyuk: *On a Family of Hypergeometric Sobolev Orthogonal Polynomials on the Unit Circle,* Constr. Math. Anal., **3** (2) (2020), 75–84.

William Ramírez
Universidad de la Costa
Department of Natural and Exact Sciences
Calle 58, 55-66, 080002, Barranquilla, Colombia
UniNettuno University
Section of Mathematics
Corso Vittorio Emanuele II, 39, 00186, Rome, Italy
ORCID: 0000-0003-4675-0221
Email address: wramirez4@cuc.edu.co

Urieles Alejandro
Universidad del Atlántico
Programa de Matemáticas
Km 7 Vía Pto. Colombia, Barranquilla, Colombia
ORCID: 0000-0002-7186-0898
Email address: alejandrourieles@mail.uniatlantico.edu.co

Clemente Cesarano
UniNettuno University
Section of Mathematics
Corso Vittorio Emanuele II, 39, 00186 Rome, Italy
ORCID: 0000-0002-1694-7907
Email address: c.cesarano@uninettunouniversity.net

CONSTRUCTIVE MATHEMATICAL ANALYSIS
7 (2024), No. SI, pp. 11-26
http://dergipark.org.tr/en/pub/cma
ISSN 2651 - 2939

Research Article

On the analytic extension of the Horn's confluent function H_6 on domain in the space $\mathbb{C}^2$

Dedicated to Professor Paolo Emilio Ricci, on occasion of his 80th birthday, with respect and friendship.

ROMAN DMYTRYSHYN*, TAMARA ANTONOVA, AND MARTA DMYTRYSHYN

ABSTRACT. The paper considers the problem of representation and extension of Horn's confluent functions by a special family of functions – branched continued fractions. An estimate of the rate of convergence for the branched continued fraction expansions of the ratios of Horn's confluent functions H_6 with real parameters is established in a new region. Here, the region refers to a domain (an open connected set) which may include all, part, or none of its boundary. Additionally, a new domain of the analytical continuation of the above-mentioned ratios is established, using their branched continued fraction expansions whose elements are polynomials in the space $\mathbb{C}^2$. These expansions can approximate solutions to certain differential equations and analytic functions represented by Horn's confluent functions H_6.

Keywords: Horn's hypergeometric function, branched continued fraction, holomorphic functions of several complex variables, analytic continuation, convergence

2020 Mathematics Subject Classification: 33C65, 32A17, 32A10, 30B40, 40A99.

1. INTRODUCTION

Hypergeometric functions have been and continue to be the subject of research for a century, surprisingly appearing in various applications in many sciences [8, 20, 28, 27, 29, 31]. Among the problems associated with the study of these functions, one of the most interesting and difficult is the representation and analytical expansion through a special family of functions – branched continued fractions [7, 14, 19]. A generalization of the classical Gaussian method is used to construct formal branched continued fraction expansions of hypergeometric functions [13, 21, 30], and the PC and PF methods are used to establish domains of analytical continuation of these functions [4, 16, 18].

In this paper, we consider the Horn's confluent function H_6, which is defined by the following double power series (see, [25])

$$\mathrm{H}_6(\alpha,\beta;\mathbf{z})=\sum_{p,q=0}^{+\infty}\frac{(\alpha)_{2p+q}}{(\beta)_{p+q}}\frac{z_1^p z_2^q}{p!q!},\quad |z_1|<1/4,\ |z_2|<+\infty,$$

where $\alpha,\beta\in\mathbb{C}$, $\beta\notin\{0,-1,-2,\ldots\}$, $(\cdot)_k$ is the Pochhammer symbol, $\mathbf{z}=(z_1,z_2)\in\mathbb{C}^2$.

Let $\mathfrak{I}_0=\{1,2,3\}$, $i(k)=(i_0,i_1,i_2,\ldots,i_k)$, and

$$\mathfrak{I}_k=\left\{i(k):\ i_0\in\mathfrak{I}_0,\ 2-\left[\frac{i_{r-1}-1}{2}\right]\le i_r\le 3-\left[\frac{i_{r-1}-1}{2}\right],\ 1\le r\le k\right\},\quad k\ge 1,$$

Received: 08.09.2024; Accepted: 02.10.2024; Published Online: 16.12.2024
*Corresponding author: Roman Dmytryshyn; roman.dmytryshyn@pnu.edu.ua
DOI: 10.33205/cma.1545452

where $[\cdot]$ denotes an integer part.

In [5], it is formally established that for each $i_0 \in \mathfrak{I}_0$

$$\begin{aligned}&\frac{\mathrm{H}_6(\alpha,\beta;\mathbf{z})}{\mathrm{H}_6(\alpha+\delta^1_{i_0}+\delta^2_{i_0},\beta+\delta^2_{i_0}+\delta^3_{i_0};\mathbf{z})}\\ &=1-\frac{\alpha}{2\beta}\delta^3_{i_0}+\sum_{i_1=2-[(i_0-1)/2]}^{3-[(i_0-1)/2]}\cfrac{u_{i(1)}(\mathbf{z})}{v_{i(1)}+\sum\limits_{i_2=2-[(i_1-1)/2]}^{3-[(i_1-1)/2]}\cfrac{u_{i(2)}(\mathbf{z})}{v_{i(2)}+\ddots}},\end{aligned}\tag{1.1}$$

where δ^j_i denotes the Kronecker delta, and, for $i(1) \in \mathfrak{I}_1$,

$$u_{i(1)}(\mathbf{z})=\begin{cases}-2\dfrac{\alpha+1}{\beta}z_1, \text{ if } i_0=1,\ i_1=2,\\ -\dfrac{z_2}{\beta}, \text{ if } i_0=1,\ i_1=3,\\ -\dfrac{(2\beta-\alpha)(\alpha+1)}{\beta(\beta+1)}z_1, \text{ if } i_0=2,\ i_1=2,\\ -\dfrac{\beta-\alpha}{\beta(\beta+1)}z_2, \text{ if } i_0=2,\ i_1=3,\\ \dfrac{\alpha}{2\beta}, \text{ if } i_0=3,\ i_1=1,\\ \dfrac{\alpha}{2\beta(\beta+1)}z_2, \text{ if } i_0=3,\ i_1=2,\end{cases}\tag{1.2}$$

for $i(k+1) \in \mathfrak{I}_{k+1}$, $k \geq 1$,

$$\begin{aligned}&u_{i(k+1)}(\mathbf{z})\\ &=\begin{cases}-\dfrac{2(\alpha+k+1-\sum_{r=0}^{k-1}\delta^3_{i_r})}{\beta+k-\sum_{r=0}^{k-1}\delta^1_{i_r}}z_1, \text{ if } i_k=1,\ i_{k+1}=2,\\ -\dfrac{z_2}{\beta+k-\sum_{r=0}^{k-1}\delta^1_{i_r}}, \text{ if } i_k=1,\ i_{k+1}=3,\\ \dfrac{(\alpha-2\beta-k-\sum_{r=0}^{k-1}(\delta^3_{i_r}-2\delta^1_{i_r}))(\alpha+k+1-\sum_{r=0}^{k-1}\delta^3_{i_r})}{(\beta+k-\sum_{r=0}^{k-1}\delta^1_{i_r})(\beta+k+1-\sum_{r=0}^{k-1}\delta^1_{i_r})}z_1, \text{ if } i_k=2,\ i_{k+1}=2,\\ -\dfrac{\beta-\alpha+\sum_{r=0}^{k-1}(\delta^3_{i_r}-\delta^1_{i_r})}{(\beta+k-\sum_{r=0}^{k-1}\delta^1_{i_r})(\beta+k+1-\sum_{r=0}^{k-1}\delta^1_{i_r})}z_2, \text{ if } i_k=2,\ i_{k+1}=3,\\ \dfrac{\alpha+k-\sum_{r=0}^{k-1}\delta^3_{i_r}}{2(\beta+k-\sum_{r=0}^{k-1}\delta^1_{i_r})}, \text{ if } i_k=3,\ i_{k+1}=1,\\ \dfrac{\alpha+k-\sum_{r=0}^{k-1}\delta^3_{i_r}}{2(\beta+k-\sum_{r=0}^{k-1}\delta^1_{i_r})(\beta+k+1-\sum_{r=0}^{k-1}\delta^1_{i_r})}z_2, \text{ if } i_k=3,\ i_{k+1}=2,\end{cases}\end{aligned}\tag{1.3}$$

and, for $i(k) \in \mathfrak{I}_k$, $k \geq 1$,

$$v_{i(k)}=1-\frac{\alpha+k-\sum_{r=0}^{k-1}\delta^3_{i_r}}{2(\beta+k-\sum_{r=0}^{k-1}\delta^1_{i_r})}\delta^3_{i_k}.\tag{1.4}$$

Here it is shown that if

$$\alpha \geq 0, \quad \beta \geq \alpha+1+\delta^1_{i_0} \quad \text{for} \quad i_0 \in \mathfrak{I}_0,\tag{1.5}$$

and there exist the positive numbers $\nu_1, \nu_2, \nu_3, \mu_1, \mu_2$, and μ_3 such that

$$\frac{2\nu_1}{\mu_2} \leq \min\left\{1-\mu_1-\frac{\nu_2}{\beta\mu_3},\ 1-\mu_2-\frac{\nu_2}{(\beta+1)\mu_3}\right\}, \quad \frac{\nu_3}{(\beta+1)\mu_2}+\mu_3 \leq \frac{1}{2},$$

then

$$\Omega_{\nu_1,\nu_2,\nu_3} = \{\mathbf{z}\in\mathbb{C}^2:\ |z_2|-\mathrm{Re}(z_2) < 2\nu_3,\ |z_k|+\mathrm{Re}(z_k) < 2\nu_k,\ k=1,2,\}$$

is the domain of the analytical continuation of the function on the left side of (1.1).

The results of the study of branched continued fraction expansions of the other Horn's hypergeometric functions can be found in [1, 17, 23, 24].

In the next section, we give the formula for the difference of two approximants of branched continued fraction expansions of the ratios of Horn's confluent functions H_6 with real parameters and prove the auxiliary Theorem 2.1 on the estimation of the rate of convergence for these expansions in a new region of the space $\mathbb{R}^2$ (that is, a domain (an open connected set) which may include all, part, or none of its boundary). In Section 3, we prove Theorem 3.2 on the new domain of the analytical extension of the above-mentioned ratios in the space $\mathbb{C}^2$ and give an important Corollary 3.1 from it.

2. Auxiliary Results

Let i_0 be an arbitrary index in $\mathfrak{I}_0$. We set, for $i(n)\in\mathfrak{I}_n$, $n\geq 1$,

$$F^{(n)}_{i(n)}(\mathbf{z}) = v_{i(n)}, \tag{2.6}$$

and for $i(k)\in\mathfrak{I}_k$, $1\leq k\leq n-1$, $n\geq 2$,

$$F^{(n)}_{i(k)}(\mathbf{z}) = v_{i(k)} + \sum_{i_{k+1}=2-[(i_k-1)/2]}^{3-[(i_k-1)/2]} \frac{u_{i(k+1)}(\mathbf{z})}{v_{i(k+1)} + \ddots + \sum\limits_{i_n=2-[(i_{n-1}-1)/2]}^{3-[(i_{n-1}-1)/2]} \dfrac{u_{i(n)}(\mathbf{z})}{v_{i(n)}}}.$$

This gives the following recurrence relations

$$F^{(n)}_{i(k)}(\mathbf{z}) = v_{i(k)} + \sum_{i_{k+1}=2-[(i_k-1)/2]}^{3-[(i_k-1)/2]} \frac{u_{i(k+1)}(\mathbf{z})}{F^{(n)}_{i(k+1)}(\mathbf{z})}, \quad i(k)\in\mathfrak{I}_k,\ 1\leq k\leq n-1,\ n\geq 2, \tag{2.7}$$

and also the following expressions

$$f^{(i_0)}_n(\mathbf{z}) = 1-\frac{\alpha}{2\beta}\delta^3_{i_0} + \sum_{i_1=2-[(i_0-1)/2]}^{3-[(i_0-1)/2]} \frac{u_{i(1)}(\mathbf{z})}{F^{(n)}_{i(1)}(\mathbf{z})}, \quad n\geq 1. \tag{2.8}$$

Suppose that $F^{(n)}_{i(k)}(\mathbf{z})\neq 0$ for all $i(k)\in\mathfrak{I}_k$, $1\leq k\leq n$, $n\geq 1$. Using the method suggested in ([11, p. 28]), we show that for $n\geq 1$ and $k\geq 1$

$$f^{(i_0)}_{n+k}(\mathbf{z}) - f^{(i_0)}_n(\mathbf{z}) = \sum_{i_1=2-[(i_0-1)/2]}^{3-[(i_0-1)/2]} \cdots \sum_{i_{n+1}=2-[(i_n-1)/2]}^{3-[(i_n-1)/2]} \frac{(-1)^n \prod_{r=1}^{n+1} u_{i(r)}(\mathbf{z})}{\prod_{r=1}^{n+1} F^{(n+k)}_{i(r)}(\mathbf{z}) \prod_{r=1}^{n} F^{(n)}_{i(r)}(\mathbf{z})}. \tag{2.9}$$

On the first step we obtain

$$\begin{aligned}
&f^{(i_0)}_{n+k}(\mathbf{z}) - f^{(i_0)}_{n}(\mathbf{z}) \\
=&1 - \frac{\alpha}{2\beta}\delta^3_{i_0} + \sum_{i_1=2-[(i_0-1)/2]}^{3-[(i_0-1)/2]} \frac{u_{i(1)}(\mathbf{z})}{F^{(n+k)}_{i(1)}(\mathbf{z})} - \left(1 - \frac{\alpha}{2\beta}\delta^3_{i_0} + \sum_{i_1=2-[(i_0-1)/2]}^{3-[(i_0-1)/2]} \frac{u_{i(1)}(\mathbf{z})}{F^{(n)}_{i(1)}(\mathbf{z})}\right) \\
=&-\sum_{i_1=2-[(i_0-1)/2]}^{3-[(i_0-1)/2]} \frac{u_{i(1)}(\mathbf{z})}{F^{(n+k)}_{i(1)}(\mathbf{z})F^{(n)}_{i(1)}(\mathbf{z})}(F^{(n+k)}_{i(1)}(\mathbf{z}) - F^{(n)}_{i(1)}(\mathbf{z})).
\end{aligned}$$

For an arbitrary integer r such that $1 \le r \le n-1$, we have

$$\begin{aligned}
&F^{(n+k)}_{i(r)}(\mathbf{z}) - F^{(n)}_{i(r)}(\mathbf{z}) \\
=&v_{i(r)} + \sum_{i_{r+1}=2-[(i_r-1)/2]}^{3-[(i_r-1)/2]} \frac{u_{i(r+1)}(\mathbf{z})}{F^{(n+k)}_{i(r+1)}(\mathbf{z})} - \left(v_{i(r)} + \sum_{i_{r+1}=2-[(i_r-1)/2]}^{3-[(i_r-1)/2]} \frac{u_{i(r+1)}(\mathbf{z})}{F^{(n)}_{i(r+1)}(\mathbf{z})}\right) \\
=&-\sum_{i_{r+1}=2-[(i_r-1)/2]}^{3-[(i_r-1)/2]} \frac{u_{i(r+1)}(\mathbf{z})}{F^{(n+k)}_{i(r+1)}(\mathbf{z})F^{(n)}_{i(r+1)}(\mathbf{z})}\left(F^{(n+k)}_{i(r+1)}(\mathbf{z}) - F^{(n)}_{i(r+1)}(\mathbf{z})\right). \qquad (2.10)
\end{aligned}$$

Since

$$F^{(n+k)}_{i(n)}(\mathbf{z}) - F^{(n)}_{i(n)}(\mathbf{z}) = \sum_{i_{n+1}=2-[(i_n-1)/2]}^{3-[(i_n-1)/2]} \frac{u_{i(n+1)}(\mathbf{z})}{F^{(n+k)}_{i(n+1)}(\mathbf{z})},$$

using the recurrence relation (2.10), at the nth step we obtain (2.9). For convenience, we rewrite (2.9) as follows

$$\begin{aligned}
f^{(i_0)}_{n+k}(\mathbf{z}) - f^{(i_0)}_{n}(\mathbf{z}) = (-1)^n &\sum_{i_1=2-[(i_0-1)/2]}^{3-[(i_0-1)/2]} \cdots \sum_{i_{n+1}=2-[(i_n-1)/2]}^{3-[(i_n-1)/2]} \frac{u_{i(1)}(\mathbf{z})}{F^{(q)}_{i(1)}(\mathbf{z})} \\
&\times \prod_{k=1}^{[(n+1)/2]} \frac{u_{i(2k)}(\mathbf{z})}{F^{(p)}_{i(2k-1)}(\mathbf{z})F^{(p)}_{i(2k)}(\mathbf{z})} \prod_{k=1}^{[n/2]} \frac{u_{i(2k+1)}(\mathbf{z})}{F^{(q)}_{i(2k)}(\mathbf{z})F^{(q)}_{i(2k+1)}(\mathbf{z})}, \qquad (2.11)
\end{aligned}$$

where $q = n+k$, $p = n$, if n is even, and $q = n$, $p = n+k$, if n is odd.

The following theorem is true:

Theorem 2.1. *Suppose that α and β are real constants such that satisfy inequalities (1.5). Then for each $i_0 \in \mathfrak{I}_0$:*

(A) *The branched continued fraction (1.1) converges to a finite value $f^{(i_0)}(\mathbf{z})$ for each $\mathbf{z} \in \Theta_{l_1,l_2}$, where*

$$\Theta_{l_1,l_2} = \{\mathbf{z} \in \mathbb{R}^2 : \ -l_1 \le z_1 \le 0, \ 0 \le z_2 \le l_2\}, \quad l_1 > 0, \ 0 < l_2 < \frac{\beta}{4}, \qquad (2.12)$$

in addition, it converges uniformly on every compact subset of an interior of the region Θ_{l_1,l_2}.

(B) *If $f^{(i_0)}_n(\mathbf{z})$ denotes the nth approximant of the branched continued fraction (1.1), then for each $\mathbf{z} \in \Theta_{l_1,l_2}$*

$$|f^{(i_0)}(\mathbf{z}) - f^{(i_0)}_n(\mathbf{z})| \le C^{(i_0)} \left(\frac{\varrho}{\varrho+1}\right)^n, \quad n \ge 1,$$

where

$$C^{(i_0)}=\begin{cases}\dfrac{2l_1(\alpha+1)(\beta+1)}{\beta(\beta-2l_2+1)}+\dfrac{2l_2}{\beta}, \text{ if } i_0=1,\\ \dfrac{l_1(2\beta-\alpha)(\alpha+1)}{\beta(\beta-2l_2+1)}+\dfrac{2l_2(\beta-\alpha)}{\beta(\beta+1)}, \text{ if } i_0=2,\\ \dfrac{\alpha}{2(\beta-2l_2)}+\dfrac{l_2\alpha}{2\beta(\beta-2l_2+1)}, \text{ if } i_0=3,\end{cases} \tag{2.13}$$

and

$$\varrho=\max\left\{\left(\frac{2l_1(\beta+1)}{\beta-2l_2+1}+\frac{2l_2}{\beta}\right)\frac{\beta}{\beta-4l_2},\ \frac{\beta}{\beta-2l_2}+\frac{l_2}{2(\beta-2l_2+1)}\right\}. \tag{2.14}$$

Proof. We will carry out the proof in the same way as in [5, Theorem 3.2]. In [5, Formula (3.22)], it is shown that

$$\begin{aligned}v_{i(k-1),3}&=1-\frac{\alpha+k-\sum_{r=0}^{k-1}\delta^3_{i_r}}{2\beta+2k-2\sum_{r=0}^{k-1}\delta^1_{i_r}}\\ &\geq\frac{1}{2},\quad i(k-1)\in\mathfrak{I}_k,\ k\geq 2,\end{aligned} \tag{2.15}$$

are valid under the condition (1.5).

Let n be an arbitrary natural number and $\mathbf{z}$ be an arbitrary fixed point in (2.12). We set

$$g_1=1-\frac{2l_2}{\beta},\ g_2=1-\frac{2l_2}{\beta+1},\ g_3=\frac{1}{2}.$$

By induction on k, we prove that

$$F^{(n)}_{i(k)}(\mathbf{z})\geq g_{i_k}, \tag{2.16}$$

where $i(k)\in\mathfrak{I}_k$, $1\leq k\leq n$.

Taking into account (1.4), (2.6), (2.12), and (2.15), it is clear that for $k=n$ inequalities (2.16) hold for $i_n=1,2,3$. Let (2.16) hold for $k=r+1$ such that $r+1\leq n$ and for all $i(r+1)\in\mathfrak{I}_r$. Then from (2.7) for $k=r$ and for any $i(r-1)\in\mathfrak{I}_{r-1}$, we have

$$\begin{aligned}F^{(n)}_{i(r)}(\mathbf{z})&=v_{i(r)}+\sum_{i_{r+1}=2}^{3}\frac{u_{i(r+1)}(\mathbf{z})}{F^{(n)}_{i(r+1)}(\mathbf{z})}\\ &\geq v_{i(r)}(\mathbf{z})-2\frac{l_2}{\beta}\\ &=1-\frac{2l_2}{\beta}\\ &=g_1,\end{aligned}$$

if $i_r=1$,

$$\begin{aligned}F^{(n)}_{i(r)}(\mathbf{z})&\geq v_{i(r)}-2\frac{l_2}{\beta+1}\\ &=1-\frac{2l_2}{\beta+1}\\ &=g_2,\end{aligned}$$

if $i_r = 2$, and

$$\begin{aligned} F^{(n)}_{i(r)}(\mathbf{z}) &\geq v_{i(r)} \\ &\geq \frac{1}{2} \\ &= g_3, \end{aligned}$$

if $i_r = 3$.

Let now n be an arbitrary integer such that $n \geq 2$. We show that

$$\sum_{i_{k+1}=2-[(i_k-1)/2]}^{3-[(i_k-1)/2]} \frac{|u_{i(k+1)}(\mathbf{z})|}{|F^{(n)}_{i(k+1)}(\mathbf{z})F^{(n)}_{i(k)}(\mathbf{z})|} \leq \frac{\varrho}{\varrho+1}, \tag{2.17}$$

where $i(k) \in \mathfrak{I}_k$, $1 \leq k \leq n-1$, and ϱ is defined by (2.14), or the same as

$$\sum_{i_{k+1}=2-[(i_k-1)/2]}^{3-[(i_k-1)/2]} \frac{|u_{i(k+1)}(\mathbf{z})|}{|F^{(n)}_{i(k+1)}(\mathbf{z})|} \leq \varrho \left(|F^{(n)}_{i(k)}(\mathbf{z})| - \sum_{i_{k+1}=2-[(i_k-1)/2]}^{3-[(i_k-1)/2]} \frac{|u_{i(k+1)}(\mathbf{z})|}{|F^{(n)}_{i(k+1)}(\mathbf{z})|} \right),$$

where $i(k) \in \mathfrak{I}_k$, $1 \leq k \leq n-1$.

Using (1.2)–(1.4), (2.12), (2.15), and (2.16), for any $i(k) \in \mathfrak{I}_k$, $1 \leq k \leq n-1$, and for any $\mathbf{z} \in \Theta_{l_1,l_2}$ we have

$$\begin{aligned} |F^{(n)}_{i(k)}(\mathbf{z})| - \sum_{i_{k+1}=2}^{3} \frac{|u_{i(k+1)}(\mathbf{z})|}{|F^{(n)}_{i(k+1)}(\mathbf{z})|} &\geq 1 - 2\frac{|u_{i(k),3}(\mathbf{z})|}{g_3} \\ &= 1 - \frac{2}{\beta + k - \sum_{r=0}^{k-1} \delta^1_{i_r}} \frac{|z_2|}{g_3} \\ &\geq 1 - \frac{4l_2}{\beta} \end{aligned}$$

and

$$\begin{aligned} \sum_{i_{k+1}=2}^{3} \frac{|u_{i(k+1)}(\mathbf{z})|}{|F^{(n)}_{i(k+1)}(\mathbf{z})|} &\leq 2\frac{\alpha + k - \sum_{r=0}^{k-1} \delta^3_{i_r} + 1}{\beta + k - \sum_{r=0}^{k-1} \delta^1_{i_r}} \frac{|z_1|}{g_2} + \frac{1}{\beta + k - \sum_{r=0}^{k-1} \delta^1_{i_r}} \frac{|z_2|}{g_3} \\ &\leq \frac{2l_1(\beta+1)}{\beta + 1 - 2l_2} + \frac{2l_2}{\beta} \\ &\leq \varrho \left(1 - \frac{4l_2}{\beta}\right), \end{aligned}$$

if $i_k = 1$,

$$\begin{aligned} |F^{(n)}_{i(k)}(\mathbf{z})| - \sum_{i_{k+1}=2}^{3} \frac{|u_{i(k+1)}(\mathbf{z})|}{|F^{(n)}_{i(k+1)}(\mathbf{z})|} &\geq 1 - 2\frac{|u_{i(k),3}(\mathbf{z})|}{g_3} \\ &= 1 - 2\frac{\beta - \alpha + \sum_{r=0}^{k-1} (\delta^3_{i_r} - \delta^1_{i_r}}{(\beta + k - \sum_{r=0}^{k-1} \delta^1_{i_r})(\beta + k + 1 - \sum_{r=0}^{k-1} \delta^1_{i_r})} \frac{|z_2|}{g_3} \\ &\geq 1 - \frac{4l_2}{\beta+1} \end{aligned}$$

and

$$\begin{aligned}\sum_{i_{k+1}=2}^{3}\frac{|u_{i(k+1)}(\mathbf{z})|}{|F^{(n)}_{i(k+1)}(\mathbf{z})|} &\le \frac{(2\beta-\alpha+k+\sum_{r=0}^{k-1}(\delta^3_{i_r}-2\delta^1_{i_r}))(\alpha+k+1-\sum_{r=0}^{k-1}\delta^3_{i_r})}{(\beta+k-\sum_{r=0}^{k-1}\delta^1_{i_r})(\beta+k-1-\sum_{r=0}^{k-1}\delta^1_{i_r})}\frac{|z_1|}{g_3}\\ &+\frac{\beta-\alpha+\sum_{r=0}^{k-1}(\delta^3_{i_r}-\delta^1_{i_r}}{(\beta+k-\sum_{r=0}^{k-1}\delta^1_{i_r})(\beta+k+1-\sum_{r=0}^{k-1}\delta^1_{i_r})}\frac{|z_2|}{g_3}\\ &\le \frac{2l_1(\beta+1)}{\beta+1-2l_2}+\frac{2l_2}{\beta+1}\\ &< \frac{2l_1(\beta+1)}{\beta+1-2l_2}+\frac{2l_2}{\beta}\\ &\le \varrho\left(1-\frac{4l_2}{\beta}\right)\\ &< \varrho\left(1-\frac{4l_2}{\beta+1}\right),\end{aligned}$$

if $i_k=2$, and last

$$\begin{aligned}|F^{(n)}_{i(k)}(\mathbf{z})|-\sum_{i_{k+1}=1}^{2}\frac{|u_{i(k+1)}(\mathbf{z})|}{|F^{(n)}_{i(k+1)}(\mathbf{z})|} &\ge v_{i(k)}\\ &\ge g_3\\ &= \frac{1}{2}\end{aligned}$$

and

$$\begin{aligned}\sum_{i_{k+1}=1}^{2}\frac{|P_{i(k+1)}(\mathbf{z})|}{|G^{(n)}_{i(k+1)}(\mathbf{z})|} &\le \frac{\alpha+k-\sum_{r=0}^{k-1}\delta^3_{i_r}}{2(\beta+k-\sum_{r=0}^{k-1}\delta^1_{i_r})}\frac{1}{g_1}\\ &+\frac{\alpha+k-\sum_{r=0}^{k-1}\delta^3_{i_r}}{(\beta+k-\sum_{r=0}^{k-1}\delta^1_{i_r})(\beta+k+1-\sum_{r=0}^{k-1}\delta^1_{i_r})}\frac{|z_2|}{g_2}\\ &\le \frac{\beta}{2(\beta-2l_2)}+\frac{l_2}{2(\beta+1-2l_2)}\\ &\le \frac{1}{2}\varrho,\end{aligned}$$

if $i_k=3$. Hence, due to the arbitrariness of $i(k)$, the validity of inequalities (2.17) follows.

Now from (1.2), (2.12), (2.13), and (2.16) it follows that

$$\sum_{i_1=2-[(i_0-1)/2]}^{3-[(i_0-1)/2]}\frac{|u_{i(1)}(\mathbf{z})|}{|F^{(q)}_{i(1)}(\mathbf{z})|}\le C^{(i_0)}\quad\text{for}\quad i_0\in\mathfrak{I}_0\quad\text{and}\quad q\ge 1. \tag{2.18}$$

Indeed,

$$\begin{aligned}\frac{|u_{1,2}(\mathbf{z})|}{|F^{(q)}_{1,2}(\mathbf{z})|}+\frac{|u_{1,3}(\mathbf{z})|}{|F^{(q)}_{1,3}(\mathbf{z})|} &\le \frac{2l_1(\alpha+1)(\beta+1)}{\beta(\beta-2l_2+1)}+\frac{2l_2}{\beta}\\ &= C^{(1)},\end{aligned}$$

if $i_0 = 1$,

$$\begin{aligned}\frac{|u_{2,2}(\mathbf{z})|}{|F^{(q)}_{2,2}(\mathbf{z})|} + \frac{|u_{2,3}(\mathbf{z})|}{|F^{(q)}_{2,3}(\mathbf{z})|} &\le \frac{l_1(2\beta-\alpha)(\alpha+1)(\beta+1)}{\beta(\beta+1)(\beta-2l_2+1)} + \frac{2l_2(\beta-\alpha)}{\beta(\beta+1)}\\ &= \frac{l_1(2\beta-\alpha)(\alpha+1)}{\beta(\beta-2l_2+1)} + \frac{2l_2(\beta-\alpha)}{\beta(\beta+1)}\\ &= C^{(2)},\end{aligned}$$

if $i_0 = 2$,

$$\begin{aligned}\frac{|u_{3,1}(\mathbf{z})|}{|F^{(q)}_{3,1}(\mathbf{z})|} + \frac{|u_{3,2}(\mathbf{z})|}{|F^{(q)}_{3,2}(\mathbf{z})|} &\le \frac{\alpha\beta}{2\beta(\beta-2l_2)} + \frac{l_2\alpha(\beta+1)}{2\beta(\beta+1)(\beta-2l_2+1)}\\ &= \frac{\alpha}{2(\beta-2l_2)} + \frac{l_2\alpha}{2\beta(\beta-2l_2+1)}\\ &= C^{(3)},\end{aligned}$$

if $i_0 = 3$.

From (2.12) and (2.16) it is clear that $F^{(q)}_{i(k)}(\mathbf{z}) \neq 0$ for $i(k) \in \mathfrak{I}_k$, $1 \le k \le q$, $q \ge 1$, and for all $\mathbf{z} \in \Theta_{l_1,l_2}$. Thus, using (2.17) and (2.18), from (2.11) for any $\mathbf{z} \in \Theta_{l_1,l_2}$ we have

$$\begin{aligned}|f^{(i_0)}_{n+k}(\mathbf{z}) - f^{(i_0)}_{n}(\mathbf{z})| &\le \sum_{i_1=2-[(i_0-1)/2]}^{3-[(i_0-1)/2]} \frac{|u_{i(1)}(\mathbf{z})|}{|F^{(q)}_{i(1)}(\mathbf{z})|}\left(\frac{\varrho}{\varrho+1}\right)^n\\ &\le C^{(i_0)}\left(\frac{\varrho}{\varrho+1}\right)^n, \quad n \ge 1,\ k \ge 1,\end{aligned}$$

where $q = n + k$, if n is even, and $q = n$, if n is odd. Finally, (A) and (B) follow when $n \to \infty$ and $k \to \infty$, respectively. □

3. Analytical Continuation

In this section, we prove the following result:

Theorem 3.2. *Let α and β be real constants satisfying the inequalities (1.5), and $\nu_1, \nu_2, \nu_3, \mu_1, \mu_2, \mu_3$ be positive numbers such that*

$$\frac{2\nu_1}{\mu_2} \le \min\left\{1-\mu_1-\frac{\nu_2}{\beta\mu_3},\ 1-\mu_2-\frac{\nu_2}{(\beta+1)\mu_3}\right\}, \quad \frac{\kappa}{2\mu_1} + \frac{\nu_3}{(\beta+1)\mu_2} \le \frac{1}{2} - \mu_3, \tag{3.19}$$

where $0 \le \kappa < 1$. Then for each $i_0 \in \mathfrak{I}_0$:

(**A**) *The branched continued fraction (1.1) converges uniformly on every compact subset of the domain*

$$\Xi_{\nu_1,\nu_2,\nu_3} = \bigcup_{\substack{\varphi\in(-\pi/4,\pi/4)\\ \mathrm{tg}(\varphi)\le\sqrt{\kappa}}} \Xi_{\nu_1,\nu_2,\nu_3,\varphi}, \tag{3.20}$$

where

$$\Xi_{\nu_1,\nu_2,\nu_3,\varphi} = \left\{\mathbf{z}\in\mathbb{C}^2:\ \frac{|z_2| - \mathrm{Re}(z_2e^{-2\varphi})}{\cos^2(\varphi)} < 2\nu_3,\ \frac{|z_k| + \mathrm{Re}(z_ke^{-2\varphi})}{\cos^2(\varphi)} < 2\nu_k,\ k=1,2\right\}, \tag{3.21}$$

to the function $f^{(i_0)}(\mathbf{z})$ holomorphic in the domain Ξ_{ν_1,ν_2,ν_3}.

(**B**) *The function $f^{(i_0)}(\mathbf{z})$ is an analytic continuation of branched continued fraction (1.1) in the domain (3.20).*

Proof. To prove (A), we use the convergence continuation theorem (see, [3, Theorem 3] and also [11, Theorem 2.17], [34, Theorem 24.2]), which extends the domain of convergence of a branched continued fraction, which is already known for a small domain, to a larger domain.

Let i_0 be an arbitrary index in $\mathfrak{I}_0$. Let us show that $\{f_n^{(i_0)}(\mathbf{z})\}$, where $f_n^{(i_0)}(\mathbf{z})$, $n \geq 1$, are defined by (2.8), is a sequence of functions holomorphic in the domain (3.20). Since each approximant of the branched continued fraction (1.1) is an entire function, it suffices to show that

$$F_{i(1)}^{(n)}(\mathbf{z}) \neq 0 \quad \text{for} \quad i(1) \in \mathfrak{I}_1,\ n \geq 1, \quad \text{and} \quad \text{for} \quad \mathbf{z} \in \Xi_{\nu_1,\nu_2,\nu_3}.$$

Let φ be an arbitrary real in $(-\pi/4, \pi/4)$ such that $\mathrm{tg}(\varphi) \leq \sqrt{\kappa}$ and $\mathbf{z}$ be an arbitrary fixed point in the domain (3.21). Under the condition (1.5) and (2.15), from (1.4) for any $i(k-1) \in \mathfrak{I}_k$, $k \geq 2$, we have

$$\begin{aligned}\mathrm{Re}(v_{i(k-1),3}e^{-i\varphi}) &= \left(1 - \frac{\alpha + k - \sum_{r=0}^{k-1}\delta_{i_r}^3}{2\beta + 2k - 2\sum_{r=0}^{k-1}\delta_{i_r}^1}\right)\mathrm{Re}(e^{-i\varphi}) \\ &\geq \frac{1}{2}\cos(\varphi),\end{aligned}$$

and for $i_k = 1$ or $i_k = 2$ we get

$$\begin{aligned}\mathrm{Re}(v_{i(k)}e^{-i\varphi}) &= \mathrm{Re}(e^{-i\varphi}) \\ &= \cos(\varphi).\end{aligned}$$

Now, using (1.4), (1.5), (2.15), and (3.21), from (1.3) for any $i(k) \in \mathfrak{I}$, $k \geq 2$, herewith $i_k = 1$ we obtain

$$\begin{aligned}|u_{i(k),2}(\mathbf{z})| - \mathrm{Re}(u_{i(k),2}(\mathbf{z})e^{-2i\varphi}) &= \frac{2(\alpha + k - \sum_{r=0}^{k-1}\delta_{i_r}^3 + 1)}{\beta + k - \sum_{r=0}^{k-1}\delta_{i_r}^1}(|z_1| + \mathrm{Re}(z_1 e^{-2i\varphi})) \\ &< 4\nu_1\cos^2(\varphi), \\ |u_{i(k),3}(\mathbf{z})| - \mathrm{Re}(u_{i(k),3}(\mathbf{z})e^{-2i\varphi}) &= \frac{|z_2| + \mathrm{Re}(z_2 e^{-2i\varphi})}{\beta + k - \sum_{r=0}^{k-1}\delta_{i_r}^1} \\ &< \frac{2\nu_2}{\beta}\cos^2(\varphi),\end{aligned}$$

and, thus,

$$\begin{aligned}\sum_{i_{k+1}=2}^{3}\frac{|u_{i(k+1)}(\mathbf{z})| - \mathrm{Re}(u_{i(k+1)}(\mathbf{z})e^{-2i\varphi})}{\mu_{i_{k+1}}\cos(\varphi)} &< \frac{4\nu_1}{\mu_2}\cos(\varphi) + \frac{2\nu_2}{\beta\mu_3}\cos(\varphi) \\ &\leq 2(1-\mu_1)\cos(\varphi) \\ &= 2(\mathrm{Re}(v_{i(k)}e^{-i\varphi}) - \mu_1\cos(\varphi)).\end{aligned}$$

When $i_k = 2$ we have

$$\begin{aligned}
&|u_{i(k),2}(\mathbf{z})| - \operatorname{Re}(u_{i(k),2}(\mathbf{z})e^{-2i\varphi}) \\
=&\frac{(2\beta - \alpha + k + \sum_{r=0}^{k-1}(\delta_{i_r}^3 - 2\delta_{i_r}^1))(\alpha + k - \sum_{r=0}^{k-1}\delta_{i_r}^3 + 1)}{(\beta + k - \sum_{r=0}^{k-1}\delta_{i_r}^1)(\beta + k - \sum_{r=0}^{k-1}\delta_{i_r}^1 + 1)}(|z_1| + \operatorname{Re}(z_1 e^{-2i\varphi})) \\
<&4\nu_1 \cos^2(\varphi),
\end{aligned}$$

$$\begin{aligned}
&|u_{i(k),3}(\mathbf{z})| - \operatorname{Re}(u_{i(k),3}(\mathbf{z})e^{-2i\varphi}) \\
=&\frac{\beta - \alpha + \sum_{r=0}^{k-1}(\delta_{i_r}^3 - \delta_{i_r}^1)}{(\beta + k - \sum_{r=0}^{k-1}\delta_{i_r}^1)(\beta + k - \sum_{r=0}^{k-1}\delta_{i_r}^1 + 1)}(|z_2| + \operatorname{Re}(z_2 e^{-2i\varphi})) \\
<&\frac{2\nu_2}{\beta + 1}\cos^2(\varphi),
\end{aligned}$$

and, thus,

$$\begin{aligned}
\sum_{i_{k+1}=2}^{3} \frac{|u_{i(k+1)}(\mathbf{z})| - \operatorname{Re}(u_{i(k+1)}(\mathbf{z})e^{-2i\varphi})}{\mu_{i_{k+1}}\cos(\varphi)} &< \frac{4\nu_1}{\mu_2}\cos(\varphi) + \frac{2\nu_2}{(\beta+1)\mu_3}\cos(\varphi) \\
&\le 2(\operatorname{Re}(v_{i(k)}e^{-i\varphi}) - \mu_2\cos(\varphi)).
\end{aligned}$$

If $i_k = 3$, we obtain

$$\begin{aligned}
|u_{i(k),1}(\mathbf{z})| - \operatorname{Re}(u_{i(k),1}(\mathbf{z})e^{-2i\varphi}) &= \frac{\alpha + k - \sum_{r=0}^{k-1}\delta_{i_r}^3}{2(\beta + k - \sum_{r=0}^{k-1}\delta_{i_r}^1)} - \frac{\alpha + k - \sum_{p=r}^{k-1}\delta_{i_r}^3}{2(\beta + k - \sum_{r=0}^{k-1}\delta_{i_r}^1)}\cos(2\varphi) \\
&\le \frac{1}{2}(1 - \cos(2\varphi)) \\
&\le \kappa\cos^2(\varphi), \\
|u_{i(k),2}(\mathbf{z})| - \operatorname{Re}(u_{i(k),2}(\mathbf{z})e^{-2i\varphi}) &= \frac{(\alpha + k - \sum_{r=0}^{k-1}\delta_{i_r}^3)(|z_2| - \operatorname{Re}(z_2 e^{-2i\varphi}))}{2(\beta + k - \sum_{r=0}^{k-1}\delta_{i_r}^1)(\beta + k + 1 - \sum_{r=0}^{k-1}\delta_{i_r}^1)} \\
&< \frac{2\nu_3}{\beta+1}\cos(\varphi),
\end{aligned}$$

and, thus,

$$\begin{aligned}
\sum_{i_{k+1}=1}^{2} \frac{|u_{i(k+1)}(\mathbf{z})| - \operatorname{Re}(u_{i(k+1)}(\mathbf{z})e^{-2i\varphi})}{\mu_{i_{k+1}}\cos(\varphi)} &< \frac{\kappa}{\mu_1}\cos(\varphi) + \frac{2\nu_3}{(\beta+1)\mu_2}\cos(\varphi) \\
&\le 2(\operatorname{Re}(v_{i(k)}e^{-i\varphi}) - \mu_3\cos(\varphi)).
\end{aligned}$$

From [6, Proposition 2], with $g_{i(k)} = \mu_{i_k}$, $i(k) \in \mathfrak{I}_k$, $k \ge 1$, it follows that

$$\operatorname{Re}(F_{i(k)}^{(n)}(\mathbf{z})e^{-i\varphi}) \ge \mu_k\cos(\varphi) > 0 \tag{3.22}$$

for $i(k) \in \mathfrak{I}_k$, $1 \le k \le n$, $n \ge 1$, and for $\mathbf{z} \in \Xi_{\nu_1,\nu_2,\nu_3,\varphi}$. Hence,

$$F_{i(1)}^{(n)}(\mathbf{z}) \ne 0 \quad \text{for} \quad i(1) \in \mathfrak{I}_1,\ n \ge 1, \quad \text{and} \quad \text{for} \quad \mathbf{z} \in \Xi_{\nu_1,\nu_2,\nu_3,\varphi},$$

and, therefore, due to the arbitrariness of φ and for $\mathbf{z} \in \Xi_{\nu_1,\nu_2,\nu_3}$. Thus, each approximants of the branched continued fraction (1.1) is a function holomorphic in the domain (3.20).

Again, let φ be an arbitrary real in $(-\pi/4, \pi/4)$ such that $\mathrm{tg}(\varphi) \le \sqrt{\kappa}$ and let $\Upsilon_{\nu_1,\nu_2,\nu_3,\varphi}$ is an arbitrary compact subset of the domain (3.21). Then there exists an open ball with center at the origin and radius ρ containing $\Upsilon_{\nu_1,\nu_2,\nu_3,\varphi}$. Using (3.22), from (2.8) for any $\mathbf{z} \in \Upsilon_{\nu_1,\nu_2,\nu_3,\varphi}$ we have

$$|f_n^{(i_0)}(\mathbf{z})| \le 1 + \frac{\alpha}{2\beta}\delta_{i_0}^3 + \sum_{i_1=2-[(i_0-1)/2]}^{3-[(i_0-1)/2]} \frac{|u_{i(1)}(\mathbf{z})|}{\mu_{i(1)}\cos(\varphi)}$$
$$= M^{(i_0)}(\Upsilon_{\nu_1,\nu_2,\nu_3,\varphi}) \quad \text{for} \quad n \ge 1,$$

where

$$M^{(i_0)}(\Upsilon_{\nu_1,\nu_2,\nu_3,\varphi}) = \begin{cases} 1 + \dfrac{2(\alpha+1)\rho}{\beta\mu_2\cos(\varphi)} + \dfrac{\rho}{\beta\mu_3\cos(\varphi)}, & \text{if } i_0 = 1, \\ 1 + \dfrac{(2\beta-\alpha)(\alpha+1)\rho}{\beta(\beta+1)\mu_2\cos(\varphi)} + \dfrac{(\beta-\alpha)\rho}{\beta(\beta+1)\mu_3\cos(\varphi)}, & \text{if } i_0 = 2, \\ 1 + \dfrac{\alpha}{2\beta} + \dfrac{\alpha}{2\beta\mu_1\cos(\varphi)} + \dfrac{\alpha\rho}{2\beta(\beta+1)\mu_2\cos(\varphi)}, & \text{if } i_0 = 3, \end{cases}$$

that is, the sequence $\{f_n^{(i_0)}(\mathbf{z})\}$ is uniformly bounded on $\Upsilon_{\nu_1,\nu_2,\nu_3,\varphi}$, and, at the same time, uniformly bounded on every compact subset of the domain (3.21).

Now, let $\Upsilon_{\nu_1,\nu_2,\nu_3}$ is an arbitrary compact subset of the domain (3.20). Let us cover $\Upsilon_{\nu_1,\nu_2,\nu_3}$ with domains of form $\Xi_{\nu_1,\nu_2,\nu_3,\varphi}$. From this cover we choose the finite subcover

$$\Xi_{\nu_1,\nu_2,\nu_3,\varphi^{(1)}},\ \Xi_{\nu_1,\nu_2,\nu_3,\varphi^{(2)}},\ \ldots,\ \Xi_{\nu_1,\nu_2,\nu_3,\varphi^{(k)}}.$$

We set

$$M^{(i_0)}(\Upsilon_{\nu_1,\nu_2,\nu_3}) = \max_{1\le r\le k} M^{(i_0)}(\Upsilon_{\nu_1,\nu_2,\nu_3,\varphi^{(r)}}).$$

Then for any $\mathbf{z} \in \Upsilon_{\nu_1,\nu_2,\nu_3}$ we have

$$|f_n^{(i_0)}(\mathbf{z})| \le M^{(i_0)}(\Upsilon_{\nu_1,\nu_2,\nu_3}) \quad \text{for} \quad n \ge 1,$$

that is, the sequence $\{f_n^{(i_0)}(\mathbf{z})\}$ is uniformly bounded on $\Upsilon_{\nu_1,\nu_2,\nu_3}$, and, hence, it is uniformly bounded on every compact subset of the domain (3.20).

Next, let

$$\tau = \min\left\{l_1,\ l_2,\ \nu_2\cos^2(\varphi)\right\}.$$

Then, according to Theorem 2.1, the branched continued fraction (1.1) converges in the domain

$$\Delta_\chi = \{\mathbf{z} \in \mathbb{R}^2 :\ -\tau < -\chi < \mathrm{Re}(z_1) < 0,\ 0 < \mathrm{Re}(z_2) < \chi < \tau\}.$$

It is clear that Δ_χ is contained in the domain (3.20) for each $0 < \chi < \tau$, in particular, $\Delta_{\tau/2} \subset \Xi_{\nu_1,\nu_2,\nu_3}$. Therefore, (A) follows by Theorem 3 [3].

To prove (B), we use the PC method (see, [2, 3]). Let i_0 be an arbitrary index in $\mathfrak{I}_0$. We set

$$R_{i(n)}^{(n)}(\mathbf{z}) = \frac{\mathrm{H}_6(\alpha+n-\sum_{r=0}^{n-1}\delta_{i_r}^3, \beta+n-\sum_{r=0}^{n-1}\delta_{i_r}^1; \mathbf{z})}{\mathrm{H}_6(\alpha+n+1-\sum_{r=0}^{n}\delta_{i_r}^3, \beta+n+1-\sum_{r=0}^{n}\delta_{i_r}^1; \mathbf{z})},\ i(n) \in \mathfrak{I},\ n \ge 1, \tag{3.23}$$

and

$$R_{i(k)}^{(n)}(\mathbf{z}) = v_{i(k)} + \sum_{i_{k+1}=2-[(i_k-1)/2]}^{3-[(i_k-1)/2]} \frac{u_{i(k+1)}(\mathbf{z})}{v_{i(k+1)} + \ddots + \sum\limits_{i_n=2-[(i_{n-1}-1)/2]}^{3-[(i_{n-1}-1)/2]} \dfrac{u_{i(n)}(\mathbf{z})}{R_{i(n)}^{(n)}(\mathbf{z})}},$$

where $i(k) \in \mathfrak{I}$, $1 \le k \le n-1$, $n \ge 2$. Then it is clear that

$$R^{(n)}_{i(k)}(\mathbf{z}) = v_{i(k)} + \sum_{i_{k+1}=2-[(i_k-1)/2]}^{3-[(i_k-1)/2]} \frac{u_{i(k+1)}(\mathbf{z})}{R^{(n)}_{i(k+1)}(\mathbf{z})}, \tag{3.24}$$

where $i(k) \in \mathfrak{I}$, $1 \le k \le n-1$, $n \ge 2$. It follows that for $n \ge 1$

$$\begin{aligned}
&\frac{\mathrm{H}_6(\alpha,\beta;\mathbf{z})}{\mathrm{H}_6(\alpha+\delta^1_{i_0}+\delta^2_{i_0},\beta+\delta^2_{i_0}+\delta^3_{i_0};\mathbf{z})}\\
=&1-\frac{\alpha}{2\beta}\delta^3_{i_0}+\sum_{i_1=2-[(i_0-1)/2]}^{3-[(i_0-1)/2]}\cfrac{u_{i(1)}(\mathbf{z})}{v_{i(1)}+\ddots+\displaystyle\sum_{i_2=2-[(i_{n+1}-1)/2]}^{3-[(i_{n+1}-1)/2]}\frac{u_{i(n+1)}(\mathbf{z})}{R^{(n+1)}_{i(n+1)}(\mathbf{z})}}\\
=&1-\frac{\alpha}{2\beta}\delta^3_{i_0}+\sum_{i_1=2-[(i_0-1)/2]}^{3-[(i_0-1)/2]}\frac{u_{i(1)}(\mathbf{z})}{R^{(n+1)}_{i(1)}(\mathbf{z})}.
\end{aligned}$$

Since $F^{(n)}_{i(k)}(\mathbf{0}) = 1$ and $R^{(n)}_{i(k)}(\mathbf{0}) = 1$ for any $i(k) \in \mathfrak{I}$, $1 \le k \le n$, $n \ge 1$, then there exist $\Lambda(1/F^{(n)}_{i(k)})$ and $\Lambda(1/R^{(n)}_{i(k)})$ (here, $\Lambda(\cdot)$ is the Taylor expansion of a function holomorphic in some neighborhood of the origin). Moreover, it is clear that $F^{(n)}_{i(k)}(\mathbf{z}) \not\equiv 0$ and $R^{(n)}_{i(k)}(\mathbf{z}) \not\equiv 0$ for all indices. Using (2.6), (2.8), (3.23), and (3.24) from (2.9) for $n \ge 1$, we have

$$\begin{aligned}
&\frac{\mathrm{H}_6(\alpha,\beta;\mathbf{z})}{\mathrm{H}_6(\alpha+\delta^1_{i_0}+\delta^2_{i_0},\beta+\delta^2_{i_0}+\delta^3_{i_0};\mathbf{z})} - f^{(i_0)}_n(\mathbf{z})\\
=&(-1)^n \sum_{i_1=2-[(i_0-1)/2]}^{3-[(i_0-1)/2]} \cdots \sum_{i_{n+1}=2-[(i_n-1)/2]}^{3-[(i_n-1)/2]} \frac{\prod_{r=1}^{n+1} u_{i(r)}(\mathbf{z})}{\prod_{r=1}^{n+1} R^{(n+1)}_{i(r)}(\mathbf{z}) \prod_{r=1}^{n} F^{(n)}_{i(r)}(\mathbf{z})}.
\end{aligned}$$

From this formula in a neighborhood of origin for any $n \ge 1$, we have

$$\Lambda\left(\frac{\mathrm{H}_6(\alpha,\beta;\mathbf{z})}{\mathrm{H}_6(\alpha+\delta^1_{i_0}+\delta^2_{i_0},\beta+\delta^2_{i_0}+\delta^3_{i_0};\mathbf{z})}\right) - \Lambda(f^{(i_0)}_n) = \sum_{\substack{k+l\ge[n+\delta^1_{i_0}+\delta^2_{i_0}]/2\\ k\ge 0,\ l\ge 0}} c^{(n)}_{k,l} z_1^k z_2^l,$$

where $c^{(n)}_{k,l}$, $k \ge 0$, $l \ge 0$, $k+l \ge [n+\delta^1_{i_0}+\delta^2_{i_0}]/2$, are some coefficients. It follows that

$$\begin{aligned}
\nu_n &= \lambda\left(\Lambda\left(\frac{\mathrm{H}_6(\alpha,\beta;\mathbf{z})}{\mathrm{H}_6(\alpha+\delta^1_{i_0}+\delta^2_{i_0},\beta+\delta^2_{i_0}+\delta^3_{i_0};\mathbf{z})}\right) - \Lambda(f^{(i_0)}_n)\right)\\
&= [n+\delta^1_{i_0}+\delta^2_{i_0}]/2
\end{aligned}$$

(here, $\lambda(\cdot)$ is a function defined on the set of all formal double power series $L(\mathbf{z})$ at the origin as follows: if $L(\mathbf{z}) \equiv 0$ then $\lambda(L) = \infty$; if $L(\mathbf{z}) \not\equiv 0$ then $\lambda(L) = k$, where k is the smallest degree of homogeneous terms for which at least one coefficient is different from zero) tends monotonically to ∞ as $n \to \infty$.

Therefore, the branched continued fraction (1.1) corresponds at the origin to

$$\Lambda\left(\frac{\mathrm{H}_6(\alpha,\beta;\mathbf{z})}{\mathrm{H}_6(\alpha+\delta^1_{i_0}+\delta^2_{i_0},\beta+\delta^2_{i_0}+\delta^3_{i_0};\mathbf{z})}\right).$$

Let Θ be a neighborhood of the origin, which is contained in the domain (3.20), and in which

$$\Lambda\left(\frac{\mathrm{H}_6(\alpha,\beta;\mathbf{z})}{\mathrm{H}_6(\alpha+\delta_{i_0}^1+\delta_{i_0}^2,\beta+\delta_{i_0}^2+\delta_{i_0}^3;\mathbf{z})}\right)=\sum_{k,l=0}^{\infty}c_{k,l}z_1^k z_2^l. \tag{3.25}$$

According to (A) and Weierstrass's theorem (see, [32, p. 288]) for arbitrary $k+l$, $k\geq 0$, $l\geq 0$, we have

$$\frac{\partial^{k+l}f_n^{(i_0)}(\mathbf{z})}{\partial z_1^k\partial z_2^l}\to\frac{\partial^{k+l}f^{(i_0)}(\mathbf{z})}{\partial z_1^k\partial z_2^l}\quad\text{as}\quad n\to\infty$$

on each compact subset of (3.20), and to the above proven, the expansion of each approximant $f_n^{(i_0)}(\mathbf{z})$, $n\geq 1$, into formal double power series and (3.25) agree for all homogeneous terms up to and including degree $([n+\delta_{i_0}^1+\delta_{i_0}^2]/2-1)$. Then for any $k+l$, $k\geq 0$, $l\geq 0$, we obtain

$$\begin{aligned}\lim_{n\to\infty}\left(\frac{\partial^{k+l}f_n^{(i_0)}}{\partial z_1^k\partial z_2^l}(\mathbf{0})\right)&=\frac{\partial^{k+l}f^{(i_0)}}{\partial z_1^k\partial z_2^l}(\mathbf{0})\\&=k!l!c_{k,l}.\end{aligned}$$

For all $\mathbf{z}\in\Theta$, it follows that

$$\begin{aligned}f^{(i_0)}(\mathbf{z})&=\sum_{k,l=0}^{\infty}\frac{1}{k!l!}\left(\frac{\partial^{k+l}f^{(i_0)}}{\partial z_1^k\partial z_2^l}(\mathbf{0})\right)z_1^k z_2^l\\&=\sum_{k,l=0}^{\infty}c_{k,l}z_1^k z_2^l.\end{aligned}$$

Finally, by the principle of analytic continuation (see, [33, p. 53]) follows (B). □

Note that if

$$\beta=2,\ \nu_1=\nu_2=\nu_3=\frac{1}{20},\ \mu_1=\mu_2=\mu_3=\frac{1}{5},\ \kappa=\frac{13}{150},$$

then it is clear that the inequalities (3.19) hold.

Setting $\alpha=0$ and $i_0=1$ (or $i_0=2$ and replacing β by $\beta-1$) in Theorem 3.2, we obtain the following result:

Corollary 3.1. *Let β be real constant such that $\beta\geq 2$, and $\nu_1,\nu_2,\nu_3,\mu_1,\mu_2,\mu_3$ be positive numbers satisfying (3.19), where $0\leq\kappa<1$. Then for $i_0=1$ (or $i_0=2$):*

(**A**) *The branched continued fraction*

$$\cfrac{1}{1+\sum\limits_{i_1=2}^{3}\cfrac{u_{i(1)}(\mathbf{z})}{v_{i(1)}+\sum\limits_{i_2=2-[(i_1-1)/2]}^{3-[(i_1-1)/2]}\cfrac{u_{i(2)}(\mathbf{z})}{v_{i(2)}+\ddots+\sum\limits_{i_k=2-[(i_{k-1}-1)/2]}^{3-[(i_{k-1}-1)/2]}\cfrac{u_{i(k)}(\mathbf{z})}{v_{i(k)}+\ddots}}}},$$

where for $i(1)\in\mathfrak{I}_1$

$$u_{i(1)}(\mathbf{z})=\begin{cases}-\dfrac{2}{\beta}z_1,\ \textit{if } i_1=2,\\[2mm]-\dfrac{z_2}{\beta},\ \textit{if } i_1=3,\end{cases}$$

for $i(k+1) \in \mathfrak{I}_{k+1}$, $k \geq 1$,

$$u_{i(k+1)}(\mathbf{z}) = \begin{cases} -\dfrac{2(k+1-\sum_{r=1}^{k-1}\delta_{i_r}^3)}{\beta+k-1-\sum_{r=1}^{k-1}\delta_{i_r}^1} z_1, \ \textit{if } i_k = 1, \ i_{k+1} = 2, \\ -\dfrac{z_2}{\beta+k-1-\sum_{r=1}^{k-1}\delta_{i_r}^1}, \ \textit{if } i_k = 1, \ i_{k+1} = 3, \\ \dfrac{(2(1-\beta)-k-\sum_{r=1}^{k-1}(\delta_{i_r}^3-2\delta_{i_r}^1))(k-\sum_{r=1}^{k-1}\delta_{i_r}^3+1)}{(\beta+k-1-\sum_{r=1}^{k-1}\delta_{i_r}^1)(\beta+k-\sum_{r=1}^{k-1}\delta_{i_r}^1)} z_1, \ \textit{if } i_k = 2, \ i_{k+1} = 2, \\ -\dfrac{\beta-1+\sum_{r=1}^{k-1}(\delta_{i_r}^3-\delta_{i_r}^1)}{(\beta+k-1-\sum_{r=1}^{k-1}\delta_{i_r}^1)(\beta+k-\sum_{r=1}^{k-1}\delta_{i_r}^1)} z_2, \ \textit{if } i_k = 2, \ i_{k+1} = 3, \\ \dfrac{k-\sum_{r=1}^{k-1}\delta_{i_r}^3}{2(\beta+k-1-\sum_{r=1}^{k-1}\delta_{i_r}^1)}, \ \textit{if } i_k = 3, \ i_{k+1} = 1, \\ \dfrac{k-\sum_{r=1}^{k-1}\delta_{i_r}^3}{2(\beta+k-1-\sum_{r=1}^{k-1}\delta_{i_r}^1)(c+k-\sum_{r=1}^{k-1}\delta_{i_r}^1)} z_2, \ \textit{if } i_k = 3, \ i_{k+1} = 2, \end{cases}$$

and for $i(k) \in \mathfrak{I}_k$, $k \geq 1$,

$$v_{i(k)} = 1 - \frac{k-\sum_{r=1}^{k-1}\delta_{i_r}^3}{2(\beta+k-1-\sum_{r=1}^{k-1}\delta_{i_r}^1)}\delta_{i_k}^3,$$

converges uniformly on every compact subset of (3.20) to the function $f^{(i_0)}(\mathbf{z})$ *holomorphic in (3.20).*

(**B**) *The function* $f^{(i_0)}(\mathbf{z})$ *is an analytic continuation of* $\mathrm{H}_6(1, c; \mathbf{z})$ *in the domain (3.20).*

Note that Theorem 3.2 and Corollary 3.1 are generalizations of Theorem 3.3 and Corollary 3.1 in [5], respectively.

4. Conclusions

In the paper, a new domain of analytical expansion of the ratios of Horn's confluent functions H_6 due to their branched continued fraction expansions is obtained. These expansions can be used as an efficient approximation tool for approximating special functions and solutions of differential equations represented by the Horn's confluent functions H_6. Recent studies of branched continued fractions (see, [9, 10, 15, 22]) open up good prospects for establishing new domains of analytical continuation of hypergeometric functions and conducting analysis of truncation errors and computational stability of their branched continued fraction expansions. Our further investigation will be devoted to the development of the approach proposed in [22] to the study of numerical stability for the above-mentioned expansions.

References

[1] T. Antonova, C. Cesarano, R. Dmytryshyn and S. Sharyn: *An approximation to Appell's hypergeometric function F_2 by branched continued fraction*, Dolomites Res. Notes Approx., **17** (1) (2024), 22–31.

[2] T. Antonova, R. Dmytryshyn and V. Goran: *On the analytic continuation of Lauricella-Saran hypergeometric function $F_K(a_1, a_2, b_1, b_2; a_1, b_2, c_3; \mathbf{z})$*, Mathematics, **11** (21) (2023), Article ID: 4487.

[3] T. Antonova, R. Dmytryshyn and V. Kravtsiv: *Branched continued fraction expansions of Horn's hypergeometric function H_3 ratios*, Mathematics, **9** (2) (2021), Article ID: 148.

[4] T. Antonova, R. Dmytryshyn and R. Kurka: *Approximation for the ratios of the confluent hypergeometric function $\Phi_D^{(N)}$ by the branched continued fractions*, Axioms, **11** (9) (2022), Article ID: 426.

[5] T. Antonova, R. Dmytryshyn and S. Sharyn: *Branched continued fraction representations of ratios of Horn's confluent function* H_6, Constr. Math. Anal., **6** (1) (2023), 22–37.

[6] T. M. Antonova: *On convergence of branched continued fraction expansions of Horn's hypergeometric function H_3 ratios*, Carpathian Math. Publ., **13** (3) (2021), 642–650.
[7] T. Antonova: *On structure of branched continued fractions*, Carpathian Math. Publ., **16** (2) (2024), 391–400.
[8] Z. e. a. Bentalha: *Representation of the Coulomb matrix elements by means of Appell hypergeometric function F_2*, Math. Phys. Anal. Geom., **21** (2018), Article ID: 10.
[9] D. I. Bodnar, O. S. Bodnar and I. B. Bilanyk: *A truncation error bound for branched continued fractions of the special form on subsets of angular domains*, Carpathian Math. Publ., **15** (2) (2023), 437–448.
[10] D. I. Bodnar, I. B. Bilanyk: *Two-dimensional generalization of the Thron-Jones theorem on the parabolic domains of convergence of continued fractions*, Ukr. Math. J., **74** (9) (2023), 1317–1333.
[11] D. I. Bodnar: *Branched Continued Fractions*, Naukova Dumka, Kyiv (1986). (In Russian)
[12] D. I. Bodnar: *Expansion of a ratio of hypergeometric functions of two variables in branching continued fractions*, J. Math. Sci., **64** (32) (1993), 1155–1158.
[13] D. I. Bodnar, O. S. Manzii: *Expansion of the ratio of Appel hypergeometric functions F_3 into a branching continued fraction and its limit behavior*, J. Math. Sci., **107** (1) (2001), 3550–3554.
[14] D. I. Bodnar: *Multidimensional C-fractions*, J. Math. Sci., **90** (5) (1998), 2352–2359.
[15] R. Dmytryshyn, C. Cesarano, I.-A. Lutsiv and M. Dmytryshyn: *Numerical stability of the branched continued fraction expansion of Horn's hypergeometric function H_4*, Mat. Stud., **61** (1) (2024), 51–60.
[16] R. Dmytryshyn, V. Goran: *On the analytic extension of Lauricella–Saran's hypergeometric function F_K to symmetric domains*, Symmetry, **16** (2) (2024), Article ID: 220.
[17] R. Dmytryshyn, I.-A. Lutsiv and O. Bodnar: *On the domains of convergence of the branched continued fraction expansion of ratio $H_4(a, d+1; c, d; \mathbf{z})/H4(a, d+2; c, d+1; \mathbf{z})$*, Res. Math., **31** (2) (2023), 19–26.
[18] R. Dmytryshyn, I.-A. Lutsiv and M. Dmytryshyn: *On the analytic extension of the Horn's hypergeometric function H_4*, Carpathian Math. Publ. **16** (1) (2024), 32–39.
[19] R. I. Dmytryshyn: *The multidimensional generalization of* g*-fractions and their application*, J. Comput. Appl. Math., **164–165** (2004), 265–284.
[20] H. Exton: *Multiple Hypergeometric Functions and Applications*, Halsted Press, Chichester (1976).
[21] C. F. Gauss: *Disquisitiones generales circa seriem infinitam* $1 + \frac{\alpha\beta}{1\cdot\gamma}x + \frac{\alpha(\alpha+1)\beta(\beta+1)}{1\cdot2\cdot\gamma(\gamma+1)}xx + \frac{\alpha(\alpha+1)(\alpha+2)\beta(\beta+1)(\beta+2)}{1\cdot2\cdot3\cdot\gamma(\gamma+1)(\gamma+3)}x^3 + etc$, In Commentationes Societatis Regiae Scientiarum Gottingensis Recentiores, Classis Mathematicae (1812), H. Dieterich: Gottingae, Germany, **2** (1813), 3–46.
[22] V. R. Hladun, D. I. Bodnar and R. S. Rusyn: *Convergence sets and relative stability to perturbations of a branched continued fraction with positive elements*, Carpathian Math. Publ., **16** (1) (2024), 16–31.
[23] V. R. Hladun, N. P. Hoyenko, O. S. Manzij and L. Ventyk: *On convergence of function $F_4(1, 2; 2, 2; z_1, z_2)$ expansion into a branched continued fraction*, Math. Model. Comput., **9** (3) (2022), 767–778.
[24] V. Hladun, R. Rusyn and M. Dmytryshyn: *On the analytic extension of three ratios of Horn's confluent hypergeometric function* H_7, Res. Math., **32** (1) (2024), 60–70.
[25] J. Horn: *Hypergeometrische Funktionen zweier Veränderlichen*, Math. Ann., **105** (1931), 381–407.
[26] N. Hoyenko, V. Hladun and O. Manzij: *On the infinite remains of the Nórlund branched continued fraction for Appell hypergeometric functions*, Carpathian Math. Publ., **6** (1) (2014), 11–25. (In Ukrainian)
[27] B. Kol, R. Shir: *The propagator seagull: general evaluation of a two loop diagram*, J. High Energy Phys., **2019** (2019), Article ID: 83.
[28] I. Kovalyov: *Rational generalized Stieltjes functions*, Constr. Math. Anal., **5** (3) (2022), 154–167.
[29] N. Ortner, P, Wagner: *On the singular values of the incomplete Beta function*, Constr. Math. Anal., **5** (2) (2022), 93–104.
[30] M. Pétréolle, A. D. Sokal and B. X. Zhu: *Lattice paths and branched continued fractions: An infinite sequence of generalizations of the Stieltjes-Rogers and Thron-Rogers polynomials, with coefficientwise Hankel-total positivity*, arXiv, (2020), arXiv:1807.03271v2.
[31] J. B. Seaborn: *Hypergeometric Functions and Their Applications*, Springer, New York (1991).
[32] B. V. Shabat: *Introduce to complex analysis. Part II. Functions of several variables*, American Mathematical Society, Providence (1992).
[33] V. S. Vladimirov: *Methods of the theory of functions of many complex variables*, The MIT Press, Cambridge (1966).
[34] H. S. Wall: *Analytic Theory of Continued Fractions*, D. Van Nostrand Co., New York (1948).

ROMAN DMYTRYSHYN
VASYL STEFANYK PRECARPATHIAN NATIONAL UNIVERSITY
57 SHEVCHENKO STR., 76018, IVANO-FRANKIVSK, UKRAINE
ORCID: 0000-0003-2845-0137
Email address: roman.dmytryshyn@pnu.edu.ua

Tamara Antonova
Lviv Polytechnic National University
12 Stepan Bandera Str., 79013, Lviv, Ukraine
ORCID: 0000-0002-0358-4641
Email address: tamara.m.antonova@lpnu.ua

Marta Dmytryshyn
West Ukrainian National University
11 Lvivska Str., 46009, Ternopil, Ukrain
ORCID: 0000-0002-0609-9764
Email address: m.dmytryshyn@wunu.edu.ua

CONSTRUCTIVE MATHEMATICAL ANALYSIS
7 (2024), No. SI, pp. 27-36
http://dergipark.org.tr/en/pub/cma
ISSN 2651 - 2939

Research Article

Hadamard matrices of genetic code and trigonometric functions

Dedicated to Professor Paolo Emilio Ricci, on occasion of his 80th birthday, with respect and friendship.

MATTHEW X. HE* AND SERGEY V. PETOUKHOV

ABSTRACT. Algebraic theory of coding is one of the modern fields of applications of algebra. Genetic matrices and algebraic biology have been the latest advances in further understanding of the patterns and rules of genetic code. Genetics code is encoded in combinations of the four nucleotides (A, C, G, T) found in DNA and then RNA. DNA defines the structure and function of an organism and contains complete genetic information. DNA paired bases of (A, C, G, T) form a geometric curve of double helix, define the 64 standard genetic triplets, and further degenerate 64 genetic codons into 20 amino acids. In trigonometry, four basic trigonometric functions ($\sin x, \tan x, \cos x, \cot x$) provided bases for Fourier analysis to encode signal information. In this paper, we use these 4 paired bases of trigonometric functions ($\sin x, \tan x, \cos x$, and $\cot x$) to generate 64 trigonometric triplets like 64 standard genetic code, further examine these 64 trigonometric functions and obtained 20 trigonometric triplets like 20 amino acids. This parallel shows a similarity connection between universal genetic codes and the universality of trigonometric functions. This connection may provide a bridge to further uncover patterns of genetic code. This demonstrates that matrix algebra is one of promising instruments and of adequate languages in bioinformatics and algebraic biology.

Keywords: Hadamard matrix, trigonometric functions, genetic code, algebraic biology.

2020 Mathematics Subject Classification: 15A15, 33B10, 92B05.

1. INTRODUCTION

The genetic code is encoded in combinations of the four nucleotides (A, C, G, T) found in DNA and the four nucleotides (A, C, G, U) found in RNA.The complementary pairs of the four nitrogenous bases in DNA are A-T (adenine and thymine), C-G (cytosine and guanine). The following table gives a complete list of 64 triplets (codons) with corresponding 20 amino acids with three (one) letter code and stop codons.

Table 1 shows that there are 64 triplets or codons. One can see that some amino acids are encoded by several different but related base triplets. Also three triplets (UAA, UAG, and UGA) are stop codons. No amino acids are corresponding to their code. The remaining 61 triplets represent 20 different amino acids. Petoukhov [18] showed the "Biperiodic table of genetic code" as illustrated below:

8×8 matrix table Table 2 shows a great symmetrical structure and has led to many discoveries [8, 9, 10, 11, 12]. By using three fundamental attributive mappings, the stochastic characteristic of the biperiodic table and symmetries in structure of genetic code were recently investigated in [8, 9, 10, 11, 12].

Received: 27.08.2024; Accepted: 04.10.2024; Published Online: 16.12.2024
*Corresponding author: Matthew X. He; hem@nova.edu
DOI: 10.33205/cma.1539666

TABLE 1. The universal genetic code and amino acids.

First Position	Second Position of Codon				Third Position
	U	C	A	G	
U	UUU Phe [F]	UCU Ser [S]	UAU Tyr [Y]	UGU Cys [C]	U
	UUC Phe [F]	UCC Ser [S]	UAC Tyr [Y]	UGC Cys [C]	C
	UUA Leu [L]	UCA Ser [S]	UAA Ter [end]	UGA Ter [end]	A
	UUG Leu [L]	UCG Ser [S]	UAG Ter [end]	UGG Trp [W]	G
C	CUU Leu [L]	CCU Pro [P]	CAU His [H]	CGU Arg [R]	U
	CUC Leu [L]	CCC Pro [P]	CAC His [H]	CGC Arg [R]	C
	CUA Leu [L]	CCA Pro [P]	CAA Gln [Q]	CGA Arg [R]	A
	CUG Leu [L]	CCG Pro [P]	CAG Gln [Q]	CGG Arg [R]	G
A	AUU Ile [I]	ACU Thr [T]	AAU Asn [N]	AGU Ser [S]	U
	AUC Ile [I]	ACC Thr [T]	AAC Asn [N]	AGC Ser [S]	C
	AUA Ile [I]	ACA Thr [T]	AAA Lys [K]	AGA Arg [R]	A
	AUG Met [M]	ACG Thr [T]	AAG Lys [K]	AGG Arg [R]	G
G	GUU Val [V]	GCU Ala [A]	GAU Asp [D]	GGU Gly [G]	U
	GUC Val [V]	GCC Ala [A]	GAC Asp [D]	GGC Gly [G]	C
	GUA Val [V]	GCA Ala [A]	GAA Glu [E]	GGA Gly [G]	A
	GUG Val [V]	GCG Ala [A]	GAG Glu [E]	GGG Gly [G]	G

TABLE 2. Biperiodic table of genetic code.

CCC	CCA	CAC	CAA	ACC	ACA	AAC	AAA
CCU	CCG	CAU	CAG	ACU	ACG	AAU	AAG
CUC	CUA	CGC	CGA	AUC	AUA	AGC	AGA
CUU	CUG	CGU	CGG	AUU	AUG	AGU	AGG
UCC	UCA	UAC	UAA	GCC	GCA	GAC	GAA
UCU	UCG	UAU	UAG	GCU	GCG	GAU	GAG
UUC	UUA	UGC	UGA	GUC	GUA	GGC	GGA
UUU	UUG	UGU	UGG	GUU	GUG	GGU	GGG

Genetic information is transferred by means of discrete elements: 4 letters of the genetic alphabet, 64 triplets, 20 amino acids, etc. General theory of signal processing utilizes the encoding of discrete signals by means of special mathematical matrices and spectral representations of signals to increase reliability and efficiency of information transfer [25, 1]. This paper considers classical trignometric functions of $\sin x, \cos x, \tan x$ and $\cot x$. These four functions form the complementary pairs $\sin x$ and $\cos x$, $\tan x$ and $\cot x$. In this paper, we use these 4 paired bases of trigonometric functions ($\sin x, \cos x, \tan x$, and $\cot x$) to generate 64 triplets similar to 64 standard genetic code, further examine these 64 trigonometric functions and obtained 20 trigonometric functions similar to 20 amino acids. This parallel shows a similarity connection between universal genetic codes and the universality of trigonometric functions. This connection may provide a bridge to further uncover patterns of genetic code. This deomnstrates that matrix algebra is one of promising instruments and of adequate languages in bioinformatics and algebraic biology.

2. HADAMARD MATRICES

By a definition a Hadamard matrix of dimension "n" is the $(n \times n)-$matrix $H(n)$ with elements "$+1$" and "-1". It satisfies the condition

$$H(n) * H(n)^T = n * I_n, \tag{2.1}$$

where $H(n)^T$ is the transposed matrix and $H(n)$ is the $(n * n)$-identity matrix. The Hadamard matrices of dimension 2^k are formed, for example, by the recursive formula $H\left(2^k\right) = H(2)^{(k)} = H(2) \otimes H\left(2^{k-1}\right)$ for $2 \leq k \in N$, where $\otimes$ denotes the Kronecker (or tensor) product, (k) means the Kronecker exponentiation, k and N are integers, $H(2)$ is showed in Figure 1. In this article, we will mark by black (white) color all cells in Hadamard matrices which contain the element "$+1$" (the element "-1" correspondingly).

Rows of a Hadamard matrix are mutually orthogonal. It means that every two different rows in a Hadamard matrix represent two perpendicular vectors, a scalar product of which is equal to 0. The element "-1" can be disposed in any of four positions in a Hadamard matrix $H(2)$.

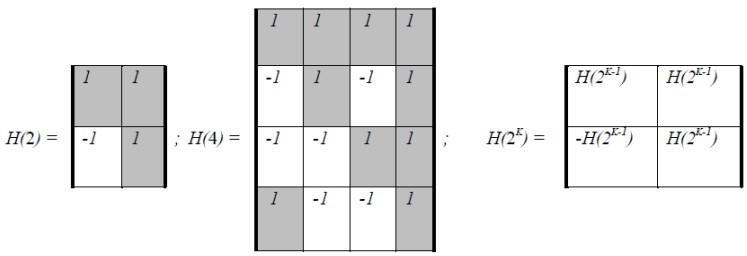

FIGURE 1. The family of Hadamard matrices $H\left(2^k\right)$ based on the Kronecker product. Matrix cells with elements "$+1$" are marked by black color.

A Kronecker product of two Hadamard matrices is a Hadamard matrix as well. A permutation of any columns or rows of a Hadamard matrix leads to a new Hadamard matrix. Hadamard matrices and their Kronecker powers are used widely in spectral methods of analysis and processing of discrete signals and in quantum computers. A transform of a vector $\bar{\mathbf{a}}$ by means of a Hadamard matrix H gives the vector $\bar{\mathbf{u}} = H * \bar{\mathbf{a}}$, which is named Hadamard spectrum. A greater analogy between Hadamard transforms and Fourier transforms exists [1]. In particular the fast Hadamard transform exists in parallel with the fast Fourier transform. The whole class of multichannel "spectrometers with Hadamard transforms" is known [27], where the principle of tape masks (or chain masks) is used, and it reminds one of the principles of a chain construction of genetic texts in DNA. Hadamard matrices are used widely in the theory of coding (for example, they are connected with Reed-Muller error correcting codes and with Hadamard codes [17]), the theory of compression of signals and images, a realization of Boolean functions by means of spectral methods, the theory of planning of multiple-factor experiments and in many other branches of mathematics.

Rows of Hadamard matrices are called Walsh functions or Hadamard functions which are used for a spectral presentation and a transfer of discrete signals [1, 3, 31]. Walsh functions can be represented in terms of product of Rademacher functions $r_n(t) = \operatorname{sign}\left(\sin 2^n \pi t\right), n = 1, 2, 3, \ldots$, which accept the two values "$+1$" and "-1" only (here "sign" is the function of a sign on argument). Sets of numerated Walsh functions (or Hadamard functions), when they

are united in square matrices, form systems depending on features of such union. Hadamard matrices are connected with Walsh-Hadamard transforms, which are the most famous among non-sinusoidal orthogonal transforms and which can be calculated by means of mathematical operations of addition and subtraction only (see more details in [1, 28, 31]). Hereinafter we will use the simplified designations of matrix elements on illustrations of Hadamard matrices: the symbol "+" or the black color of a matrix cell means the element "+1"; the the symbol "−" or the white color of a matrix cell means the element "−1". The theory of discrete signals pays special attention to quantities of changes of signs "+" and "−" along each row and each column in Hadamard matrices. These quantities are connected with an important notion of "sequency" as a generalization of notion of "frequency" [1, p. 85]. Normalized Hadamard matrices are unitary operators. They serve as one of the important instruments to create quantum computers, which utilize so called Hadamard gates (as evolution of the closed quantum system is unitary) [16].

Algebraic biology knows already examples of applications of Walsh functions (alongside with other systems of basic functions) to spectral analysis of various aspects of genetic algorithms and sequences [6, 2, 5, 14, 24, 31, 32]. The book [32] contains a review of investigations made by various authors about Walsh orthogonal functions in physiological systems of supra-cellular levels as well. We investigate whether structures of the genetic code have such direct relations with Hadamard matrices which can justify systematic applications of Walsh-Hadamard functions to spectral and other analysis of many inherited biological structures of various levels. This paper proposes relevant evidences about connections of Hadamard matrices with the genetic code in its Kronecker's matrix form of presentation.

We note that standard genetic code can be constructed by Kronecker product process from a 2×2 to 4×4 and then 8×8 matrices as illustrated in Figure 2.

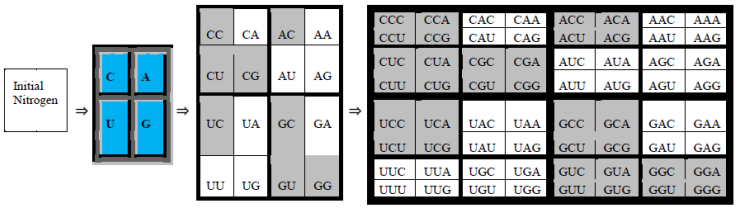

FIGURE 2. Genetic code matrices.

This 8×8 matrix represents a universal genetic code. It served as a basis for the central dogma of microbiology (DNA→RNA→Protein). The shapes of DNA motions form DNA double hélix [7]. Mathematical structure of DNA code has been viewed as the other secrets of life [26]. Four bases of trignometric functions of $\sin x, \cos x, \tan x$, and $\cot x$ may offer further insights of DNA bases of A, C, G, and T.

3. HADAMARD MATRIX OF TRIGONOMETRIC FUNCTIONS

The fundamental elements of trigonometry are $\sin x, \cos x, \tan x$, and $\cot x$. These 4 elements form the trigonometry relation base pairs $T = [\sin x, \tan x; \cos x, \cot x]$ like DNA base pairs [A, T; G, C]. This T matrix evolves from a 2×2 matrix to a 4×4 matrix and then to an 8×8 matrix as illustrated below:

TABLE 3. 2×2 matrix $T^{[1]}$.

$\sin x$	$\tan x$
$\cot x$	$\cos x$

TABLE 4. 4×4 matrix $T^{[2]}$.

$\sin x \sin x$	$\sin x \tan x$	$\tan x \sin x$	$\tan x \tan x$
$\sin x \cot x$	$\sin x \cos x$	$\tan x \cot x$	$\tan x \cos x$
$\cot x \sin x$	$\cot x \tan x$	$\cos x \sin x$	$\cos x \tan x$
$\cot x \cot x$	$\cot x \cos x$	$\cos x \cot x$	$\cos x \cos x$

TABLE 5. 8×8 matrix $T^{[3]}$.

$\sin x \sin x \sin x$	$\sin x \sin x \tan x$	$\sin x \tan x \sin x$	$\sin x \tan x \tan x$	$\tan x \sin x \sin x$	$\tan x \sin x \tan x$	$\tan x \tan x \sin x$	$\tan x \tan x \tan x$
$\sin x \sin x \cot x$	$\sin x \sin x \cos x$	$\sin x \tan x \cot x$	$\sin x \tan x \cos x$	$\tan x \sin x \cot x$	$\tan x \sin x \cos x$	$\tan x \tan x \cot x$	$\tan x \tan x \cos x$
$\sin x \cot x \sin x$	$\sin x \cot x \tan x$	$\sin x \cos x \sin x$	$\sin x \cos x \tan x$	$\tan x \cot x \sin x$	$\tan x \cot x \tan x$	$\tan x \cos x \sin x$	$\tan x \cos x \tan x$
$\sin x \cot x \cot x$	$\sin x \cot x \cos x$	$\sin x \cos x \cot x$	$\sin x \cos x \cos x$	$\tan x \cot x \cot x$	$\tan x \cot x \cos x$	$\tan x \cot x \cos x$	$\tan x \cos x \cos x$
$\cot x \sin x \sin x$	$\cot x \sin x \tan x$	$\cot x \tan x \sin x$	$\cot x \tan x \tan x$	$\cos x \sin x \sin x$	$\cos x \sin x \tan x$	$\cos x \tan x \sin x$	$\cos x \tan x \tan x$
$\cot x \sin x \cot x$	$\cot x \sin x \cos x$	$\cot x \tan x \cot x$	$\cot x \tan x \cos x$	$\cos x \sin x \cot x$	$\cos x \sin x \cos x$	$\cos x \tan x \cot x$	$\cos x \tan x \cos x$
$\cot x \cot x \sin x$	$\cot x \cot x \tan x$	$\cot x \cos x \sin x$	$\cot x \cos x \tan x$	$\cos x \cot x \sin x$	$\cos x \cot x \tan x$	$\cos x \cos x \sin x$	$\cos x \cos x \tan x$
$\cot x \cot x \cot x$	$\cot x \cot x \cos x$	$\cot x \cos x \cot x$	$\cot x \cos x \cos x$	$\cos x \cot x \cot x$	$\cos x \cot x \cos x$	$\cos x \cos x \cot x$	$\cos x \cos x \cos x$

Either addition or multiplication can be applied to each cell of these 64 triplets as illustrated below in the case of **multiplication operation**:

TABLE 6. 8×8 matrix $T^{[3]}$ with multiplication $(\times)$.

$\sin^3 x$	$\sin^2 x \tan x$	$\sin^2 x \tan x$	$\tan^2 x \sin x$	$\sin^2 x \tan x$	$\tan^2 x \sin x$	$\tan^2 x \sin x$	$\tan^3 x$
$\sin^2 x \cot x$	$\sin^2 x \cos x$	$\sin x \tan x \cot x$	$\sin x \tan x \cos x$	$\tan x \sin x \cot x$	$\tan x \sin x \cos x$	$\tan^2 x \cot x$	$\tan^2 x \cos x$
$\sin^2 x \cot x$	$\sin x \cot x \tan x$	$\sin^2 x \cos x$	$\sin x \cos x \tan x$	$\tan x \cot x \sin x$	$\tan^2 x \cot x$	$\tan x \cos x \sin x$	$\tan^2 x \cos x$
$\cot^2 x \sin x$	$\sin x \cot x \cos x$	$\sin x \cos x \cot x$	$\cos^2 x \sin x$	$\cos^2 x \tan x$	$\tan x \cot x \cos x$	$\tan x \cos x \cot x$	$\cos^2 x \tan x$
$\sin^2 x \cot x$	$\cot x \sin x \tan x$	$\cot x \tan x \sin x$	$\tan^2 x \cot x$	$\sin^2 x \cos x$	$\cos x \sin x \tan x$	$\cos x \tan x \sin x$	$\tan^2 x \cos x$
$\cot^2 x \sin x$	$\cot x \sin x \cos x$	$\cot^2 x \tan x$	$\cot x \tan x \cos x$	$\cos x \sin x \cot x$	$\cos^2 x \sin x$	$\cos x \tan x \cot x$	$\cos^2 x \tan x$
$\cot^2 x \sin x$	$\cot^2 x \tan x$	$\cot x \cos x \sin x$	$\cot x \cos x \tan x$	$\cos x \cot x \sin x$	$\cos x \cot x \tan x$	$\cos^2 x \sin x$	$\cos^2 x \tan x$
$\cot^3 x$	$\cot^2 x \cos x$	$\cot^2 x \cos x$	$\cos^2 x \cot x$	$\cot^2 x \cos x$	$\cos^2 x \cot x$	$\cos^2 x \cos x$	$\cos^3 x$

This 8×8 matrix has 64 cells. Applying addition or multiplication operation to each cell, it degenerates into 20 different cells due to the commutative nature of addition/multiplication operation like 20 amino were acids degenerated from the 64 universal genetic code. These 20 different cells and frequency distribution are illustrated below:

TABLE 7. Trigonometric functions.

Different Matrix Cell with Addition $(+)$	Different Matrix Cell with Addition $(\times)$	Frequency from 8×8 Matrix $T^{[3]}$
$3\sin x$	$\sin^3 x$	1
$3\cos x$	$\cos^3 x$	1
$3\tan x$	$\tan^3 x$	1
$3\cot x$	$\cot^3 x$	1
$2\sin x + \cos x$	$\sin^2 x \cos x$	3
$2\sin x + \tan x$	$\sin^2 x \tan x$	3
$2\sin x + \cot x$	$\sin^2 x \cot x$	3
$2\cos x + \sin x$	$\cos^2 x \sin x$	3
$2\cos x + \tan x$	$\cos^2 x \tan x$	3
$2\cos x + \cot x$	$\cos^2 x \cot x$	3
$2\tan x + \sin x$	$\tan^2 x \sin x$	3
$2\tan x + \cos x$	$\tan^2 x \cos x$	3
$2\tan x + \cot x$	$\tan^2 x \cot x$	3
$2\cot x + \sin x$	$\cot^2 x \sin x$	3
$2\cot x + \cos x$	$\cot^2 x \cos x$	3
$2\cot x + \tan x$	$\cot^2 x \tan x$	3
$\sin x + \cos x + \tan x$	$\sin x \cos x \tan x$	6
$\sin x + \cos x + \cot x$	$\sin x \cos x \cot x$	6
$\sin x + \tan x + \cot x$	$\sin x \tan x \cot x$	6
$\cos x + \tan x + \cot x$	$\cos x \tan x \cot x$	6
20	**20**	**64**

Each cell of this matrix represents an relation curve. The graphical representations of these curves (with addition/multiplication) are shown below:

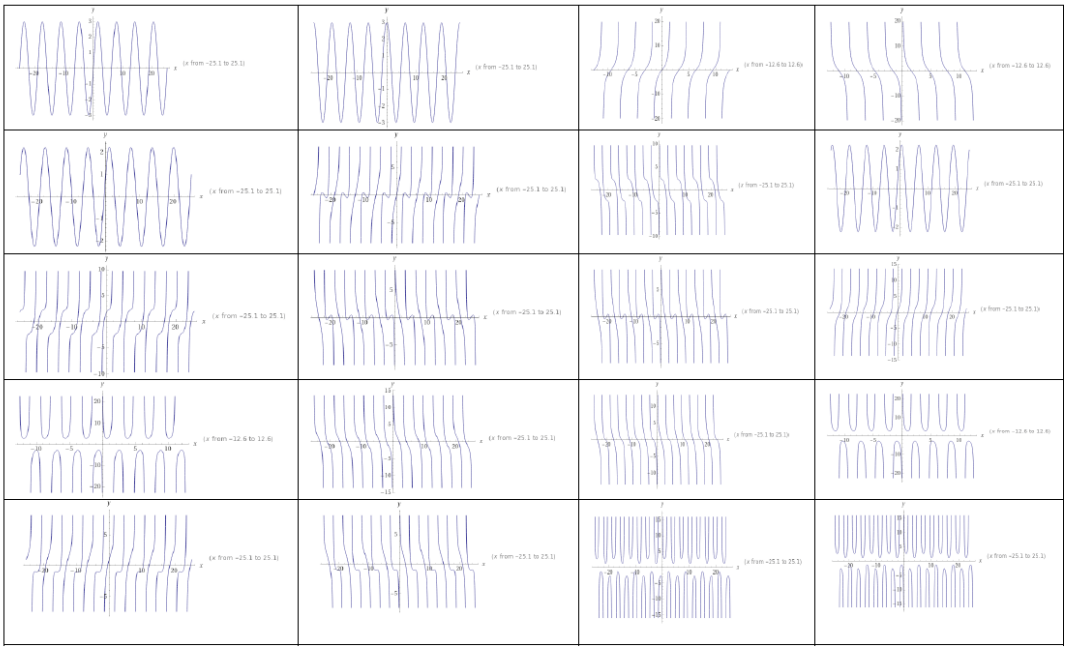

FIGURE 3. Twenty trigonometric curves with addition.

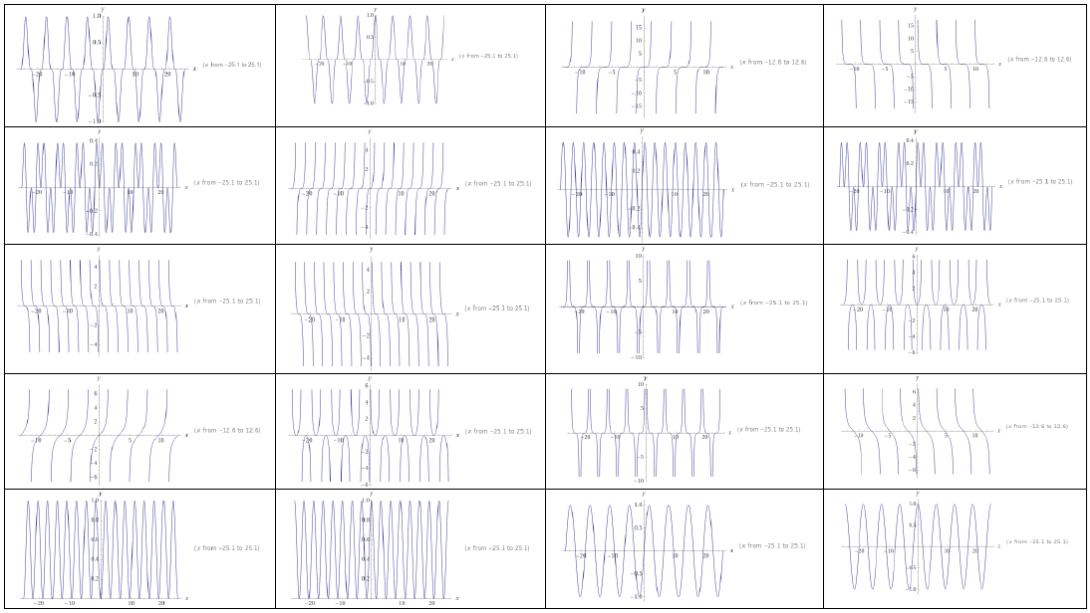

FIGURE 4. Twenty trigonometric curves with multiplication.

These curves are either bounded or unbounded. These curves may serve as basis to model the expressions of human thoughts like the 20 amino acids as the building blocks of the proteins. The orthogonal relationships of sine and cosine functions along with these building blocks of thinking frequency curves provide the basis for Fourier series that can be used to represent various thinking frequency curves. Throughout the history of humankind, trigonometry as human mind activities, has been applied in almost every area from geometry to nature [24].

4. MATRIX GENETICS AND ALGEBRAIC BIOLOGY

Matrix genetics which can be interpreted as a part of algebraic biology on the genetic systems by means of their matrix forms of presentation. One can name additionally the following main reasons for an initial choice of such form of presentation of molecular ensembles of the genetic code:

- Information is usually stored in computers in the form of matrices.
- Noise-immunity codes are constructed on the basis of matrices.
- Quantum mechanics utilizes matrix operators through the connections with matrix forms of presentation of the genetic code. The significance of matrix approach is emphasized by the fact that quantum mechanics arises in a form of matrix mechanics as formulated by W. Heisenberg.
- Complex and hypercomplex numbers, which are utilized in physics and mathematics, possess matrix forms of their presentation. The notion of number is the main notion of mathematics and mathematical natural sciences. In view of this, investigation of a possible connection of the genetic code to multi-dimensional numbers in their matrix presentations can lead to very significant results.

- Matrix analysis is one of the main investigation tools in mathematical natural sciences. The study of possible analogies between matrices, which are specific for the genetic code, and famous matrices from other branches of sciences can be heuristic and useful.
- Matrices, which are a kind of union of many components in a single whole, are subordinated to certain mathematical operations, which determine substantial connections between collectives of many components. These kinds of connections can be essential for collectives of genetic elements of different levels as well.

Matrix genetics are developed during last decade intensively [8, 9, 10, 11, 18, 19, 20, 21, 22]. Let us list some of interesting results which were obtained in these works:

- new phenomenological rules of evolution of the genetic code;
- multi-dimensional algebras for modelling and for analysing the genetic code systems;
- hidden interrelations between the golden section and parameters of genetic multiplets;
- relations between the Pythagorean musical scale and an important class of quint genetic matrices which show a molecular genetic basis with a sense of musical harmony and of aesthetics of proportions;
- cyclic algebraic principles in the structure of matrices of the genetic code;
- materials for a chronocyclic conception, which connects structures of the genetic system with chrono-medicine and a problem of an internal clock of organisms, etc.

Spectral methods of decomposition of signals on orthogonal systems of functions such as $\sin(x)$ and $\cos(x)$ have proved themselves for a long time as especially important in the theory of signals and informatics in general. Researchers of genetic informatics attempt to address to them already (see, for example, the works [13, 15] which pay attention to the importance of spectral methods in this field). But an infinite quantity of orthogonal systems of functions exists. It is difficult for researchers of molecular-genetic systems to make a choice of one of infinite number of possible orthogonal systems as an adequate one for spectral methods in the field of genetic informatics. They should make here rather a volitional choice, risking the waste of many years of work in the case of the failure of such a choice. They make this choice usually, proceeding from secondary reasons, which do not have a direct relation to genetic systems. For example, they choose the system of orthogonal harmonious functions, which is applied in the classical frequency Fourier-analysis, because this system has extensive applications in technical fields.

The results described in our article show the relation of the genetic code with the orthogonal systems of functions, which relate to Hadamard matrices, and which possess a special meaning for genetic informatics and its spectral methods. The orthogonal systems of functions connected with Hadamard matrixes are picked out by nature from the infinite set of basic systems for their deep connection with an essence of molecular-genetic coding. A consistent investigation of bioinformatics systems should be done from the viewpoint of the theory of Hadamard matrices and their applications. In particular, the comparative analysis of various genetic sequences on their Hadamard spectrums is interesting. The described results give important help in a choice of research tool from an infinite set of orthogonal systems of functions and from a set of variants of noise-immunity codes.

In the spectral analysis of genetic sequences (for example, their correlation functions), it is meaningful to spend their decomposition on orthogonal vectors-rows of Hadamard genomatrices, instead of on trigonometric functions of the frequency Fourier-analysis. Investigations of Hadamard spectrums in mathematical genetics are perspective and well-founded. Especially since some works are already known as applications of Walsh functions (alongside with other systems of basic functions) to spectral analysis of various aspects of genetic algorithms

and sequences [6, 2, 5, 14, 23, 29, 30]. The book [32, p. 416] contains a review of works about applications of Walsh orthogonal functions in some other fields of physiology.

The discovery of connections of the genetic matrices with Hadamard matrices leads to many new possible investigations using methods of symmetries, of spectral analysis, etc. One can expect that those Walsh-Hadamard functions, which are related to the described genetic Hadamard matrices, will be used effectively in the spectral analysis of genetic sequences. It seems that investigations of structural and functional principles of bio-information systems from the viewpoint of quantum computers and of unitary Hadamard operators are very promising. A comparison of orthogonal systems of Walsh-Hadamard functions in molecular-genetic structures and in genetically inherited macro-physiological systems can give new understanding to an interrelation of various levels in biological organisms. Data about the genetic Hadamard matrices together with data about algebras of the genetic code can lead to new understanding of genetic code systems, to new effective algorithms of information processing and, perhaps, to new directions in the field of quantum computers.

REFERENCES

[1] N. Ahmed, K. Rao: *Orthogonal transforms for digital signal processing*, New-York: Springer-Verlag Inc (1975).

[2] Y. A. Geadah, M. J. Corinthios: *Natural, dyadic and sequency order algorithms and processors for the Walsh-Hadamard transform*, IEEE Trans. Comput., **C-26** (1977), 25–40.

[3] A. V. Geramita: *Orthogonal designs: quadratic forms and Hadamard matrices*, London: Dekker (1979).

[4] A. Gierer, K. W. Mundry: *Production of mutants of tobacco mosaic virus by chemical alteration of its ribonucleic acid in vitro*, Nature (London), **182** (1958), 1457–1458.

[5] D. E. Goldberg: *Genetic algorithms and Walsh functions*, Complex Systems, **3** (2) (1989), 129–171.

[6] S. Forrest, M. Mitchell: *The performance of genetic algorithms on Walsh polynomials: Some anomalous results and their explanation*, In R.K.Belew and L.B.Booker, (editors), Proceedings of the Fourth International Conference on Genetic Algorithms, p.182-189, San Mateo, CA: Morgan Kaufmann.

[7] M. D. Frank-Kamenetskiy: *The most principal molecule*, Moscow: Nauka (1988).

[8] M. He: *Double helical sequences and doubly stochastic matrices*, In S. Petoukhov (Ed.).Symmetry in genetic information, Symmetry: Culture and Science, Budapest, 307–330.

[9] M. He: *Symmetry in Structure of Genetic Code*, Proceedings of the 3rd All-Russian Interdisciplinary Scientific Conference "Ethics and the Science of Future. Unity in Diversity", Feb. 12-14, Moscow, 80–85.

[10] M. He: *Genetic Code, Attributive Mappings and Stochastic Matrices*, Bulletin for Mathematical Biology, **66** (5) (2003), 965–973.

[11] M. He, S. Petoukhov: *Harmony of living nature, symmetries of genetic systems and matrix genetics*, International journal of integrative medicine, **1** (1) (2007), 41–43.

[12] M. He, S. V. Petoukhov and P. E. Ricci: *Genetic code, Hamming distance and stochastic matrices*, Bulletin for Mathematical Biology, **66** (5) (2004), 965–973.

[13] H. Kargupta: *A striking property of genetic code-like transformations*, Complex systems, **11** (2001), 57–70.

[14] M. H. Lee, M. Kaveh: *Fast Hadamard transform based on a simple matrix factorization*, IEEE Trans. Acoust., Speech, Signal Processing, **ASSSP-34** (6) (1986), 1666–1667.

[15] V. V. Lobzin, V. P. Chechetkin: *The order and correlations in genome sequences of DNK*, Achievements of physical sciences (Uspehi fizicheskih nauk), **170** (1) (2000), 57–81 (in Russian).

[16] M. A. Nielsen, I. L. Chuang: *Quantum computation and quantum information*, Cambridge: Cambridge University Press (2001).

[17] W. W. Peterson, E. J. Weldon: *Error-correcting codes*, Cambridge: MIT Press (1972).

[18] S. V. Petoukhov: *Genetic codes: binary sub-alphabets, bi-symmetric matrices and golden section; Genetic codes: numeric rules of degeneracy and the chronocyclic theory*, Symmetry:Culture and Science, **12**(1) (2001), 255–306.

[19] S. V. Petoukhov: *The rules of degeneracy and segregations in genetic codes. The chronocyclic conception and parallels with Mendel's laws*, In M.He, G.Narasimhan, S.Petoukhov (Ed.), Advances in Bioinformatics and its Applications, Series in Mathematical Biology&Medicine, Singapore: World Scientific, 8 (2005), (pp. 512-532).

[20] S. V. Petoukhov: *Hadamard matrices and quint matrices in matrix presentations of molecular genetic systems*, Symmetry: Culture and Science, **16**(3) (2005), 247–266.

[21] S. V. Petoukhov: *Matrix genetics, algebras of the genetic code, noise-immunity*, Moscow: RCD (2008) (in Russian).

[22] S. V. Peteukhov: *Matrix genetics, part 2: the degeneracy of the genetic code and the octave algebra with two quasi-real units (the "Yin-Yang octave algebra")*, 1-27, retrieved March, 08, from http://arXiv:0803.3330.
[23] A. Shiozaki: *A model of distributed type associated memory with quantized Hadamard transform*, Biol. Cybern., **38** (1) (1980), 19–22.
[24] P. E. Ricci, J. Gielis: *From Pythagoras to Fourier and From Geometry to Nature*, Athena, Publishing (2021).
[25] B. Sklar: *Digital communication. Fundamentals and applications*, New-York: Prentice Hall (2001).
[26] I. Stewart: *Life's other secret: The new mathematics of the living world*, New-York: Penguin (1999).
[27] A. Yu. Tolmachev: *New optic spectrometers*, Leningrad: Leningrad University (1976) (in Russian).
[28] A. M. Trahtman, V. A. Trahtman: *The foundations of the theory of discrete signals on finite intervals*, Moscow: Sovetskoie Radio (1975) (in Russian).
[29] M. Vose, A. Wright: *The simple genetic algorithm and the Walsh transform: Part I, theory*, Journal of Evolutionary Computation, **6** (3) (1998), 253–274.
[30] M. S. Waterman (Ed.): *Mathematical methods for DNA sequences*, Florida: CRC Press, Inc (1999).
[31] R. Yarlagadda, J. Hershey: *Hadamard matrix analysis and synthesis with applications to communications and signal/image processing*, . London: Kluwer Academic Publ (1997).
[32] L. A. Zalmanzon: *Fourier, Walsh and Haar transformations and their application in control, communication and other systems*, Moscow: Nauka (1989) (in Russian).

MATTHEW X. HE
NOVA SOUTHEASTERN UNIVERSITY
DEPARTMENT OF MATHEMATICS
FL 33314 , FT. LAUDERDALE, USA
ORCID: 0000-0002-7918-621X
Email address: hem@nova.edu

SERGEY V. PETOUKHOV
MECHANICAL ENGINEERING RESEARCH INSTITUTE OF RUSSIAN ACADEMY OF SCIENCES
MOSCOW, RUSSIA
ORCID: 0000-0001-7355-1813
Email address: spetoukhov@gmail.com

CONSTRUCTIVE MATHEMATICAL ANALYSIS
7 (2024), No. SI, pp. 37-49
http://dergipark.org.tr/en/pub/cma
ISSN 2651 - 2939

Research Article

The Jinc- function: a note on the relevant generalizations and applications

Dedicated to Professor Paolo Emilio Ricci, on occasion of his 80th birthday, with respect and friendship.

ALESSANDRO CURCIO*, GIUSEPPE DATTOLI, AND EMANUELE DI PALMA

ABSTRACT. Jinc and sinc-functions are well known special functions with important applications in Spectral theory, Fourier Optics and diffraction problems from circular apertures. The first are less widely known than the latter and should be more properly framed within the context of special functions. In this article, we present a unified point of view to the relevant generalizations, propose generalized forms and touch on application perspectives.

Keywords: Jinc-function, Fourier-optics, Quantum-diffraction.

2020 Mathematics Subject Classification: 35A01, 65L10, 65L12, 65L20, 65L70.

1. INTRODUCTION

The Jinc-function naturally emerges in problems such as the diffraction of spherical/plane waves converging on circular apertures [2, 5].
Its definition involves the use of the cylindrical Bessel of first order, according to the identity [1]:

$$Jinc(x) = \frac{J_1(x)}{\left(\frac{x}{2}\right)}$$
$$J_\alpha(x) = \left(\frac{x}{2}\right)^\alpha \sum_{r=0}^{\infty} \frac{(-1)^r \left(\frac{x}{2}\right)^{2r}}{\Gamma(r+\alpha+1)\, r!} \equiv \alpha\, th - \text{order first kind cylindrical bessel.} \tag{1.1}$$

A current definition is $Jinc(x) = J_1(x)/x$, but the adoption of the form in equation 1.1 is more convenient for the generalizations considered in this article. In the case of the Fraunhofer diffraction by circular apertures, the scattered Airy pattern distribution exhibits a Jinc-like behavior, with respect to the radial coordinate, namely [9, 3]:

$$F(x,y) = Jinc\left(\sqrt{x^2+y^2}\right). \tag{1.2}$$

In order to fix the terms of the forthcoming discussion, we start from equation (1.1) rewritten as:

$$Jinc(x) = \sum_{r=0}^{\infty} \frac{(-1)^r \left(\frac{x}{2}\right)^{2r}}{(1+r)!r!}. \tag{1.3}$$

Received: 01.07.2024; Accepted: 13.10.2024; Published Online: 16.12.2024
*Corresponding author: Alessandro Curcio; alessandro.curcio@uniroma1.it
DOI: 10.33205/cma.1507441

The umbral image [15] of (1.3) is a simple Gaussian and can be written as:

$$Jinc(x) = \hat{c}e^{-\hat{c}\left(\frac{x}{2}\right)^2}\varphi_0. \tag{1.4}$$

The operator $\hat{c}$ is the umbral operator, satisfying the property:

$$\hat{c}^\alpha \hat{c}^\beta = \hat{c}^{\alpha+\beta} \tag{1.5}$$

and characterized by the following action on the umbral vacuum φ_0:

$$\hat{c}^\alpha \varphi_0 = \frac{1}{\Gamma(\alpha+1)}. \tag{1.6}$$

Since we have reduced the Jinc-function to a Gaussian, namely an elementary transcendent function, we can evaluate the relevant integral using straightforward methods. Therefore, writing

$$\int_{-\infty}^{\infty} Jinc(x)dx = \hat{c}\int_{-\infty}^{+\infty} e^{-\hat{c}\left(\frac{x}{2}\right)^2}dx\varphi_0 \tag{1.7}$$

and, treating the umbral operator $\hat{c}$ as an ordinary constant, we find:

$$\hat{c}\int_{-\infty}^{+\infty} e^{-\hat{c}\left(\frac{x}{2}\right)^2}dx\varphi_0 = 2\hat{c}\sqrt{\frac{\pi}{\hat{c}}}\varphi_0 = 2\sqrt{\pi}\hat{c}^{\frac{1}{2}}\varphi_0. \tag{1.8}$$

The use of equations (1.5) and (1.5) yields:

$$2\sqrt{\pi}\hat{c}^{\frac{1}{2}}\varphi_0 = 2\sqrt{\pi}\frac{1}{\Gamma\left(\frac{3}{2}\right)} \tag{1.9}$$

and, therefore, we eventually find:

$$\int_{-\infty}^{\infty} Jinc(x)\,dx = 4. \tag{1.10}$$

The function in equation (1.2) realizes what is known as ***sombrero*** $(somb(x))$ function and, from the mathematical point of view, is the Fourier transform of the 2-d circle function [10, 6].
Although this aspect of the problem will be touched on in the final section, here we like to mention another important property.
Thus, we consider the integral:

$$L(x) = \int_{-\infty}^{+\infty} Jinc\left(\sqrt{x^2+y^2}\right)\,dy. \tag{1.11}$$

The use of the previously outlined umbral technique yields:

$$\begin{aligned}
&\int_{-\infty}^{+\infty} Jinc\left(\sqrt{x^2+y^2}\right)\,dy = \hat{c}e^{-\hat{c}\left(\frac{x}{2}\right)^2}\int_{-\infty}^{+\infty} e^{-\hat{c}\left(\frac{y}{2}\right)^2}dy\varphi_0\\
=&2\sqrt{\pi}\,\hat{c}^{\frac{1}{2}}e^{-\hat{c}\left(\frac{x}{2}\right)^2}\varphi_0 = 2\sqrt{\pi}\sum_{r=0}^{\infty}(-1)^r\frac{\hat{c}^{r+\frac{1}{2}}\left(\frac{x}{2}\right)^{2r}}{r!}\varphi_0\\
=&2\sqrt{\pi}\sum_{r=0}^{\infty}(-1)^r\frac{\left(\frac{x}{2}\right)^{2r}}{r!\Gamma\left(r+\frac{3}{2}\right)}.
\end{aligned} \tag{1.12}$$

In conclusion, if we apply the definition of Bessel function in equation (1.1), we end up with:

$$L(x) = 2\sqrt{\pi}\frac{J_{\frac{1}{2}}(x)}{\left(\frac{x}{2}\right)^{\frac{1}{2}}}. \tag{1.13}$$

For future convenience we also note that the use of the series definition of the Struve function [7, 11, 12],

$$\mathcal{H}_\alpha(x) = \sum_{r=0}^{\infty} \frac{(-1)^r}{\Gamma\left(r+\frac{3}{2}\right)\Gamma\left(r+\alpha+\frac{3}{2}\right)}\left(\frac{x}{2}\right)^{2r+\alpha+1} \tag{1.14}$$

allows to write:

$$\int_{-\infty}^{+\infty} Jinc\left(\sqrt{x^2+y^2}\right)\, dy = \sqrt{\frac{8\pi}{x}}\mathcal{H}_{-\frac{1}{2}}(x). \tag{1.15}$$

This introduction has been addressed to assess the formal environment in which we develop the forthcoming discussion. The paper consists of two further sections, in which we propose a generalization of the Jinc and their link with previously known families of special functions and the concluding section is dedicated to comments on the relevant applications.

2. Generalized Forms of Jinc's

The genesis of the function (1.1) is associated with the Fourier transform of the $circ(x)$ function, which is defined as:

$$circ(r) = \begin{matrix} 1, r < 1 \\ \frac{1}{2}, r = 0 \\ 0, r > 0. \end{matrix} \tag{2.16}$$

The relevant Fourier transform is:

$$\begin{aligned} \hat{F}\left(circ(r)\right) &= somb(\rho) \\ somb(\rho) &= 2\pi\, Jinc\left(2\pi\rho\right). \end{aligned} \tag{2.17}$$

The analogy with the $\mathrm{sinc}(x) = \sin(x)/x$ has a twofold origin. It is, indeed, associated with the Fourier transform of the step function, but it is also corroborated by the analogy between the first two cylindrical Bessel ($J_{0,1}(x)$) with the circular functions $(\cos(x), \sin(x))$. Postponing a deeper discussion on this point to the final section, here we note that the $jinc$ function is well behaved at the origin:

$$\lim_{x\to 0} Jinc(x) = 1 \tag{2.18}$$

If we introduce the n-th order Jinc as (with n any real):

$$Jinc_n(x) = \frac{J_n(x)}{\left(\frac{x}{2}\right)^n}, \tag{2.19}$$

we find that they are well behaved at the origin ($Jinc_n(0) = 1/\Gamma(n+1)$) and that:

$$\begin{aligned} L(x) &= 2\sqrt{\pi} Jinc_{\frac{1}{2}}(x) \\ Jinc(x) &= Jinc_1(x). \end{aligned} \tag{2.20}$$

The point we like to rise is that the function defined in eq. (2.19) are by no means new. They are indeed expressible in terms of the so called Tricomi fuctions, namely:

$$C_n(x) = \sum_{r=0}^{\infty} \frac{(-1)^r x^r}{r!\,\Gamma(n+r+1)} \tag{2.21}$$

so that:

$$Jinc_n(x) = C_n\left(-\left(\frac{x}{2}\right)^2\right). \tag{2.22}$$

Most of the properties of the Tricomi functions can be extended to the Jinc functions as it will be shown below. The 0-th order Tricomi is known as the Laguerre exponential and is an eigenfunctions of the Laguerre derivative [14], namely:

$$[\partial_x x \partial_x]\, C_0(\lambda x) = -\lambda C_0(\lambda x) \tag{2.23}$$

which, translated to the $Jinc_0(x)$, yields:

$$\frac{1}{x}\partial_x x \partial_x Jinc_0(\lambda x) = -\lambda^2 Jinc_0(\lambda x) \tag{2.24}$$

while for the associated differential equation we find:

$$\begin{aligned} &xz'' + z' + xz(x) = 0 \\ &z = Jinc_0(x). \end{aligned} \tag{2.25}$$

The n-th order Tricomi are eigenfunctions of the operator $-[\partial_x x \partial_x + n\partial_x]$, therefore the equations for the $Jinc_n(x)$ writes:

$$\begin{aligned} &xz'' + (1+n)z' + xz(x) = 0 \\ &z = Jinc_n(x). \end{aligned} \tag{2.26}$$

The previous equations exhibit a Bessel-like form and will be further discussed in the forthcoming section.
As already noted the umbral methods offer an efficient tool to work out the relevant properties. Accordingly, it is straightforward to get:

$$\begin{aligned} &Jinc_n(x) = \hat{c}^n e^{-\hat{c}\left(\frac{x}{2}\right)^2}\varphi_0 \\ &\int_{-\infty}^{\infty} Jinc_n(x)dx = \hat{c}^n \int_{-\infty}^{+\infty} e^{-\hat{c}\left(\frac{x}{2}\right)^2} dx\varphi_0 = 2\sqrt{\pi}\hat{c}^{n-\frac{1}{2}}\varphi_0 = 2\frac{\sqrt{\pi}}{\Gamma\left(n+\frac{1}{2}\right)}. \end{aligned} \tag{2.27}$$

Furthermore, the use of the following properties of the Gaussian under successive derivatives

$$\begin{aligned} &\partial_x^n e^{-ax^2} = (-1)^n H_n(2ax, -a)e^{-ax^2} \\ &H_n(x,y) = n!\sum_{r=0}^{\left\lfloor \frac{n}{2} \right\rfloor} \frac{x^{n-2r}y^r}{(n-2r)!r!} \end{aligned} \tag{2.28}$$

can be exploited to work out, in finite terms, the following higher order derivatives:

$$\partial_x^m Jinc_n(x) = (-1)^m \hat{c}^n H_m\left(\frac{\hat{c}}{2}x, -\frac{\hat{c}}{4}\right) e^{-\hat{c}\left(\frac{x}{2}\right)^2}\varphi_0. \tag{2.29}$$

The use of the second of equation (2.28) and of the first of (2.27) yields the desired result:

$$\partial_x^m Jinc_n(x) = \left(-\frac{1}{2}\right)^m \sum_{r=0}^{\left\lfloor \frac{m}{2} \right\rfloor} \frac{(-1)^r m! x^{n-r}}{(m-2r)!r!} Jinc_{m+n-r}(x). \tag{2.30}$$

It is evident that the use of the mathematical means, we have outlined, is fairly useful to explore the properties of a Bessel-like family of functions, which have been only tangentially studied within the context of the relevant applications.
In the recent past [2], the possibility of introducing more general forms of Jinc functions has been discussed within the context of studies regarding their application to focusing and diffraction of circular apertures.
The functions introduced in [2], in terms of $Jinc_n(x)$ reads:

$$\Phi inc_n(x) = -\frac{1}{2}\sum_{r=0}^{n}(-1)^r \frac{n!}{(n-r)!} Jinc_{r+1}(x) \tag{2.31}$$

In umbral terms equation (2.31) we can cast eq. (2.31) as a combination of Gaussians, namely:

$$\Phi inc_n(x) = -\frac{\hat{c}}{2}\sum_{r=0}^{n}(-1)^r \frac{n!}{(n-r)!} \hat{c}^r e^{-\hat{c}\left(\frac{x}{2}\right)^2} \varphi_0 \tag{2.32}$$

and, according to equation (2.27), we obtain:

$$\int_{-\infty}^{+\infty} \Phi inc_n(x)\, dx = -\sqrt{\pi}\sum_{r=0}^{n}(-1)^r \frac{n!}{(n-r)!}\frac{1}{\Gamma\left(r+\frac{3}{2}\right)}. \tag{2.33}$$

Furthermore, keeping the derivative of the Φinc as expressed in equation (2.32), we obtain:

$$\begin{aligned} \partial_x \Phi inc_n(x) &= -\frac{x}{4}\sum_{r=0}^{n}(-1)^r \frac{n!}{(n-r)!} \hat{c}^{r+2} e^{-\hat{c}\left(\frac{x}{2}\right)^2} \varphi_0 \\ &= \frac{x}{2(n+1)}\left[\Phi inc_{n+1}(x) + \frac{1}{2} Jinc_1(x)\right] \end{aligned} \tag{2.34}$$

the n-th derivative can be computed in finite form, using the procedure leading to equation (2.30).
Before closing this section, we discuss the evaluation of the generating function of the Φinc, in particular we consider the derivation of the following infinite sum:

$$G_\Phi(x;\xi) = \sum_{n=0}^{\infty} \frac{\xi^n}{n!} \Phi inc_n(x). \tag{2.35}$$

In order to write equation (2.35) in finite form, we note that, on account of the fact that $r! = \int_0^\infty e^{-t} t^r dt$, it is possible to set:

$$\begin{aligned} \sum_{r=0}^{n}(-1)^r \frac{n!}{(n-r)!} a^r &= \sum_{r=0}^{n}(-1)^r \frac{n!}{(n-r)!}\int_0^\infty e^{-t}\,(ta)^r\, dt \\ &= \int_0^\infty e^{-t}\,(1-ta)^n\, dt \end{aligned} \tag{2.36}$$

applying this identity to the umbral form in equation (2.32), we find:

$$-\frac{\hat{c}}{2}\sum_{r=0}^{n}(-1)^r \frac{n!}{(n-r)!} \hat{c}^r e^{-\hat{c}\left(\frac{x}{2}\right)^2} \varphi_0 = -\frac{\hat{c}}{2}\int_0^\infty (1-\hat{c}t)^n e^{-t} dt e^{-\hat{c}\left(\frac{x}{2}\right)^2} \varphi_0 \tag{2.37}$$

and, accordingly:

$$\sum_{n=0}^{\infty}\frac{\xi^n}{n!}\,\Phi inc_n(x) = -\frac{\hat{c}}{2}\sum_{n=0}^{\infty}\frac{\xi^n}{n!}\int_0^{\infty}(1-\hat{c}t)^n e^{-t}dt e^{-\hat{c}\left(\frac{x}{2}\right)^2}\varphi_0$$
$$= -\frac{\hat{c}}{2}e^{\xi}\int_0^{\infty} e^{-t}e^{-\hat{c}\left(t\xi+\left(\frac{x}{2}\right)^2\right)}dt\varphi_0. \tag{2.38}$$

Therefore, in conclusion, we find:

$$\sum_{n=0}^{\infty}\frac{\xi^n}{n!}\,\Phi inc_n(x) = -\frac{\hat{c}}{2}e^{\xi}\int_0^{\infty} e^{-t}e^{-\hat{c}\left(t\xi+\left(\frac{x}{2}\right)^2\right)}dt\varphi_0$$
$$= -\frac{e^{\xi}}{2}\int_0^{\infty} e^{-t}Jinc_1\left(2\sqrt{t\xi+\left(\frac{x}{2}\right)^2}\right)dt. \tag{2.39}$$

The same technique eventually yields:

$$\sum_{n=0}^{\infty}\frac{\xi^n}{n!}\,Jinc_n(x) = Jinc_1\left(2\sqrt{t\xi+\left(\frac{x}{2}\right)^2}\right). \tag{2.40}$$

In the forthcoming section we discuss, along with the relevant use in applications, the impact $Jinc_n(x)$ in the study of further Bessel-like functions.

3. JINC FUNCTIONS , CIRCULAR FUNCTIONS, PRODUCTS OF JINC FUNCTIONS AND DOUBLE VACUA UMBRAL IMAGES

The use of the Umbral/Algebraic methods, touched in the previous sections, has allowed a fairly significant level of freedom in defining a class of functions, "interpolating" between Bessel and circular functions [15]. A step further in this direction allows the possibility of defining the cosine function in terms of its Gaussian image [15]:

$$\cos(x) = e^{-{}_{(2,1)}\hat{d}\,x^2}\gamma_0$$
$${}_{(\alpha,\beta)}\hat{d}^k\gamma_0 = \frac{\Gamma(k+1)}{\Gamma(\alpha\,k+\beta)}. \tag{3.41}$$

The sine function can accordingly be written as:

$$\sin(x) = 2x_{(2,1)}\hat{d}e^{-{}_{2,1}\hat{d}\,x^2}\gamma_0 \tag{3.42}$$

thus, getting the following Gaussian image for the sinc:

$$\mathrm{sinc}(x) = 2_{(2,1)}\hat{d}e^{-{}_{2,1}\hat{d}\,x^2}\gamma_0. \tag{3.43}$$

The use of the paradigm underlying the derivation of the integrals discussed in the previous section, yields the well- known result:

$$\int_{-\infty}^{+\infty}\mathrm{sinc}(x)\,dx = 2_{(2,1)}\hat{d}^{\frac{1}{2}}\gamma_0 = 2\sqrt{\pi}\frac{\Gamma\left(\frac{3}{2}\right)}{\Gamma(2)} = \pi \tag{3.44}$$

which leads to further mathematical speculations, associated with the derivation of integrals like

$$\begin{aligned}\int_{-\infty}^{+\infty} \operatorname{sinc}(\alpha\, x^2+\beta\, x)\, dx &= 2_{(2,1)}\hat{d}\int_{-\infty}^{+\infty} e^{-_{(2,1)}\hat{d}\left(\alpha\, x^2+\beta\, x\right)} dx\gamma_0 \\ &= 2\sqrt{\frac{\pi}{\alpha}}{}_{(2,1)}\hat{d}^{\frac{1}{2}} e^{_{(2,1)}\hat{d}\frac{\beta^2}{4\alpha}}\gamma_0\end{aligned} \tag{3.45}$$

which has been obtained by writing in umbral form the elementary Gaussian identity:

$$\int_{-\infty}^{+\infty} e^{-(\alpha\, x^2+\beta\, x)}\, dx = \sqrt{\frac{\pi}{\alpha}} e^{\frac{\beta^2}{4\alpha}}. \tag{3.46}$$

The point to be clarified is whether the last term in equation (3.45) has any meaning from the mathematical point of view. The use of the properties of the umbral operator${}_{2,1}\hat{d}$ yields (the correctness of the result has been checked numerically):

$$\begin{aligned}&\int_{-\infty}^{+\infty} \operatorname{sinc}(\sqrt{\alpha\, x^2+\beta\, x})\, dx \\ =&2\sqrt{\frac{\pi}{\alpha}}\sum_{r=0}^{\infty}\frac{\Gamma\left(r+\frac{3}{2}\right)}{r!\Gamma(2(r+1))}\left(\frac{\beta}{2\sqrt{\alpha}}\right)^{2r} \\ =&\frac{\pi}{\sqrt{\alpha}}\, I_0\left(\frac{\beta}{2\sqrt{\alpha}}\right)\end{aligned} \tag{3.47}$$

providing a further example of integral representation of O-th order cylindrical Bessel, whose implications will be discussed in a forthcoming dedicated article.
Regarding however the case involving the Jinc functions we obtain:

$$\int_{-\infty}^{+\infty} Jinc_n(2\sqrt{\alpha\, x^2+\beta\, x})\, dx = \sqrt{\frac{\pi}{\alpha}} Jinc_{n-1/2}\left(\frac{\beta^2}{4\alpha}\right). \tag{3.48}$$

We have so far used the Gaussian as umbral image of Bessel-like functions. It is however well known that any image can be used to get an umbral representation of a given function and the choice is matter of convenience and one can choose the most suitable for the solution of a given problem. In the following we apply this statement to the derivation of integrals involving squares of Jinc functions.
To this aim we remind that the squares of Bessel functions can be written as [4]:

$$[J_n(x)]^2 = \sum_{r=0}^{\infty}\frac{(-1)^r\left(\frac{x}{2}\right)^{2r+2n}\Gamma\left[2r+1\right]}{r!^2\Gamma(r+n+1)^2}. \tag{3.49}$$

Therefore, defining

$$JJinc_n(x) = \left[\frac{J_n(x)}{\left(\frac{x}{2}\right)^n}\right]^2 \tag{3.50}$$

we find:

$$JJinc_n(x) = \sum_{r=0}^{\infty}\frac{(-1)^r\left(\frac{x}{2}\right)^{2r}\Gamma\left[2r+1\right]}{r!^2\Gamma(r+n+1)^2}. \tag{3.51}$$

The function $J_0(x)$ can usefully be exploited as umbral image $JJinc_n(x)$ and, indeed, we write:

$$\begin{aligned} JJinc_n(x) &= \hat{c}^n J_0\left(\sqrt{\hat{b}}x\right)\varphi_0 \\ \hat{b}^r\varphi_0 &= \frac{\Gamma(2\,r+1)}{\Gamma(r+1)}. \end{aligned} \tag{3.52}$$

Furthermore, by keeping into account that

$$\int_{-\infty}^{+\infty} J_0\left(\sqrt{b}x\right)\,dx = \frac{2}{\sqrt{b}} \tag{3.53}$$

we find:

$$\int_{-\infty}^{+\infty} JJinc_n\left(x\right)\,dx = 2\,\hat{b}^{n-\frac{1}{2}}\varphi_0 = 2\frac{\Gamma\left[2\,\left(n-\frac{1}{2}\right)+1\right]}{\Gamma\left(\left(n-\frac{1}{2}\right)+1\right)^2} = 2\frac{\Gamma\left(2n\right)}{\Gamma\left(n+\frac{1}{2}\right)^2}. \tag{3.54}$$

Let us now remind that:

$$\left[J_n(x)\right]^2 = \sum_{r=0}^{\infty}\frac{(-1)^r\left(\frac{x}{2}\right)^{2r+2n}\Gamma\left[2r+1\right]}{r!^2\Gamma(r+n+1)^2}. \tag{3.55}$$

A final point we touch here is the study of the following generalized Jinc function :

$$JJinc_{\mu.\nu}(x) = \frac{J_\nu(x)J_\mu(x)}{\left(\frac{x}{2}\right)^{\mu+\nu}} = \sum_{k=0}^{\infty}\frac{(-1)^k\Gamma(\nu+\mu+2k+1)}{k!\Gamma(\nu+k+1)\Gamma(\mu+k+1)\Gamma(\mu+\nu+k+1)}\left(\frac{x}{2}\right)^{2k} \tag{3.56}$$

which can be reduced to a easily manageable image by the use of the following two vacuum operators

$$\begin{aligned} \hat{b}_1^\nu &= e^{\nu\frac{\partial}{\partial z_1}} \\ \hat{b}_2^\mu &= e^{\mu\frac{\partial}{\partial z_2}} \end{aligned} \tag{3.57}$$

acting on the vacuum

$$\varphi_0 = \frac{\Gamma(z_1+z_2+1)}{\Gamma(z_1+1)\Gamma(z_2+1)} \tag{3.58}$$

in such a way that:

$$\hat{b}_1^\nu\hat{b}_2^\mu\varphi_0|_{z_1=z_2=0} = \frac{\Gamma(\mu+\nu+1)}{\Gamma(\mu+1)\Gamma(\nu+1)}. \tag{3.59}$$

If we use now the image

$$Jinc_{\mu+\nu}(x) = \frac{J_{\nu+\mu}(x)}{\left(\frac{x}{2}\right)^{\mu+\nu}}, \tag{3.60}$$

we can end up with

$$JJinc_{\mu,\nu}(x) = \hat{b}_1^\nu\hat{b}_2^\mu Jinc_{\mu+\nu}(\sqrt{\hat{b}_1\hat{b}_2}x)\varphi_0 \tag{3.61}$$

and get the relevant infinite integral as reported below:

$$\begin{aligned}&\hat{b}_1^{\nu}\hat{b}_2^{\mu}\int_{-\infty}^{+\infty} Jinc_{\mu+\nu}(\sqrt{\hat{b}_1\hat{b}_2}x)dx\,\varphi_0\\ =&2\sqrt{\pi}\frac{\hat{b}_1^{\nu}\hat{b}_2^{\mu}}{\Gamma\left(\mu+\nu+\frac{1}{2}\right)}\hat{b}_1^{-\frac{1}{2}}\hat{b}_2^{-\frac{1}{2}}\varphi_0\\ =&2\sqrt{\pi}\frac{\Gamma(\mu+\nu)}{\Gamma\left(\mu+\nu+\frac{1}{2}\right)\Gamma\left(\mu+\frac{1}{2}\right)\Gamma\left(\nu+\frac{1}{2}\right)}.\end{aligned} \tag{3.62}$$

We have so far treated the Jinc functions and the associated generalizations using a fairly abstract point of view, in the forthcoming part we will discuss physical applications where this type of functions are used. In particular we discuss the case of the Fraunhofer diffraction in two-iris wave-particle duality experiments, where integrals Involving functions of the type $Jinc_{\mu+\nu}(x)$ play a crucial role.

4. Relevant applications of Jinc functions in Physics

Jinc functions play a fundamental role in several contexts of physics, due to the fact that the Fourier transform of a uniform distribution over a finite circular area of radius r_0 coincides with the area of the circle πr_0^2 multiplied by a Jinc function:

$$\int_0^{2\pi} d\varphi \int_0^{\infty} drrcirc\left(\frac{r}{r_0}\right) e^{-ikr\cos(\phi-\varphi)} = 2\pi\int_0^{r_0} drrJ_0(kr) = \pi r_0^2 Jinc(kr_0). \tag{4.63}$$

In the following we are going to list a few topical applications of the above result.

4.1. **High-power lasers.** Chirped Pulse Amplification (CPA) is the most common technique used to amplify laser beams to unprecedented levels of peak power, up to the PetaWatt level. CPA is based on the principle that a short seed pulse is amplified while stretched, to avoid damages in the active media. A laser beam that enters the amplifier with a gaussian profile (or any other bell-shape distribution), is firstly amplified on-axis, where there is a larger amount of seeding energy. Once the saturation level is reached by the photon energy amplified on-axis, the tails of the profile start accumulating energy more efficiently than the central part of the beam. For high-gain, multi-pass amplifiers, the final effect on the seed beam, at the end of the amplification process, is that of a super-gaussian distribution, which can be assimilated to a circular uniform distribution of radius r_0. The flat-profile beam is then recompressed and focused for laser-matter interactions at high-intensity. Considering an aperture of the focusing element that is much larger than the beam diameter, the laser field at the focal plane is evaluated via the Kirchoff's integral [8]:

$$E(r, z=f) = \frac{-ike^{ik\left(f-\frac{r^2}{2f}\right)}}{f}\int_0^{\infty} dr'r'E_0(r')J_0\left(\frac{kr'r}{f}\right) = \frac{-ike^{ik\left(f-\frac{r^2}{2f}\right)}}{f}\pi r_0^2 Jinc\left(\frac{kr_0r}{f}\right), \tag{4.64}$$

where f is the focal length and $k = 2\pi/\lambda$, with λ the radiation wavelength. The flat-profile of the laser beam impinging on the focusing optics has been defined as $E_0(r) = E_0 circ(r/r_0)$. Thus, the radiation intensity in the focal point is:

$$I = \frac{c\varepsilon_0}{2}|E(r,f)|^2 = \frac{c\varepsilon_0\pi^2k^2r_0^4}{2f^2}Jinc^2\left(\frac{kr_0r}{f}\right), \tag{4.65}$$

where c is the speed of light in vacuum and ε_0 is the vacuum dielectric constant. A criterion to evaluate the beam radius R at the focal plane, is to impose that the argument of the Jinc function is equal to the first zero of the Bessel J_1, defined as $j_1 \simeq 3.832$:

$$\frac{kr_0R}{f} = j_1 \to R = \frac{j_1 f}{kr_0} = \frac{j_1 \lambda f}{2\pi r_0}. \tag{4.66}$$

Typical values are $\lambda = 1\ \mu m$, $f = 1\ m$, $r_0 = 0.1\ m$. This means that the focal spot radius is $R \simeq 6\ \mu m << r_0$. The evaluation of the total laser energy passes through an integral of the type:

$$\begin{aligned} &\int_0^\infty drrJinc^2\left(\frac{kr_0 r}{f}\right) = \int_0^\infty drrJinc^2(\kappa r) \\ &= \hat{c}_1\hat{c}_2 \int_0^\infty drre^{-\hat{c}_1\left(\frac{\kappa r}{2}\right)^2} e^{-\hat{c}_2\left(\frac{\kappa r}{2}\right)^2} \varphi_0^{(1)}\varphi_0^{(2)} = \frac{2\hat{c}_1\hat{c}_2\varphi_0^{(1)}\varphi_0^{(2)}}{\kappa^2(\hat{c}_1+\hat{c}_2)} = \frac{2}{\kappa^2} = \frac{\lambda^2 f^2}{2\pi^2 r_0^2} = \frac{2R^2}{j_1^2}, \end{aligned} \tag{4.67}$$

where we have defined the action of the entangled umbral operators $\hat{c}_1$ and $\hat{c}_2$ on the double vacuum $\varphi_0^{(1)}\varphi_0^{(2)}$ as:

$$\left(\frac{\hat{c}_1\hat{c}_2}{\hat{c}_1+\hat{c}_2}\right)^\alpha \varphi_0^{(1)}\varphi_0^{(2)} \equiv \frac{1}{\Gamma(\alpha+1)}. \tag{4.68}$$

4.2. **Diffraction limits in optics, acoustics and telecommunications.** The Jinc function is also known as Airy pattern. The first zero of the Bessel J_1 determines the limits of the so-called Airy disk. The airy patterns were discovered in the context of astronomical observation, where it was observed that the size of stars appeared different depending on the instrumentation. The aperture of the lenses of telescopes limits the resolution of these instruments. This can be seen using Eq. 4.66. Let's assume here a lens of radius r_0, used to focus a uniform wavefront of light of larger size compared to the optical aperture. If the distance between two far objects is d, then $\theta = d/f$ will be, approximately, the angular separation from the observer's point of view, placed at the focal plane. The minimum resolvable distance is then [8]:

$$\frac{d}{f} \simeq \theta \simeq 1.22\frac{\lambda}{2r_0}. \tag{4.69}$$

The same limits and description apply to focusing elements used in acoustics and to antennas exploited in telecommunications.

4.3. **Fraunhofer diffraction in two-iris wave-particle duality experiments.** Fraunhofer diffraction affects any plane wavefront passing through a circular aperture, determining a a Jinc function pattern (see Eq. 4.64). This description also underlies the two-iris experiment for the verification of the wave-particle duality. Considering a quantum particle that can pass a wall only through two different circular holes, with centers in $x = \pm a$, both of radius r_0, the wave function ψ of the particle evaluated at a certain distance R from the holes is given in the Born approximation by [8]:

$$\psi = \psi_1 + \psi_2, \psi_{1,2}(r,t) \simeq e^{i\frac{pz}{\hbar}} + f_{1,2}(\theta_x,\theta_y)\frac{e^{i\frac{pr}{\hbar}}}{r} \tag{4.70}$$

$$f_{1,2}(\theta_x,\theta_y) = -\frac{mV_0L}{\hbar^2}\int_0^{r_0} drrJ_0\left(\tilde{q}_{1,2}r\right) = -\frac{mV_0Lr_0^2}{2\hbar^2}Jinc\left(\tilde{q}_{1,2}r_0\right), \quad \tilde{q}_{1,2} \simeq \frac{p}{\hbar}\sqrt{\left(\theta_x \mp \frac{a}{R}\right)^2 + \theta_y^2},$$

where V_0 and L are empirical constants, m is the mass of the particle, $\hbar$ is the Planck constant,

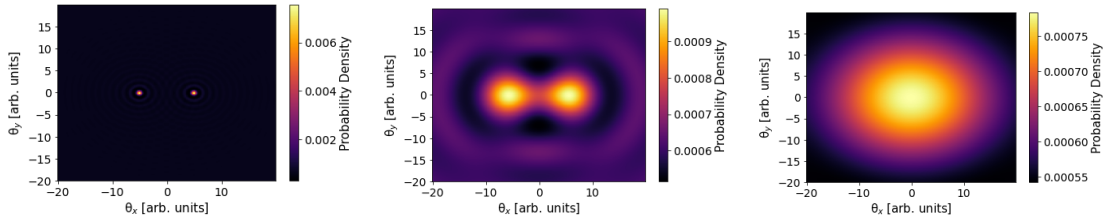

FIGURE 1. Probability density $|\psi_1+\psi_2|^2$ for the two-iris experiment. From left to right the momentum of the particle decreases.

$\theta_{x,y}$ are the observation angles in the plane of the two holes and in the perpendicular one, respectively, and p is the momentum of the particle. The partial wave functions $\psi_{1,2}$, represent the passage of the particle through one or the other iris, respectively. Fig. 1 shows the outcome of the two-iris experiment, based on the Eq. 4.70. From left to right the momentum of the particle decreases, reaching values comparable to $\hbar/r_0$, leading to diffraction phenomena. From the leftest situation, showing very localized particle states, mirroring the two entrance irises, one moves to the rightest situation where the interference is such to create a maximum probability at the center. The normalization of the wavefunction is achieved via integrals of the type:

$$
\begin{aligned}
&\int d\theta_x \int d\theta_y Jinc(\tilde{q}_1 r_0) Jinc(\tilde{q}_2 r_0) \\
=&\hat{c}_1\hat{c}_2 \int d\theta_x \int d\theta_y e^{-\hat{c}_1\left(\frac{\tilde{q}_1 r_0}{2}\right)^2} e^{-\hat{c}_2\left(\frac{\tilde{q}_2 r_0}{2}\right)^2} \varphi_0^{(1)}\varphi_0^{(2)} = \frac{4\pi\hbar^2}{p^2 r_0^2} Jinc\left(\frac{2par_0}{\hbar R}\right) \\
&\int d\theta_x \int d\theta_y Jinc^2(\tilde{q}_{1,2} r_0) \\
=&\hat{c}_1\hat{c}_2 \int d\theta_x \int d\theta_y e^{-\hat{c}_1\left(\frac{\tilde{q}_{1,2} r_0}{2}\right)^2} e^{-\hat{c}_2\left(\frac{\tilde{q}_{1,2} r_0}{2}\right)^2} \varphi_0^{(1)}\varphi_0^{(2)} = 4\pi\left(\frac{\hat{c}_1\hat{c}_2}{\hat{c}_1+\hat{c}_2}\right)\varphi_0^{(1)}\varphi_0^{(2)} = 4\pi.
\end{aligned}
\tag{4.71}
$$

It is worth noting that integrals in Eqs. 4.71 would, normally, be very difficult to solve without the umbral approach.

5. DISCUSSION

The article has provided a comprehensive treatment of Jinc functions and of the relevant applications. The mathematical tools we have employed to study the relevant properties has been the use of the indicial umbral calculus [15]. Such a choice has been dictated by mere convenience and other means can be usefully exploited. To give an example we consider the use of the generating function method.
To this aim we remind the Jacobi-Anger generating function [4]

$$
\sum_{n=-\infty}^{+\infty} t^n J_n(x) = e^{\frac{x}{2}\left(t-\frac{1}{t}\right)} \tag{5.72}
$$

which, once applied to the Jinc, yields:

$$
\sum_{n=-\infty}^{+\infty} t^n Jinc_n(x) = e^{t-\frac{x^2}{4t}}. \tag{5.73}
$$

We use this last identity to evaluate the integral:

$$Iinc_n(\alpha) = \int_{-\infty}^{+\infty} e^{-\alpha\, x^2} Jinc_n(2\sqrt{\beta\, x})dx. \tag{5.74}$$

Multiplying both sides of (5.74) by t^n and summing on the index n we find:

$$\sum_{n=-\infty}^{+\infty} t^n Iinc_n(\alpha.\beta) = e^t \int_{-\infty}^{+\infty} e^{-\alpha\, x^2 - \frac{\beta\, x}{t}} dx = \sqrt{\frac{\pi}{\alpha}} e^{t + \frac{\beta^2}{4\alpha\, t^2}}. \tag{5.75}$$

In order to get the explicit expression of the integral in (5.74) we note that:

$$\begin{aligned} e^{t+\frac{x}{t^2}} &= \sum_{n=-\infty}^{+\infty} t^n (x^n C_n^{(2)}(x)) \\ C_n^{(1.2)}(x) &= \sum_{s=0}^{\infty} \frac{x^{2s}}{(n+2s)!s!}, \end{aligned} \tag{5.76}$$

where $C_n^{(2)}(x)$ is an n-th order Bessel-Wright function [13]. Therefore expanding the rhs of (5.75) and equating the t-like power coefficients, we end up with:

$$Iinc_n(\alpha, \beta) = \sqrt{\frac{\pi}{\alpha}} C_n^{(2)}\left(\frac{\beta^2}{4\alpha}\right). \tag{5.77}$$

References

[1] E. W. Weisstein: *Jinc Function,From MathWorld–A Wolfram Web Resource*, `https://mathworld.wolfram.com/JincFunction.html`

[2] R. Bracewell, P. B. Kahn: *The Fourier transform and its applications* American Journal of Physics, **34** (8) (1966), 712.

[3] Y. Li, E. Wolf: *Three-dimensional intensity distribution near the focus in systems of different Fresnel numbers*, J. Opt. Soc. Am. A, **1** (8) (1984), 801-–808.

[4] L. C. Andrews: *Special functions for engineers and applied mathematicians*, Macmillan, USA (1985).

[5] A. E. Siegman: *Lasers*, University Science Books, USA (1986).

[6] W. i. R. Hendee, P. N. T. Wells: *The Perception of Visual Information*, Springer, New York (1997).

[7] G. E. Andrews, R. Askey and R. Roy: *Special Functions*, Cambridge University Press, Cambridge (1999).

[8] M. Born, E. Wolf: *Principles of Optics*, Cambridge University Press, Cambridge (1999).

[9] Q. Cao: *Generalized Jinc functions and their application to focusing and diffraction of circular apertures*, J. Opt. Soc. Am. A, **20** (4) (2003), 661–667.

[10] R. E. Blahut: *Theory of remote image formation*, Cambridge University Press, Cambridge (2004).

[11] K. B. Oldham, J. Myland and J. Spanier: *An Atlas of Functions: with Equator, the Atlas Function Calculator*, Springer New York (2010).

[12] D. Babusci, G. Dattoli, K. Górska and K. A. Penson: *The spherical Bessel and Struve functions and operational methods*, Appl. Math. Comput., **238** (2014), 1–6.

[13] G. Dattoli, E. Di Palma, S. Licciardi and E. Sabia: *From Circular to Bessel Functions: A Transition through the Umbral Method*, Fractal and Fractional, **1** (1) (2017), Article ID: 9.

[14] D. Babusci, G. Dattoli, S. Licciardi and E. Sabia: *Mathematical Metods for Physicists*, World Scientific, Singapur (2019).

[15] S. Licciardi, G. Dattoli: *Guide to the Umbral Calculus*. World Scientific, Singapur (2022).

Alessandro Curcio
Sapienza University
SBAI Department
Via A. Scarpa 14, 00161 Rome, Italy
ORCID: 0000-0002-1777-5078
Email address: `alessandro.curcio@uniroma1.it`

GIUSEPPE DATTOLI
ENEA FRASCATI RESEARCH CENTER
VIA ENRICO FERMI 45, 00044 ROME, ITALY
ORCID: 0000-0003-0244-8434
Email address: pinodattoli@libero.it

EMANUELE DI PALMA
ENEA FRASCATI RESEARCH CENTER
VIA ENRICO FERMI 45, 00044 ROME, ITALY
ORCID: 0000-0002-6257-622X
Email address: emanuele.dipalma@enea.it

CONSTRUCTIVE MATHEMATICAL ANALYSIS
7 (2024), No. SI, pp. 50-00
http://dergipark.org.tr/en/pub/cma
ISSN 2651 - 2939

Research Article

Analytical results for a linear hardening elasto-plastic spring investigated via a hemivariational formulation

Dedicated to Professor Paolo Emilio Ricci, on occasion of his 80th birthday, with respect and friendship.

LUCA PLACIDI*, ANIL MISRA, ABDOU KANDALAFT, MOHAMMAD MAHDI NAYEBAN, AND NURETTIN YILMAZ

ABSTRACT. We investigate the linear hardening phenomena with a method that is not standard in the literature, i.e. with a hemivariational method. As a result, we do not introduce any flow rules, and the number of assumptions is reduced to the generalized variational principle with proper definition of a new set of kinematic descriptors and, as a function of them, with a new definition of the energy functional. The variational framework guarantees the rationality of the deduction. Analytical derivation of the force displacement hysteretic loop is also derived and, finally, the dissipation energy is furnished with respect to either the final value of the dissipation energy potential or the corresponding area of the hysteretic loop.

Keywords: Linear hardening, hysteretic loop, variational method, plasticity.

2020 Mathematics Subject Classification: code, code.

1. INTRODUCTION

Linear hardening behavior of a class of materials is well-known in the literature [7, 21], and the methods for its study are also explored in many aspects [74, 75]. However, we will examine the possibility of a new approach with some advantages. The first is that the number of assumptions is reduced, and the second is that analytical solutions [18, 78] are derived with no use of flow rules. We need to say that elastic models can be derived in different ways, i.e. by assuming the balance of forces, of moments and therefore of the corresponding Partial Differential Equations (PDEs) and Boundary Conditions (BCs) as first principles or by assuming an energetic approach, where the assumptions are based on an action principle, and the PDEs and BCs are derived as a consequence of these first assumptions [8, 27, 23, 36, 32]. In standard continuum elastic models, fundamental problems arise, see e.g. [19, 49, 50], as well as the necessity of higher order gradient generalization [4, 35, 1] also for the dynamic case [33, 57]. These kinds of generalizations are particularly important for materials with microstructures, made e.g. with additive manufacturing techniques [10, 11, 12], for fiber-reinforced composites [13, 29, 46, 52, 51, 69], for composite structure [34], and for biological applications [43, 44, 76, 61, 2]. Thus, variational approaches have been developed also for microstructural materials [26, 28]. Also thermomechanical problems [53, 56, 70, 72] can be used via a purely variational procedure [40]. Besides, the use of 3D printers has improved the investigation of metamaterials, made with a microstructure that can be designed, as pantographic

Received: 13.08.2024; Accepted: 15.10.2024; Published Online: 16.12.2024
*Corresponding author: Luca Placidi; luca.placidi@uninettunouniversity.net
DOI: 10.33205/cma.1532828

materials [15, 24, 25, 31, 80], where higher order gradient is essential for the modelling. Higher order gradient elastic theories are therefore suitable for those materials with microstructure. However, the number of constitutive parameters of a general higher order gradient theory is so large that the problem of their identification is an open one, and deserves specific techniques [38, 37]. In order to avoid the identification of a large number of parameters, one can use the same strategy of Cauchy and Navier [14, 62] for homogeneous linear and isotropic materials aimed to solve the elastic granular micromechanic problem [9] for anisotropic [30] and generalized continuous [45, 47, 64, 63, 81, 82]. Granular micromechanic is ideal for concrete [16, 17] and for any materials with a strengthening microstructure [20] with the necessity to model the bond behavior [48]. Variational principles for elastic materials are therefore standard. For the dissipative case, e.g. for the viscoelastic case [41, 42, 54], the variational strategy must be generalized [71, 5, 65]. For damage [83, 77, 79] and plasticity [3] such a strategy is also different. Variational approaches in plasticity are not new [39, 22, 55]. The aim of this work is to use a hemivariational procedure, conceived for granular micromechanics [59, 58, 60, 66, 67], for a one degree of freedom problem with linear hardening behavior. Such a one degree of freedom model can be used into two ways to construct a continuum model with the same linear hardening behavior. The first is to build a discrete mode and use standard homogenization technique [68, 73]. The second is to use granular micromechanics [66]. As an outlook of this work, we will consider the fatigue problem [6].

2. Formulation of the problem

2.1. **Definition of the Action functional and plastic kinematic descriptors.**

The action A

$$A = \int_{t_{in}}^{t_{fi}} \left\{ U + W - U^{ext} \right\} dt \tag{2.1}$$

is a functional of the fundamental kinematical quantities u, λ_t, and λ_c, i.e. of the functions, $\hat{u}$, $\hat{\lambda}_t$ and $\hat{\lambda}_c$,

$$A = \mathcal{A}\left(\hat{u}, \hat{\lambda}_t, \hat{\lambda}_c\right). \tag{2.2}$$

$\hat{u}$, $\hat{\lambda}_t$, and $\hat{\lambda}_c$ are all functions of time t (where t_{in} is the initial time and t_{fi} is the final time),

$$u = \hat{u}\left(t\right), \qquad \lambda_t = \hat{\lambda}_t\left(t\right), \qquad \lambda_c = \hat{\lambda}_c\left(t\right), \qquad \forall t \in \left[t_{in}, t_{fi}\right], \tag{2.3}$$

and called, respectively, the displacement and plastic multipliers in tension and compression. The plastic multipliers are also called, respectively, the tension and the compression plastic displacement accumulations. The reason for these names is as follows. The elastic displacement u_{el}

$$u_{el} = u - u_{pl}, \tag{2.4}$$

is defined as the difference between the total displacement u and the plastic displacement u_{pl}, that is defined as the difference between the tension and compression plastic accumulations, i.e. between the two plastic multipliers, viz.,

$$u_{pl} = \lambda_t - \lambda_c. \tag{2.5}$$

The values U, W, and U^{ext} are the elastic, the dissipation, and the external energies which are functionals of the fundamental kinematical fields,

$$U = \mathcal{U}\left(\hat{u}, \hat{\lambda}_t, \hat{\lambda}_c\right), \quad W = \mathcal{W}\left(\hat{\lambda}_t, \hat{\lambda}_c\right), \quad U^{ext} = \mathcal{U}^{ext}\left(\hat{u}\right).$$

The explicit form of the functionals $\mathcal{U}$, $\mathcal{W}$ and $\mathcal{U}^{ext}$ is prescribed constitutively. Here we restrict to the condition that the dissipation energy functionals depend only upon the plastic multipliers and the external energy functional $\mathcal{U}^{ext}$ only upon the total displacement.

2.2. **Kinematic and thermodynamic restrictions of motion.**

2.2.1. *Boundary conditions in time.* An initial datum on plastic multipliers must be assumed at $t = t_{in}$,

$$\lambda_{t0} = \hat{\lambda}_t\left(t = t_{in}\right), \quad \lambda_{c0} = \hat{\lambda}_c\left(t = t_{in}\right), \tag{2.6}$$

as well as initial and final displacements,

$$u_{in} = \hat{u}\left(t_{in}\right), \qquad u_{fi} = \hat{u}\left(t_{fi}\right), \tag{2.7}$$

both at the initial $t = t_{in}$ and at the final $t = t_{fi}$ instants of times. Conditions (2.7) can also be omitted in the present quasi-static formulation but they should be taken into account when the kinetic energy in (2.1) is considered.

2.2.2. *Definition of motion.* A motion is defined as a family, fulfilling (2.6) and (2.7), of displacements $u = \hat{u}\left(t\right)$ and of plastic multipliers $\lambda_t = \hat{\lambda}_t\left(t\right)$ and $\lambda_c = \hat{\lambda}_c\left(t\right)$ for those discrete values of times defined as follows,

$$t = t_i = t_{in} + i\Delta t, \qquad \forall i = 0, \ldots, N, \qquad t_{in} = t_0, \qquad t_{fi} = t_N = t_0 + N\Delta t.$$

The increments, across two successive instants of times, of displacement

$$\Delta u = \hat{u}\left(t_{i+1}\right) - \hat{u}\left(t_i\right), \tag{2.8}$$

and of plastic multipliers

$$\Delta\lambda_t = \hat{\lambda}_t\left(t_{i+1}\right) - \hat{\lambda}_t\left(t_i\right), \quad \Delta\lambda_c = \hat{\lambda}_c\left(t_{i+1}\right) - \hat{\lambda}_c\left(t_i\right), \tag{2.9}$$

at time $t = t_i$ are defined in (2.8) and (2.9).

2.2.3. *Admissible variation of motion.* The set AM_t is that of kinematically admissible displacements $(2.3)_1$, fulfilling the (2.7) in the non-quasi-static case and any kinematical restrictions imposed by the problem, e.g., by the external constraints, at time t. The set AV_t is that of their admissible variations,

$$u \in AM_t, \qquad \delta\hat{u} \in AV_t.$$

Two examples are as follows. The first is for a force-control problem, where the displacement u is not prescribed, the variation $\delta\hat{u}$ is arbitrary, and we have

$$AV_t \equiv \mathbb{R}, \qquad \forall t \in \left(t_{in}, t_{fi}\right)$$

for any values of time, in the non-quasi-static case different from the initial and the final ones because of (2.7). The second is for a displacement-control problem, where the displacement is prescribed, and the only admissible value for its variation $\delta\hat{u}$ is zero, i.e. $\delta\hat{u} = 0$; as a consequence the set of admissible variations

$$AV_t = \{0\}, \qquad \forall t \in \left[t_{in}, t_{fi}\right]$$

is composed only of the zero value. The kinematical quantities λ_t and λ_c are assumed to be irreversible and therefore can not reduce their values. Thus, their admissible variations are all the positive numbers, viz.,

$$\delta\hat{\lambda}_t \in \mathbb{R}^+, \quad \delta\hat{\lambda}_c \in \mathbb{R}^+. \tag{2.10}$$

The kinematical irreversibility of the plastic multipliers justifies the relation of their names with the accumulation of tension and compression plastic displacements. It is worth noting

that the plastic displacement defined in (2.5) is not irreversible. The irreversibility conditions on the two plastic multipliers that are assumed in (2.10), induce the necessity to generalize the variational principle into a hemivariational principle, that is discussed in the next subsection.

2.3. **The hemivariational principle.** The variation $\delta\mathcal{A}$ of the action functional (2.2) is defined with respect to the variations of the kinematic descriptors (2.3),

$$\delta\mathcal{A} = \mathcal{A}\left(\hat{u}+\delta\hat{u}, \hat{\lambda}_t+\delta\hat{\lambda}_t, \hat{\lambda}_c+\delta\hat{\lambda}_c\right) - \mathcal{A}\left(\hat{u}, \hat{\lambda}_t, \hat{\lambda}_c\right), \tag{2.11}$$

and its increment $\Delta\mathcal{A}$ is defined with respect to those increments defined in (2.8) and (2.9), that yields

$$\Delta\mathcal{A} = \mathcal{A}\left(\hat{u}+\Delta\hat{u}, \hat{\lambda}_t+\Delta\hat{\lambda}_t, \hat{\lambda}_c+\Delta\hat{\lambda}_c\right) - \mathcal{A}\left(\hat{u}, \hat{\lambda}_t, \hat{\lambda}_c\right). \tag{2.12}$$

The hemivariational principle is formulated as follows: The following variational inequality holds

$$\Delta\mathcal{A} \leq \delta\mathcal{A} \tag{2.13}$$

for the solution (2.3) and for any admissible variations

$$\forall\delta\hat{u} \in AV_t, \qquad \forall\delta\hat{\lambda}_t \in \mathbb{R}^+, \quad \forall\delta\hat{\lambda}_c \in \mathbb{R}^+. \tag{2.14}$$

Finally, the only thermodynamic restriction, among the positive definiteness of the elastic energy functional $\mathcal{U}$, involves the dissipation energy, that is assumed to be a non-decreasing function of time,

$$\Delta\mathcal{W}\left(\hat{\lambda}_t, \hat{\lambda}_c\right) = \mathcal{W}\left(\hat{\lambda}_t+\Delta\hat{\lambda}_t, \hat{\lambda}_c+\Delta\hat{\lambda}_c\right) - \mathcal{W}\left(\hat{\lambda}_t, \hat{\lambda}_c\right) \geqslant 0. \tag{2.15}$$

3. The case of an elasto-plastic linear kinematic hardening spring

3.1. **Definition of the energy functionals.** The elastic energy is assumed to be quadratic with respect to the elastic displacement u_{el} defined in (2.4) and proportional to the elastic stiffness k_{el}, i.e.,

$$U = \mathcal{U}\left(\hat{u}, \hat{\lambda}_t, \hat{\lambda}_c\right) = \frac{1}{2}k_{el}u_{el}^2 = \frac{1}{2}k_{el}\left(u-u_{pl}\right)^2 = \frac{1}{2}k_{el}\left(u-\lambda_t+\lambda_c\right)^2. \tag{3.16}$$

The dissipation energy is defined with the following incomplete quadratic form of the irreversible plastic kinematic descriptors,

$$W = \sigma\left(\lambda_t+\lambda_c\right) + \frac{1}{2}h\left(\lambda_t-\lambda_c\right)^2, \tag{3.17}$$

where σ is the initial plastic yielding point, and h is the hardening parameter. Positive definition of the numbers of the three constitutive coefficients of the model, i.e.,

$$k_{el} > 0, \qquad \sigma > 0, \qquad h > 0,$$

guarantees not only the positive definiteness of the elastic energy functional $\mathcal{U}$ but also the assumed thermodynamic restriction (2.15).

The external energy

$$U^{ext} = \mathcal{U}^{ext}\left(\hat{u}\right) = Fu, \tag{3.18}$$

is defined with the external force F, that is a function of time,

$$F = \hat{F}\left(t\right). \tag{3.19}$$

Thus, the action functional is given by the insertion of (3.16), (3.17) and (3.18) into (2.1)

$$\mathcal{A} = \int_{t_{in}}^{t_{fi}} \left[\frac{1}{2} k_{el} \left(u - \lambda_t + \lambda_c \right)^2 + \sigma \left(\lambda_t + \lambda_c \right) + \frac{1}{2} h \left(\lambda_t - \lambda_c \right)^2 - Fu \right] dt, \tag{3.20}$$

and its variation is,

$$\begin{aligned} \delta\mathcal{A} = \int_{t_{in}}^{t_{fi}} \{ & \left[k_{el} \left(u - \lambda_t + \lambda_c \right) - F \right] \delta\hat{u} \\ & + \left[-k_{el} \left(u - \lambda_t + \lambda_c \right) + \sigma + h \left(\lambda_t - \lambda_c \right) \right] \delta\hat{\lambda}_t + \left[k_{el} \left(u - \lambda_t + \lambda_c \right) + \sigma - h \left(\lambda_t - \lambda_c \right) \right] \delta\hat{\lambda}_c \} dt, \end{aligned}$$

or, in compact form,

$$\delta\mathcal{A} = \int_{t_{in}}^{t_{fi}} \{ \left[k_{el} \left(u - u_{pl} \right) - F \right] \delta\hat{u} + \left[k_{el} + h \right] \left[\left(\lambda_t - \lambda_{ty} \right) \delta\hat{\lambda}_t + \left(\lambda_c - \lambda_{cy} \right) \delta\hat{\lambda}_c \right] \} dt, \tag{3.21}$$

where λ_{ty} and λ_{cy} are the plastic yielding tension and the plastic yielding compression, respectively, i.e.,

$$\lambda_{ty} = \lambda_c + \frac{k_{el} u - \sigma}{k_{el} + h}, \tag{3.22}$$

$$\lambda_{cy} = \lambda_t - \frac{k_{el} u + \sigma}{k_{el} + h}. \tag{3.23}$$

The increment $\Delta\mathcal{A}$ of the action functional (2.12) is derived from (3.21),

$$\Delta\mathcal{A} = \int_{t_{in}}^{t_{fi}} \{ \left[k_{el} \left(u - \lambda_t + \lambda_c \right) - F \right] \Delta\hat{u} + \left[k_{el} + h \right] \left[\left(\lambda_t - \lambda_{ty} \right) \Delta\hat{\lambda}_t + \left(\lambda_c - \lambda_{cy} \right) \Delta\hat{\lambda}_c \right] \} dt. \tag{3.24}$$

3.2. **Euler-Lagrange equations for the linear kinematic hardening spring.** The variational inequality (2.13) is valid for any admissible variations in (2.14). Let us define an arbitrary function of time $f \in AV_t$ belonging to the admissible displacement variations AV_t and calculate the variational inequality (2.13) with the following admissible variation

$$\left(\delta\hat{u}, \delta\hat{\lambda}_t, \delta\hat{\lambda}_c \right) = \left(f, \Delta\hat{\lambda}_t, \Delta\hat{\lambda}_c \right),$$

and then with another admissible variation that is similar to the previous one but with opposite f, i.e.,

$$\left(\delta\hat{u}, \delta\hat{\lambda}_t, \delta\hat{\lambda}_c \right) = \left(-f, \Delta\hat{\lambda}_t, \Delta\hat{\lambda}_c \right),$$

both for arbitrary $f \in AV_t$. Thus, we obtain two inequalities, that imply the following Euler-Lagrange equation

$$\left[k_{el} \left(u - \lambda_t + \lambda_c \right) - F \right] f = 0, \qquad \forall f \in AV_t, \tag{3.25}$$

that, by assuming no restrictions on $f \in AV_t$, we easily derive the standard form of the elasto-plastic linear kinematic hardening spring response,

$$k_{el} \left(u - \lambda_t + \lambda_c \right) = k_{el} \left(u - u_{pl} \right) = F. \tag{3.26}$$

Thus, let us calculate the variational inequality (2.13) by assuming the following particular admissible variation evaluated on the corresponding increment of the solution but doubling that of the tension plastic multiplier,

$$\left(\delta\hat{u}, \delta\hat{\lambda}_t, \delta\hat{\lambda}_c\right) = \left(\Delta\hat{u}, 2\Delta\hat{\lambda}_t, \Delta\hat{\lambda}_c\right), \tag{3.27}$$

and then with another admissible variation that is similar to the previous one but keeping the plastic multiplier in tension at zero,

$$\left(\delta\hat{u}, \delta\hat{\lambda}_t, \delta\hat{\lambda}_c\right) = \left(\Delta\hat{u}, 0, \Delta\hat{\lambda}_c\right). \tag{3.28}$$

It is easy to derive that the two obtained inequalities imply another Euler-Lagrange equation for the plastic multiplier in tension in the form of the following KKT condition,

$$\left[\lambda_t - \lambda_{ty}\right] \Delta\lambda_t = 0. \tag{3.29}$$

In the same way we obtain the other plastic KKT conditions,

$$\left[\lambda_c - \lambda_{cy}\right] \Delta\lambda_c = 0. \tag{3.30}$$

It is worth to be noted that the variations (3.27) and (3.28) are both admissible because the increments on the solutions are always non-negative as it is prescribed in (2.14). Besides, a variation $\delta\hat{\lambda}_t = -\Delta\hat{\lambda}_t$, for the same reason, is not admissible.

3.3. **A resume of the governing equations.** The governing equations of the present linear hardening spring are given by the coupling effects of eqns. (3.26), (3.29) and (3.30) with the insertion, respectively, of (2.5), (3.22) and (3.23),

$$\left[\lambda_t - \lambda_c - \frac{k_{el}u - \sigma}{k_{el} + h}\right] \Delta\lambda_t = 0, \tag{3.31}$$

$$\left[\lambda_c - \lambda_t + \frac{k_{el}u + \sigma}{k_{el} + h}\right] \Delta\lambda_c = 0, \tag{3.32}$$

$$k_{el}\left(u - \lambda_t + \lambda_c\right) = F. \tag{3.33}$$

The explicit method consists of the following numerical strategy once the displacement history u is prescribed for all the time steps. From (3.31), we evaluate λ_t by assuming the other multiplier λ_c at the previous time step. Thus, from (3.32), we evaluate λ_c by assuming the other multiplier λ_t at the previous time step. Finally, we calculate the reaction F from (3.33) and repeat this scheme for every time steps.

4. The cycling loading of the elasto-plastic linear kinematic hardening spring

4.1. **The cyclic loading history.** The cyclic loading history is prescribed in terms of the displacement field and graphically represented in Fig. 1. The period of oscillation of the imposed displacement is $4\bar{t}$. The oscillation range is $2\overline{u}$, where $\overline{u}$ is assumed to be larger than σ/k_{el}.

We investigate, in the following six subsections of Section 4, the six phases of the loading history. We will call these stages of the loading history as follows: elastic reversible one, plastic irreversible one, elastic reversible two, plastic irreversible two, elastic reversible three, and plastic irreversible three. We will later justify the names of these phases. It is worth noting here that in the elastic phases, the dissipation energy is constant with respect to time, and in the plastic phases, the dissipation energy is an increasing function with respect to time. Besides, on the one hand, during the elastic phases, an eventual unloading process follows the loading path (reversibility of the process), and on the other hand, during the plastic phases, an eventual unloading process follows another path (irreversibility of the process).

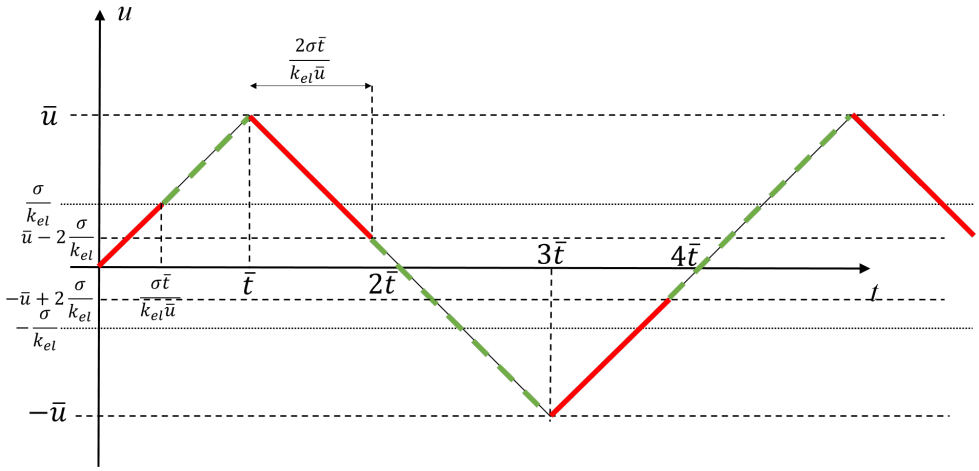

FIGURE 1. The cyclic loading history in terms of the imposed displacement u vs the time t. Each period is divided into six phases. Three phases (red-thick lines) are denoted elastic and three (green-dashed lines) are denoted plastic.

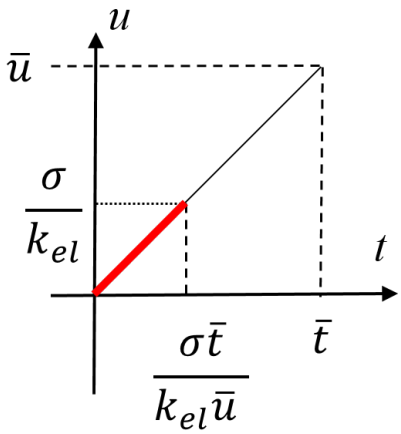

FIGURE 2. Elastic reversible phase one of the loading history in terms of the imposed displacement u vs time t.

4.2. **Elastic reversible phase one.** At the beginning of the loading history (i.e. at $t = t_{in} = 0$) the displacement and both the plastic multipliers are null

$$u\left(t = t_{in} = 0\right) = \lambda_c\left(t = t_{in} = 0\right) = \lambda_t\left(t = t_{in} = 0\right) = 0. \tag{4.34}$$

Besides, the displacement u is imposed to evolve according to Fig. 1, and it is therefore limited, in the elastic reversible phase one, to be

$$u < \frac{\sigma}{k_{el}}, \qquad \forall t \in [0, \frac{\sigma\bar{t}}{k_{el}\bar{u}}], \tag{4.35}$$

lower than the ratio σ/k_{el} as remarked in Fig. 2. Besides, the plastic yielding tension and

compression are at the beginning from (3.22), (3.23) and (4.34) both negative,

$$\lambda_{ty}\left(t=t_{in}=0\right)=-\frac{\sigma}{k_{el}+h}<0,\qquad \lambda_{cy}\left(t=t_{in}=0\right)=-\frac{\sigma}{k_{el}+h}<0. \tag{4.36}$$

On the one hand, from (3.23) and because u is an increasing function of time for this elastic reversible phase one (see Fig. 2), the plastic yielding compression λ_{cy} is a decreasing function of time, which guarantees that it is constrained to be negative for all the times in this initial part of the loading history,

$$\dot{u}>0,\quad \Rightarrow\quad \dot{\lambda}_{cy}=-\frac{k_{el}\dot{u}}{k_{el}+h}<0,\quad \Rightarrow\quad \lambda_{cy}\left(t\right)<0,\qquad \forall t\in[0,\frac{\sigma\bar{t}}{k_{el}\bar{u}}].$$

Thus, the KKT condition (3.30) is satisfied only by setting to zero the increment $\Delta\lambda_c$ and therefore also the values of the plastic multiplier in compression λ_c for all the times in this initial part of the loading history,

$$\lambda_c\left(t\right)=0,\qquad \forall t\in[0,\frac{\sigma\bar{t}}{k_{el}\bar{u}}]. \tag{4.37}$$

On the other hand, from (3.22) and because u is an increasing function of time for this elastic reversible phase one (see Fig. 2), the plastic yielding tension λ_{ty} is an increasing function of time. However, from (3.22), (4.35) and (4.37), it remains negative for all times in this initial part of the loading history,

$$\lambda_{ty}\left(t\right)=\lambda_c+\frac{k_{el}u-\sigma}{k_{el}+h}=\frac{k_{el}u-\sigma}{k_{el}+h}<0,\qquad \forall t\in[0,\frac{\sigma\bar{t}}{k_{el}\bar{u}}].$$

Thus, also the KKT condition (3.29) is satisfied only setting to zero the increment $\Delta\lambda_t$ and therefore also the values of the plastic multiplier in tension for all the times in this initial part of the loading history,

$$\lambda_t\left(t\right)=0,\qquad \forall t\in[0,\frac{\sigma\bar{t}}{k_{el}\bar{u}}]. \tag{4.38}$$

The conditions (4.37) and (4.38) justify to call elastic this first part of the loading history. The spring response has been derived from (3.26), (4.37) and (4.38), and takes the following simple form

$$k_{el}u=F,\qquad \forall t\in[0,\frac{\sigma\bar{t}}{k_{el}\bar{u}}], \tag{4.39}$$

that is also represented in Fig. 3.

If, in an arbitrary moment of this elastic reversible phase we change the sign of the loading velocity $\dot{u}$ then the KKT conditions (3.29) and (3.30) will be both satisfied with the same constant values of plastic multipliers (4.37) and (4.38) and therefore the response is the same calculated in (4.39) and graphically reported in Fig. 3. This reversible behavior justifies the name "reversible" of this phase of the loading history.

4.3. **The plastic irreversible phase one.** In the second part of the loading history, the displacement u is imposed to evolve according to Fig. 1, and it is therefore limited, in the plastic irreversible phase one, to be

$$\frac{\sigma}{k_{el}}<u<\bar{u},\qquad \forall t\in[\frac{\sigma\bar{t}}{k_{el}\bar{u}},\bar{t}]$$

as represented in Fig. 4. Thus, the yielding compression from (3.23) is still a decreasing function

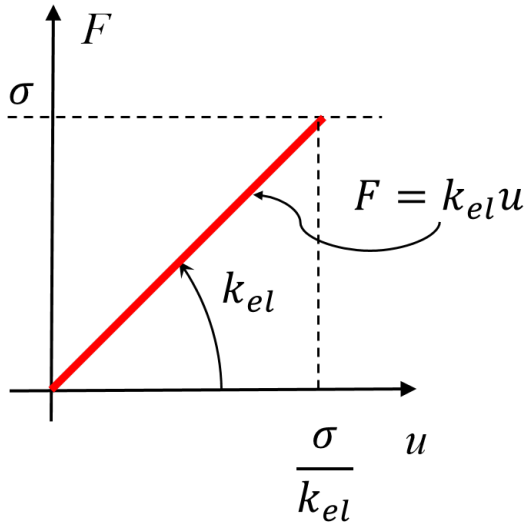

FIGURE 3. Elastic reversible phase one response. We plot the reaction force F vs the imposed displacement u.

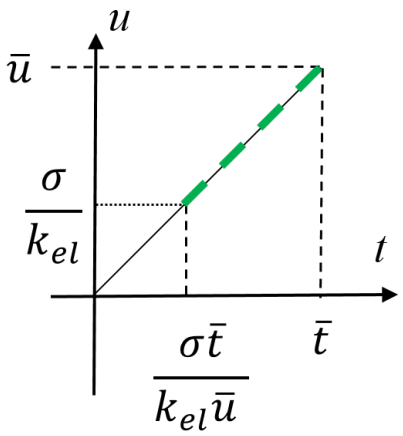

FIGURE 4. The plastic irreversible phase one of the loading history in terms of the imposed displacement u vs time t.

of time, and therefore, it remains negative,

$$\lambda_{cy} < 0, \qquad \forall t \in [\frac{\sigma \bar{t}}{k_{el}\bar{u}}, \bar{t}]. \tag{4.40}$$

This means that the KKT condition (3.30) can be satisfied only setting to zero the increment $\Delta\lambda_c$ and therefore also the values of the plastic multiplier in compression for all the times in this part of the loading history,

$$\lambda_c\,(t) = 0, \qquad \forall t \in [\frac{\sigma \bar{t}}{k_{el}\bar{u}}, \bar{t}]. \tag{4.41}$$

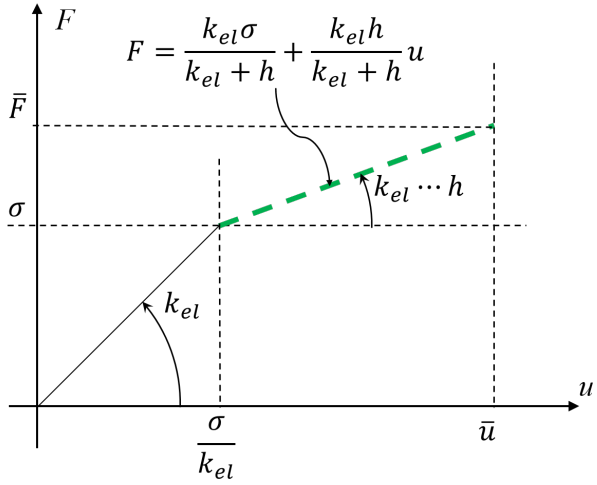

FIGURE 5. Plastic irreversible phase one response is highlighted with the green-dashed line. We plot the reaction force F vs the imposed displacement u.

Besides, the yielding tension from (3.22) and (4.41) becomes positive,

$$\lambda_{ty} = \frac{k_{el}u - \sigma}{k_{el}+h} > 0, \qquad \forall t \in [\frac{\sigma \bar{t}}{k_{el}\bar{u}}, \bar{t}],$$

and the KKT condition (3.29) is satisfied in terms of the plastic multiplier in tension by

$$\lambda_t(t) = \lambda_{ty} = \frac{k_{el}u - \sigma}{k_{el}+h}, \qquad \forall t \in [\frac{\sigma \bar{t}}{k_{el}\bar{u}}, \bar{t}]. \tag{4.42}$$

The spring response, according to (3.26), (4.41) and (4.42), is as follows,

$$k_{el}\left(u - \lambda_t(t) + \lambda_c(t)\right) = k_{el}\left(u - \frac{k_{el}u - \sigma}{k_{el}+h}\right) = F, \qquad \forall t \in [\frac{\sigma \bar{t}}{k_{el}\bar{u}}, \bar{t}],$$

that means

$$F = k_{el}\left(\frac{hu + \sigma}{k_{el}+h}\right) = \frac{k_{el}}{k_{el}+h}\sigma + \frac{hk_{el}}{k_{el}+h}u, \qquad \forall t \in [\frac{\sigma \bar{t}}{k_{el}\bar{u}}, \bar{t}], \tag{4.43}$$

that is a spring with a residual (with no displacement $u = 0$) force equal to

$$\frac{k_{el}}{k_{el}+h}\sigma,$$

and a stiffness

$$\frac{hk_{el}}{k_{el}+h}, \tag{4.44}$$

that is the equivalent stiffness of the series of two springs, one with stiffness k_{el} and one with stiffness h. The response is therefore represented in Fig. 5. As a matter of fact, from (4.42) the final value of the plastic multiplier in tension is

$$\lambda_t(t = \bar{t}) = \frac{k_{el}\bar{u} - \sigma}{k_{el}+h} > 0 \tag{4.45}$$

and from (4.43), the final value of the reaction force is

$$\hat{F}\left(t=\bar{t}\right)=\overline{F}=k_{el}\frac{\sigma+h\overline{u}}{k_{el}+h}. \tag{4.46}$$

In this phase, the dissipation energy is derived by the insertion of (4.41) and (4.42) into (3.17).

If, in an arbitrary moment $t=\widetilde{t}$ at $u=u\left(t=\widetilde{t}\right)=\widetilde{u}$ of this plastic irreversible phase, we change the sign of the loading velocity $\dot{u}$, then the KKT conditions (3.29) and (3.30) would both be satisfied setting to zero the increments $\Delta\lambda_t$ and $\Delta\lambda_c$, and therefore, the value of the plastic multiplier in compression would be still the same of that already calculated in (4.41)

$$\lambda_c\left(t\right)=\widetilde{\lambda}_c=0, \qquad \forall t>\widetilde{t},$$

and that in tension would be from (4.42)

$$\lambda_t\left(t\right)=\widetilde{\lambda}_t=\frac{k_{el}\widetilde{u}-\sigma}{k_{el}+h}, \qquad \forall t>\widetilde{t},$$

and therefore the response would be

$$k_{el}\left(u-\widetilde{\lambda}_t+\widetilde{\lambda}_c\right)=k_{el}\left(u-\frac{k_{el}\widetilde{u}-\sigma}{k_{el}+h}\right)=F, \qquad \forall t>\widetilde{t},$$

that is different from that calculated in (4.43). In particular, the tangent stiffness would be k_{el} and not the series reported in (4.44). This irreversible behavior justifies the name "irreversible" of this phase of the loading history.

4.4. **The elastic reversible phase two.** In the third part of the loading history, the displacement u is imposed to evolve according to Fig. 1. Thus, it changes the sign of its time derivative $\dot{u}$, and therefore, the spring is in an unloading phase. Besides, in this elastic reversible phase two, it is limited to be

$$\overline{\bar{u}}=\bar{u}-2\frac{\sigma}{k_{el}}<u<\bar{u}, \qquad \forall t\in[\bar{t},\bar{t}+2\frac{\sigma\bar{t}}{k_{el}\bar{u}}], \tag{4.47}$$

and it is graphically represented in Fig. 6. Thus, the yielding tension is from (3.22) a decreasing function of time, and therefore, it is always lower than the final value $\lambda_t\left(t=\bar{t}\right)$ of the plastic multiplier in tension calculated in (4.45), that is the last one taken during the previous plastic irreversible one part of the loading history,

$$\lambda_{ty}<\lambda_t\left(t=\bar{t}\right)=\frac{k_{el}\bar{u}-\sigma}{k_{el}+h}, \qquad \forall t\in[\bar{t},\bar{t}+2\frac{\sigma\bar{t}}{k_{el}\bar{u}}]. \tag{4.48}$$

The KKT condition (3.29) is satisfied only setting to zero the increment $\Delta\lambda_t$, and therefore, also keeping constant the values of the plastic multiplier in tension for all the times in this part of the loading history,

$$\lambda_t\left(t\right)=\frac{k_{el}\bar{u}-\sigma}{k_{el}+h}, \qquad \forall t\in[\bar{t},\bar{t}+2\frac{\sigma\bar{t}}{k_{el}\bar{u}}]. \tag{4.49}$$

Besides, the yielding compression is from (3.23) an increasing function of time,

$$\lambda_{cy}=\frac{k_{el}\bar{u}-\sigma}{k_{el}+h}-\frac{k_{el}u+\sigma}{k_{el}+h}=\frac{k_{el}\left(\bar{u}-u\right)-2\sigma}{k_{el}+h}<0, \qquad \forall t\in[\bar{t},\bar{t}+2\frac{\sigma\bar{t}}{k_{el}\bar{u}}], \tag{4.50}$$

but it remains negative in the prescribed range (4.47) of the present third phase of the loading history so that we still have that the KKT condition (3.30) can be satisfied only by setting to

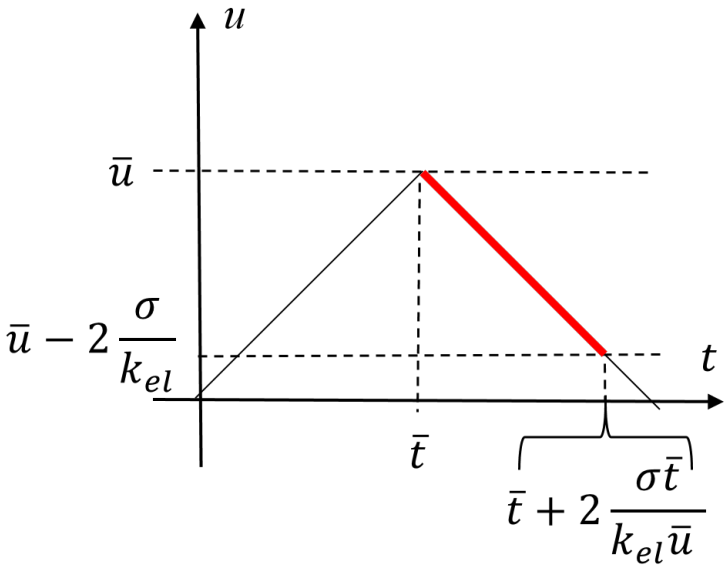

FIGURE 6. The elastic reversible phase two of the loading history in terms of the imposed displacement u vs time t.

zero the increment $\Delta\lambda_c$, and therefore, also the values of the plastic multiplier in compression for all the times in this part of the loading history,

$$\lambda_c(t) = 0, \qquad \forall t \in [\bar{t}, \bar{t} + 2\frac{\sigma\bar{t}}{k_{el}\bar{u}}]. \tag{4.51}$$

The spring response is, according to (3.26), (4.49) and (4.51), as follows,

$$k_{el}\left(u - \lambda_t(t) + \lambda_c(t)\right) = k_{el}\left(u - \frac{k_{el}\bar{u} - \sigma}{k_{el} + h}\right) = F = \hat{F}(t), \qquad \forall t \in [\bar{t}, \bar{t} + 2\frac{\sigma\bar{t}}{k_{el}\bar{u}}], \tag{4.52}$$

that is a spring with a residual (with no displacement $u = 0$) force equal to

$$k_{el}\left(\frac{\sigma - k_{el}\bar{u}}{k_{el} + h}\right),$$

and the same initial elastic stiffness

$$k_{el}.$$

The two plastic multipliers do not change their values, and this justifies calling elastic this part of the loading history. The response is therefore represented according to Fig. 7. As a matter of fact the final value of the reaction force is from (4.52)

$$F = \hat{F}\left(t = \bar{t} + 2\frac{\sigma\bar{t}}{k_{el}\bar{u}}\right) = \overline{\overline{F}} = \overline{F} - 2\sigma.$$

If, in an arbitrary moment of this elastic reversible phase, we change the sign of the loading velocity $\dot{u}$, then the KKT conditions (3.29) and (3.30) will be both satisfied with the same constant values of plastic multipliers (4.49) and (4.51), and therefore, the response is the same as calculated in (4.52) and graphically reported in Fig. 7. This reversible behavior justifies the name "reversible" for this phase of the loading history.

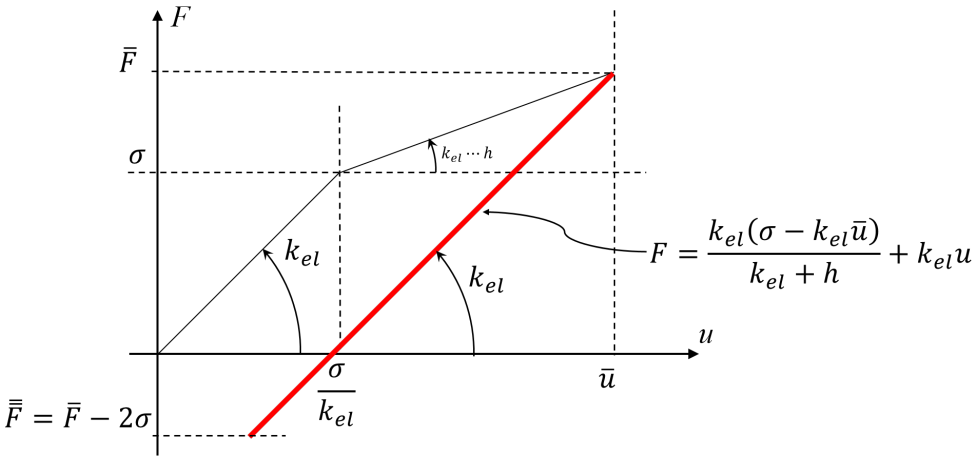

FIGURE 7. Elastic reversible phase two response is highlighted with the red-thick line. We plot the reaction force F vs the imposed displacement u.

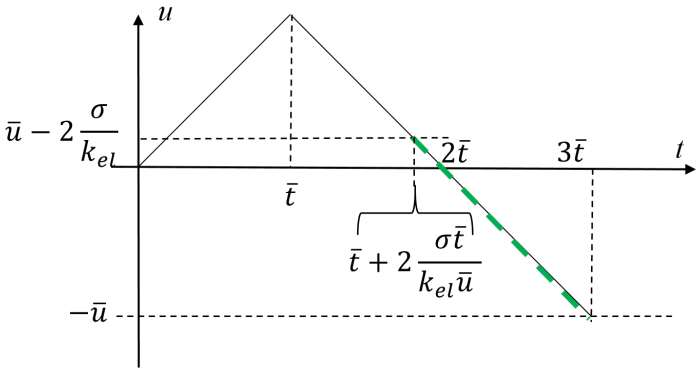

FIGURE 8. The plastic irreversible phase two of the loading history in terms of the imposed displacement u vs time t.

4.5. **The plastic irreversible phase two.** In the fourth part of loading history, the displacement u is imposed to evolve according to Fig. 1. Besides, in this plastic irreversible phase two, the spring is still in an unloading phase and it is limited to be

$$-\bar{u} < u < \bar{u} - 2\frac{\sigma}{k_{el}}, \qquad \forall t \in [\bar{t} + 2\frac{\sigma\bar{t}}{k_{el}\bar{u}}, 3\bar{t}], \tag{4.53}$$

and it is graphically represented in Fig. 8.

The yielding tension is from (3.22) again a decreasing function of time (because the displacement u is a decreasing function of time), and therefore, it continues to be always lower than the value (that was constant in the previous stage) of the plastic multiplier λ_t in (4.49),

$$\lambda_{ty} < \lambda_t\left(t = \bar{t} + 2\frac{\sigma\bar{t}}{k_{el}\bar{u}}\right) = \frac{k_{el}\bar{u} - \sigma}{k_{el} + h}, \qquad \forall t \in [\bar{t} + 2k_{el}\bar{u}, 3\bar{t}]. \tag{4.54}$$

Thus, the KKT condition is satisfied only setting to zero the increment $\Delta\lambda_t$, and therefore also the values of the plastic multiplier in tension for all the times in this part of the loading history,

$$\lambda_t(t) = \frac{k_{el}\bar{u} - \sigma}{k_{el} + h}, \qquad \forall t \in [\bar{t} + 2\frac{\sigma\bar{t}}{k_{el}\bar{u}}, 3\bar{t}]. \tag{4.55}$$

Besides, the yielding compression is from (3.23) an increasing function of time (because the displacement u is a decreasing function of time),

$$\lambda_{cy}(t) = \frac{k_{el}\bar{u} - \sigma}{k_{el} + h} - \frac{k_{el}u + \sigma}{k_{el} + h} = \frac{k_{el}(\bar{u} - u) - 2\sigma}{k_{el} + h} > \lambda_c\left(\bar{t} + 2\frac{\sigma\bar{t}}{k_{el}\bar{u}}\right) = 0, \qquad \forall t \in [\bar{t} + 2\frac{\sigma\bar{t}}{k_{el}\bar{u}}, 3\bar{t}], \tag{4.56}$$

but now it is positive (and therefore because of (4.51) greater than the plastic multiplier in compression in the previous stage) in the prescribed range (4.53) of the fourth part of the loading history so that the KKT condition condition (3.30) is satisfied by,

$$\lambda_c(t) = \lambda_{cy}(t) = \frac{k_{el}(\bar{u} - u) - 2\sigma}{k_{el} + h}, \qquad \forall t \in [\bar{t} + 2\frac{\sigma\bar{t}}{k_{el}\bar{u}}, 3\bar{t}]. \tag{4.57}$$

The spring response is, according to (3.26), (4.55) and (4.57), as follows,

$$k_{el}(u - \lambda_t(t) + \lambda_c(t)) = k_{el}\left(u - \frac{k_{el}\bar{u} - \sigma}{k_{el} + h} + \frac{k_{el}(\bar{u} - u) - 2\sigma}{k_{el} + h}\right) = F,$$

that means

$$\frac{k_{el}h}{k_{el} + h}u - k_{el}\frac{\sigma}{k_{el} + h} = \hat{F}(t), \qquad \forall t \in [\bar{t} + 2\frac{\sigma\bar{t}}{k_{el}\bar{u}}, 3\bar{t}], \tag{4.58}$$

that is a spring with a residual (with no displacement $u = 0$) force equal to

$$-k_{el}\frac{\sigma}{k_{el} + h},$$

and a stiffness (4.44), that is the equivalent stiffness of the series of two springs, one with stiffness k_{el} and one with stiffness h. The response is therefore represented according to Fig. 9.

As a matter of facts, from (4.57) the final value of plastic multiplier in compression is

$$\lambda_c(t = 3\bar{t}) = \frac{k_{el}(\bar{u} - u(t = 3\bar{t})) - 2\sigma}{k_{el} + h} = \frac{k_{el}(\bar{u} - (-\bar{u})) - 2\sigma}{k_{el} + h} = 2\frac{k_{el}\bar{u} - \sigma}{k_{el} + h}, \tag{4.59}$$

and from (4.58) the final value of the reaction response is

$$\hat{F}(t = 3\bar{t}) = \frac{k_{el}h}{k_{el} + h}u(t = 3\bar{t}) - k_{el}\frac{\sigma}{k_{el} + h} = -\frac{k_{el}h}{k_{el} + h}\bar{u} - k_{el}\frac{\sigma}{k_{el} + h} = -k_{el}\frac{\sigma + h\bar{u}}{k_{el} + h} = -\overline{F}.$$

If, in an arbitrary moment $t = \widetilde{t}$ at $u = u(t = \widetilde{t}) = \widetilde{u}$ of this plastic irreversible phase, we change the sign of the loading velocity $\dot{u}$ then the KKT conditions (3.29) and (3.30) would both be satisfied setting to zero the increments $\Delta\lambda_t$ and $\Delta\lambda_c$, and therefore, the value of the plastic multiplier in tension would be still the same of that already calculated in (4.55)

$$\lambda_t(t) = \widetilde{\lambda}_t = \frac{k_{el}\bar{u} - \sigma}{k_{el} + h}, \qquad \forall t > \widetilde{t},$$

and that in compression would be from (4.57)

$$\lambda_c(t) = \widetilde{\lambda}_c = \frac{k_{el}(\bar{u} - \widetilde{u}) - 2\sigma}{k_{el} + h}, \qquad \forall t > \widetilde{t},$$

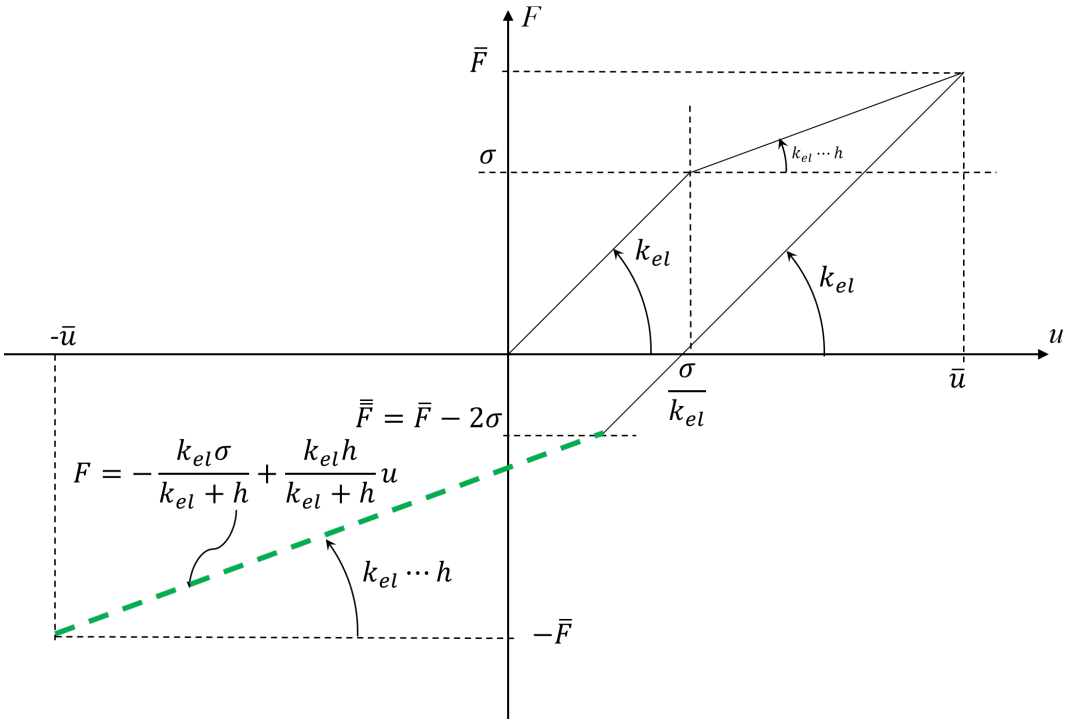

FIGURE 9. Plastic irreversible phase two response is highlighted with the green-dashed line. We plot the reaction force F vs the imposed displacement u.

and therefore, the response would be

$$k_{el}\left(u-\widetilde{\lambda}_t+\widetilde{\lambda}_c\right)=k_{el}\left(u-\frac{k_{el}\widetilde{u}-\sigma}{k_{el}+h}+\frac{k_{el}\left(\bar{u}-\widetilde{u}\right)-2\sigma}{k_{el}+h}\right)=k_{el}\left(u-\frac{2k_{el}\widetilde{u}-k_{el}\bar{u}+\sigma}{k_{el}+h}\right)$$
$$=F,\qquad \forall t>\widetilde{t},$$

that is different from that calculated in (4.58). In particular the tangent stiffness would be k_{el} and not the series reported in (4.44). This irreversible behavior justifies the name "irreversible" of this phase of the loading history.

4.6. **The elastic reversible phase three.** In the fifth part of the loading history, the displacement u is imposed to evolve according to Fig. 1. Thus, it changes the sign of its time derivative $\dot{u}$ and therefore the spring is again in a loading phase. Besides, in this elastic reversible phase three it is limited to be

$$-\bar{u}<u<-\bar{u}+2\frac{\sigma}{k_{el}},\qquad \forall t\in[3\bar{t},3\bar{t}+2\frac{\sigma\bar{t}}{k_{el}\bar{u}}], \tag{4.60}$$

and it is graphically represented in Fig. 10. The yielding compression is from (3.23) a decreasing function of time (because the displacement u is an increasing function of time) so that it remains

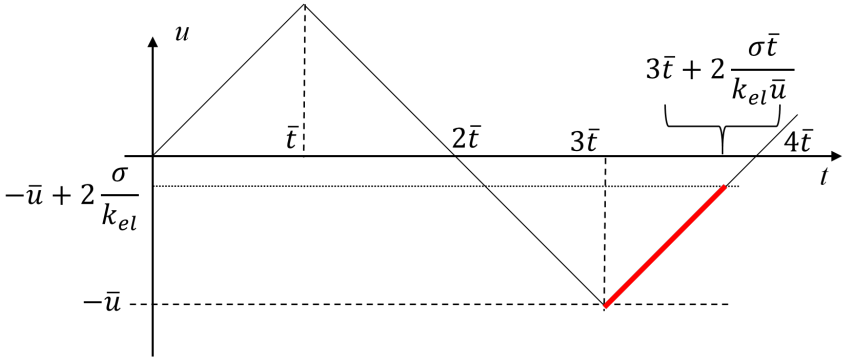

FIGURE 10. The elastic reversible phase three of the loading history in terms of the imposed displacement u vs time t.

always lower than the last value (4.59) of the previous stage of the loading history,

$$\lambda_{cy}(t) < \lambda_{cy}(t=3\bar{t}) = \lambda_c(t=3\bar{t}) = 2\frac{k_{el}\bar{u}-\sigma}{k_{el}+h}, \qquad \forall t \in [3\bar{t}, 3\bar{t}+2\frac{\sigma\bar{t}}{k_{el}\bar{u}}].$$

Thus, the KKT condition (3.30) for the plastic multiplier in compression is satisfied only setting to zero the increment $\Delta\lambda_c$ and therefore it yields also constant the function of the plastic multiplier in compression for all the times in this part of the loading history,

$$\lambda_c(t) = 2\frac{k_{el}\bar{u}-\sigma}{k_{el}+h}, \qquad \forall t \in [3\bar{t}, 3\bar{t}+2\frac{\sigma\bar{t}}{k_{el}\bar{u}}]. \tag{4.61}$$

Besides, the yielding tension (because the displacement u is an increasing function of time) is an increasing function of time but still lower than the previous value $\lambda_t(t=3\bar{t})$ of the plastic multiplier in tension

$$\lambda_{ty} = 2\frac{k_{el}\bar{u}-\sigma}{k_{el}+h} + \frac{k_{el}u-\sigma}{k_{el}+h} < \lambda_t(t=3\bar{t}) = \frac{k_{el}\bar{u}-\sigma}{k_{el}+h}, \qquad \forall t \in [3\bar{t}, 3\bar{t}+2\frac{\sigma\bar{t}}{k_{el}\bar{u}}].$$

Thus, the KKT condition (3.29) for the plastic multiplier in tension is satisfied only setting to zero the increment $\Delta\lambda_t$ and therefore it yields also constant the function of the plastic multiplier in tension for all the times in this part of the loading history,

$$\lambda_t(t) = \lambda_t(t=3\bar{t}) = \frac{k_{el}\bar{u}-\sigma}{k_{el}+h}, \qquad \forall t \in [3\bar{t}, 3\bar{t}+2\frac{\sigma\bar{t}}{k_{el}\bar{u}}]. \tag{4.62}$$

From (4.61) and (4.62) we have that plastic multipliers are constant and this justifies to call elastic the present fifth phase of the loading history. The spring response is, according to (3.26), (4.61) and (4.62), as follows,

$$k_{el}(u-\lambda_t(t)+\lambda_c(t)) = k_{el}\left(u - \frac{k_{el}\bar{u}-\sigma}{k_{el}+h} + 2\frac{k_{el}\bar{u}-\sigma}{k_{el}+h}\right) = F,$$

that means

$$k_{el}u + k_{el}\left(\frac{k_{el}\bar{u}-\sigma}{k_{el}+h}\right) = \hat{F}(t), \qquad \forall t \in [3\bar{t}, 3\bar{t}+2\frac{\sigma\bar{t}}{k_{el}\bar{u}}], \tag{4.63}$$

that is a spring with a residual (with no displacement $u=0$) force equal to

$$k_{el}\left(\frac{k_{el}\bar{u}-\sigma}{k_{el}+h}\right),$$

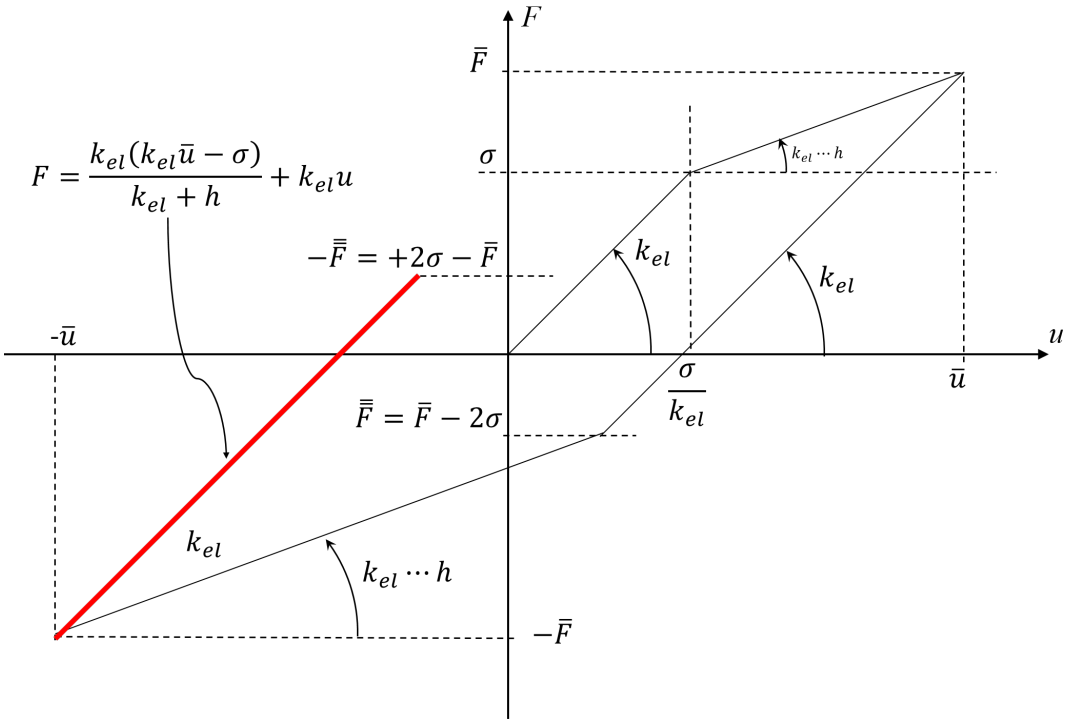

FIGURE 11. Elastic reversible phase three response is highlighted with the red-thick line. We plot the reaction force F vs the imposed displacement u.

and a stiffness

$$k_{el}.$$

The response is therefore graphically represented in Fig. 11.

As a matter of facts the final value of the reaction force is from (4.63)

$$\hat{F}\left(t = 3\bar{t} + 2\frac{\sigma\bar{t}}{k_{el}\bar{u}}\right) = k_{el}\left(-\bar{u} + 2\frac{\sigma}{k_{el}}\right) + k_{el}\left(\frac{k_{el}\bar{u} - \sigma}{k_{el} + h}\right) = 2\sigma - k_{el}\frac{h\bar{u} + \sigma}{k_{el} + h} = 2\sigma - \overline{F} = -\overline{\overline{F}}.$$

If, in an arbitrary moment of this elastic reversible phase we change the sign of the loading velocity $\dot{u}$ then the KKT conditions (3.29) and (3.30) will be both satisfied with the same constant values of plastic multipliers (4.61) and (4.62) and therefore the response is the same as calculated in (4.63) and graphically reported in Fig. 11. This reversible behavior justifies the name "reversible" for this phase of the loading history.

4.7. **The plastic irreversible phase three.** In the sixth part of the loading history the displacement u is imposed to evolve according to Fig. 1. Besides, in this plastic irreversible phase three, the spring is still in a loading phase and it is limited to be

$$-\bar{u} + 2\frac{\sigma}{k_{el}} < u < \bar{u}, \qquad \forall t \in [3\bar{t} + 2\frac{\sigma\bar{t}}{k_{el}\bar{u}}, 5\bar{t}], \tag{4.64}$$

and it is graphically represented in Fig. 12. The yielding compression is from (3.23) again a decreasing function of time (because the displacement u is still an increasing function of

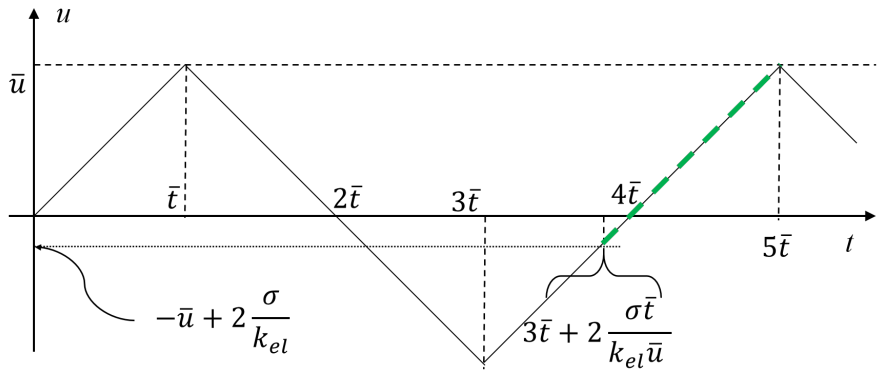

FIGURE 12. The plastic irreversible phase three of the loading history in terms of the imposed displacement u vs time t.

time), and therefore it is always lower than the final value in (4.61) of the plastic multiplier in compression of the previous part of the loading history

$$\lambda_{cy} < \lambda_c\left(t = 3\bar{t} + 2\frac{\sigma\bar{t}}{k_{el}\bar{u}}\right) = 2\frac{k_{el}\bar{u} - \sigma}{k_{el} + h}, \qquad \forall t \in [3\bar{t} + 2\frac{\sigma\bar{t}}{k_{el}\bar{u}}, 5\bar{t}]. \tag{4.65}$$

Thus, the KKT condition (3.30) is satisfied only setting to zero the increment $\Delta\lambda_c$ and therefore it yields also constant the function of the plastic multiplier in compression for all the times in this part of the loading history,

$$\lambda_c(t) = 2\frac{k_{el}\bar{u} - \sigma}{k_{el} + h}, \qquad \forall t \in [3\bar{t} + 2\frac{\sigma\bar{t}}{k_{el}\bar{u}}, 5\bar{t}]. \tag{4.66}$$

Besides, the yielding tension is from (3.22) an increasing function of time (because the displacement u is still an increasing function of time),

$$\lambda_{ty}(t) = 2\frac{k_{el}\bar{u} - \sigma}{k_{el} + h} + \frac{k_{el}u - \sigma}{k_{el} + h} = \frac{k_{el}(2\bar{u} + u) - 3\sigma}{k_{el} + h} > \frac{k_{el}\bar{u} - \sigma}{k_{el} + h} = \lambda_t(t = 3\bar{t}), \quad \forall t \in [3\bar{t} + 2\frac{\sigma\bar{t}}{k_{el}\bar{u}}, 5\bar{t}]. \tag{4.67}$$

It is greater than, because of (4.62), the value of the plastic multiplier in tension $\lambda_t(t = 3\bar{t})$ at the previous last instant of time of the fifth part of the loading history. Thus, the KKT condition (3.29) is satisfied by,

$$\lambda_t(t) = \lambda_{ty}(t) = \frac{k_{el}(2\bar{u} + u) - 3\sigma}{k_{el} + h}, \qquad \forall t \in [3\bar{t} + 2\frac{\sigma\bar{t}}{k_{el}\bar{u}}, 5\bar{t}]. \tag{4.68}$$

The spring response is, according to (3.26), (4.66) and (4.68), as follows,

$$F = k_{el}(u - \lambda_t(t) + \lambda_c(t)) = k_{el}\left(u - \frac{k_{el}(2\bar{u} + u) - 3\sigma}{k_{el} + h} + 2\frac{k_{el}\bar{u} - \sigma}{k_{el} + h}\right),$$

that means

$$\frac{k_{el}h}{k_{el} + h}u + k_{el}\frac{\sigma}{k_{el} + h} = \hat{F}(t), \qquad \forall t \in [3\bar{t} + 2\frac{\sigma\bar{t}}{k_{el}\bar{u}}, 5\bar{t}], \tag{4.69}$$

that is a spring with a residual (with no displacement $u = 0$) force equal to

$$k_{el}\frac{\sigma}{k_{el} + h},$$

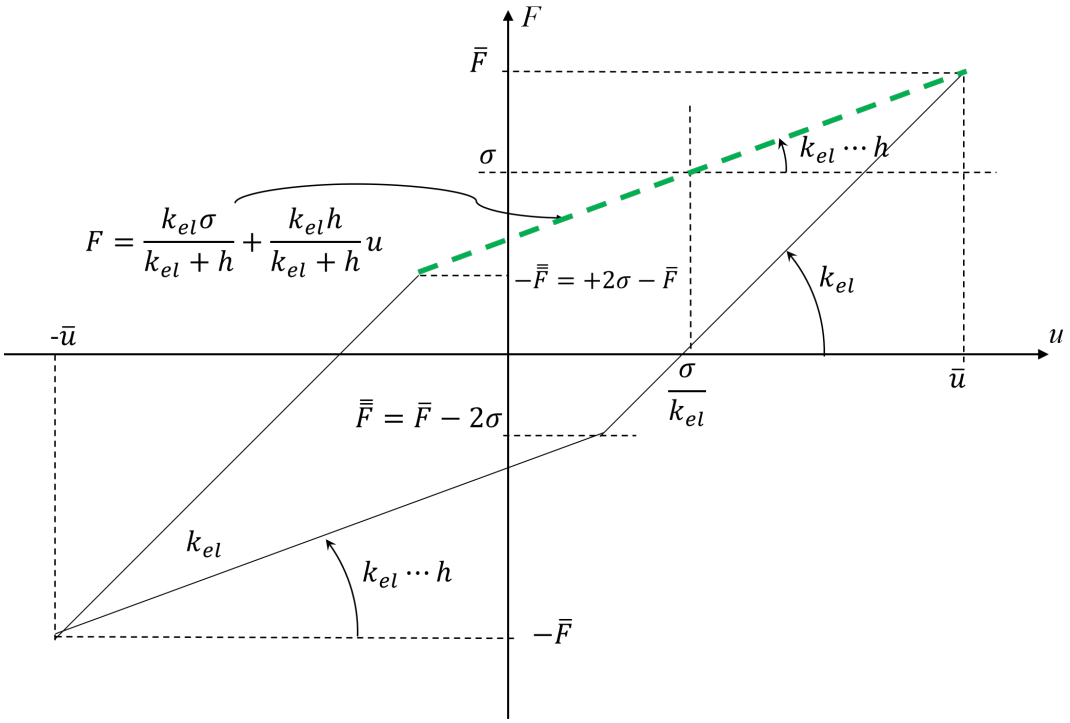

FIGURE 13. Plastic irreversible phase three response is highlighted with the green-dashed line. We plot the reaction force F vs the imposed displacement u.

and a stiffness (4.44), that is the equivalent stiffness of the series of two springs, one with stiffness k_{el} and one with stiffness h. The response is therefore represented according to Fig. 13.

As a matter of facts, from (4.68) the final value of plastic multiplier in tension is

$$\lambda_t\left(t=5\bar{t}\right)=\frac{k_{el}\left(2\bar{u}+u\left(t=5\bar{t}\right)\right)-3\sigma}{k_{el}+h}=\frac{k_{el}\left(2\bar{u}+\bar{u}\right)-3\sigma}{k_{el}+h}=3\frac{k_{el}\bar{u}-\sigma}{k_{el}+h} \tag{4.70}$$

and from (4.69) the final value of the reaction response is

$$\hat{F}\left(t=5\bar{t}\right)=\frac{k_{el}h}{k_{el}+h}u\left(t=5\bar{t}\right)+k_{el}\frac{\sigma}{k_{el}+h}=\frac{k_{el}h}{k_{el}+h}\bar{u}+k_{el}\frac{\sigma}{k_{el}+h}=k_{el}\frac{\sigma+h\bar{u}}{k_{el}+h}=\bar{F}.$$

If, in an arbitrary moment $t=\widetilde{t}$ at $u=u\left(t=\widetilde{t}\right)=\widetilde{u}$ of this plastic irreversible phase, we change the sign of the loading velocity $\dot{u}$ then the KKT conditions (3.29) and (3.30) would both be satisfied setting to zero the increments $\Delta\lambda_t$ and $\Delta\lambda_c$ and therefore the value of the plastic multiplier in compression would be still the same of that already calculated in (4.66)

$$\lambda_c\left(t\right)=\widetilde{\lambda}_c=2\frac{k_{el}\bar{u}-\sigma}{k_{el}+h},\qquad\forall t>\widetilde{t},$$

and that in tension would be from (4.68)

$$\lambda_t\left(t\right)=\widetilde{\lambda}_t=\frac{k_{el}\left(2\bar{u}+\widetilde{u}\right)-3\sigma}{k_{el}+h},\qquad\forall t>\widetilde{t},$$

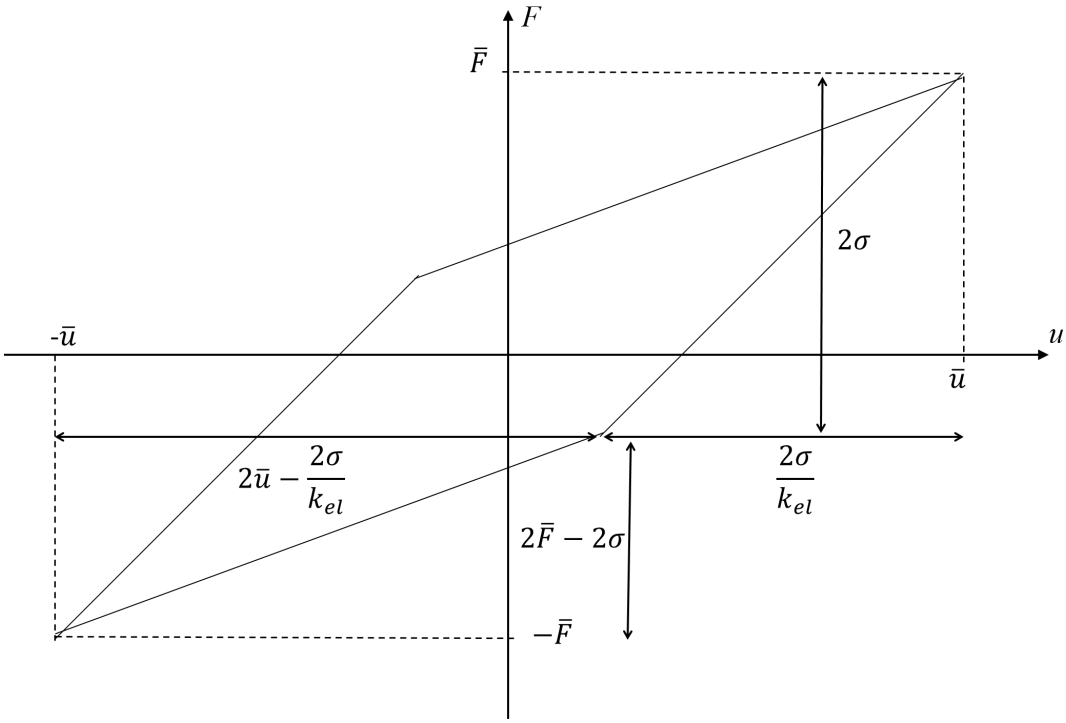

FIGURE 14. Measures for calculating the dissipated area of the hysteretic loop.

and therefore the response would be

$$k_{el}\left(u-\widetilde{\lambda}_t+\widetilde{\lambda}_c\right)=k_{el}\left(u-\frac{k_{el}\left(2\bar{u}+\widetilde{u}\right)-3\sigma}{k_{el}+h}+2\frac{k_{el}\bar{u}-\sigma}{k_{el}+h}\right)=k_{el}\left(u-\frac{k_{el}\widetilde{u}-\sigma}{k_{el}+h}\right)$$
$$=F, \qquad \forall t>\widetilde{t},$$

that is different from that calculated in (4.69). In particular the tangent stiffness would be k_{el} and not the series reported in (4.44). This irreversible behavior justifies the name "irreversible" of this phase of the loading history.

4.8. **Dissipated energy per unit cycle.** The dissipated energy per unit cycle can be calculated into two ways. The first is simply by measuring the area within the hysteretic loop

The area of the external rectangle R_e is

$$R_e = 2\overline{F}2\sigma = 4\sigma\overline{F}.$$

The areas A above and bottom the hysteretic area H_y are the same so that

$$H_y = R_e - 2A = R_e - 2\left(R_s + T_l + T_a\right).$$

Such areas are composed by two triangles and one small rectangle R_s with area

$$R_s = \left(2\overline{F} - 2\sigma\right)\frac{2\sigma}{k_{el}}.$$

Let us consider the below area. The below triangle T_l is

$$T_l = \frac{1}{2}\left(2\overline{u} - \frac{2\sigma}{k_{el}}\right)\left(2\overline{F} - 2\sigma\right),$$

the above triangle T_a is

$$T_a = \frac{1}{2}\left(\frac{2\sigma}{k_{el}}\right)(2\sigma).$$

Combining the previous equations, we obtain

$$H_y = 4\sigma\overline{F} - 2\left[\left(2\overline{F} - 2\sigma\right)\frac{2\sigma}{k_{el}} + \frac{1}{2}\left(2\overline{u} - \frac{2\sigma}{k_{el}}\right)\left(2\overline{F} - 2\sigma\right) + \frac{1}{2}\left(\frac{2\sigma}{k_{el}}\right)(2\sigma)\right] = 4\sigma\left(\overline{u} - \frac{\overline{F}}{k_{el}}\right),$$

that, from (4.46) we have

$$H_y = 4\sigma\left(\frac{k_{el}\overline{u} - \sigma}{k_{el} + h}\right).$$

Another way is to calculate the dissipation energy (3.17) at the displacement within the plastic irreversible phase three (4.64)

$$u = \frac{\sigma}{k_{el}}.$$

From (4.66) we have

$$\lambda_c = 2\frac{k_{el}\bar{u} - \sigma}{k_{el} + h},$$

and from (4.68)

$$\lambda_t = \frac{k_{el}\left(2\bar{u} + \frac{\sigma}{k_{el}}\right) - 3\sigma}{k_{el} + h},$$

that implies that the two accumulations are the same and the dissipation(3.17) is

$$W = 4\sigma\frac{k_{el}\bar{u} - \sigma}{k_{el} + h} = H_y,$$

that is consistent with the area H_y of the hysteretic cycle.

4.9. **Evolution of the plastic multipliers.** In the previous subsections, we have calculated analytically, among the reaction force evolution F, also both the plastic multipliers λ_t and λ_c. Besides, a graphical evolution of the hysteretic loop is also furnished. In this subsection, we want to give an analogous graphical evolution also of the plastic multipliers λ_t and λ_c and, because of (2.5) also of the plastic displacement u_{pl}. In Fig. 15, we show such an evolution versus time. We observe that for elastic phases both λ_t and λ_c are constant. As a consequence, also the plastic displacement u_{pl} is constant. Besides, the investigated plastic phases are 3. During the first and the third plastic phase, only λ_c is constant, and λ_t linearly evolves. During the second plastic phase only λ_t is constant, and λ_c linearly evolves. As a consequence, during the first and the third plastic phase, the plastic displacement u_{pl} linearly increases, and during the second plastic phase, it linearly decreases.

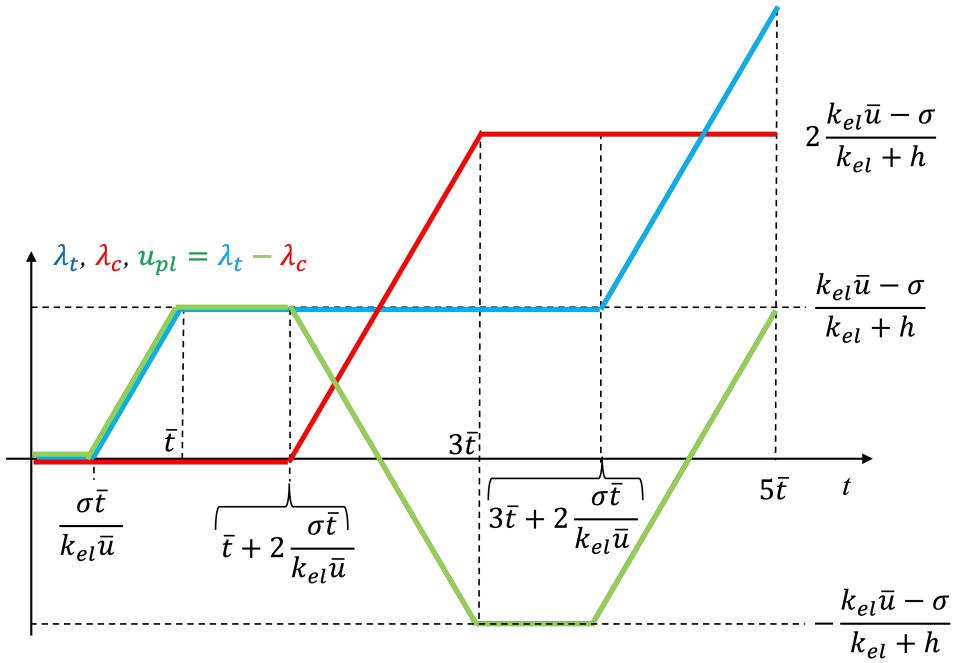

FIGURE 15. Evolutions of the plastic multipliers λ_t (blue line) and λ_c (red line) and of plastic displacement $u_{pl} = \lambda_t - \lambda_c$ (green line) are shown as a function of time.

5. CONCLUSION

A hemivariational derivation of the linear hardening spring is derived analytically. Three kinematical descriptors have been used, i.e. one displacement u and two plastic multipliers λ_t and λ_c. The two plastic multipliers are interpreted as the plastic displacement accumulation in tension and in compression, and the plastic displacement u_{pl} is therefore simply assumed to be the difference $u_{pl} = \lambda_t - \lambda_c$ between the two plastic multipliers. On the one hand, variation of displacement δu is assumed to be arbitrary. On the other hand, mono-lateral constraints $\dot{\lambda}_t \geq 0$ and $\dot{\lambda}_c \geq 0$ are assumed on both the plastic multipliers, i.e. their variations $\delta\lambda_t$ and $\delta\lambda_c$ can only be positive $\delta\lambda_t \geq 0$ and $\delta\lambda_c \geq 0$ because they can only increase with time. This is the reason why a hemivariational principle has been used. The last assumptions concern only the functional form of the elastic energy U, that is quadratic with respect to the elastic part $u_{el} = u - u_{pl}$ of the displacement function, of the dissipation energy W, that is assumed to be quadratic with respect to the plastic displacement u_{pl} and on the external energy U^{ext}, that is assumed to be linear with the displacement u. Besides, the elastic energy is also assumed to be proportional with respect to the elastic stiffness k_{el}, the dissipation energy is assumed to be proportional to the hardening coefficient h, and the external energy is proportional to the dual of the displacement, that is the external force F. Thus, only two constitutive coefficients k_{el} and h have been assumed and no flow rules has been introduced. Models for linear hardening phenomena are present in the literature. These models are equivalent to the present one. However, in this approach, the generalization of the response is easier because it is connected only to the form of the dissipation energy. Thus, we finally observe that linearity of the hardening behaviour explored in this paper has been achieved by considering a quadratic term in

the dissipation energy (3.17). This has had the consequence of a linear evolution of the plastic multipliers with respect to the imposed displacement. Thus, adding higher order terms of plastic multipliers in the form of the dissipation energy would modify such a linear hardening behavior. For example, a quartic dissipation energy would imply a cubic hardening behavior.

REFERENCES

[1] B. E. Abali, W. H. Müller and F. dell'Isola: *Theory and computation of higher gradient elasticity theories based on action principles*, Archive of Applied Mechanics, **87** (2017), 1495–1510.

[2] I. Ahmad, H. Ahmad, P. Thounthong, Y. Chu and C. Cesarano: *Solution of multi-term time-fractional PDE models arising in mathematical biology and physics by local meshless method*, Symmetry, **12** (2020), Article ID: 1195.

[3] E. Aifantis: *Pattern formation in plasticity*, Internat. J. Engrg. Sci., **33** (1995), 2161–2178.

[4] J. Alibert, P. Seppecher and F. Dell'Isola: *Truss modular beams with deformation energy depending on higher displacement gradients*, Math. Mech. Solids, **8** (2003), 51–73

[5] A. Al-Jaser, C. Cesarano, B. Qaraad and L. Iambor: *Second-Order Damped Differential Equations with Superlinear Neutral Term: New Criteria for Oscillation*, Axioms, **13** (2024), Article ID: 234.

[6] U. Andreaus, P. Baragatti: *Fatigue crack growth, free vibrations, and breathing crack detection of aluminium alloy and steel beams*, J. Strain Anal. Eng. Des., **44** (2009), 595–608.

[7] E. Artioli, F. Auricchio and L. Veiga: *Generalized midpoint integration algorithms for J2 plasticity with linear hardening*, Int. J. Numer. Methods Eng., **72** (2007), 422–463.

[8] N. Auffray, F. Dell'Isola, V. Eremeyev, A. Madeo and G. Rosi: *Analytical continuum mechanics à la Hamilton–Piola least action principle for second gradient continua and capillary fluids*, Math. Mech. Solids, **20** (2015), 375–417.

[9] E. Barchiesi, A. Misra, L. Placidi and E. Turco: *Granular micromechanics-based identification of isotropic strain gradient parameters for elastic geometrically nonlinear deformations*, ZAMM Z. Angew. Math. Mech., **101** (11) (2021), Article ID: e202100059.

[10] M. Bragaglia, F. Lamastra, P. Russo, L. Vitiello, M. Rinaldi, F. Fabbrocino and F. Nanni: *A comparison of thermally conductive polyamide 6-boron nitride composites produced via additive layer manufacturing and compression molding*, Polym. Compos., **42** (2021), 2751–2765.

[11] M. Bragaglia, L. Paleari, F. Lamastra, D. Puglia, F. Fabbrocino and F. Nanni: *Graphene nanoplatelet, multiwall carbon nanotube, and hybrid multiwall carbon nanotube–graphene nanoplatelet epoxy nanocomposites as strain sensing coatings*, J. Reinf. Plast. Comp., **40** (2021), 632–643.

[12] M. Bragaglia, L. Paleari, F. Lamastra, P. Russo, F. Fabbrocino and F. Nanni: *Oleylamine functionalization of boron nitride nano-platelets for Polyamide-6 thermally conductive injection moulded composites*, J. Thermoplast. Compos. Mater., **36** (2023), 2862–2882.

[13] A. Caporale, R. Luciano and E. Sacco: *Micromechanical analysis of interfacial debonding in unidirectional fiber-reinforced composites*, Comput. Struct., **84** (2006), 2200–2211.

[14] A. Cauchy: *Sur l'èquilibre et le mouvement d'un système de points matèriels sollicitès par des forces d'attraction ou de rèpulsion mutuelle*, In: Oeuvres Complètes: Series 2. Cambridge Library Collection - Mathematics, Cambridge University Press, (2009) 227–252.

[15] A. Ciallella, I. Giorgio, E. Barchiesi, G. Alaimo, A. Cattenone, B. Smaniotto, A. Vintache, F. D'Annibale, F. Dell'Isola, F. Hild and Others: *A 3D pantographic metamaterial behaving as a mechanical shield: experimental and numerical evidence*, Mater. Des., **237** (2023), Article ID: 112554.

[16] L. Contrafatto, M. Cuomo and S. Gazzo: *A concrete homogenisation technique at meso-scale level accounting for damaging behaviour of cement paste and aggregates*, Comput. Struct., **173** (2016), 1–18.

[17] L. Contrafatto, M. Cuomo and L. Greco: *Meso-scale simulation of concrete multiaxial behaviour*, Eur. J. Environ. Civ. En., **21** (7–8) (2016), 896–911.

[18] F. Cornacchia, F. Fabbrocino, N. Fantuzzi, R. Luciano and R. Penna: *Analytical solution of cross-and angle-ply nano plates with strain gradient theory for linear vibrations and buckling*, Mech. Adv. Mater. Struct., **28** (2021), 1201–1215.

[19] M. Cuomo, L. Contrafatto and L. Greco: *A variational model based on isogeometric interpolation for the analysis of cracked bodies*, Int. J. Eng. Sci., **80** (2014), 173–188.

[20] C. D'Ambra, G. Lignola, A. Prota, F. Fabbrocino and E. Sacco: *FRCM strengthening of clay brick walls for out of plane loads*, Compos. B: Eng., **174** (2019), Article ID: 107050.

[21] F. De Angelis: *A comparative analysis of linear and nonlinear kinematic hardening rules in computational elastoplasticity*, Tech. Mech., **32** (2012), 164–173.

[22] G. Del Piero: *The variational structure of classical plasticity*, Math. Mech. Complex Syst., **6** (3) (2018), 137–180.

[23] F. Dell'Isola, S. Eugster, R. Fedele and P. Seppecher: *Second-gradient continua: From Lagrangian to Eulerian and back*, Math. Mech. Solids, **27** (2022), 2715–2750.

[24] F. Dell'Isola, I. Giorgio and U. Andreaus: *Elastic pantographic 2D lattices: a numerical analysis on static response and wave propagation*, Proc. Est. Acad. Sci., **64** (2015), 219–225.
[25] F. Dell'Isola, I. Giorgio, M. Pawlikowski and N. Rizzi: *Large deformations of planar extensible beams and pantographic lattices: heuristic homogenization, experimental and numerical examples of equilibrium*, Proc. R. Soc. A, **472** (2016), Article ID: 20150790.
[26] F. dell'Isola, M. Guarascio and K. Hutter: *A variational approach for the deformation of a saturated porous solid. A second-gradient theory extending Terzaghi's effective stress principle*, Arch. Appl. Mech., **70** (5) (2000), 323–337.
[27] F. Dell'Isola, A. Misra: *Principle of Virtual Work as Foundational Framework for Metamaterial Discovery and Rational Design*, C. R. Mecanique, **351** (2023), 1–25.
[28] F. Dell'Isola, A. Madeo and P. Seppecher: *Boundary conditions at fluid-permeable interfaces in porous media: A variational approach*, Int. J. Solids Struct., **46** (2009), 3150–3164.
[29] F. Dell'Isola, D. Steigmann: *A two-dimensional gradient-elasticity theory for woven fabrics*, J. Elast., **18** (2015), 113–125.
[30] C. Dharmawardhana, A. Misra, S. Aryal, P. Rulis and W. Ching: *Role of interatomic bonding in the mechanical anisotropy and interlayer cohesion of CSH crystals*, Cem. Concr. Res., **52** (2013), 123–130.
[31] V. Eremeyev, F. Dell'Isola, C. Boutin and D. Steigmann: *Linear pantographic sheets: existence and uniqueness of weak solutions*, J. Elast., **132** (2017), 175–196.
[32] S. Eugster, F. Dell'Isola, R. Fedele and P. Seppecher: *Piola transformations in second-gradient continua*, Mech. Res. Commun., **120** (2022), Article ID: 103836.
[33] F. Fabbrocino, G. Carpentieri: *Three-dimensional modeling of the wave dynamics of tensegrity lattices*, Compos. Struct., **173** (2017), 9–16.
[34] F. Fabbrocino, I. Farina: *Loading noise effects on the system identification of composite structures by dynamic tests with vibrodyne*, Compos. B: Eng., **115** (2017), 376–383.
[35] R. Fedele: *Piola's approach to the equilibrium problem for bodies with second gradient energies. Part I: First gradient theory and differential geometry*, Contin. Mech. Thermodyn., **34** (2022), 445–474.
[36] R. Fedele: *Third-gradient continua: nonstandard equilibrium equations and selection of work conjugate variables*, Math. Mech. Solids, **27** (2022), 2046–2072.
[37] R. Fedele, A. Ciani and F. Fiori: *X-ray microtomography under loading and 3D-volume digital image correlation A review*, Fundam. Inform., **135** (2014), 171–197.
[38] R. Fedele, M. Filippini and G. Maier: *Constitutive model calibration for railway wheel steel through tension-torsion tests*, Comput. Struct., **83** (2005), 1005–1020.
[39] F. Freddi, G. Royer-Carfagni: *Regularized variational theories of fracture: a unified approach*, J. Mech. Phys. Solids, **58** (2010), 1154–1174.
[40] I. Giorgio: *A variational formulation for one-dimensional linear thermoviscoelasticity*, Math. Mech. Complex Syst., **9** (2022), 397–412.
[41] I. Giorgio, U. Andreaus, D. Scerrato and F. Dell'Isola: *A visco-poroelastic model of functional adaptation in bones reconstructed with bio-resorbable materials*, Biomech. Model. Mechanobiol., **15** (2016), 1325–1343.
[42] I. Giorgio, U. Andreaus, F. Dell'Isola and T. Lekszycki: *Viscous second gradient porous materials for bones reconstructed with bio-resorbable grafts*, Extreme Mech. Lett., **13** (2017), 141–147.
[43] I. Giorgio, M. De Angelo, E. Turco and A. Misra: *A Biot–Cosserat two-dimensional elastic nonlinear model for a micromorphic medium*, Contin. Mech. Thermodyn., **32** (2019), 1357–1369.
[44] I. Giorgio, F. Dell'Isola, U. Andreaus, F. Alzahrani, T. Hayat and T. Lekszytcki: *On mechanically driven biological stimulus for bone remodeling as a diffusive phenomenon*, Biomech. Model. Mechanobiol., **18** (2019), 1639–1663.
[45] I. Giorgio, F. Dell'Isola and A. Misra: *Chirality in 2D Cosserat media related to stretch-micro-rotation coupling with links to granular micromechanics*, Int. J. Solids Struct., **202** (2020), 28–38.
[46] I. Giorgio, R. Grygoruk, F. Dell'Isola and D. Steigmann: *Pattern formation in the three-dimensional deformations of fibered sheets*, Mech. Res. Commun., **69** (2015), 164–171.
[47] I. Giorgio, F. Hild, E. Gerami, F. Dell'Isola and A. Misra: *Experimental verification of 2D Cosserat chirality with stretch-micro-rotation coupling in orthotropic metamaterials with granular motif*, Mech. Res. Commun., **126** (2022), Article ID: 104020.
[48] E. Grande, G. Milani, A. Formisano, B. Ghiassi and F. Fabbrocino: *Bond behaviour of FRP strengthening applied on curved masonry substrates: numerical study*, Int. J. Mason. Res. Innov., **5** (2020), 303–320.
[49] L. Greco, M. Cuomo: *An implicit G1 multi patch B-spline interpolation for Kirchhoff–Love space rod*, Comput. Methods Appl. Mech. Eng., **269** (2014), 173–197.
[50] L. Greco, M. Cuomo: *An isogeometric implicit G1 mixed finite element for Kirchhoff space rods*, Comput. Methods Appl. Mech. Eng., **298** (2016), 325–349.
[51] F. Greco, L. Leonetti, R. Luciano and P. Trovalusci: *Multiscale failure analysis of periodic masonry structures with traditional and fiber-reinforced mortar joints*, Compos. B: Eng., **118** (2017), 75–95.

[52] A. Grimaldi, R. Luciano: *Tensile stiffness and strength of fiber-reinforced concrete*, J. Mech. Phys. Solids, **48** (2000), 1987–2008.
[53] G. Khoury, C. Majorana, F. Pesavento and B. Schrefler: *Modelling of heated concrete*, Mag. Concr. Res.", **54** (2002), 77–101.
[54] D. Kumar, F. Ayant and C. Cesarano: *Analytical Solutions of Temperature Distribution in a Rectangular Parallelepiped*, Axioms, **11** (2022), Article ID: 488.
[55] J. Larsen: *A new variational principle for cohesive fracture and elastoplasticity*, Mech. Res. Commun., **58** (2014), 133-138.
[56] C. Majorana, V. Salomoni and B. Schrefler: *Hygrothermal and mechanical model of concrete at high temperature*, Mater. Struct., **31** (1998), 378–386.
[57] G. Mancusi, F. Fabbrocino, L. Feo and F. Fraternali: *Size effect and dynamic properties of 2D lattice materials*, Compos. B: Eng., **112** (2017), 235–242.
[58] A. Misra, P. Poorsolhjouy: *Granular micromechanics model for damage and plasticity of cementitious materials based upon thermomechanics*, Math. Mech. Solids, **25** (10) (2015), Article ID: 1081286515576821.
[59] A. Misra, V. Singh: *Micromechanical model for viscoelastic materials undergoing damage*, Contin. Mech. Thermodyn., **25** (2013), 343–358.
[60] A. Misra, V. Singh: *Thermomechanics-based nonlinear rate-dependent coupled damage-plasticity granular micromechanics model*, Contin. Mech. Thermodyn., **27** (4-5) (2015), Article ID: 787.
[61] M. M. Nava, R. Fedele and M. T. Raimondi: *Computational prediction of strain-dependent diffusion of transcription factors through the cell nucleus*, Biomech. Model. Mechanobiol., **15** (2016), 983–993.
[62] C. Navier: *Memoire sur les lois de l'equilibre et du mouvement des corps solides elastiques*, Academie des Sciences, (1827).
[63] N. Nejadsadeghi, F. Hild and A. Misra: *Parametric experimentation to evaluate chiral bars representative of granular motif*, Int. J. Mech. Sci., **221** (2022), Article ID: 107184.
[64] N. Nejadsadeghi, A. Misra: *Extended granular micromechanics approach: a micromorphic theory of degree n*, Math. Mech. Solids, **25** (2020), 407–429.
[65] C. Liu, Y. Zhong: *Existence and multiplicity of periodic solutions for nonautonomous second-order discrete Hamiltonian systems*, Constr. Math. Anal., **3** (2020), 178–188.
[66] L. Placidi, E. Barchiesi, A. Misra and D. Timofeev: *Micromechanics-based elasto-plastic–damage energy formulation for strain gradient solids with granular microstructure*, Contin. Mech. Thermodyn., **33** (2021), 2213–2241.
[67] P. Poorsolhjouy, A. Misra: *Effect of intermediate principal stress and loading-path on failure of cementitious materials using granular micromechanics*, Int. J. Solids Struct., **108** (2017), 139–152.
[68] Y. Rahali, I. Giorgio, J. Ganghoffer and F. Dell'Isola: *Homogenization à la Piola produces second gradient continuum models for linear pantographic lattices*, Int. J. Eng. Sci., **97** (2015), 148–172.
[69] G. Ramaglia, G. Lignola, F. Fabbrocino and A. Prota: *Numerical investigation of masonry strengthened with composites*, Polymers, **10** (2018), Article ID: 334.
[70] B. Schrefler, P. Brunello, D. Gawin, C. Majorana and F. Pesavento: *Concrete at high temperature with application to tunnel fire*, Comput. Mech., **29** (2002), 43–51.
[71] D. Scerrato, I. Giorgio, A. Madeo, A. Limam and F. Darve: *A simple non-linear model for internal friction in modified concrete*, Int. J. Eng. Sci., **80** (2014), 136–152.
[72] B. Schrefler, C. Majorana, G. Khoury and D. Gawin: *Thermo-hydro-mechanical modelling of high performance concrete at high temperatures*, Eng. Comput., **19** (2002), 787–819.
[73] P. Seppecher, J. Alibert and F. Dell'Isola: *Linear elastic trusses leading to continua with exotic mechanical interactions*, J. Phys. Conf. Ser., **319** (2011), Article ID: 012018.
[74] J. Simo, T. Hughes: *Computational inelasticity*, Springer Science & Business Media, (2006).
[75] J. Simo, R. Taylor: *Quasi-incompressible finite elasticity in principal stretches. Continuum basis and numerical algorithms*, Comput. Methods Appl. Mech. Eng., **85** (1991), 273–310.
[76] R. Sarikaya, Q. Ye, L. Song, C. Tamerler, P. Spencer and A. Misra: *Probing the mineralized tissue-adhesive interface for tensile nature and bond strength*, J. Mech. Behav. Biomed. Mater., **120** (2021), Article ID:104563.
[77] M. Spagnuolo, K. Barcz, A. Pfaff, F. Dell'Isola and P. Franciosi: *Qualitative pivot damage analysis in aluminum printed pantographic sheets: numerics and experiments*, Mech. Res. Commun., **83** (2017), 47–52.
[78] G. Tocci Monaco, N. Fantuzzi, F. Fabbrocino and R. Luciano: *Semi-analytical static analysis of nonlocal strain gradient laminated composite nanoplates in hygrothermal environment*, J. Braz. Soc. Mech. Sci. Eng., **43** (2021), Article ID: 274.
[79] E. Turco, F. Dell'Isola, N. Rizzi, R. Grygoruk, W. Müller and C. Liebold: *Fiber rupture in sheared planar pantographic sheets: Numerical and experimental evidence*, Mech. Res. Commun., **76** (2016), 86–90.
[80] E. Turco, M. Golaszewski, I. Giorgio and F. D'Annibale: *Pantographic lattices with non-orthogonal fibres: Experiments and their numerical simulations*, Compos. B: Eng., **118** (2017), 1–14.
[81] Y. Yang, A. Misra: *Higher-order stress-strain theory for damage modeling implemented in an element-free Galerkin formulation*, CMES - Comput. Model. Eng. Sci., **64** (1) (2010), 1–36.

[82] Y. Yang, A. Misra: *Micromechanics based second gradient continuum theory for shear band modeling in cohesive granular materials following damage elasticity*, Int. J. Solids Struct., **49** (18) (2012), 2500–2514.

[83] M. E. Yildizdag, L. Placidi and E. Turco: *Modeling and numerical investigation of damage behavior in pantographic layers using a hemivariational formulation adapted for a Hencky-type discrete model*, Contin. Mech. Thermodyn., **35** (2023), 1481–1494.

Luca Placidi
International Telematic University Uninettuno
Section of Mathematics
Corso Vittorio Emanuele II, 39, 00186, Rome, Italy
ORCID: 0000-0002-1461-3997
Email address: luca.placidi@uninettunouniversity.net

Anil Misra
Florida International University
Department of Mathematics and Statistics
Deuxieme Maison, 430, 11101 SW 13th St, Miami, USA
ORCID: 0000-0002-9761-2358
Email address: anmisra@fiu.edu

Abdou Kandalaft
University of Catania
Department of Mathematics and Computer Science
Piazza Università, 2, 95131, Catania, Italy
ORCID: 0000-0002-1556-0540
Email address: abdou.kandalaft@phd.unict.it

Mohammad Mahdi Nayeban
University of Catania
Department of Mathematics and Computer Science
Piazza Università, 2, 95131, Catania, Italy
ORCID: 0009-0000-1302-2901
Email address: mohammad.nayeban@phd.unict.it

Nurettin Yilmaz
Università dell'Aquila
Department of Information Engineering, Computer Science and Mathematics
via Vetoio (Coppito), 1 – 67100 L'Aquila, Italy
ORCID: 0009-0007-9362-0928
Email address: nurettin.yilmaz@graduate.univaq.it

CONSTRUCTIVE MATHEMATICAL ANALYSIS
7 (2024), No. SI, pp. 76-92
http://dergipark.org.tr/en/pub/cma
ISSN 2651 - 2939

Research Article

Adaptive residual subsampling algorithms for kernel interpolation based on cross validation techniques

Dedicated to Professor Paolo Emilio Ricci, on occasion of his 80th birthday, with respect and friendship.

ROBERTO CAVORETTO*, ADEEBA HAIDER, SANDRO LANCELLOTTI, DOMENICO MEZZANOTTE, AND AMIR NOORIZADEGAN

ABSTRACT. In this article, we present an adaptive residual subsampling scheme designed for kernel based interpolation. For an optimal choice of the kernel shape parameter we consider some cross validation (CV) criteria, using efficient algorithms of k-fold CV and leave-one-out CV (LOOCV) as a special case. In this framework, the selection of the shape parameter within the residual subsampling method is totally automatic, provides highly reliable and accurate results for any kind of kernel, and guarantees existence and uniqueness of the kernel based interpolant. Numerical results show the performance of this new adaptive scheme, also giving a comparison with other computational techniques.

Keywords: Adaptive interpolation, meshfree methods, radial basis function approximation, shape parameter optimization, cross validation schemes.

2020 Mathematics Subject Classification: 65D05, 65D12, 65D15.

1. INTRODUCTION

In [12] an adaptive residual subsampling method depending on radial basis function (RBF) interpolation is presented. The computational technique guarantees, on the one hand, the non-singularity of the interpolation matrix (and so existence and uniqueness of the interpolant) and, on the other, allows an optimal selection of the kernel shape parameter through application of a maximum profile likelihood estimation criterion. This twofold advantage is obtained by using strictly positive definite kernels that are radially symmetric [19]. Each of these positive features do not usually occur in the original method [18], as well as in its modified version [40]. Indeed, while in [18] the adaptive method is characterized by a kernel shape parameter that can vary at each node, thus breaking the above-mentioned symmetry and accordingly compromising the proof of matrix non-singularity, in [12] this issue is solved by an optimal choice of a *unique* shape parameter for all nodes. As a result, for practical purposes, any kind of radial kernel can be used and the adaptive scheme can be iteratively and automatically applied without any user's action. Other examples of adaptive interpolation algorithms can be found in literature, see e.g. [1, 7, 24, 38] and references therein.

In this work, we propose a change in the decision strategy regarding the choice of the optimal shape parameter associated with the kernel within the residual subsampling method [12]. In this context, we opt for use of some *cross validation* (CV) criteria. In fact, CV is a popular technique in statistics which, instead of the usually unknown solution, makes use of the given

Received: 19.07.2024; Accepted: 01.11.2024; Published Online: 16.12.2024
*Corresponding author: Roberto Cavoretto; roberto.cavoretto@unito.it
DOI: 10.33205/cma.1518603

data to predict optimal values of model parameters for data fitting. The main idea is to split the data into a training set and a validation one, then utilizing some form of error norm obtained by gauging the accuracy of the fit built from information on the training set at points of the validation set [21]. Here, we focus on some possible options of CV algorithms to be applied within the residual subsampling method. More precisely, we consider the k-fold CV formulated as an extended version of Rippa's scheme [30], which includes original Rippa's algorithm [34] as a particular case. The latter is an especially popular version of CV, known as leave-one-out cross validation (LOOCV), and corresponds to using a training set consisting of all of the data points except one, which in turn is the sole member of the validation set. In the setting of kernel or RBF methods the LOOCV scheme appears in several papers such as [7, 22, 26, 36, 37], to name a few. Since the LOOCV method is also efficiently implemented in the MATLAB `crossval` routine [31], it will also be used in this study as a term of comparison for our procedures.

The aim of this work is therefore to introduce a CV criterion for an optimal choice of the kernel shape parameter within the adaptive residual subsampling method. The use of k-fold CV or LOOCV strategies provides greater flexibility and sometimes efficiency than the maximum profile likelihood estimation criterion in [12]. Indeed, this study shows how the CV techniques are valid alternative within residual subsampling schemes, even if – due to several variables involved – is not possible to declare a clear and complete superiority of a specific CV scheme compared to other ones. However, the resulting algorithm allows a totally automatic computation of the shape parameter, i.e., any user's action is not required, either initially, and a single optimal shape parameter is found at any iteration and for each data point set. In this framework, the interpolation problem is well-posed and hence the kernel interpolant exists uniquely, obviously provided that the kernel matrix is positive definite (see e.g. [21]). Moreover, the use of CV techniques has some predictive role to control the ill-conditioning of the interpolation matrix, in particular when in the iterative/adaptive method the number of interpolation points grows. Finally, as our numerical results show, an application of CV criteria formulated in the framework of extended Rippa's scheme generally results in an adaptive interpolation scheme more efficient than commonly used MATLAB routines. The new adaptive method is tested in one and two dimensions and highlights good performance in term of both computational accuracy and efficiency.

The paper is organized as follows. In Section 2, we introduce some preliminaries on multivariate RBF/kernel based interpolation. Section 3 presents CV criteria to find optimal values of the kernel shape parameter in the interpolation method. In Section 4, we describe the adaptive residual subsampling scheme. In Section 5, we report some numerical results, showing accuracy and efficiency of the different CV schemes and providing a comparison with other algorithms. Section 6 concludes this article.

2. Preliminaries

RBF or kernel based methods are powerful and effective tools for multivariate data interpolation. In this section, we introduce some basic notations and a few theoretical results for kernel based interpolation. For further details, we refer the reader to [3, 21, 39].

2.1. **Multivariate interpolation and positive definite functions.**

Scattered data fitting is in general one of the fundamental problems in the field of approximation theory and its applications. In order to have a well-posed problem formulation, we need to recall the concepts of positive definite matrices, and strictly positive definite functions. Indeed, such functions provide a direct entry into meshfree approximation methods [19].

To give a precise definition of the scattered data interpolation problem, we assume to have a finite set $X = \{\boldsymbol{x}_i\}_{i=1}^N \subseteq \Omega$ of data points (or nodes) for some region Ω in $\mathbb{R}^d$, $d \geq 1$, and the corresponding scalar-valued data $f_i \in \mathbb{R}$. These values are often obtained by sampling some (unknown) function f at the data points, i.e. $y_i = f(\boldsymbol{x}_i)$, $i = 1, \ldots, N$. So we are now ready for a precise formulation of the multivariate interpolation problem.

Problem 2.1. *Given data $(\boldsymbol{x}_i, y_i)$, $i = 1, \ldots, N$, with $\boldsymbol{x}_i \in \mathbb{R}^d$, $d \geq 1$, and $y_i \in \mathbb{R}$, find a (continuous) function s such that*

$$s(\boldsymbol{x}_i) = y_i, \qquad i = 1, \ldots, N. \tag{2.1}$$

A suitable and common approach to solving this problem is to take the function s as a linear combination of certain *basis functions* B_j, i.e.,

$$s(\boldsymbol{x}) = \sum_{j=1}^{N} c_j B_j(\boldsymbol{x}), \qquad \boldsymbol{x} \in \Omega. \tag{2.2}$$

Solving the interpolation problem under this assumption leads to a linear system of the form

$$\mathsf{A}\boldsymbol{c} = \boldsymbol{y},$$

where the entries of the *interpolation matrix* A are given by $\mathsf{A}_{ij} = B_j(\boldsymbol{x}_i)$, $i, j = 1, \ldots, N$, $\boldsymbol{c} = (c_1, c_2, \ldots, c_N)^T$, and $\boldsymbol{y} = (y_1, \ldots, y_N)^T$.

Problem 2.1 is *well-posed*, i.e., a solution to a problem exists and is unique, if and only if the matrix A is non-singular.

In order to have basis functions B_j, $j = 1, \ldots, N$, that generate non-singular matrices A for any set of distinct nodes, we recall the special class of positive definite (PD) matrices.

Definition 2.1. *A real symmetric matrix A is called positive semi-definite if its associated quadratic form is non-negative, i.e.,*

$$\sum_{i=1}^{N} \sum_{j=1}^{N} c_i c_j \mathsf{A}_{ij} \geq 0 \tag{2.3}$$

for $\boldsymbol{c} = (c_1, \ldots, c_N)^T \in \mathbb{R}^N$. If the quadratic form (2.3) is zero only for $\boldsymbol{c} \equiv \boldsymbol{0}$, then A is called positive definite.

An important property which involves all PD matrices is that, if A is a PD matrix, all its eigenvalues are positive and therefore A is non-singular (but not vice versa). In general, then, it is convenient to consider basis functions B_j of the form (2.2) which are the shifts of a certain function centred at $\boldsymbol{x}_j$, i.e. $B_j(\cdot) = \Phi(\cdot - \boldsymbol{x}_j)$, so that interpolation matrix is positive definite. For this reason, we introduce the concept of *strictly positive definite (SPD) function*.

Definition 2.2. *A complex-valued continuous function $\Phi : \mathbb{R}^d \to \mathbb{C}$ is called positive definite on $\mathbb{R}^d$ if*

$$\sum_{i=1}^{N} \sum_{j=1}^{N} c_i \overline{c_j} \Phi\left(\boldsymbol{x}_i - \boldsymbol{x}_j\right) \geq 0 \tag{2.4}$$

for any N pairwise different data points $\boldsymbol{x}_1, \ldots, \boldsymbol{x}_N \in \mathbb{R}^d$, and $\boldsymbol{c} = (c_1, \ldots, c_N)^T \in \mathbb{C}^N$. The function Φ is called strictly positive definite on $\mathbb{R}^d$ if the quadratic form (2.4) is zero only for $\boldsymbol{c} \equiv \boldsymbol{0}$.

It is also possible to characterize real-valued (S)PD functions using only real coefficients. In fact, Definition 2.2 implies that only functions whose quadratic form is real are candidates

for (S)PD functions. A characterization of such functions is given in the following theoretical result.

Theorem 2.1 ([19]). *A real-valued continuous function Φ is positive definite on $\mathbb{R}^d$ if and only if it is even and*

$$\sum_{i=1}^{N}\sum_{j=1}^{N} c_i c_j \Phi\left(\boldsymbol{x}_i - \boldsymbol{x}_j\right) \geq 0 \tag{2.5}$$

for any N pairwise different data points $\boldsymbol{x}_1, \ldots, \boldsymbol{x}_N \in \mathbb{R}^d$, and $\boldsymbol{c} = (c_1, \ldots, c_N)^T \in \mathbb{R}^N$. The function Φ is called strictly positive definite on $\mathbb{R}^d$ if the quadratic form (2.5) is zero only for $\boldsymbol{c} \equiv \boldsymbol{0}$.

A celebrated result on PD functions is the integral characterization given by Bochner's theorem.

Theorem 2.2 (**Bochner**, [19]). *A (complex-valued) function $\Phi \in C(\mathbb{R}^d)$ is positive definite on $\mathbb{R}^d$ if and only if it is the Fourier transform of a finite non-negative Borel measure μ on $\mathbb{R}^d$, i.e.*

$$\Phi(\boldsymbol{x}) = \hat{\mu}(\boldsymbol{x}) = \frac{1}{\sqrt{(2\pi)^d}} \int_{\mathbb{R}^d} e^{-i\boldsymbol{x}\cdot\boldsymbol{y}} d\mu(\boldsymbol{y}), \qquad \boldsymbol{x} \in \mathbb{R}^d.$$

2.2. **Kernel based interpolation.** Given a compact domain $\Omega \subset \mathbb{R}^d$, we assume that the N distinct data points are defined by the set $X = \{\boldsymbol{x}_i\}_{i=1}^N \subseteq \Omega$, while the associated data values are given by $y_i = f(\boldsymbol{x}_i) \in \mathbb{R}$, $i = 1, \ldots, N$, the latter being obtained by sampling some function $f : \Omega \to \mathbb{R}$. For Problem 2.1 we want to determine a function $s : \Omega \to \mathbb{R}$ satisfying the interpolation conditions (2.1).

We can thus express the interpolant s as a linear combination of kernels $\kappa_\varepsilon : \Omega \times \Omega \to \mathbb{R}$ depending on the so-called shape parameter $\varepsilon > 0$, i.e.

$$s(\boldsymbol{x}) = \sum_{j=1}^{N} c_j \kappa_\varepsilon(\boldsymbol{x}, \boldsymbol{x}_j), \qquad \boldsymbol{x} \in \Omega. \tag{2.6}$$

The solution of this interpolation problem results in the symmetric linear system

$$\mathsf{A}_\varepsilon \boldsymbol{c} = \boldsymbol{y}, \tag{2.7}$$

where A_ε is the interpolation (or kernel) matrix with entries $(\mathsf{A}_\varepsilon)_{ij} = \kappa_\varepsilon(\boldsymbol{x}_i, \boldsymbol{x}_j)$, $i, j = 1, \ldots, N$, while $\boldsymbol{c}$ and $\boldsymbol{y}$ are defined as above. Specifically, we remark that if the kernel κ_ε is symmetric and SPD, the matrix A_ε is PD for any data point set X, and the coefficients c_j in (2.6) can uniquely be found.

Starting from the kernel κ_ε in (2.6) we may define a SPD RBF $\phi : \mathbb{R}_0^+ \to \mathbb{R}$ such that

$$\kappa_\varepsilon(\boldsymbol{x}, \boldsymbol{x}_j) = \phi_\varepsilon(||\boldsymbol{x} - \boldsymbol{x}_j||_2) = \phi_\varepsilon(r) := \phi(\varepsilon r), \qquad \forall \boldsymbol{x}, \boldsymbol{x}_j \in \Omega,$$

where $||\cdot||_2$ denotes the Euclidean norm on $\mathbb{R}^d$. It is noteworthy to observe that the choice of a suitable shape parameter ε is usually relevant in radial kernel methods, even if it is known to be a big issue (see e.g. [13, 20, 25, 32], or [21, Chapter 14]). Some popular examples of SPD RBFs are listed below, together with their smoothness degrees and related abbreviations (see

[19]):

$$\phi_\varepsilon(r) = \begin{cases} \exp(-\varepsilon^2 r^2), & \text{Gaussian } C^\infty & \text{GA} \\ (1+\varepsilon^2 r^2)^{-1/2}, & \text{Inverse MultiQuadric } C^\infty & \text{IMQ} \\ \exp(-\varepsilon r)(\varepsilon^3 r^3 + 6\varepsilon^2 r^2 + 15\varepsilon r + 15), & \text{Matérn } C^6 & \text{M6} \\ \exp(-\varepsilon r)(\varepsilon^2 r^2 + 3\varepsilon r + 3), & \text{Matérn } C^4 & \text{M4} \\ \exp(-\varepsilon r)(\varepsilon r + 1), & \text{Matérn } C^2 & \text{M2}. \end{cases}$$

Additionally, the solution of the linear system (2.7) turns out often to be quite sensitive to changes in the data, and the choice of ε can greatly influence the numerical result. A way to measure the computational stability of this interpolation method consists in calculating the condition number of A_ε. As the kernel κ_ε is symmetric and SPD, the conditioning of the kernel matrix A_ε can simply be computed as the ratio between the largest and the smallest eigenvalue ($\lambda_{\max}$ and $\lambda_{\min}$, respectively) of A_ε as:

$$\text{cond}(\mathsf{A}_\varepsilon) = ||\mathsf{A}_\varepsilon||_2 ||\mathsf{A}_\varepsilon^{-1}||_2 = \frac{\lambda_{\max}}{\lambda_{\min}}. \tag{2.8}$$

In order to give some error estimates, we introduce the so-called native space associated with the kernel κ_ε, which is a reproducing kernel Hilbert space $\mathcal{N}_{\kappa_\varepsilon}(\Omega)$ with inner product $(\cdot,\cdot)_{\mathcal{N}_{\kappa_\varepsilon}(\Omega)}$, i.e., $f(\boldsymbol{x}) = (f, \kappa_\varepsilon(\cdot,\boldsymbol{x}))_{\mathcal{N}_{\kappa_\varepsilon}(\Omega)}$, for all $f \in \mathcal{N}_{\kappa_\varepsilon}(\Omega)$ and $\boldsymbol{x} \in \Omega$. Moreover, $H_{\kappa_\varepsilon}(\Omega) = \text{span}\{\kappa_\varepsilon(\cdot,\boldsymbol{x}), \boldsymbol{x} \in \Omega\}$ is a pre-Hilbert space with reproducing kernel κ_ε and equipped with the bilinear form $(\cdot,\cdot)_{\kappa_\varepsilon}$. The native space $\mathcal{N}_{\kappa_\varepsilon}(\Omega)$ of κ_ε is its completion w.r.t. the κ_ε-norm $||\cdot||_{\kappa_\varepsilon}$ so that $||f||_{\kappa_\varepsilon} = ||f||_{\mathcal{N}_{\kappa_\varepsilon}(\Omega)}$ for all $f \in H_{\kappa_\varepsilon}(\Omega)$ (see [19]). Now, we can thus provide a generic error bound in terms of the well-known *power function* $P_{\kappa_\varepsilon,X}$.

Theorem 2.3 ([19]). *Let $\Omega \subseteq \mathbb{R}^d$, $\kappa_\varepsilon \in C(\Omega \times \Omega)$ be strictly positive definite on $\mathbb{R}^d$, and suppose that $X = \{\boldsymbol{x}_i\}_{i=1}^N$ has distinct points. Then, for all $f \in \mathcal{N}_{\kappa_\varepsilon}(\Omega)$, we have*

$$|f(\boldsymbol{x}) - s(\boldsymbol{x})| \le P_{\kappa_\varepsilon,X}(\boldsymbol{x}) ||f||_{\mathcal{N}_{\kappa_\varepsilon}(\Omega)}, \quad \boldsymbol{x} \in \Omega.$$

The first error estimate of Theorem 2.3 can then be improved as shown in the following theorem.

Theorem 2.4 ([19]). *Let $\Omega \subseteq \mathbb{R}^d$ be bounded and satisfy an interior cone condition. Suppose that $\kappa_\varepsilon \in C^{2k}(\Omega \times \Omega)$ is symmetric and strictly positive definite. Then, for all $f \in \mathcal{N}_{\kappa_\varepsilon}(\Omega)$, there exist constants h_0, $C > 0$ (independent of $\boldsymbol{x}$, f and κ_ε) such that*

$$|f(\boldsymbol{x}) - s(\boldsymbol{x})| \le C h_{X,\Omega}^k \sqrt{C_{\kappa_\varepsilon}(\boldsymbol{x})}\, \|f\|_{\mathcal{N}_{\kappa_\varepsilon}(\Omega)},$$

provided $h_{X,\Omega} \le h_0$. Here

$$C_{\kappa_\varepsilon}(\boldsymbol{x}) = \max_{|\boldsymbol{\beta}|=2k,\, \boldsymbol{w},\boldsymbol{z} \in \Omega \cap B(\boldsymbol{x}, c_2 h_{X,\Omega})} \left| D_2^{\boldsymbol{\beta}} \kappa_\varepsilon(\boldsymbol{w},\boldsymbol{z}) \right|,$$

with $B(\boldsymbol{x}, c_2 h_{X,\Omega})$ denoting the ball of radius $c_2 h_{X,\Omega}$ centred at $\boldsymbol{x}$, and $h_{X,\Omega}$ being the fill distance

$$h_{X,\Omega} = \sup_{\boldsymbol{x} \in \Omega} \min_{\boldsymbol{x}_j \in X} ||\boldsymbol{x} - \boldsymbol{x}_j||_2.$$

Theorem 2.4 says that interpolation with a C^{2k} smooth kernel κ_ε has approximation order k. Accordingly, we can deduce that:

(a) for C^∞ SPD kernels, the approximation order k is arbitrarily high;
(b) for SPD kernels with limited smoothness, the approximation order is limited by the kernel smoothness.

For more refined error bounds, the reader may refer to [39].

3. Cross validation criteria for the shape parameter choice

In Section 2, we compute the interpolant s in (2.6) by solving the linear system (2.7), where the kernel matrix A_ε is symmetric and PD. By the uncertainty or trade-off principle [35, 33] we know that using a standard RBF one cannot have high accuracy and stability at the same time. In fact, when the best level of accuracy is typically achieved, i.e., in the flat limit $\varepsilon \to 0$, the interpolation matrix may be very ill-conditioned. A good compromise between numerical accuracy and computational stability needs to be found. It is therefore important to devise suitable techniques that allow us to make a reliable prediction of ε. In fact, the approximation quality is often strongly influenced by the shape parameter, and consequently several strategies have been proposed in the literature for its tuning, see e.g. [8, 15, 23, 36] and [21, Chapter 14].

In this work, we discuss three possible versions of CV algorithms, which we will apply in the residual subsampling method for kernel based interpolation. Hereinafter, firstly we consider the k-fold CV formulated as an extended version of Rippa's algorithm [30], including original Rippa's LOOCV scheme [34] as a particular case (i.e., when $k = N$); then, we refer to the LOOCV method that is implemented in the MATLAB `crossval` routine [31].

3.1. Extended Rippa's scheme.

Supposing to have N data points, in the k-fold CV the data set is divided into k (possibly equal-sized) disjoint subsets, $k \leq N$. Then, iteratively, $k \in \mathbb{N}$ different models are built upon $k-1$ training folds and their performance is evaluated on the respective remaining validation fold. An alternative CV scheme is the so-called leave-p-out cross validation (LpOCV) [16], $p \in \mathbb{N}$, $p < N$, where all possible combinations of p elements of the data set are taken into account as validation set. Since such a computation is very demanding in many situations, k-fold CV is usually preferred. In this work, with an abuse of notation, we refer to LpOCV meaning k-fold CV with $k \approx N/p$. A stochastic extension of extended Rippa's scheme can be found in [29].

To formulate extended Rippa's scheme in the k-fold CV setting [30], considering one of the k folds, we define a vector $\boldsymbol{p} = (p_1, \ldots, p_v)^T$ of distinct validation indices $p_j \in \{1, \ldots, N\}$, $v \in \mathbb{N}$, $v < N$. The data set is subdivided into a training data set $\mathcal{T}$ consisting of $N - v$ points $(\boldsymbol{x}_j, y_j)$ with $j \notin \boldsymbol{p}$, meaning the indices that are not elements of $\boldsymbol{p}$, and a validation data set $\mathcal{V}$ formed by the remaining v points $(\boldsymbol{x}_{p_j}, y_{p_j})$, $j = 1, \ldots, v$.

For a fixed ε, we define the partial RBF interpolant constructed upon $\mathcal{T}$ as

$$s^{[\boldsymbol{p}]}(\boldsymbol{x}) = \sum_{j=1,\ j\notin\boldsymbol{p}}^{N} c_j^{[\boldsymbol{p}]} \kappa_\varepsilon(\boldsymbol{x}, \boldsymbol{x}_j).$$

The column vector $\boldsymbol{c}^{[\boldsymbol{p}]} = (c_j^{[\boldsymbol{p}]})_{j\notin\boldsymbol{p}}$ is found by solving the system of linear equations

$$\mathsf{A}_\varepsilon^{\boldsymbol{p},\boldsymbol{p}} \boldsymbol{c}^{[\boldsymbol{p}]} = \boldsymbol{y}^{\boldsymbol{p}}, \tag{3.9}$$

where $\mathsf{A}_\varepsilon^{\boldsymbol{p},\boldsymbol{p}} = (\mathsf{A}_\varepsilon)_{i,j}$, with $i, j \notin \boldsymbol{p}$, and $\boldsymbol{y}^{\boldsymbol{p}} = (y_j)_{j\notin\boldsymbol{p}}$. Notice that by writing $\boldsymbol{c}^{\boldsymbol{p}} = (c_i)_{j\notin\boldsymbol{p}}$ and $\boldsymbol{c}_{\boldsymbol{p}} = (c_j)_{j\in\boldsymbol{p}}$ we are, in practice, considering some subvectors of $\boldsymbol{c}$, while $\boldsymbol{c}^{[\boldsymbol{p}]}$ represents the solution of the linear system (3.9). Thus, in general, we have that $\boldsymbol{c}^{[\boldsymbol{p}]} \neq \boldsymbol{c}^{\boldsymbol{p}}$.

To extend Rippa's algorithm, our aim is to compute the validation errors at $\mathcal{V}$, i.e.,

$$\boldsymbol{e}_{\boldsymbol{p}} := \boldsymbol{e}_{\boldsymbol{p}}(\varepsilon) = \boldsymbol{y}_{\boldsymbol{p}} - s^{[\boldsymbol{p}]}(\boldsymbol{x}_{\boldsymbol{p}}) = (y_{p_1} - s^{[\boldsymbol{p}]}(\boldsymbol{x}_{p_1}), \ldots, y_{p_v} - s^{[\boldsymbol{p}]}(\boldsymbol{x}_{p_v}))^T \tag{3.10}$$

by means of (2.7) and without solving (3.9). Thus, from [30, Theorem 1], if A_ε and $\boldsymbol{c}$ are as in (2.7), the vector of ε-dependent errors $\boldsymbol{e}_{\boldsymbol{p}} = \boldsymbol{e}_{\boldsymbol{p}}(\varepsilon)$ in (3.10) related to the points $\boldsymbol{x}_{p_1}, \ldots, \boldsymbol{x}_{p_v}$ is the unique solution of the linear system

$$(\mathsf{A}_\varepsilon^{-1})_{\boldsymbol{p},\boldsymbol{p}} \boldsymbol{e}_{\boldsymbol{p}} = \boldsymbol{c}_{\boldsymbol{p}}, \qquad \boldsymbol{e}_{\boldsymbol{p}} \in \mathbb{R}^v, \tag{3.11}$$

where $(\mathsf{A}_\varepsilon^{-1})_{\boldsymbol{p},\boldsymbol{p}} = (\mathsf{A}_\varepsilon^{-1})_{i,j}$, with $i,j \in \boldsymbol{p}$, and $\boldsymbol{c_p} = (c_i)_{i\in\boldsymbol{p}}$, and the vectorized index $\boldsymbol{p}$ extracts the i-th rows and j-th columns subsystem with $i,j \in \boldsymbol{p}$ of the original matrix.

Concatenating all k validation error vectors $\boldsymbol{e}(\varepsilon) = (\boldsymbol{e}_{\boldsymbol{p}_1}^T, \ldots, \boldsymbol{e}_{\boldsymbol{p}_k}^T)^T(\varepsilon)$ of all k folds yields the vector of errors, and we define the LpOCV optimal value by

$$\varepsilon_* = \arg\min_{\varepsilon} ||\boldsymbol{e}(\varepsilon)||, \tag{3.12}$$

where $||\cdot||$ is any norm used in the minimization problem, for instance, the ∞-norm. So from (3.11) and (3.12) the LpOCV cost function to be minimized is given by

$$\text{L}p\text{OCV}(\varepsilon) = ||\boldsymbol{e}(\varepsilon)||_\infty. \tag{3.13}$$

In particular, by setting $\boldsymbol{p} = p \in \{1,\ldots,N\}$ in (3.10) and (3.11), we get to original Rippa's scheme [34], i.e.

$$e_p(\varepsilon) = y_p - s^{[p]}(\boldsymbol{x}_p) = \frac{c_p}{(\mathsf{A}_\varepsilon^{-1})_{p,p}}.$$

Indeed, when we set $k = N$ in the k-fold CV, this choice is equivalent to consider the LpOCV with $p = 1$, thus defining the LOOCV, because each validation fold consists of a single point. The resulting LOOCV scheme computes an exact N-fold CV, which has been widely employed by the scientific community and also generalized to other contexts e.g. in [5, 10, 11, 14, 22].

3.2. **Other MATLAB CV techniques.** CV is a model assessment technique that is commonly used to evaluate the performance of machine learning algorithms in making predictions on new data sets that it has not been trained on. This is carried out by creating a partition of the known data set in two subsets: a subset is used to train the algorithm, while the remaining one is applied for model validation. More precisely, each CV phase involves randomly partitioning the original data set into a training set and a validation set. The former is then used to train a supervised learning algorithm, whereas the latter is considered to evaluate its performance. This process is repeated several times and the average CV error is used as a performance indicator [31].

Among the most usual techniques of CV, already implemented in MATLAB, we here mention for our purposes only two as follows:

a) **k-fold CV**: It partitions data into k randomly chosen subsets (or folds) of roughly equal size. One subset is employed for validation of the model trained using the remaining subsets. This process is repeated k times such that each subset is used exactly once for validation. Across all k partitions the average error is computed. This approach is one of the most popular CV techniques even if it can be quite expensive from the computational point of view since the model needs to be trained repeatedly.

b) **LOOCV**: It partitions data using the k-fold approach, k being equal to the total number N of data. This data is used once as a validation set.

MATLAB software enables to use both k-fold CV and LOOCV algorithms through suitable application of `crossval` and `cvpartition` routines.

4. Adaptive residual subsampling scheme

In this section, we present our adaptive residual subsampling procedure, which allows us to refine and coarsen the node distribution by applying a kernel based interpolation process. More precisely, this scheme is used to approximate an unknown target function on uniformly distributed points, and then the residual error is evaluated at midpoints. The latter are added to the point set when the residual is over a prescribed refinement threshold, whereas they are

removed from that set when they are under a predefined coarsening threshold. Hereinafter, we give a more detailed explanation of this adaptive scheme.

We firstly introduce a finite sequence of data point sets, which in the iterative procedure are denoted by

$$X^{(0)}, X^{(1)}, \cdots, X^{(kmax)},$$

so that the $(k+1)$-th set $X^{(k+1)}$ is obtained from the k-th one, i.e. $X^{(k)} = \{\boldsymbol{x}_i^{(k)}\}_{i=1}^{N^{(k)}}$, after applying some refinement and/or coarsening procedures till a maximum number $kmax$ of iterations. This adaptive process thus brings to an update of the node distribution based on the computation of residual errors evaluated on some suitable test points. The iterative scheme we are constructing follows the common paradigm to solve, estimate, refine and/or coarsen till stop criteria are satisfied, or $kmax$ is reached.

Then, after defining a set of test points $T^{(k)} = \{\boldsymbol{t}_i^{(k)}\}_{i=1}^{N_{T^{(k)}}} \subset \Omega$, for $k \geq 0$, we compute the residual absolute error

$$\xi(\boldsymbol{t}_i^{(k)}) = \left| s(\boldsymbol{t}_i^{(k)}) - f(\boldsymbol{t}_i^{(k)}) \right|, \qquad \boldsymbol{t}_i^{(k)} \in T^{(k)}, \tag{4.14}$$

the interpolating function s being here constructed on the set $X^{(k)}$, and $N_{T^{(k)}}$ defining the number of points belonging to $T^{(k)}$.

The residual in (4.14) provides a measure of the error between the approximate solution and the function value computed at the test set $T^{(k)}$. In particular, the absolute error $\xi(\boldsymbol{t}_i^{(k)})$ is expected to be small when the test point $\boldsymbol{t}_i^{(k)}$ is on or close to a smooth region, while it is expected to be large when $\boldsymbol{t}_i^{(k)}$ lies in a part of the domain characterized by a low regularity or close to a discontinuous region.

Remark 4.1. *At the earliest stage (i.e. for $k = 0$), the test set $T^{(0)}$ is defined by starting from $X^{(0)} \equiv X$, whereas in the next iterations (i.e. for $k \geq 1$), the test set $T^{(k)}$ depends on both the sets $X^{(k)}$ and $X^{(k-1)}$.*

The residual (4.14) is used as an error indicator to define two different sets of our adaptive scheme, namely a refinement set and a coarsening one, called $X^{(k)}_{\text{refine}}$ and $X^{(k)}_{\text{coarse}}$, respectively. Therefore, introducing two positive thresholds θ_{refine} and θ_{coarse}, with $\theta_{\text{coarse}} < \theta_{\text{refine}}$, we can act as follows:

(1) If the error $\xi(\boldsymbol{t}_i^{(k)})$ in (4.14) is larger than θ_{refine}, the test point $\boldsymbol{t}_i^{(k)}$ is added in the set $X^{(k)}_{\text{refine}}$, and so $X^{(k)}$ is replaced by $X^{(k)} \cup X^{(k)}_{\text{refine}}$.

(2) If the error $\xi(\boldsymbol{t}_i^{(k)})$ in (4.14) is smaller than θ_{coarse}, the test point is moved from the set $X^{(k)}$ to the set $X^{(k)}_{\text{coarse}}$, and so $X^{(k)}$ is then updated with $X^{(k)} \backslash X^{(k)}_{\text{coarse}}$.

Accordingly, the set $X^{(k+1)}$ is adaptively obtained by adding the set $X^{(k)}_{\text{refine}}$ to the set $X^{(k)}$ and deleting the set $X^{(k)}_{\text{coarse}}$, i.e.,

$$X^{(k+1)} = \left\{ X^{(k)} \cup X^{(k)}_{\text{refine}} \right\} \backslash X^{(k)}_{\text{coarse}}.$$

The iterative method concludes once the process of addition/removal was completed, returning the final set $X^{(k^*)}$, k^* denoting the last iteration.

Analysing the proposed method, we note that it turns out to be dependent on the error (4.14). Indeed, at each iteration k, the adaptive procedure generates a kernel based interpolant of the form (2.6) defined on the set $X^{(k)}$, thus requiring to make some extra evaluations of the function f at the test points $\boldsymbol{t}_i^{(k)}$, $\forall i$. Since the function evaluation might be costly (or,

for instance, in real world applications, even not available at all), one could think of using an alternative strategy creating a local approximation around $\boldsymbol{t}_i^{(k)}$ and using the latter (instead of function value) in (4.14). A pseudo-code of this adaptive scheme is outlined in Algorithm 1. Similar computational techniques have already been studied in e.g. [6, 40].

Algorithm 1: Adaptive residual subsampling scheme

STEP 1 Assume $X^{(0)} \equiv X$

STEP 2 Fix $\theta_{\text{refine}} > \theta_{\text{coarse}} > 0$

STEP 3 While $k \leq kmax$ & $X^{(k)}_{\text{refine}} \cup X^{(k)}_{\text{coarse}} \neq \emptyset$

3.1: Compute $\varepsilon_*^{(k)}$ minimizing (3.13)

3.2: Solve the system (2.7) on $X^{(k)}$ and get the interpolant (2.6)

3.3: Define $T^{(k)}$

3.4: Evaluate the residual $\xi(\boldsymbol{t}_i^{(k)})$ in (4.14)

3.5: Define

$$X^{(k)}_{\text{refine}} = \{\boldsymbol{t}_i^{(k)} \in T^{(k)} \,:\, \xi(\boldsymbol{t}_i^{(k)}) > \theta_{\text{refine}},\, i = 1, \ldots, N_{T^{(k)}}\}$$
$$X^{(k)}_{\text{coarse}} = \{\boldsymbol{x}_i^{(k)} \in X^{(k)} \,:\, \xi(\boldsymbol{t}_i^{(k)}) < \theta_{\text{coarse}},\, i = 1, \ldots, N_{T^{(k)}}\}$$

3.6: Construct the set

$$X^{(k+1)} = \left\{X^{(k)} \cup X^{(k)}_{\text{refine}}\right\} \setminus X^{(k)}_{\text{coarse}}$$

5. NUMERICAL EXPERIMENTS

In this section, we analyze computational accuracy and efficiency of the residual subsampling scheme, which is implemented in MATLAB for adaptive 1D and 2D interpolation. All programs are run on a laptop with an Intel(R) Core(TM) i7-1065G7 CPU 1.50 GHz processor with 16 GB RAM.

In these tests we highlight the performance of k-fold CV algorithms including LOOCV as a special case, firstly focusing on approximation error and computational time and then emphasizing on iteration number (# iter), final number of points required to achieve convergence (N_{fin}), and conditioning of the kernel matrix (cond(A_ε)). Furthermore, we also compare numerical results obtained by considering a benchmark MATLAB implementation of LOOCV via `crossval` routine and those deriving from the adaptive method in [12]. To show how the adaptive CV based methods work, we consider various types of radial kernels involving both infinity and finite regularity like GA, IMQ, M6, M4 and M2. In such a case, we select the shape parameter ε as discussed in Section 3. In particular, the optimal values of the shape parameter are found by minimizing a cost function via the MATLAB `fminbnd` routine with a default tolerance of 10^{-4} and searching ε in the range $[0.2, 20]$.

To analyze the precision of the adaptive scheme, we compute the root mean square error (RMSE), i.e.,

$$\text{RMSE} = \frac{1}{\sqrt{N_e}}||f - s||_2 = \sqrt{\frac{1}{N_e}\sum_{i=1}^{N_e}[f(\boldsymbol{\xi}_i) - s(\boldsymbol{\xi}_i)]^2},$$

where the $\boldsymbol{\xi}_i$ is a uniform (equally-spaced or gridded) data set consisting of N_e evaluation points.

The matrix conditioning in (2.8) is estimated by using the MATLAB `cond` command, whereas the execution or CPU time of the adaptive algorithm is computed in seconds. We remark that the CPU time reported in this article is the result of an average obtained by sequentially running the code 100 times.

5.1. **Results in 1D interpolation.** In this subsection, we focus on adaptive 1D interpolation. All these tests are carried by starting from an initial point set $X^{(0)} \equiv X$, which consists of $N^{(0)} = 13$ equally-spaced points in the interval $\Omega = [-1, 1]$. Then, to connect the sets $X^{(k)}$ and $T^{(k)}$ within the adaptive method, for $k \geq 0$, we define the set $T^{(k)}$ of test points that are the midpoints taken from (sorted) interpolation nodes, i.e.

$$T^{(k)} = \{t_i^{(k)} = 0.5(x_i^{(k)} + x_{i+1}^{(k)}),\ i = 1, \ldots, N^{(k)} - 1\}.$$

The threshold values are assumed to be equal to $\theta_{\text{refine}} = 10^{-6}$ and $\theta_{\text{coarse}} = 10^{-8}$. However, in the comparison among the different residual subsampling algorithms, the refinement threshold θ_{refine} varies, while the coarsening one is kept fixed at the value $\theta_{\text{coarse}} = 10^{-8}$.

In order to validate in depth our adaptive algorithms, we consider the following benchmark target (or test) functions:

$$f_1(x) = \frac{1}{1 + 25x^2}, \qquad f_2(x) = 2\sin(5)\cos\left[\frac{10(x+1)}{2}\right] + \sin\left[\frac{5(x+1)}{2}\right],$$

where f_1 is the Runge function, and f_2 represents a trigonometric function (see [18, 40]).

In Tables 1, 2, 3 and 4, we present the results obtained by applying the adaptive residual subsampling method and using 10-fold CV and LOOCV schemes for the shape parameter choice. From these tables we get some useful information regarding the algorithm execution, i.e. the number of iterations and the final number of points required to achieve convergence. Specifically, we remark that the average approximation error (RMSE) is significantly smaller than the prescribed value θ_{refine}. Moreover, the automatic shape parameter choice also allows us to control the conditioning of the interpolation matrix that is always smaller than 10^{+17}. At the same time, we observe a high level of precision of the numerical method (roughly around the order of 10^{-7} or 10^{-8}). Indeed, taking into consideration the various situations, condition number and execution time assume quite similar values.

kernel	# iter	N_{fin}	RMSE	cond(A_ε)	time
GA	4	53	9.6e-8	2.3e+9	0.5
IMQ	4	51	1.8e-7	1.6e+8	0.4
M6	24	37	2.9e-7	2.3e+14	1.7
M4	5	81	6.1e-8	2.7e+10	0.5
M2	12	107	1.9e-7	6.7e+11	1.1

TABLE 1. Results with 10-fold CV for f_1.

In Tables 5 and 6, we compare our adaptive CV based methods, specifically the 10-fold CV and LOOCV, deriving from extended Rippa's scheme in Subsection 3.1, with the method [12]

kernel	# iter	N_{fin}	RMSE	cond(A_ε)	time
GA	4	51	2.3e-7	1.5e+10	0.4
IMQ	4	51	9.4e-8	8.2e+13	0.4
M6	7	99	1.8e-7	1.3e+8	0.6
M4	11	55	1.6e-7	2.0e+9	0.8
M2	7	99	1.8e-7	1.3e+8	0.6

TABLE 2. Results with LOOCV for f_1.

kernel	# iter	N_{fin}	RMSE	cond(A_ε)	time
GA	2	25	1.6e-7	3.9e+17	0.3
IMQ	3	49	2.1e-8	8.8e+17	0.4
M6	9	52	1.1e-7	4.1e+15	0.7
M4	7	66	2.5e-7	7.2e+15	0.7
M2	12	118	2.5e-7	6.8e+13	1.0

TABLE 3. Results with 10-fold CV for f_2.

kernel	# iter	N_{fin}	RMSE	cond(A_ε)	time
GA	3	20	7.8e-8	2.1e+14	0.3
IMQ	2	25	2.1e-7	1.2e+16	0.3
M6	11	116	2.6e-7	6.1e+13	0.9
M4	10	53	1.8e-7	7.3e+13	0.7
M2	11	116	2.6e-7	6.1e+13	0.9

TABLE 4. Results with LOOCV for f_2.

and another one characterized by the implementation of LOOCV, called LOOCV*, through the MATLAB `crossval` routine, as described in Subsection 3.2. In this experimentation, all tests have been run by M4 kernel. From the variation of the threshold θ_{refine}, we can observe that, on average, 10-fold CV and LOOCV turn out to be comparable to method [12] in terms of both number of nodes and execution time (necessary to achieve convergence). Though deducing the superiority of one approach in regard to another is not easy, we can state that the LOOCV is more efficient than LOOCV*. This fact is clearly evident when the value of θ_{refine} becomes smaller and smaller and so the threshold request is more demanding.

5.2. **Results in 2D interpolation.** In this subsection, we consider adaptive 2D interpolation. These experiments are run by taking an initial node set $X^{(0)} \equiv X$, containing $N^{(0)} = 320$

θ_{refine}	method [12]		10-fold CV		LOOCV		LOOCV*	
	N_{fin}	time	N_{fin}	time	N_{fin}	time	N_{fin}	time
1e-04	33	0.3	33	0.3	33	0.3	31	0.3
1e-05	39	0.4	39	0.3	39	0.3	39	0.4
1e-06	54	1.4	81	0.4	55	0.7	47	1.7

TABLE 5. Comparison among residual subsampling methods using M4 for f_1. Note that * refers to the use of the MATLAB `crossval` routine [31].

θ_{refine}	method [12]		10-fold CV		LOOCV		LOOCV*	
	N_{fin}	time	N_{fin}	time	N_{fin}	time	N_{fin}	time
1e-04	35	0.3	44	0.4	33	0.3	32	0.7
1e-05	44	0.4	48	0.5	45	0.4	45	2.4
1e-06	58	0.7	66	0.6	53	0.6	68	11.8

TABLE 6. Comparison among residual subsampling methods using M4 for f_2. Note that * refers to the use of the MATLAB `crossval` routine [31].

uniformly distributed points on $\Omega = [-1, 1]^2$. Then, we update the node set $X^{(k)}$ by applying the adaptive subsampling procedure described in Section 4. To correlate the interpolation node set $X^{(k)}$ with the corresponding test point set $T^{(k)}$, for $k \geq 0$, we compute the halfway points of $T^{(k)}$, as in [12]. As refinement threshold we set $\theta_{\text{refine}} = 10^{-4}$, while the coarsening threshold is $\theta_{\text{coarse}} = 10^{-8}$.

In our tests we analyze the performance of our algorithms taking the data values by three test functions. The first is known as a Franke-type function [40], i.e.,

$$f_3(x,y) = \exp\left[-0.1\left(x^2+y^2\right)\right] + \exp\left[-5\left((x-0.5)^2+(y-0.5)^2\right)\right] + \exp\left[-15((x+0.2)^2+(y+0.4)^2)\right] + \exp\left[-9\left((x+0.8)^2+(y-0.8)^2\right)\right].$$

The second is a hyperbolic tan function

$$f_4(x,y) = \frac{1}{9}\tanh\left[\frac{9}{2}(y-x)\right] + 1,$$

while the third is the exponential function [40] given by

$$f_5(x,y) = \exp\left[-60((x-0.35)^2+(y-0.25)^2)\right] + 0.2.$$

In Tables 7, 8, 9 and 10, we provide a numerical analysis to show how the adaptive residual subsampling methods based on CV techniques work when they are applied to solve some unknown functions characterized by quick variations in the domain Ω. As already done in the one dimensional case, in the above-mentioned tables we provide a detailed summary regarding the performance of the bivariate algorithm. Specifically, it collects the number of iterations needed to get convergence, the corresponding final number of nodes, the approximation error, the condition number of the kernel matrix and the total CPU time. From this study we point

out that both methods, involving 10-fold CV and LOOCV, enable the algorithm to converge in a relatively small number of iterations (namely, between 1 and 5). Moreover, the adaptive procedure is able to avoid an excessive additions of points because – in all considered examples – the final number of nodes is always less than 1000. This fact has a twofold importance: on the one hand the conditioning is kept under control, on the other the executing time takes a few seconds only. As regards the CPU time, we point the reader out that the type of radial kernel and so its smoothness can influence the convergence speed of the numerical scheme, which is subjected to an automatic addition or removal of points.

kernel	# iter	N_{fin}	RMSE	cond(A_ε)	time
GA	2	386	9.6e-6	5.1e+17	1.3
IMQ	2	321	5.0e-6	7.4e+15	1.0
M6	2	681	6.3e-6	3.2e+13	3.3
M4	3	496	1.5e-5	1.2e+13	2.5
M2	5	852	2.3e-5	7.9e+8	9.9

TABLE 7. Results with 10-fold CV for f_3.

kernel	# iter	N_{fin}	RMSE	cond(A_ε)	time
GA	2	550	3.1e-7	1.2e+19	2.3
IMQ	1	315	7.4e-6	9.7e+12	0.5
M6	3	369	2.0e-5	5.9e+14	2.1
M4	5	508	2.1e-5	7.7e+9	4.3
M2	4	860	2.3e-5	7.9e+8	5.4

TABLE 8. Results with LOOCV for f_3.

kernel	# iter	N_{fin}	RMSE	cond(A_ε)	time
GA	3	806	1.8e-5	2.3e+13	5.1
IMQ	2	654	9.3e-6	3.7e+11	2.2
M6	2	623	1.1e-5	2.6e+8	2.8
M4	2	622	6.3e-6	8.1e+8	2.4
M2	3	690	1.3e-5	1.5e+7	4.7

TABLE 9. Results with 10-fold CV for f_4.

kernel	# iter	N_{fin}	RMSE	cond(A_ε)	time
GA	3	938	1.2e-5	7.0e+11	5.9
IMQ	1	320	2.4e-5	7.4e+11	0.6
M6	4	387	1.4e-5	5.1e+9	2.4
M4	3	428	1.0e-5	1.2e+9	2.0
M2	4	593	1.4e-5	4.9e+7	4.8

TABLE 10. Results with LOOCV for f_4.

Finally, in order to highlight the benefit coming from the use of the new adaptive scheme, we conclude this section by making a comparison among different k-fold CV methods. In Table 11 we report the numerical results obtained by considering some specific values of k in the k-fold CV. Indeed, in this study we assume $k = 5, 25, 50, 100$ and $k = N$, where the latter results in the particular case of LOOCV. From this table, we can observe that all the CV techniques produce good results. The main differences in the algorithm performance seems to be dependent on the kind of radial kernel used. Conversely, for a fixed kernel, as evident focusing on each row of Table 11, the final number of interpolation points (required to satisfy the thresholds θ_{refine} and θ_{coarse}) and the CPU time are enough similar. In conclusion, these numerical experiments for 2D adaptive interpolation show that the use of CV techniques are efficient and effective for the selection of the kernel shape parameter but, at the same time, it is not possible to declare a clear and complete superiority of a CV scheme compared to other ones.

kernel	5-fold CV		25-fold CV		50-fold CV		100-fold CV		LOOCV	
	N_{fin}	time	N_{fin}	time	N_{fin}	time	N_{fin}	time	N_{fin}	time
GA	1243	13.1	1420	33.4	1330	19.6	1327	9.7	1231	9.7
IMQ	824	3.5	881	4.7	806	4.0	800	4.0	1053	7.4
M6	780	4.7	782	5.1	783	5.1	783	5.1	784	5.1
M4	683	7.2	683	7.6	684	7.0	689	7.7	682	7.0
M2	846	11.7	818	11.6	816	10.7	818	11.8	828	11.8

TABLE 11. Comparison among different k-fold CV methods for f_5.

6. CONCLUSIONS

In this work, we proposed the use of various CV criteria for selecting optimal kernel shape parameters within the adaptive residual subsampling method. More precisely, we focused on extended Rippa's scheme, considering k-fold CV and LOOCV as a special case. The application of such strategies in an interpolation framework showed that CV based techniques are valid alternative compared to other computational methods such as maximum likelihood estimation approaches. Indeed, the resulting CV based schemes revealed good level of flexibility and accuracy, also turning out to be more efficient than commonly used MATLAB routines.

As future work we expect to extend the application area of the adaptive CV based schemes to variably scaled kernels and discontinuous functions (see e.g. [2, 17, 27, 28]). Moreover, we also consider the chance to implement efficient residual subsampling algorithms for partition of unity methods (see e.g. [4, 7, 9]).

Acknowledgments

The authors sincerely thank the reviewers for their constructive and valuable comments. This work has been supported by the INdAM Research group GNCS as part of the GNCS-INdAM 2024 project "Metodi kernel e polinomiali per l'approssimazione e l'integrazione: teoria e software applicativo". The work of R.C. and D.M. has been supported by the Spoke 1 "FutureHPC & BigData"of ICSC - Centro Nazionale di Ricerca in High-Performance Computing, Big Data and Quantum Computing, funded by European Union - NextGenerationEU. Moreover, the work has been supported by the Fondazione CRT, project 2022 "Modelli matematici e algoritmi predittivi di intelligenza artificiale per la mobilità sostenibile". This research has been accomplished within the RITA "Research ITalian network on Approximation", the UMI Group TAA "Approximation Theory and Applications", and the SIMAI Activity Group ANA&A "Numerical and Analytical Approximation of Data and Functions with Applications". The work of A.N. has financially been supported by the National Science and Technology Council of Taiwan under grant numbers 112-2811-E-002-020-MY3.

References

[1] M. Bozzini, L. Lenarduzzi and R. Schaback: *Adaptive interpolation by scaled multiquadrics*, Adv. Comput. Math., **16** (2002), 375–387.
[2] M. Bozzini, L. Lenarduzzi, M. Rossini and R. Schaback: *Interpolation with variably scaled kernels*, IMA J. Numer. Anal., **35** (2015), 199–219.
[3] M. D. Buhmann: *Radial Basis Functions: Theory and Implementation*, Cambridge Monogr. Appl. Comput. Math., vol. 12, Cambridge Univ. Press, Cambridge (2003).
[4] R. Cavoretto, A. De Rossi, E. Perracchione and E. Venturino: *Reliable approximation of separatrix manifolds in competition models with safety niches*, Int. J. Comput. Math., **92** (2015), 1826–1837.
[5] R. Cavoretto, A. De Rossi: *A two-stage adaptive scheme based on RBF collocation for solving elliptic PDEs*, Comput. Math. Appl., **79** (2020), 3206–3222.
[6] R. Cavoretto, A. De Rossi: *Adaptive refinement procedures for meshless RBF unsymmetric and symmetric collocation methods*, Appl. Math. Comput., **382** (2020), 125354.
[7] R. Cavoretto: *Adaptive radial basis function partition of unity interpolation: A bivariate algorithm for unstructured data*, J. Sci. Comput., **87** (2021), Article ID: 41.
[8] R. Cavoretto, A. De Rossi, M. S. Mukhametzhanov and Y. D. Sergeyev: *On the search of the shape parameter in radial basis functions using univariate global optimization methods*, J. Global Optim., **79** (2021), 305–327.
[9] R. Cavoretto, A. De Rossi and W. Erb: *Partition of unity methods for signal processing on graphs*, J. Fourier Anal. Appl., **27** (2021), Article ID: 66.
[10] R. Cavoretto: *Adaptive LOOCV-based kernel methods for solving time-dependent BVPs*, Appl. Math. Comput., **429** (2022), Article ID: 127228.
[11] R. Cavoretto, A. De Rossi, A. Sommariva and M. Vianello: *RBFCUB: A numerical package for near-optimal meshless cubature on general polygons*, Appl. Math. Lett., **125** (2022), Article ID: 107704.
[12] R. Cavoretto, A. De Rossi: *An adaptive residual sub-sampling algorithm for kernel interpolation based on maximum likelihood estimations*, J. Comput. Appl. Math., **418** (2023), Article ID: 114658.
[13] R. Cavoretto, A. De Rossi and S. Lancellotti: *Bayesian approach for radial kernel parameter tuning*, J. Comput. Appl. Math., **441** (2024), Article ID: 115716.
[14] R. Cavoretto, A. De Rossi, F. Dell'Accio, F. Di Tommaso, N. Siar, A. Sommariva and M. Vianello: *Numerical cubature on scattered data by adaptive interpolation*, J. Comput. Appl. Math., **444** (2024), Article ID: 115793.
[15] R. Cavoretto, A. De Rossi, A. Haider and S. Lancellotti: *Comparing deterministic and statistical optimization techniques for the shape parameter selection in RBF interpolation*, Dolomites Res. Notes Approx., **17** (2024), 48–55.
[16] A. Celisse, S. Robin: *Nonparametric density estimation by exact leave-p-out cross-validation*, CSDA, **52** (2008), 2350–2368.

[17] S. De Marchi: *Padua points and fake nodes for polynomial approximation: old, new and open problems*, Constr. Math. Anal., **5** (2022), 14–36.
[18] T. A. Driscoll, A. R. H. Heryudono, *Adaptive residual subsampling methods for radial basis function interpolation and collocation problems*, Comput. Math. Appl., **53** (2007), 927–939.
[19] G. E. Fasshauer: *Meshfree Approximation Methods with MATLAB*, Interdisciplinary Mathematical Sciences, vol. 6, World Scientific Publishing Co., Singapore (2007).
[20] G. E. Fasshauer: *Positive definite kernels: Past, present and future*, Dolomites Res. Notes Approx., **4** (2011), 21–63.
[21] G. E. Fasshauer, M. J. McCourt: *Kernel-based Approximation Methods using MATLAB*, Interdisciplinary Mathematical Sciences, Vol. 19, World Scientific Publishing Co., Singapore (2015).
[22] G. E. Fasshauer, J. G. Zhang: *On choosing "optimal" shape parameters for RBF approximation*, Numer. Algorithms, **45** (2007), 345–368.
[23] B. Fornberg, J. Zuev: *The Runge phenomenon and spatially variable shape parameters in RBF interpolation*, Comput. Math. Appl., **54** (2007), 379–398.
[24] K. Gao, G. Mei, S. Cuomo, F. Piccialli and N. Xu: *ARBF: adaptive radial basis function interpolation algorithm for irregularly scattered point sets*, Soft Computing, **24** (2020), 17693–17704.
[25] A. Golbabai, E. Mohebianfar and H. Rabiei: *On the new variable shape parameter strategies for radial basis functions*, Comput. Appl. Math., **34** (2015), 691–704.
[26] F. J. Hickernell, Y. C. Hon: *Radial basis function approximations as smoothing splines*, Appl. Math. Comput., **102** (1999), 1–24.
[27] M. Karimnejad Esfahani, S. De Marchi and F. Marchetti: *Moving least squares approximation using variably scaled discontinuous weight function*, Constr. Math. Anal., **6** (2023), 38–54.
[28] L. Lenarduzzi, R. Schaback: *Kernel-based adaptive approximation of functions with discontinuities*, Appl. Math. Comput., **307** (2017), 113–123.
[29] L. Ling, F. Marchetti: *A stochastic extended rippa's algorithm for LpOCV*, Appl. Math. Lett., **129** (2022), Article ID: 107955.
[30] F. Marchetti: *The extension of Rippa's algorithm beyond LOOCV*, Appl. Math. Lett., **120** (2021), Article ID: 107262.
[31] MATLAB version: *9.13.0.2553342 (R2022b) Update 9*, Natick, Massachusetts, The MathWorks Inc. (2022).
[32] A. Noorizadegan, C.-S. Chen, R. Cavoretto and A. De Rossi: *Efficient truncated randomized SVD for mesh-free kernel methods*, Comput. Math. Appl., **164** (2024), 12–20.
[33] A. Noorizadegan, R. Schaback: *Introducing the evaluation condition number: A novel assessment of conditioning in radial basis function methods*, Eng. Anal. Bound. Elem., **166** (2024), Article ID: 105827.
[34] S. Rippa: *An algorithm for selecting a good value for the parameter c in radial basis function interpolation*, Adv. Comput. Math., **11** (1999), 193–210.
[35] R. Schaback: *Error estimates and condition numbers for radial basis function interpolation*, Adv. Comput. Math., **3** (1995), 251–264.
[36] M. Scheuerer: *An alternative procedure for selecting a good value for the parameter c in RBF-interpolation*, Adv. Comput. Math., **34** (2011), 105–126.
[37] M. Scheuerer, R. Schaback and M. Schlather: *Interpolation of spatial data – A stochastic or a deterministic problem?*, European J. Appl. Math., **24** (2013), 601–629.
[38] G. K. Veni, C. Satyanarayana and M. C. Krishnareddy: *Residual error based adaptive method with an optimal variable scaling parameter for RBF interpolation*, International Journal of Applied Mechanics and Engineering, **28** (2023), 37–46.
[39] H. Wendland: *Scattered Data Approximation*, Cambridge Monogr. Appl. Comput. Math., vol. 17, Cambridge Univ. Press, Cambridge (2005).
[40] Q. Zhang, Y. Zhao and J. Levesley: *Adaptive radial basis function interpolation using an error indicator*, Numer. Algorithms, **76** (2017), 441–471.

ROBERTO CAVORETTO
UNIVERSITY OF TURIN
DEPARTMENT OF MATHEMATICS "GIUSEPPE PEANO "
VIA CARLO ALBERTO 10, 10123, TURIN, ITALY
ORCID: 0000-0001-6076-4115
Email address: roberto.cavoretto@unito.it

ADEEBA HAIDER
UNIVERSITY OF TURIN
DEPARTMENT OF MATHEMATICS "GIUSEPPE PEANO "
VIA CARLO ALBERTO 10, 10123, TURIN, ITALY
ORCID: 0009-0001-4198-1808
Email address: adeeba.haider@unito.it

SANDRO LANCELLOTTI
UNIVERSITY OF TURIN
DEPARTMENT OF MATHEMATICS "GIUSEPPE PEANO "
VIA CARLO ALBERTO 10, 10123, TURIN, ITALY
ORCID: 0000-0003-4253-3561
Email address: sandro.lancellotti@unito.it

DOMENICO MEZZANOTTE
UNIVERSITY OF TURIN
DEPARTMENT OF MATHEMATICS "GIUSEPPE PEANO "
VIA CARLO ALBERTO 10, 10123, TURIN, ITALY
ORCID: 0000-0001-5154-6538
Email address: domenico.mezzanotte@unito.it

AMIR NOORIZADEGAN
NATIONAL TAIWAN UNIVERSITY
DEPARTMENT OF CIVIL ENGINEERING
10617, TAIPEI, TAIWAN
ORCID: 0000-0003-3191-0990
Email address: amirnoori23@ntu.edu.tw

CONSTRUCTIVE MATHEMATICAL ANALYSIS
7 (2024), No. SI, pp. 93-113
http://dergipark.org.tr/en/pub/cma
ISSN 2651 - 2939

Research Article

Maxwell orthogonal polynomials

Dedicated to Professor Paolo Emilio Ricci, on occasion of his 80th birthday, with respect and friendship.

ÁNGEL ÁLVAREZ-PAREDES*, RUYMÁN CRUZ-BARROSO, AND FRANCISCO MARCELLÁN

ABSTRACT. In the framework of the theory of semiclassical linear functionals in this contribution, we deal with the sequence of orthogonal polynomials associated with the linear functional $\langle L, p\rangle = \int_0^\infty p(x)e^{-x^2}dx$, where $p \in \mathbb{P}$, the linear space of polynomials with complex coefficients. The class of L is one and we deduce a differential/difference equation (structure relation) for the sequence of orthogonal polynomials. The Laguerre-Freud equations that the coefficients of the three term recurrence relation satisfy are deduced. The connection with discrete Painlevé IV equations is emphasized. Finally, we analyze the lowering and raising operators (ladder operators) for such polynomials in order to find a second order linear differential equation they satisfy. As a consequence, an electrostatic interpretation of their zeros is formulated.

Keywords: Maxwell linear functional, Stieltjes function, Pearson equation, Ladder operators, Laguerre-Freud equations, electrostatic interpretation, Painlevé equations.

2020 Mathematics Subject Classification: 42C05, 33C50.

1. INTRODUCTION

Let consider the sequence of orthogonal polynomials associated with a linear functional L defined from a weight function $w(x) = e^{-x^2}$ supported on the positive real semi-axis by $\langle L, p\rangle = \int_0^\infty p(x)e^{-x^2}dx$. The linear functional belongs to a wide class called semiclassical ([13]). Indeed, they are semiclassical of class $s = 1$. The concept of class allows to introduce a hierarchy of linear functionals that constitutes an alternative to the Askey tableau based on the hypergeometric character of the corresponding sequence of orthogonal polynomials. Semiclassical orthogonal polynomials appear in the seminal paper [16], where weight functions whose logarithmic derivatives are rational functions were considered. A second order linear differential equation that the corresponding sequence of orthogonal polynomials is obtained. The theory of semiclassical orthogonal polynomials has been developed by P. Maroni (see [12, 13]) and combine techniques of functional analysis, distribution theory, z and Fourier transforms, ordinary differential equations, among others, in order to deduce algebraic and structural properties of such polynomials. Many of the most popular families of orthogonal polynomials coming from Mathematical Physics as Hermite, Laguerre, Jacobi and Bessel are semiclassical (of class $s = 0$) but other families appearing in the literature are also semiclassical. For instance, semiclassical families of class $s = 1$ are described in [1]. As a sample in [7] truncated Hermite polynomials associated with the normal distribution supported on a symmetric interval of the real line have been considered. They are semiclassical of class $s = 2$.

Received: 09.07.2024; Accepted: 03.11.2024; Published Online: 16.12.2024
*Corresponding author: Francisco Marcellán; pacomarc@ing.uc3m.es
DOI: 10.33205/cma.1513303

The coefficients of the three term relation satisfied by orthogonal polynomials associated with a semiclassical linear functional satisfy coupled non linear difference equations (Laguerre-Freud equations, see [2]) which are related to discrete Painlevé equations, see [11, 17] among others. On the other hand, ladder operators (lowering and raising) are associated with semi-classical orthogonal polynomials. Their construction is based on the so called first structure relation , see [13], they satisfy. As a consequence, you can deduce a second order linear differential equation that the polynomials satisfy. Notice that the coefficients are polynomials with degrees depending of the class.

In the framework of random matrices, several authors have considered Gaussian unitary ensembles with one or two discontinuities (see [10]). Therein it is proved that the logarithmic derivative of the Hankel determinants generated by the normal (Gaussian) weight with two jump discontinuities in the scaled variables tends to the hamiltonian of a coupled Painlevé II system and it satisfies a second order PDE. The asymptotics of the coefficients of the three term recurrence relation for the corresponding orthogonal polynomials is deduced. They are related to the solutions of the coupled Painlevé II system. The techniques are based on the analysis of ladder operators associated with such orthogonal polynomials. For more information, see [3, 4].

Integrable systems also provide nice examples of semiclassical orthogonal polynomials. They are related to time perturbations of a weight function (Toda, Langmuir lattices). For more information, see [18].

It is important to highlight that, according to S. Belmehdi and A. Ronveaux (see [2]), the MOPS associated with the linear functional L defined as above is known as the family of Maxwell polynomials. Nevertheless, in the literature, the name Maxwell polynomials is quoted when you deal with the weight function $\omega(x) = x^2 e^{-x^2}$, supported on the positive real semi-axis (see, for instance, [6]). They appear in many problems of kinetic theory since involve the evaluation of averages over a Maxwellian distribution function $f^M(c)$, where c is the particle speed. The equilibrium average value of a function $F(c)$ is defined by

$$\overline{F} = \int f^M(c) F(c) dc = \frac{4}{\sqrt{\pi}} \int_0^\infty x^2 e^{-x^2} F(x) dx.$$

Here $f^M(c) = (m/2\pi kT)^{3/2} e^{-mc^2/2kT}$, m is the mass and $x = (m/2kT)^{1/2}$ is the dimesionless speed. They are called speed polynomials.

In the literature, see [15], among others, Gaussian quadrature rules are analyzed for weight functions $w(x) = x^p e^{-x^2}$ supported on the positive real semi-axis. They constitute an useful tool in the solution of the Boltzman and/or Fokker-Planck equations. It is important to point out that the coefficients of the three term recurrence relations for the corresponding sequences of orthogonal polynomials satisfy nonlinear equations which are numerically unstable. In [15] extended precision arithmetic is used to generate the recurrence coefficients to high order. As a consequence, the polynomials and associated quadrature weights and nodes are deduced.

Maxwell polynomials are used in various fields for different purposes, such as in pseudo-spectral collocation schemes. Among the numerous characteristics that make these polynomials desirable for pseudo-spectral discretization schemes for the velocity variable, one may emphasize their capability to handle semi-infinite intervals, the convenient distribution of their zeros that balances clustering around zero, where increased resolution is often needed, with the sampling at increasingly larger distances from the origin, and their optimal location for the computation of integrals involving a Maxwell-Boltzmann distribution. For further details, see [9, 14].

On the other hand, strong asymptotic properties of orthogonal polynomials with respect to weights $\omega(x) = x^{\alpha}e^{-Q(x)}$, where $\alpha > -1$ and Q is a polynomial of degree m with positive leading coefficient, have been analyzed in [19]. An application to prove universality in random matrix theory is also provided therein.

The presentation is structured as follows. In Section 2, a basic background concerning linear functionals, orthogonal polynomials is given. The semiclassical case is emphasized. Section 3 deals with the Pearson equation associated with the Maxwell linear functional. As a consequence you get the first order linear differential equation that the Stieltjes function satisfy. Section 4 focuses the attention on the Laguerre-Freud equations satisfied by the coefficients of the three-term recurrence relation associated with the Maxwell polynomials. The connection with discrete IV Painlevé equation is stated. Finally, in Section 5, the expressions of the ladder operators are given as well as the second order linear differential equation these polynomials satisfy. The electrostatic interpretation of their zeros is deduced.

2. Basic background

Let $\mathbb{P}$ be the linear space of polynomials in one variable with complex coefficients and let $\mathbb{P}_n$ be the $(n+1)$-dimensional subspace of polynomials of degree less than or equal to n. Let $L : \mathbb{P} \to \mathbb{C}$ be a linear functional and denote by μ_n the moments of L on the monomial basis:

$$L[x^n] = \langle L, x^n\rangle := \mu_n. \tag{2.1}$$

A sequence $\{p_n\}_{n\geq 0}$, with $p_n \in \mathbb{P}_n\backslash\mathbb{P}_{n-1}$ for all $n \geq 0$ ($\mathbb{P}_{-1} = \emptyset$), is said to be an orthogonal polynomial sequence (OPS) with respect to L if

$$\langle L, p_k p_n\rangle = h_n\delta_{k,n}, \quad k, n \in \mathbb{N}\cup\{0\}, \quad h_n \neq 0, \tag{2.2}$$

where $\delta_{k,n}$ denotes the Kronecker delta symbol. We will denote by $\{P_n\}_{n\geq 0}$ the OPS with P_n monic, for all $n \geq 0$ (MOPS) and by $\{\tilde{p}_n\}_{n\geq 0}$ the orthonormal family (ONPS) i.e., $h_n = 1$ in (2.2), for all $n \geq 0$ (this family is unique under the condition that all the leading coefficients are positive).

We recall (see [5]) that a linear functional L defined on $\mathbb{P}$ is said to be quasi-definite if an OPS with respect to L exists. A quasi-definite linear functional L is positive-definite when $h_n > 0$ in (2.2), $n \geq 0$. In this case, L can be represented in terms of a positive Borel measure μ supported on the real line as $\langle L, p\rangle = \int_{\mathbb{R}} p(x)d\mu(x)$ for $p \in \mathbb{P}$, L has real moments and thus, MOPS and ONPS have real coefficients. Also, the zeros of p_n are real, distinct, located in the interior of the convex hull of the support of μ and they interlace with those of p_{n+1}.

It is very well known that MOPS and ONPS satisfy three term recurrence relations (TTRR).

Theorem 2.1. *Let $\{P_n\}_{n\geq 0}$ and $\{\tilde{p}_n\}_{n\geq 0}$ be the MOPS and ONPS with respect to the linear functional L given by (2.1), respectively. Define $\alpha_n = \frac{\langle L, xP_n^2\rangle}{\langle L, P_n^2\rangle}$, $\forall n \geq 0$, and $\beta_m = \frac{\langle L, P_m^2\rangle}{\langle L, P_{m-1}^2\rangle} > 0$, $\forall m \geq 1$. Setting $P_{-1}(x) \equiv \tilde{p}_{-1}(x) \equiv 0$, $P_0(x) \equiv 1$ and $\tilde{p}_0(x) \equiv \frac{1}{\sqrt{\mu_0}}$, then it holds for all $n \geq 0$,*

$$P_{n+1}(x) = (x - \alpha_n)\, P_n(x) - \beta_n P_{n-1}(x), \tag{2.3}$$

$$x\tilde{p}_n(x) = \sqrt{\beta_{n+1}}\tilde{p}_{n+1}(x) + \alpha_n\tilde{p}_n(x) + \sqrt{\beta_n}\tilde{p}_{n-1}(x). \tag{2.4}$$

We consider also the reproducing kernel $K_n(x, y) = \sum_{k=0}^{n}\tilde{p}_k(x)\tilde{p}_k(y)$, that satisfies the reproducing property $\langle L_y, K_n(x, y)q(y)\rangle = \int K_n(x, y)q(y)\, d\mu(y) = q(x)$, for all $q \in \mathbb{P}_n$. The well

known Christoffel-Darboux and confluent formulas are

$$K_n(x,y) = \sqrt{\beta_{n+1}} \cdot \frac{\tilde{p}_{n+1}(x)\tilde{p}_n(y) - \tilde{p}_n(x)\tilde{p}_{n+1}(y)}{x-y}, \qquad x \neq y, \tag{2.5}$$

$$K_n(x,x) = \sqrt{\beta_{n+1}} \cdot \left[\tilde{p}'_{n+1}(x)\tilde{p}_n(x) - \tilde{p}'_n(x)\tilde{p}_{n+1}(x)\right] > 0, \tag{2.6}$$

respectively.

The following definition of D-semiclassical linear functionals (with respect to the derivative operator) is a natural generalization of the D-classical functionals.

Definition 2.1. *A quasi-definite functional L is said to be semiclassical if there exist nonzero polynomials ϕ and ψ, where ϕ is monic, $\deg\phi \geq 0$, and $\deg\psi \geq 1$, such that L satisfies the distributional Pearson equation*

$$D(\phi L) = \psi L. \tag{2.7}$$

Furthermore, an OPS associated with L is called a semiclassical sequence of orthogonal polynomials. Recall that the adjoints of the derivative and multiplication operators are $\langle DL, p\rangle = -\langle L, p'\rangle$ and $\langle xL, p\rangle = \langle L, xp\rangle$, respectively (see [13]*).*

One can observe that $\deg\psi \geq 1$. Indeed, if $\psi(x) = \psi_0 \neq 0$, then

$$0 = -\langle \phi L, 0\rangle = \langle D(\phi L), 1\rangle = \langle \psi L, 1\rangle = \langle L, \psi\rangle = \psi_0\mu_0 \quad \text{with} \quad \mu_0 = \langle L, 1\rangle .$$

Thus, $\mu_0 = 0$, contradicting the quasi-definiteness of L. Clearly, we also need the polynomial ϕ to be nonzero in order to guarantee that L is quasi-definite. To prevent any potential conflict arising from the quasi-definite nature of the semiclassical functional L, a new requirement has to be imposed: if $\phi(x) = \sum_{k=0}^{r} a_k x^k$ and $\psi(x) = \sum_{k=0}^{t} b_k x^k$ ($r \geq 0$, $t \geq 1$), then for any $n \geq 0$ it must hold $na_r + b_{r-1} \neq 0$ when $r = t+1$, to ensure that all the moments are well defined. Indeed, from (2.7) we can write $\langle D(\phi L), x^n\rangle = \langle \psi u, x^n\rangle$, which implies $\langle u, n\phi x^{n-1} + \psi x^n\rangle = 0$ for all $n \geq 0$. So, the Pearson equation is equivalent for $n \geq 0$ in this case to

$$n \cdot \sum_{k=0}^{r} a_k \mu_{n+k-1} + \sum_{k=0}^{r-1} b_k \mu_{n+k} = 0,$$

implying

$$(na_r + b_{r-1})\mu_{n+r-1} = -\sum_{k=0}^{r-2} (na_{k+1} + b_k)\mu_{n+k} - na_0\mu_{n-1}, \quad n \geq 0.$$

Consequently, if there is n_0 such that $n_0 a_r + b_{r-1} = 0$, we see that μ_{n_0+r-1} cannot be computed from the previous identity. This circumstance may potentially give inconsistencies with the quasi-definiteness of L. When L is semiclassical, it is possible that (2.7) not to be minimal due to the non-uniqueness of the polynomials ϕ and ψ. Specifically, for any non-zero polynomial q, one can see that

$$D(q\phi L) = q'\phi L + qD(\phi L) = q'\phi L + q\psi L = (q'\phi + q\psi)L.$$

Therefore, L satisfies $D(\tilde{\phi}L) = \tilde{\psi}L$, with $\tilde{\phi} = q\phi$ and $\tilde{\psi} = q'\phi + q\psi$. Moreover,

$$\deg(q\phi) = \deg q + \deg\phi \ \text{ and } \ \deg(q'\phi + q\psi) = \deg q + \max\left\{\deg\phi - 1, \deg\psi\right\}.$$

Therefore, a semiclassical linear functional exhibits various Pearson equations based on the choices of polynomials ϕ and ψ. Defining the class of a semiclassical linear functional L stems from the minimum degree choices of ϕ and ψ, given by

$$s(L) = \min\max\left\{\deg\phi - 2, \deg\psi - 1\right\},$$

where the minimum is taken among all pairs of polynomials ϕ and ψ such that (2.7) holds. It is noteworthy that D-classical linear functionals, such as Hermite, Laguerre, Jacobi, and Bessel polynomials, fall under the category of semiclassical ones with class $s = 0$. In this respect, a proof of the following two results can be found in [13].

Theorem 2.2. *For any semiclassical linear functional L, the polynomials ϕ and ψ in (2.7) such that $s(L) = \max\{\deg\phi - 2, \deg\psi - 1\}$ are unique up to a constant factor.*

Proposition 2.1. *Let L be a semiclassical linear functional and let ϕ and ψ be nonzero polynomials, with $\deg\phi = r$ and $\deg\psi = t$, such that (2.7) is satisfied. Consider $s = \max\{r - 2, t - 1\}$. Then $s = s(L)$, if and only if*

$$\prod_{c:\ \phi(c)=0} \left(|\psi(c) - \phi'(c)| + \left|\langle L, \theta_c\psi(x) - \theta_c^2\phi(x)\rangle\right|\right) > 0,$$

where

$$\theta_c q(x) := \frac{q(x) - q(c)}{x - c}, \quad q \in \mathbb{P}.$$

We can consider from the moment sequence its z-transform, that yields a formal power series

$$S(z) = \sum_{n=0}^{\infty} \frac{\mu_n}{z^{n+1}} \tag{2.8}$$

that is referred in the literature as Stieltjes function (see [8, 13]). Semiclassical functionals are introduced alongside various characterizations. It is worth noting that some of these characterizations naturally extend the criteria used for defining class functions. We refer to [8, 13] for the proof of the following:

Proposition 2.2. *Let L be a quasi-definite functional, $\{P_n\}_{n\geq 0}$ its associated MOPS and s a nonnegative integer. The following statements are equivalent:*

(1) L is semiclassical of class s.

(2) There exist two non-zero polynomials ϕ and ψ, with $\deg\phi = r \geq 0$ and $\deg\psi = t \geq 1$, such that the Stieltjes function S associated with L given by (2.8) satisfies $\phi\mathcal{S}' + (\phi' - \psi)\mathcal{S} = C$, with $C = L\cdot\theta_0(\phi' - \psi) + DL\cdot\theta_0\phi$, where ϕ, $\phi' - \psi$ and C are coprime (they do not share common zeros). Notice that

$$L\cdot q(x) := \langle L, \frac{xq(x) - yq(y)}{x - y}\rangle, \quad q \in \mathbb{P}.$$

(3) There exist a monic polynomial ϕ, $\deg\phi = r$, with $0 \leq r \leq s + 2$, such that

$$\phi(x)P'_{n+1}(x) = \sum_{k=n-s}^{n+r} \lambda_{n+1,k}P_k(x), \quad n \geq s, \quad \lambda_{n+1,n-s} \neq 0. \tag{2.9}$$

If $s \geq 1$, $r \geq 1$, and $\lambda_{s+1,0} \neq 0$, then s is the class of L.

Now, using the TTRR (2.3) for MOPS, (2.9) can be rewritten in a shorter form (see [13]):

Theorem 2.3. *Let L be a semiclassical functional of class s and $\{P_n\}_{n\geq 0}$ its corresponding MOPS. Then it holds (lowering operator)*

$$\left[\phi(x)D_x - \frac{C_{n+1}(x) - C_0(x)}{2}\right] P_{n+1}(x) = -D_{n+1}(x)P_n(x), \quad n \geq 0, \tag{2.10}$$

where $\{C_n\}_{n\geq 0}$ *and* $\{D_n\}_{n\geq 0}$ *satisfy*

$$C_0(x) = -\psi(x) + \phi'(x), \quad C_{n+1}(x) = -C_n(x) + \frac{2D_n(x)}{\beta_n}(x-\alpha_n), \quad n \geq 0, \tag{2.11}$$

with $D_{-1} = 0$, $D_0 = (L\cdot\theta_0\phi)' - (L\cdot\theta_0\psi)$ *and*

$$D_{n+1}(x) = -\phi(x) + \frac{\beta_n}{\beta_{n-1}}D_{n-1}(x) + (x-\alpha_n)^2\frac{D_n(x)}{\beta_n} - (x-\alpha_n)C_n(x), \quad n \geq 0.$$

The expressions of the previous theorem lead to the so-called ladder operators associated with the semiclassical functional L. Indeed, using (2.11) and the TTRR (2.9), we can deduce from (2.10) that the raising operator is given by

$$\left[\phi(x)D_x + \frac{C_{n+2}(x) + C_0(x)}{2}\right]P_{n+1}(x) = \frac{D_{n+1}(x)}{\beta_{n+1}}P_{n+2}(x), \quad n \geq 0.$$

This relation, together with (2.11) are essential to deduce a second-order linear differential equation satisfied by the polynomials $\{P_n\}_{n\geq 0}$ (see [8, 13]):

$$J(x,n)P''_{n+1}(x) + K(x,n)P'_{n+1}(x) + M(x,n)P_{n+1}(x) = 0, \quad n \geq 0,$$

where, for $n \geq 0$,

$$\begin{aligned}
J(x,n) &= \phi(x)D_{n+1}(x),\\
K(x,n) &= (\phi'(x) + C_0(x))D'_{n+1}(x) - \phi(x)D'_{n+1}(x),\\
M(x,n) &= \frac{C_{n+1}(x) - C_0(x)}{2}D'_{n+1}(x) - \frac{C'_{n+1}(x) - C'_0(x)}{2}D_{n+1}(x) - D_{n+1}(x)\sum_{k=0}^{n}\frac{D_k(x)}{\beta_k}.
\end{aligned}$$

Remark 2.1. *Observe that the degrees of the polynomials* J, K, M *are at most* $2s+2$, $2s+1$, *and* $2s$, *respectively, where* s *denotes the class of the linear functional.*

In [3, 4], assuming that the linear functional is positive-definite, it is associated with a weight function, and under some integrability conditions, raising and lowering operators for orthogonal polynomials with respect to a weight function supported on the real line are derived, as well as a second-order linear differential equation satisfied by these polynomials (particularly, in [4], the case of orthogonal polynomials with discontinuous weights is studied). Let $-\infty < a < b < \infty$ and $\{P_n\}_{n\geq 0}$ be the MOPS associated with the linear functional L defined over $\mathbb{P}$ such that $\langle L, p\rangle = \int_a^b p(x)\omega(x)dx$, with $\omega(x) := e^{-v(x)}$, where v is a twice continuously differentiable and convex function for $x \in [a,b]$. If h_n is given by (2.2) and α_n, β_n are the coefficients of the TTRR (2.3), then the actions of the ladder operators on P_n and P_{n-1} are (see [3]):

$$\left(\frac{d}{dx} + B_n(x)\right)P_n(x) = \beta_n A_n(x)P_{n-1}(x), n \geq 1, \tag{2.12}$$

$$-\left(\frac{d}{dx} - B_n(x) - v'(x)\right)P_{n-1}(x) = A_{n-1}(x)P_n(x), n \geq 1, \tag{2.13}$$

where

$$A_n(x) := \frac{1}{h_n}\int_a^b \frac{v'(x) - v'(y)}{x-y}P_n^2(y)\omega(y)\,dy + \frac{P_n^2(y)\omega(y)}{h_n(y-x)}\Bigg|_{y=a}^{y=b}, \tag{2.14}$$

$$B_n(x) := \frac{1}{h_{n-1}}\int_a^b \frac{v'(x) - v'(y)}{x-y}P_{n-1}(y)P_n(y)\omega(y)\,dy + \frac{P_n(y)P_{n-1}(y)\omega(y)}{h_{n-1}(y-x)}\Bigg|_{y=a}^{y=b}. \tag{2.15}$$

Observe that $A_n > 0$ due to the convexity of v. Thus, the lowering and raising operators are given, respectively, by

$$L_n = \frac{d}{dx} + B_n(x) \quad \text{and} \quad R_n = -\left(\frac{d}{dx} - B_n(x) - v'(x)\right).$$

In addition, the coefficient functions in the ladder operators, $A_n(z)$ and $B_n(z)$, satisfy

$$B_{n+1}(x) + B_n(x) = (x - \alpha_n)A_n(x) - v'(x),$$
$$B_{n+1}(x) - B_n(x) = \frac{\beta_{n+1}A_{n+1}(x) - \beta_n A_{n-1}(x) - 1}{x - \alpha_n}.$$

Remark 2.2. *The raising and lowering operators are adjoint within the context of a Hilbert space endowed with the inner product $\langle f, g\rangle = \int_a^b f(x)g(x)w(x)dx$. Note that the adjoint relationship between raising and lowering operators persists even within the framework of classical orthogonal polynomials, which adds an intriguing layer to their general setting.*

Furthermore, the combination of the raising and lowering operators leads to a second-order linear differential equation.

Theorem 2.4 ([3]). *Under the above conditions, the MOPS $\{P_n\}_{n\geq 0}$ associated with the linear functional L satisfy*

$$R_n\left[\frac{1}{A_n(x)}\left(L_n P_n(x)\right)\right] = \frac{h_{n-1}}{h_n}A_{n-1}(x)P_n(x), \quad n \geq 1,$$

or equivalently,

$$P_n''(x) + S_n(x)P_n'(x) + Q_n(x)P_n(x) = 0, \quad n \geq 1,$$

where

$$S_n(x) = -\left[v'(x) + \frac{A_n'(x)}{A_n(x)}\right]$$

and

$$Q_n(x) = A_n(x)\left(\frac{B_n(x)}{A_n(x)}\right)' - B_n(x)[v'(x) + B_n(x)] + A_n(x)A_{n-1}(x)\frac{h_{n-1}}{h_n}$$
$$= -B_n'(x) - B_n(x)\frac{A_n'(x)}{A_n(x)} - B_n(x)[v'(x) + B_n(x)] + \frac{h_{n-1}}{h_n}A_n(x)A_{n-1}(x).$$

3. Pearson equation, moments and Stieltjes function

Throughout the rest of the paper we will focus our attention on the study of the truncated Hermite positive-definite linear functional L_M, defined by

$$L_M[p] = \langle L_M, p\rangle = \int_0^\infty p(x)e^{-x^2}\,dx, \quad p \in \mathbb{P} = \mathbb{R}[x]. \tag{3.16}$$

We will recognize L_M as a D-semiclassical functional of class $s = 1$. To prove this, we begin by examining the associated Pearson equation. We will then derive a second-order linear recurrence equation for its moments. Using the z-transform of the moment sequence (the Stieltjes function), we will obtain a first-order linear differential equation satisfied by this function. Subsequently, we will derive the Laguerre-Freud equations. Finally, we will construct the ladder operators and explore the electrostatic interpretation of the zeros of the corresponding orthogonal polynomials.

The Pearson equation representing the linear functional (3.16) can be expressed as follows.

Proposition 3.3. *Let $p \in \mathbb{R}[x]$, $\phi(x) = x$ and $\psi(x) = 1 - 2x^2$. Then, the linear functional L_M defined by (3.16) satisfies the Pearson equation established in (2.7).*

Proof. For $p \in \mathbb{R}[x]$ it follows that

$$\begin{aligned}\langle D(\phi L_M), p\rangle &= -\langle L_M, \phi p'\rangle = -\int_0^\infty \phi(x)p'(x)e^{-x^2}dx \\ &= \int_0^\infty p(x)\left(1-2x^2\right)e^{-x^2}dx - \underbrace{\left[\phi(x)p(x)e^{-x^2}\right]_0^\infty}_{=0} = \langle L_M, \psi p\rangle \\ &= \langle \psi L_M, p\rangle .\end{aligned}$$

□

From Proposition 3.3 we see that L_M is a D-semiclassical functional whose class does not exceed $s = 1$. In Remark 3.4 we will show that the class is indeed $s = 1$, see further.

Remark 3.3. *Since $\psi(x) = \phi'(x) - 2x\phi(x)$, the Pearson equation from Proposition 3.3 can be rewritten as*

$$-\langle D(\phi L_M), p\rangle = \langle L_M, \phi p'\rangle = -\langle L_M, (\phi' - 2x\phi)p\rangle = \langle L_M, (2x\phi - \phi')p\rangle . \tag{3.17}$$

Regarding the corresponding moments of the linear functional (3.16), by setting $s = x^2$ we can write for all $n \geq 0$,

$$\mu_{2n} = \langle L_M, x^{2n}\rangle = \int_0^\infty x^{2n}e^{-x^2}dx = \frac{1}{2}\int_0^\infty s^{n-\frac{1}{2}}e^{-s}ds = \frac{1}{2}\cdot\Gamma\left(n+\frac{1}{2}\right), \tag{3.18}$$

$$\mu_{2n+1} = \langle L_M, x^{2n+1}\rangle = \int_0^\infty x^{2n+1}e^{-x^2}dx = \frac{1}{2}\int_0^\infty s^{n}e^{-s}ds = \frac{1}{2}\cdot\Gamma\left(n+1\right) = \frac{n!}{2}. \tag{3.19}$$

To deduce a second-order homogeneous difference equation that characterizes the moments associated with the linear functional L_M, we can make use of the Pearson equation given by (3.17):

Proposition 3.4. *Let $\mu_n = \langle L_M, x^n\rangle$, $n \geq 0$. Then, $\{\mu_n\}_{n\geq 0}$ satisfies*

$$2\mu_{n+2} - (n+1)\mu_n = 0, \quad n \geq 0, \tag{3.20}$$

with initial conditions $\mu_0 = \frac{\sqrt{\pi}}{2}$ and $\mu_1 = \frac{1}{2}$.

Proof. From (3.17) with $p(x) = x^n$, we get

$$\langle L_M, n\phi(x)x^{n-1}\rangle = \langle L_M, (2x\phi(x) - \phi'(x))x^n\rangle . \tag{3.21}$$

Since $\phi(x) = x$ and $2x\phi(x) - \phi'(x) = 2x^2 - 1$, we can write $\langle L_M, n\phi(x)x^{n-1}\rangle = n\langle L_M, x^n\rangle = n\mu_n$ and $\langle L_M, (2x\phi(x) - \phi'(x))x^n\rangle = 2\langle L_M, x^{n+2}\rangle - \langle L_M, x^n\rangle = 2\mu_{n+2} - \mu_n$. Therefore, (3.21) is equivalent to (3.20). The initial conditions follows directly by taking $n = 0$ in (3.18)-(3.19). □

Concerning the corresponding Stieltjes function (2.8), we can prove the following

Proposition 3.5. *Let $\mu_n = \langle L_M, x^n\rangle$, $n \geq 0$. Then, the Stieltjes function $\mathcal{S}(z)$ associated with the linear functional L_M satisfies the first-order non-homogeneous linear ordinary differential equation*

$$z\mathcal{S}'(z) + 2z^2\mathcal{S}(z) = 2(\mu_1 + z\mu_0), \tag{3.22}$$

or equivalently,

$$\phi(z)\mathcal{S}'(z) + [\phi'(z) - \psi(z)]\,\mathcal{S}(z) = 2(\mu_1 + \phi(z)\mu_0),$$

where $\phi(z) = z$ and $\psi(z) = 1 - 2z^2$.

Proof. If we apply the z-transform to (3.20), we get

$$2\sum_{n=0}^{\infty}\frac{\mu_{n+2}}{z^{n+2}}-\sum_{n=0}^{\infty}(n+1)\frac{\mu_n}{z^{n+2}}=0.$$

Since

$$\sum_{n=0}^{\infty}\frac{\mu_{n+2}}{z^{n+2}}=z\left[\mathcal{S}(z)-\frac{\mu_0}{z}-\frac{\mu_1}{z^2}\right]\quad\text{and}\quad\sum_{n=0}^{\infty}(n+1)\frac{\mu_n}{z^{n+2}}=-D_z\mathcal{S}(z),$$

it follows that

$$2z\left[\mathcal{S}(z)-\frac{\mu_0}{z}-\frac{\mu_1}{z^2}\right]+\mathcal{S}'(z)=0$$

and we conclude (3.22). □

Remark 3.4. *Observe that from Proposition 2.2 and (3.22), we get*

$$C(z)=2(\mu_1+z\mu_0). \tag{3.23}$$

Taking into account that $\phi(z)=z$, $\psi(z)=1-2z^2$, $\phi(0)=(\phi'-\psi)(0)=0$ and $C(0)=2\mu_1\neq 0$, the Stieltjes function associated with L_M, satisfies

$$\phi(z)\mathcal{S}'(z)+[\phi'(z)-\psi(z)]\,\mathcal{S}(z)=C(z),$$

where C is given by (3.23) and ϕ, $\phi'-\psi$, and C are coprime. Therefore, from Proposition 2.2 we conclude that L_M is a D-semiclassical functional of class $s=1$.

4. Laguerre-Freud equations

The equations governing the coefficients of the TTRR (2.3), which are typically nonlinear in nature, are recognized in the literature as Laguerre-Freud equations (see, for instance, [2]). It is noteworthy that these equations can be viewed as discrete analogues of the well-established Painlevé equations (see [11]). The aim of this section is to obtain the Laguerre-Freud equations for the Maxwell linear functional given by (3.16). We start with a structure relation satisfied by Maxwell polynomials:

Theorem 4.5. *Let $\{P_n\}_{n\geq 0}$ be the MOPS associated with the linear functional defined in (3.16) and α_n, β_n the corresponding coefficients in the TTRR (2.3). Then the polynomials P_n satisfy the structure relation*

$$\phi(x)P'_{n+1}(x)=(n+1)P_{n+1}(x)+\lambda_{n+1,n}P_n(x)+\lambda_{n+1,n-1}P_{n-1}(x),\quad n\geq 1, \tag{4.24}$$

where $\lambda_{n+1,n}=2\beta_{n+1}\left(\alpha_{n+1}+\alpha_n\right)$ and $\lambda_{n+1,n-1}=2\beta_{n+1}\beta_n$.

Proof. From Proposition 2.2 with $s=1$ and $r=\deg\phi=1$, the structure relation satisfied by the MOPS with respect to the semiclassical functional defined in (3.16) becomes for all $n\geq 1$,

$$\phi(x)P'_{n+1}(x)=(n+1)P_{n+1}(x)+\lambda_{n+1,n}P_n(x)+\lambda_{n+1,n-1}P_{n-1}(x),$$

where

$$\lambda_{n+1,n}=\frac{\langle L_M,\phi P'_{n+1}P_n\rangle}{\|P_n\|^2}\qquad\text{and}\qquad\lambda_{n+1,n-1}=\frac{\langle L_M,\phi P'_{n+1}P_{n-1}\rangle}{\|P_{n-1}\|^2}.$$

Indeed, one can observe that if we write $xP'_{n+1} = (n+1)P_{n+1} + \sum_{k=0}^{n} \lambda_{n+1,k} P_k$, then

$$\begin{aligned}\lambda_{n+1,k} &= \frac{\langle L_M, xP'_{n+1}P_k\rangle}{\|P_k\|^2} = \frac{\langle L_M, x\left[(P_{n+1}P_k)' - P_{n+1}P'_k\right]\rangle}{\|P_k\|^2} \\ &= \frac{\langle xL_M, (P_{n+1}P_k)' - P_{n+1}P'_k\rangle}{\|P_k\|^2} = \frac{-\langle D(xL_M), P_{n+1}P_k\rangle - \langle xL_M, P_{n+1}P'_k\rangle}{\|P_k\|^2} \\ &= \frac{-\langle (1-2x^2)L_M, P_{n+1}P_k\rangle - \langle L_M, xP_{n+1}P'_k\rangle}{\|P_k\|^2},\end{aligned}$$

where we have used (3.17) in the last equality. Hence,

$$\lambda_{n+1,k} = \begin{cases} 0, & \text{if } k < n-1, \\ 2\frac{\|P_{n+1}\|^2}{\|P_{n-1}\|^2}, & \text{if } k = n-1, \\ 2\frac{\langle L_M, x^2 P_{n+1}P_n\rangle}{\|P_n\|^2}, & \text{if } k = n. \end{cases}$$

From the TTRR (2.3) we can write

$$\begin{cases} xP_{n+1}(x) = P_{n+2}(x) + \alpha_{n+1}P_{n+1}(x) + \beta_{n+1}P_n(x), \\ xP_n(x) = P_{n+1}(x) + \alpha_n P_n(x) + \beta_n P_{n-1}(x), \end{cases}$$

which implies that

$$\langle L_M, x^2 P_{n+1}P_n\rangle = \langle L_M, xP_{n+1}xP_n\rangle = \alpha_{n+1}\|P_{n+1}\|^2 + \alpha_n\beta_{n+1}\|P_n\|^2.$$

Therefore, for all $n \geq 1$ we get

$$\begin{aligned}\lambda_{n+1,n} &= 2(\alpha_{n+1}\beta_{n+1} + \alpha_n\beta_{n+1}) = 2\beta_{n+1}(\alpha_{n+1} + \alpha_n), \\ \lambda_{n+1,n-1} &= 2\beta_{n+1}\beta_n,\end{aligned}$$

and the proof is concluded. □

Theorem 4.6. *The coefficients α_n and β_n of the TTRR (2.3) for the linear functional defined in (3.16) satisfy for all $n \geq 1$ the Laguerre-Freud equations*

$$\alpha_n^2 + \beta_{n+1} + \beta_n = n + \frac{1}{2}, \tag{4.25}$$

$$2\beta_{n+2}\alpha_{n+2} + \alpha_{n+1}(2\beta_{n+2} - 2\beta_{n+1} - 1) - 2\alpha_n\beta_{n+1} = 0, \tag{4.26}$$

with initial conditions $\beta_1 = \frac{1}{2} - \frac{1}{\pi}$, $\beta_2 = \frac{\pi(\pi-3)}{(\pi-2)^2}$ and $\alpha_1 = \frac{2}{(\pi-2)\sqrt{\pi}}$.

Proof. Let $\{P_n\}_{n\geq 0}$ be the MOPS with respect to the linear functional L_M given by (3.16). Taking $p = P_n^2$ in (2.7) with $\phi(x) = x$ and $\psi(x) = 1 - 2x^2$, we get

$$-2\langle L_M, P_n\phi P'_n\rangle = \langle L_M, \psi P_n^2\rangle, \quad n \geq 1. \tag{4.27}$$

The right side of (4.27) can be rewritten as

$$\langle L_M, \psi P_n^2\rangle = \langle L_M, (1-2x^2)P_n^2\rangle = \langle L_M, P_n^2\rangle - 2\langle L_M, x^2 P_n^2\rangle, \quad n \geq 1. \tag{4.28}$$

From (2.2) we have that $\langle L_M, P_n^2\rangle = h_n$ and

$$\begin{aligned} x^2P_n(x) &= x\left[P_{n+1}(x) + \alpha_n P_n(x) + \beta_n P_{n-1}(x)\right] \\ &= xP_{n+1}(x) + \alpha_n xP_n(x) + \beta_n xP_{n-1}(x) \\ &= P_{n+2}(x) + \alpha_{n+1}P_{n+1}(x) + \beta_{n+1}P_n(x) + \alpha_n P_{n+1}(x) + \alpha_n^2 P_n(x) \\ &+ \alpha_n\beta_n P_{n-1}(x) + \beta_n P_n(x) + \alpha_{n-1}\beta_n P_{n-1}(x) + \beta_n\beta_{n-1}P_{n-2}(x) \\ &= P_{n+2}(x) + (\alpha_{n+1}+\alpha_n)P_{n+1}(x) + (\alpha_n^2 + \beta_{n+1} + \beta_n)P_n(x) \\ &+ \beta_n(\alpha_n + \alpha_{n-1})P_{n-1}(x) + \beta_n\beta_{n-1}P_{n-2}(x), \end{aligned}$$

so (4.28) is equivalent to

$$\langle L_M, \psi P_n^2\rangle = h_n - 2\left(\alpha_n^2 + \beta_{n+1} + \beta_n\right)h_n = \left[1 - 2\left(\alpha_n^2 + \beta_{n+1} + \beta_n\right)\right]h_n, \quad n \geq 1. \tag{4.29}$$

In addition, from (4.24) we have that

$$\phi(x)P_n'(x) = nP_n(x) + 2\beta_n\left(\alpha_n + \alpha_{n-1}\right)P_{n-1}(x) + 2\beta_n\beta_{n-1}P_{n-2}(x), \quad n \geq 1,$$

so the left side of (4.27) becomes

$$\begin{aligned} -2\langle L_M, P_n\phi P_n'\rangle &= -2\langle L_M, P_n\left[nP_n + 2\beta_n\left(\alpha_n + \alpha_{n-1}\right)P_{n-1} + 2\beta_n\beta_{n-1}P_{n-2}\right]\rangle \\ &= -2nh_n. \end{aligned} \tag{4.30}$$

Finally, equating (4.29) and (4.30) we obtain $-2n = 1 - 2\left(\alpha_n^2 + \beta_{n+1} + \beta_n\right)$ and (4.25) is deduced.

On the other hand, since $xP_{n+1}' = (xP_{n+1})' - P_{n+1}$ and $\langle L_M, P_{n+1}P_n\rangle = 0$, we see that

$$\begin{aligned} \lambda_{n+1,n} &= \frac{\langle L_M, xP_{n+1}'P_n\rangle}{\|P_n\|^2} = \frac{\langle L_M, (xP_{n+1})'P_n\rangle}{\|P_n\|^2} \\ &= \frac{\langle L_M, \left(P_{n+2}' + \alpha_{n+1}P_{n+1}' + \beta_{n+1}P_n'\right)P_n\rangle}{\|P_n\|^2} = \frac{\langle L_M, P_{n+2}'P_n\rangle}{\|P_n\|^2} + \alpha_{n+1}(n+1). \end{aligned}$$

Let us write

$$P_{n+2}(x) = x^{n+2} + \sum_{k=0}^{n+1}\delta_{n+2,k}x^k = x^{n+2} + \delta_{n+2,n+1}x^{n+1} + \ldots,$$

so

$$P_{n+2}'(x) = (n+2)x^{n+1} + \sum_{k=1}^{n+1}k\delta_{n+2,k}x^{k-1} = (n+2)x^{n+1} + (n+1)\delta_{n+2,n+1}x^n + \ldots$$

It follows that

$$\frac{\langle L_M, P_{n+2}'P_n\rangle}{\|P_n\|^2} = \frac{(n+2)\langle L_M, x^{n+1}P_n\rangle}{\|P_n\|^2} + (n+1)\delta_{n+2,n+1}.$$

Since $x^{n+1} = P_{n+1}(x) - \delta_{n+1,n}x^n - \ldots$, we have $\langle L_M, x^{n+1}P_n\rangle = -\delta_{n+1,n}\|P_n\|^2$. Then,

$$\lambda_{n+1,n} = -(n+2)\delta_{n+1,n} + (n+1)\delta_{n+2,n+1} + (n+1)\alpha_{n+1}. \tag{4.31}$$

Alternatively, identifying coefficients of x^n in (4.24), we can observe that

$$\lambda_{n+1,n} + (n+1)\delta_{n+1,n} = n\delta_{n+1,n} \quad \Rightarrow \quad \lambda_{n+1,n} = -\delta_{n+1,n}.$$

Since $xP_{n+1}(x) = P_{n+2}(x) + \alpha_{n+1}P_{n+1}(x) + \beta_{n+1}P_n(x)$ we get $\delta_{n+1,n} = \delta_{n+1,n+1} + \alpha_{n+1}$, and this allows us to recover (4.31). Therefore, we can write

$$\begin{cases} 2\beta_{n+1}(\alpha_{n+1} + \alpha_n) &= -\delta_{n+1,n}, \\ 2\beta_{n+2}(\alpha_{n+2} + \alpha_{n+1}) &= -\delta_{n+2,n+1}, \end{cases}$$

and this implies

$$\alpha_{n+1} = 2\beta_{n+2}(\alpha_{n+2} + \alpha_{n+1}) - 2\beta_{n+1}(\alpha_{n+1} + \alpha_n), \quad n \geq 1.$$

which is equivalent to (4.26). The initial values α_1, β_1 and β_2 can be obtained by direct computation (see Remark 4.5 and Theorem 4.8 further). □

A second recurrence relation for the parameters of the TTRR (2.3) which is of interest can be obtained as follows. Let $\{\tilde{p}_n\}_{n\geq 0}$ be the ONPS associated with the linear functional defined in (3.16), with TTRR given by (2.4) and $\tilde{p}_n = \frac{1}{\sqrt{h_n}}P_n$ with h_n defined in (2.2). If we multiply by $x^2e^{-x^2}$ in the confluent formula (2.6) and we integrate over $[0, \infty)$, it follows that

$$\sum_{k=0}^{n} \int_0^\infty x^2\tilde{p}_k^2(x)e^{-x^2}dx = \sqrt{\beta_{n+1}}\left[\int_0^\infty \tilde{p}'_{n+1}(x)x^2\tilde{p}_n(x)e^{-x^2}dx - \int_0^\infty \tilde{p}_{n+1}(x)\tilde{p}'_n(x)x^2e^{-x^2}dx\right]. \tag{4.32}$$

The integration by parts in the first member of (4.32) yields

$$\begin{aligned} \int_0^\infty x\tilde{p}_k^2(x)xe^{-x^2}dx &= \frac{1}{2}\int_0^\infty \left[\tilde{p}_k^2(x) + 2x\tilde{p}_k(x)\tilde{p}'_k(x)\right]e^{-x^2}dx \\ &= \frac{1}{2} + \int_0^\infty x\tilde{p}_k(x)\tilde{p}'_k(x)e^{-x^2}dx = \frac{1}{2} + k. \end{aligned}$$

Therefore, we have that

$$\sum_{k=0}^{n} \int_0^\infty x^2\tilde{p}_k^2(x)e^{-x^2}dx = \sum_{k=0}^{n} \frac{1}{2} + k = \frac{1}{2}(n+1)^2. \tag{4.33}$$

Regarding the right-hand side of (4.32), notice that

$$\begin{aligned} &\int_0^\infty \tilde{p}'_{n+1}(x)x^2\tilde{p}_n(x)e^{-x^2}dx - n\int_0^\infty \tilde{p}_{n+1}(x)\frac{\sqrt{h_{n+1}}}{\sqrt{h_n}}\tilde{p}_{n+1}(x)x^2e^{-x^2}dx \\ &= -n\sqrt{\beta_{n+1}} - \int_0^\infty \tilde{p}_{n+1}(x)\left(2x\tilde{p}_n(x)e^{-x^2}\right)dx - \int_0^\infty \tilde{p}_{n+1}(x)x^2\tilde{p}'_n(x)e^{-x^2}dx \\ &+2\int_0^\infty \tilde{p}_{n+1}(x)\tilde{p}_n(x)x^3e^{-x^2}dx \\ &= -n\sqrt{\beta_{n+1}} - 2\sqrt{\beta_{n+1}} - n\sqrt{\beta_{n+1}} \\ &= -2(n+1)\sqrt{\beta_{n+1}} + 2\int_0^\infty \tilde{p}_{n+1}(x)\tilde{p}_n(x)x^3e^{-x^2}dx. \end{aligned}$$

Now, from (2.4) we get

$$\begin{aligned}x^2\tilde{p}_n(x) =&\sqrt{\beta_{n+1}}\left[\sqrt{\beta_{n+2}}\tilde{p}_{n+2}(x)+\alpha_{n+1}\tilde{p}_{n+1}(x)+\sqrt{\beta_{n+1}}\tilde{p}_n(x)\right]\\ &+\alpha_n\left[\sqrt{\beta_{n+1}}\tilde{p}_{n+1}(x)+\alpha_n\tilde{p}_n(x)+\sqrt{\beta_n}\tilde{p}_{n-1}(x)\right]\\ &+\sqrt{\beta_n}\left[\sqrt{\beta_n}\tilde{p}_n(x)+\alpha_{n-1}\tilde{p}_{n-1}(x)+\sqrt{\beta_{n-1}}\tilde{p}_{n-2}(x)\right]\\ =&\sqrt{\beta_{n+1}\beta_{n+2}}\tilde{p}_{n+2}(x)+\left(\sqrt{\beta_{n+1}}\alpha_{n+1}+\alpha_n\sqrt{\beta_{n+1}}\right)\tilde{p}_{n+1}(x)\\ &+\left(\beta_{n+1}+\alpha_n^2+\beta_n\right)\tilde{p}_n(x),\end{aligned}$$

and by making use of the TTRR (2.4) with n replaced by $n+1$ it follows that

$$\int_0^\infty x^3\tilde{p}_{n+1}(x)\tilde{p}_n(x)e^{-x^2}dx=\sqrt{\beta_{n+1}}\left[\beta_{n+2}+\alpha_{n+1}\left(\alpha_{n+1}+\alpha_n\right)+\beta_{n+1}+\alpha_n^2+\beta_n\right],$$

which implies that the right-hand side of (4.32) reads as

$$2\beta_{n+1}\left[\beta_{n+2}+\alpha_{n+1}\left(\alpha_{n+1}+\alpha_n\right)+\beta_{n+1}+\alpha_n^2+\beta_n-(n+1)\right]. \tag{4.34}$$

If we equate (4.33) and (4.34),

$$\begin{aligned}(n+1)^2&=4\beta_{n+1}\left[\beta_{n+2}+\alpha_{n+1}\left(\alpha_{n+1}+\alpha_n\right)+\beta_{n+1}+\alpha_n^2+\beta_n-(n+1)\right]\\ &=4\beta_{n+1}\left[n+\frac{3}{2}+\alpha_n\left(\alpha_n+\alpha_{n+1}\right)+\beta_n-n-1\right]\\ &=4\beta_{n+1}\left[\frac{1}{2}+\beta_n+\alpha_n\left(\alpha_n+\alpha_{n+1}\right)\right].\end{aligned}$$

Therefore, we have proved the following

Theorem 4.7. *The coefficients α_n and β_n of the TTRR (2.3) for the linear functional defined in (3.16) satisfy the Laguerre-Freud equations (4.25) and*

$$4\beta_{n+1}\left[\frac{1}{2}+\beta_n+\alpha_n\left(\alpha_n+\alpha_{n+1}\right)\right]=(n+1)^2,\quad n\geq 1, \tag{4.35}$$

with initial conditions $\beta_1=\frac{1}{2}-\frac{1}{\pi}$, $\beta_2=\frac{\pi(\pi-3)}{(\pi-2)^2}$ and $\alpha_1=\frac{2}{(\pi-2)\sqrt{\pi}}$.

Moreover, one can easily see that (4.35) can be rewritten as

$$(n+1)^2=4\beta_{n+1}\left[\frac{1}{2}+\alpha_n\alpha_{n+1}+n+\frac{1}{2}-\beta_{n+1}\right]=4\beta_{n+1}\left[n+1-\beta_{n+1}+\alpha_n\alpha_{n+1}\right],$$

which implies that

$$4\beta_{n+1}\alpha_n\alpha_{n+1}=(n+1)^2-4(n+1)\beta_{n+1}+4\beta_{n+1}^2=(n+1-2\beta_{n+1})^2,$$

or equivalently,

$$16\beta_{n+1}^2\alpha_n^2\alpha_{n+1}^2=(n+1-2\beta_{n+1})^4. \tag{4.36}$$

On the other hand, from (4.25) we have that $2\beta_{n+1}+2\beta_n+2\alpha_n^2=2n+1$ and hence, $2\alpha_n^2=n+1-2\beta_{n+1}+n-2\beta_n$. Thus, (4.36) becomes

$$4\beta_{n+1}^2(n+1-2\beta_{n+1}+n-2\beta_n)(n+2-2\beta_{n+2}+n+1-2\beta_{n+1})=(n+1-2\beta_{n+1})^4,$$

or, alternatively,

$$\beta_{n+1}^2\left(\frac{n+1}{2}-\beta_{n+1}+\frac{n}{2}-\beta_n\right)\left(\frac{n+2}{2}-\beta_{n+2}+\frac{n+1}{2}-\beta_{n+1}\right)=\left(\frac{n+1}{2}-\beta_{n+1}\right)^4.$$

Setting $g_n = \frac{n}{2} - \beta_n$, the previous equation turns into

$$g_{n+1}^4 = \left(\frac{n+1}{2} - g_{n+1}\right)^2 (g_{n+1}g_n)\,(g_{n+2} + g_{n+1}), \quad n \geq 1,$$

which is a discrete Painlevé IV equation (denoted in the literature as $d - P_{IV}$). We refer to [17, p. 10] and [18, Section 4] for more details.

Finally, one can observe that

$$\alpha_n^2 = n + \frac{1}{2} - \beta_n - \beta_{n+1} = n + \frac{1}{2} + \left(g_n - \frac{n}{2}\right) = g_n + g_{n+1}.$$

Remark 4.5. *Concerning the initial conditions, from the relation $\beta_n = \frac{h_n}{h_{n-1}}$ $(n \geq 1)$ that follows from Theorem 2.1, where $h_n = \|P_n\|^2 = \langle L_M, P_n^2\rangle$, and from the explicit expressions for the moments (3.18)-(3.19) it is an easy exercise to check that*

$$P_0(x) \equiv 1, \qquad P_1(x) = x - \frac{1}{\sqrt{\pi}}, \qquad P_2(x) = x^2 - \frac{\sqrt{\pi}}{\pi - 2}x + \frac{4-\pi}{2(\pi-2)},$$

which implies $\beta_1 = \frac{1}{2} - \frac{1}{\pi}$ and $\beta_2 = \frac{\pi(\pi-3)}{(\pi-2)^2}$. Therefore, we get

$$g_1 = \frac{1}{2} - \beta_1 = \frac{1}{\pi}, \qquad g_2 = 1 - \beta_2 = 1 - \frac{\pi(\pi-3)}{(\pi-2)^2} = \frac{4-\pi}{(\pi-2)^2}. \tag{4.37}$$

Thus, the following result has been proved.

Theorem 4.8. *Let α_n and β_n be the coefficients of the TTRR (2.3) for the linear functional defined in (3.16) and let $\{g_n\}_{n\geq 0}$ be defined by $g_n = \frac{n}{2} - \beta_n$. Then, $\{g_n\}_{n\geq 0}$ satisfy the $d - P_{IV}$ equation*

$$g_{n+1}^4 = \left(\frac{n+1}{2} - g_{n+1}\right)^2 (g_{n+1} + g_n)\,(g_{n+2} + g_{n+1}), \quad n \geq 1,$$

with initial conditions given by (4.37). In addition, for all $n \geq 1$ we have $\alpha_n^2 = g_n + g_{n+1}$.

To conclude this section, we will study the asymptotic behavior of the coefficients α_n and β_n. Our aim is to find the leading behavior of an asymptotic series solution for the recurrence relations discussed previously, that is, the first term in the expansion. Since α_n and β_n are all positive and approach infinity as $n \to \infty$, we can write

$$\alpha_n = n^r \tilde{\alpha}_n \quad \text{and} \quad \beta_n = n^s \tilde{\beta}_n,$$

where $\tilde{\alpha}_n$ and $\tilde{\beta}_n$ approach positive constants A and B respectively, as $n \to \infty$. Hence, let us consider $\alpha_n \sim An^r$ and $\beta_n \sim Bn^s$ as $n \to \infty$, where r and s are unknown positive constants and $\sim$ means *asymptotic to*. Substituting these asymptotic forms into the recurrence relation (4.25) yields

$$B^2 n^{2r} + 2An^s = n + \frac{1}{2}.$$

We require that this equation hold for all $n > 0$ so that $s = 1$ and $2r = 1$. Then, the coefficients A and B satisfy the equation

$$B^2 + 2A = 1. \tag{4.38}$$

On the other hand, if we replace the asymptotic expressions in (4.35), then

$$4A(n+1)\left[\frac{1}{2} + An + Bn^{\frac{1}{2}}\left(Bn^{\frac{1}{2}} + B(n+1)^{\frac{1}{2}}\right)\right] = (n+1)^2,$$

which is equivalent to

$$4A\left[\frac{1}{2}+An+B^2n\left(1+\left(1+\frac{1}{n}\right)^{\frac{1}{2}}\right)\right]=(n+1).$$

Again, since this equation also hold for all $n>0$, we have

$$4A\left(A+2B^2\right)=1. \tag{4.39}$$

Now, we need to solve the nonlinear system of equations formed by (4.38) and (4.39). Note that we can write $2B^2=2-4A$ due to (4.38), so (4.39) can be turned into $4A\,(2-3A)=1\Leftrightarrow 12A^2-8A+1=0$, whose solutions are $A_1=\frac{1}{2}\Rightarrow B_1=0$ and $A_2=\frac{1}{6}\Rightarrow B_2=\sqrt{\frac{2}{3}}$. Given that α_n and β_n are positive for all n, so A and B must both be positive. Thus, $A=\frac{1}{6}$ and $B_2=\sqrt{\frac{2}{3}}$ is the only possible solution, so the leading behavior is given by

$$\alpha_n\sim\frac{1}{6}n\quad\text{and}\quad\beta_n\sim\sqrt{\frac{2n}{3}}.$$

5. Ladder operators and electrostatic interpretation of the zeros

In this section, we construct first the ladder operators for the semiclassical functional of class $s=1$ defined by (3.16). Then, a second-order linear differential equation (in x) for the Maxwell polynomial P_{n+1} will be obtained, as well as the electrostatic interpretation of the zeros of these polynomials.

Theorem 5.9. *Let the lowering operator L_{n+1} be defined by $L_{n+1}=A_{n+1}(x)D_x-B_{n+1}(x)$ for all $n\geq 0$, where*

$$A_{n+1}(x)=\frac{\phi(x)}{2\beta_{n+1}(x-\alpha_n)+\lambda_{n+1,n}}\quad\text{and}\quad B_{n+1}(x)=\frac{n+1-2\beta_{n+1}}{2\beta_{n+1}(x-\alpha_n)+\lambda_{n+1,n}},$$

with $\phi(x)=x$ and $\lambda_{n+1,n}=2\beta_{n+1}(\alpha_{n+1}+\alpha_n)$. Then,

$$L_{n+1}P_{n+1}=P_n,\qquad n\geq 0. \tag{5.40}$$

Proof. From (4.24) we have that

$$\phi(x)P'_{n+1}(x)=(n+1)P_{n+1}(x)+\lambda_{n+1,n}P_n(x)+2\beta_{n+1}\beta_nP_{n-1}(x).$$

Using the TTRR (2.3), we can see that $\beta_nP_{n-1}(x)=(x-\alpha_n)P_n(x)-P_{n+1}(x)$, so the previous expression is equivalent to

$$\begin{aligned}\phi(x)P'_{n+1}(x)&=(n+1)P_{n+1}(x)+\lambda_{n+1,n}P_n(x)+2\beta_{n+1}\left[(x-\alpha_n)P_n(x)-P_{n+1}(x)\right]\\&=\left(n+1-2\beta_{n+1}\right)P_{n+1}(x)+\left[2\beta_{n+1}(x-\alpha_n)+\lambda_{n+1,n}\right]P_n(x).\end{aligned} \tag{5.41}$$

Therefore, we can write

$$\left[\phi D_x-(n+1-2\beta_{n+1})\right]P_{n+1}(x)=\left[2\beta_{n+1}(x-\alpha_n)+\lambda_{n+1,n}\right]P_n(x),$$

and (5.40) follows. □

Theorem 5.10. *Let the raising operator R_{n+1} be defined by $R_{n+1} = C_{n+1}(x)D_x + E_{n+1}(x)$, for all $n \geq 0$, where*

$$C_{n+1}(x) = -\frac{\phi(x)}{2(x-\alpha_n) + \frac{\lambda_{n+1,n}}{\beta_{n+1}}},$$

$$E_{n+1}(x) = \frac{n+1-2\beta_{n+1} + \left(2(x-\alpha_n) + \frac{\lambda_{n+1,n}}{\beta_{n+1}}\right)(x-\alpha_{n+1})}{2(x-\alpha_n) + \frac{\lambda_{n+1,n}}{\beta_{n+1}}},$$

with $\phi(x) = x$ and $\lambda_{n+1,n} = 2\beta_{n+1}(\alpha_{n+1} + \alpha_n)$. Then,

$$R_{n+1}P_{n+1} = P_{n+2}, \qquad n \geq 0. \tag{5.42}$$

Proof. Using the TTRR (2.3), it is clear that $P_n = \frac{1}{\beta_{n+1}}\left[(x-\alpha_{n+1})P_{n+1} - P_{n+2}\right]$, where $\beta_{n+1} > 0$, so (5.41) can be rewritten as

$$\begin{aligned}\phi P'_{n+1} &= (n+1-2\beta_{n+1})\,P_{n+1} + \frac{1}{\beta_{n+1}}\left[2\beta_{n+1}(x-\alpha_n) + \lambda_{n+1,n}\right]\left[(x-\alpha_{n+1})P_{n+1} - P_{n+2}\right] \\ &= \left[n+1-2\beta_{n+1} + \left(2(x-\alpha_n) + \frac{\lambda_{n+1,n}}{\beta_{n+1}}\right)(x-\alpha_{n+1})\right]P_{n+1} \\ &\quad - \left(2(x-\alpha_n) + \frac{\lambda_{n+1,n}}{\beta_{n+1}}\right)P_{n+2}.\end{aligned}$$

Thus,

$$\begin{aligned}&\left[\phi D_x - n - 1 + 2\beta_{n+1} - \left(2(x-\alpha_n) + \frac{\lambda_{n+1,n}}{\beta_{n+1}}\right)(x-\alpha_{n+1})\right]P_{n+1} \\ &= -\left(2(x-\alpha_n) + \frac{\lambda_{n+1,n}}{\beta_{n+1}}\right)P_{n+2},\end{aligned}$$

and (5.42) follows. □

Considering the definition of the lowering operator L_{n+1} in Theorem 5.9, we can derive a second-order linear differential equation in terms of x for P_{n+1}.

Theorem 5.11. *Let the second-order linear differential operator $\mathcal{D}_{n+1}$ be defined for all $n \geq 0$ by*

$$\begin{aligned}\mathcal{D}_{n+1} =& \beta_n A_n(x)A_{n+1}(x)D_x^2 \\ &+ \left[\beta_n\left(A_n(x)\left(A'_{n+1}(x) - B_{n+1}(x)\right) - A_{n+1}(x)B_n(x)\right) + \alpha_n A_{n+1}(x) - xA_{n+1}(x)\right]D_x \\ &+ \beta_n\left[B_n(x)B_{n+1} - A_n(x)B'_{n+1}(x)\right] + xB_{n+1}(x) - \alpha_n B_{n+1}(x) + 1.\end{aligned}$$

Then, $\mathcal{D}_{n+1}P_{n+1} = 0$, for all $n \geq 0$.

Proof. By (2.3), we have that $xP_n(x) = P_{n+1}(x) + \alpha_n P_n(x) + \beta_n P_{n-1}(x)$, which can be rewritten in terms of (5.40) as

$$xL_{n+1}P_{n+1}(x) = P_{n+1}(x) + \alpha_n L_{n+1}P_{n+1}(x) + \beta_n L_n L_{n+1}P_{n+1}(x).$$

For a function f of x, we can observe that

$$\begin{aligned}L_n L_{n+1}f(x) &= \left[A_n(x)D_x - B_n(x)\right]\cdot\left[A_{n+1}(x)f'(x) - B_{n+1}(x)f(x)\right] \\ &= A_n(x)\left[A'_{n+1}(x)f'(x) + A_{n+1}(x)f''(x) - B'_{n+1}(x)f(x) - B_{n+1}(x)f'(x)\right] \\ &\quad - B_n(x)\left[A_{n+1}(x)f'(x) - B_{n+1}(x)f(x)\right].\end{aligned}$$

Hence, for $f = P_{n+1}$ it follows that

$$\begin{aligned}
0 &= [\beta_n L_n L_{n+1} - xL_{n+1} + \alpha_n L_{n+1} + 1]\, f(x) \\
&= \beta_n A_n(x) A_{n+1}(x) f''(x) \\
&+ \beta_n \left[A_n(x)\left(A'_{n+1}(x) - B_{n+1}(x)\right) - A_{n+1}(x)B_n(x)\right] f'(x) \\
&+ [\alpha_n A_{n+1}(x) - xA_{n+1}(x)]\, f'(x) \\
&+ \beta_n \left[B_n(x)B_{n+1} - A_n(x)B'_{n+1}(x)\right] f(x) \\
&+ [xB_{n+1}(x) - \alpha_n B_{n+1}(x) + 1]\, f(x),
\end{aligned}$$

and the result is obtained. □

Let us consider the ladder operators discussed in [3, 4] so that we can obtain the electrostatic interpretation of the zeros in a simpler way. Let P_n be the monic orthogonal polynomial of degree n associated with the linear functional in (3.16). Recalling (2.12) and (2.13), we have

$$\frac{1}{\beta_n \tilde{A}_n(x)} \left(\frac{d}{dx} + \tilde{B}_n(x)\right) P_n(x) = P_{n-1}(x), \quad n \geq 1,$$

and

$$-\frac{1}{\tilde{A}_{n-1}(x)} \left(\frac{d}{dx} - \tilde{B}_n(x) - v'(x)\right) P_{n-1}(x) = P_n(x), \quad n \geq 1,$$

where $\tilde{A}_n(x)$ and $\tilde{B}_n(x)$ are given by (2.14) and (2.15), respectively. In the case of the linear functional L_M defined in (3.16), we observe that $a = 0$, $b = \infty$, $v(x) = x^2$ and $\omega(x) = e^{-x^2}$. Therefore, since $\langle L_M, P_n^2 \rangle = h_n$ and $\langle L_M, P_n P_{n-1} \rangle = 0$, we have

$$\begin{aligned}
\tilde{A}_n(x) &= \frac{2}{h_n} \int_0^\infty P_n^2(y) e^{-y^2} dy + \frac{P_n^2(y) e^{-y^2}}{h_n(y-x)} \Big|_{y=0}^{y=\infty} = \frac{2}{h_n} \langle L_M, P_n^2 \rangle + \frac{1}{h_n} \cdot \frac{P_n^2(0)}{x} \\
&= 2 + \frac{1}{h_n} \cdot \frac{P_n^2(0)}{x}, \\
\tilde{B}_n(x) &= \frac{2}{h_{n-1}} \int_0^\infty P_{n-1}(y) P_n(y) e^{-y^2} dy + \frac{P_n(y) P_{n-1}(y) e^{-y^2}}{h_{n-1}(y-x)} \Big|_{y=0}^{y=\infty} \\
&= \frac{2}{h_{n-1}} \langle L_M, P_n P_{n-1} \rangle + \frac{1}{h_{n-1}} \cdot \frac{P_n(0) P_{n-1}(0)}{x} = \frac{1}{h_{n-1}} \cdot \frac{P_n(0) P_{n-1}(0)}{x}.
\end{aligned}$$

Then, the lowering and raising operators are also determined, respectively, by

$$\tilde{L}_n = \frac{1}{\beta_n \tilde{A}_n(x)} \left(\frac{d}{dx} + \tilde{B}_n(x)\right), \quad n \geq 1, \tag{5.43}$$

$$\tilde{R}_n = -\frac{1}{\tilde{A}_{n-1}(x)} \left(\frac{d}{dx} - \tilde{B}_n(x) - 2x\right), \quad n \geq 1. \tag{5.44}$$

Moreover, from Theorem 2.4, we have that P_n satisfies the second-order linear ordinary differential equation

$$P_n''(x) - \left(\frac{\tilde{A}'_n(x)}{\tilde{A}_n(x)} - 2x\right) P_n'(x) + Q_n(x) P_n(x) = 0, \quad n \geq 1,$$

where

$$\frac{\tilde{A}'_n(x)}{\tilde{A}_n(x)} = -\frac{P_n^2(0)}{x(2h_n x + P_n^2(0))}$$

and

$$
\begin{aligned}
Q_n(x) &= -\tilde{B}_n'(x) - \tilde{B}_n(x)\frac{\tilde{A}_n'(x)}{\tilde{A}_n(x)} - \tilde{B}_n(x)\left[\tilde{B}_n(x) - 2x\right] + \frac{h_{n-1}}{h_n}\tilde{A}_n(x)\tilde{A}_{n-1}(x) \\
&= \frac{P_n^3(0)P_{n-1}(0)}{h_{n-1}x^2(2h_nx + P_n^2(0))} - \frac{P_n^2(0)P_{n-1}^2(0) + h_{n-1}P_n(0)P_{n-1}(0)}{h_{n-1}^2x^2} \\
&+ \frac{2P_n(0)P_{n-1}(0)}{h_{n-1}} + 4\frac{h_{n-1}}{h_n} + \frac{2}{h_n}\frac{P_{n-1}^2(0)}{x} + 2\frac{h_{n-1}}{h_n^2}\frac{P_n^2(0)}{x} \\
&+ \frac{1}{h_nh_{n-1}}\frac{P_n^2(0)P_{n-1}^2(0)}{x^2}, \quad n \geq 1.
\end{aligned} \tag{5.45}
$$

Therefore, we have proved the following

Theorem 5.12. *Let the lowering and the raising operators be defined by (5.43) and (5.44), respectively. Then, $\tilde{R}_nP_n = P_{n+1}$ and $\tilde{L}_nP_n = P_{n-1}$, for $n \geq 1$. Moreover, if we define the second-order linear differential operator $\tilde{\mathcal{D}}_n$ as*

$$
\tilde{\mathcal{D}}_n = D_x^2 + \left(\frac{P_n^2(0)}{x(2h_nx + P_n^2(0))} + 2x\right)D_x + Q_n(x), \quad n \geq 1, \tag{5.46}
$$

where Q_n is given by (5.45), then $\tilde{\mathcal{D}}_nP_n = 0$, for all $n \geq 1$.

To end, we can obtain an electrostatic interpretation of the zeros of the corresponding OPS by means of Theorem 5.12. Indeed, let us denote by $\{x_{n,k}\}_{k=1}^n$ the zeros of P_n in increasing order, i.e.,

$$
P_n(x_{n,k}) = 0,\ 1 \leq k \leq n, \quad \text{and} \quad x_{n,1} < x_{n,2} < \cdots < x_{n,n}.
$$

Evaluating the operator $\tilde{\mathcal{D}}_n$ given by (5.46) at $x = x_{n,k}$, we see that

$$
\frac{P_n''(x_{n,k})}{P_n'(x_{n,k})} = -\frac{P_n^2(0)}{x(2h_nx + P_n^2(0))} - 2x_{n,k} = D_x\left[\ln(\tilde{A}_n(x_{n,k}))\right] - 2x_{n,k}, \quad n \geq 1, \tag{5.47}
$$

where $\tilde{A}_n$ is given by

$$
\tilde{A}_n(x) = 2 + \frac{1}{h_n}\cdot\frac{P_n^2(0)}{x} = \frac{2h_nx + P_n^2(0)}{h_nx}. \tag{5.48}
$$

Theorem 5.13. *The zeros of $P_n(x)$ correspond to the equilibrium positions of n unit-charged particles distributed within the interval $(0, \infty)$ under the influence of the potential*

$$
V_n(x) = x^2 + \ln|x| - \ln\left|x + \frac{P_n^2(0)}{2h_n}\right|. \tag{5.49}
$$

Proof. If we write $P_n(x) = \prod_{k=1}^n(x - x_{n,k})$, then according to [8, Ch. 10],

$$
\left.\frac{P_{n+1}''(x)}{P_{n+1}'(x)}\right|_{x=x_{n,k}} = \sum_{j=1,j\neq k}^n \frac{2}{x_{n,k} - x_{n,j}},
$$

and so, (5.47) implies that

$$
\begin{aligned}
&\sum_{j=1,j\neq k}^n \frac{2}{x_{n,k} - x_{n,j}} + 2x_{n,k} + \frac{P_n^2(0)}{x_{n,k}(2h_nx_{n,k} + P_n^2(0))} \\
&= \sum_{j=1,j\neq k}^n \frac{2}{x_{n,k} - x_{n,j}} + 2x_{n,k} - D_x\left[\ln(\tilde{A}_n(x_{n,k}))\right] = 0,
\end{aligned}
$$

or equivalently,

$$\frac{\partial E_n}{\partial x_{n,k}} = 0, \quad k = 1, \dots, n,$$

where the total energy of the system, $E_n := E_n(x_{n,1}, \dots, x_{n,n})$ is given by

$$E_n = -2 \sum_{1 \le j < k \le n} \ln |x_{n,k} - x_{n,j}| + \sum_{k=1}^{n} \left[x_{n,k}^2 - \ln \left(\tilde{A}_n(x_{n,k}) \right) \right]. \tag{5.50}$$

Due to (5.48), it is clear that

$$\begin{aligned} \frac{\tilde{A}_n'(x)}{\tilde{A}_n(x)} &= D_x \left[\ln \left(\tilde{A}_n(x) \right) \right] = D_x \left[\ln \left(2h_n x + P_n^2(0) \right) - \ln \left(h_n x \right) \right] \\ &= \frac{2h_n}{2h_n x + P_n^2(0)} - \frac{1}{x} = \frac{1}{x + \frac{P_n^2(0)}{2h_n}} - \frac{1}{x}. \end{aligned}$$

Therefore, we can rewrite (5.50) as

$$E_n = -2 \sum_{1 \le j < k \le n} \ln |x_{n,k} - x_{n,j}| + \sum_{k=1}^{n} \left[x_{n,k}^2 + \ln |x_{n,k}| - \ln \left| x_{n,k} + \frac{P_n^2(0)}{2h_n} \right| \right]$$

and consequently, the external potential V_n is expressed as (5.49). □

Remark 5.6. *Regarding the value of $P_n(0)$, it is important to note that it can be generated iteratively. Indeed, by the TTRR (2.3), one has that*

$$P_{n+1}(0) + \alpha_n P_n(0) + \beta_n P_{n-1}(0) = 0, \quad n \ge 1, \qquad P_0(0) = 1, \quad P_1(0) = -\frac{1}{\sqrt{\pi}}.$$

Moreover, considering that $\frac{P_n^2(0)}{2h_n} > 0$, we have an extra charge located at $-\frac{P_n^2(0)}{2h_n} < 0$. Additionally, it can be observed that there is a negative charge at the origin, which attracts the positive ones.

6. Concluding remarks

In this paper, we have analyzed a semiclassical linear functional of class 1 defined by the weight function $w(x) = e^{-x^2}$ supported in the positive real semi-axis. We deduce the Laguerre-Freud equations for the coefficients of the three term recurrence relation that the corresponding sequence of orthogonal polynomials satisfy. These coefficients are given in terms of a sequence satisfying a discrete Painlevé IV equation. In a next step the ladder operators associated with such a sequence of orthogonal polynomials are obtained. As a consequence, we get a second order linear differential equation with polynomial coefficients that such orthogonal polynomials satisfy. Thus an electrostatic interpretation of their zeros is discussed.

7. Acknowledgements

Authors thank the valuable comments by the referees. They have contributed to improve the presentation of the manuscript. The work of Francisco Marcellán has been supported by the research project [PID2021- 122154NB-I00] *Ortogonalidad y Aproximación con Aplicaciones en Machine Learning y Teoría de la Probabilidad* funded by MICIU/AEI/10.13039/501100011033 and by "ERDF A Way of making Europe".

REFERENCES

[1] S. Belmehdi: *On semi-classical linear functionals of class $s = 1$. Classification and integral representations*, Indag. Math. (New Series), **3** (3) (1992), 253–275.

[2] S. Belmehdi: A. Ronveaux, *Laguerre-Freud's equations for the recurrent coefficients of semi-classical orthogonal polynomials*, J. Approx. Theory, **76** (3) (1994), 351–368.

[3] Y. Chen, M. E. H. Ismail: *Ladder operators and differential equations for orthogonal polynomials*, J. Phys. A: Math. Gen., **30** (22) (1997), 7817–7829.

[4] Y. Chen, G. Pruessner: *Orthogonal polynomials with discontinuous weights*, J. Phys. A: Math. Gen., **38** (12) (2005), L191–L199.

[5] T. S. Chihara: *An Introduction to Orthogonal Polynomials*, New York, Dover Publications (2011).

[6] A. S. Clarke, B. Shizgal: *On the Generation of Orthogonal Polynomials Using Asymptotic Methods for Recurrence Coefficients*, J. Comput. Phys., **104** (1) (1993), 140–149.

[7] D. Dominici, F. Marcellán: *Truncated Hermite polynomials*, J. Difference Equ. Appl., **29** (7) (2023), 701–732.

[8] J. C. García-Ardila, F. Marcellán and M. E. Marriaga: *Orthogonal Polynomials and Linear Functionals. An Algebraic Approach and Applications*, Berlin, European Mathematical Society (2021).

[9] M. Landreman, D. R. Ernst: *New velocity-space discretization for continuum kinetic calculations and Fokker–Planck collisions*, J. Comput. Phys., **243** (2013), 130–150.

[10] S. Lyu, Y. Chen: *Gaussian unitary ensembles with two jump discontinuities, PDEs and the coupled Painlevé II and IV systems*, Stud. Appl. Math., **146** (1) (2021), 118–138.

[11] A. P. Magnus: *Freud's equations for orthogonal polynomials as discrete Painlevé equations*, in *Symmetries and Integrability of Difference Equations*, P. A. Clarkson and F. W. Nijhoff, Eds., Cambridge University Press., London Math. Soc. Lect. Note Ser., vol **255**, 228–343, 1999.

[12] P. Maroni: *Prolégomènes à l' étude des polynômes orthogonaux semi-classiques*, Ann. Mat. Pura Appl. (4), **149** (1987), 165–184.

[13] P. Maroni: *Une théorie algébrique des polynômes orthogonaux. Application aux polynômes orthogonaux semi-classiques*, in *Orthogonal Polynomials and Their Applications*, C. Brezinski et al., Eds., IMACS Ann. Comput. Appl. Math., vol. **9**, 95–130, Baltzer, Basel (1991).

[14] T. Sánchez-Vizuet, A. J. Cerfon: *Pseudo spectral collocation with Maxwell polynomials for kinetic equations with energy diffusion*, Plasma Phys. Control. Fusion, **60** (2) (2018), Article ID: 025018.

[15] B. Shizgal: *A Gaussian quadrature procedure for use in the solution of the Boltzmann equation and related problems*, J. Comput. Phys., **41** (2) (1981), 309–328.

[16] J. Shohat: *A differential equation for orthogonal polynomials*, Duke Math. J., **5** (1939), 401–417.

[17] W. Van Assche: *Orthogonal Polynomials and Painlevé Equations*, Cambridge, Cambridge University Press (2018).

[18] W. Van Assche: *Orthogonal and Multiple Orthogonal Polynomials, Random Matrices, and Painlevé Equations,* in *Orthogonal Polynomials and Their Applications*, Mama Foupouagnigni and Wolfram Koepf, Eds., 629–683, Cham Springer International Publishing (2020).

[19] M. Vanlessen: *Strong Asymptotics of Laguerre-Type Orthogonal Polynomials and Applications in Random Matrix Theory*, Constr. Approx., **25** (2) (2007), 125–175.

ÁNGEL ÁLVAREZ-PAREDES
UNIVERSIDAD CARLOS III DE MADRID
DEPARTMENT OF MATHEMATICS
28911 LEGANÉS, MADRID, SPAIN
ORCID: 0000-0000-0000-0000
Email address: angalvar@math.uc3m.es

RUYMÁN CRUZ-BARROSO
LA LAGUNA UNIVERSITY
DEPARTMENT OF MATHEMATICAL ANALYSIS AND INSTITUTO DE MATEMÁTICAS Y SUS APLICACIONES (IMAULL)
38271 LA LAGUNA, TENERIFE, CANARY ISLANDS, SPAIN
ORCID: 0000-0001-8002-1829
Email address: rcruzb@ull.edu.es

FRANCISCO MARCELLÁN
UNIVERSIDAD CARLOS III DE MADRID
DEPARTMENT OF MATHEMATICS
28911 LEGANÉS, MADRID, SPAIN
ORCID: 0000-0003-4331-4475
Email address: pacomarc@ing.uc3m.es

CONSTRUCTIVE MATHEMATICAL ANALYSIS
7 (2024), No. SI, pp. 114-128
http://dergipark.org.tr/en/pub/cma
ISSN 2651 - 2939

Research Article

Approximation of the Hilbert transform on $(0, +\infty)$ by using discrete de la Vallée Poussin filtered polynomials

Dedicated to Professor Paolo Emilio Ricci, on occasion of his 80th birthday, with respect and friendship.

DONATELLA OCCORSIO*

ABSTRACT. In the present paper, is proposed a method to approximate the Hilbert transform of a given function f on $(0, +\infty)$ employing truncated de la Vallée discrete polynomials recently studied in [25]. The method generalizes and improves in some sense that introduced in [24] based on a truncated Lagrange interpolating polynomial, since is faster convergent and simpler to apply. Moreover, the additional parameter defining de la Vallée polynomials helps to attain better pointwise approximations. Stability and convergence are studied in weighted uniform spaces and some numerical tests are provided to asses the performance of the procedure.

Keywords: Hilbert transform, discrete de la Vallèe-Poussin approximation, generalized Laguerre polynomials, approximation by polynomials.

2020 Mathematics Subject Classification: 65D30, 41A05.

1. INTRODUCTION

Let $\mathcal{H}(f,t)$ be the Hilbert transform of f

$$\mathcal{H}(f,t) = \int_0^\infty \frac{f(x)}{x-t} w(x)dx, \tag{1.1}$$

where $w(x) = e^{-x}x^\alpha$ is a Laguerre weight, and the integral in (1.1) is understood in the Cauchy principal value sense. In numerical analysis and in approximation theory, the approximation of Hilbert transforms over bounded or unbounded regions, represents a relevant topic, since it arises in several problems of the applied sciences, such as image analysis, optics, signal processing, fluid mechanics, electrodynamics. A collection of problems can be found in [13, Vol I , II]. In addition, Hilbert transforms and their derivatives can appear in singular and hypersingular integral equations, which in turn are possible tools to model several physics problems [20, 14, 15]. The literature dealing with numerical methods to approximate Hilbert transforms is rich. We cite among them [9, 21, 1, 12, 3, 5, 22, 7, 8, 10, 23] and the references contained in it. Concerning the approximation of $\mathcal{H}(f,t)$ by global methods based on Laguerre zeros, we recall two product-type integration rules, one obtained by approximating f by truncated Lagrange polynomials [5], the other by discrete de la Vallée Poussin polynomials [25]. In both these rules, the coefficients are obtained by recurrence relations depending on t, and hence requiring a considerable computational effort when $\mathcal{H}(f,t)$ is needed for a large number of points. So they are efficient, but "expensive". Another significant and reliable approach is given by the truncated Gauss-Laguerre rule, suitable "modified" to overcome numerical instability due to

Received: 01.08.2024; Accepted: 10.10.2024; Published Online: 16.12.2024
*Corresponding author: Donatella Occorsio; donatella.occorsio@unibas.it
DOI: 10.33205/cma.1541668

the closeness of some Gaussian node to the singularity t [8]. Such rule largely applied also in other contexts (see e.g. [4, 8, 2]) is simpler than the previous ones, but not employable in methods for solving integral equations, since it requires the choice between two sequence of Gauss-Laguerre nodes, according to the position of the singularity t. To overcome in some sense the aforesaid issues, in [24] it was introduced a method to approximate the function

$$\mathcal{F}(f,t)=\int_0^\infty \frac{f(x)-f(t)}{x-t}w(x)dx,$$

by means of suitable truncated Lagrange polynomials based on Laguerre zeros (say it L-method), and to compute $\mathcal{H}(f,t)=\mathcal{F}(f,t)+f(t)\mathcal{H}(\mathbf{1},t)$. By this way, for any t are required always the same samples of $\mathcal{F}(f)$. In the present paper, we want to generalize the L-method and improve it in some sense, proposing to approximate $\mathcal{F}(f)$ by the sequence of discrete de la Vallée Poussin (VP) polynomials $V_n^m(w,\mathcal{F}(f))$, recently introduced and studied in [25]. Analogously to the L-method, the polynomial $V_n^m(w,\mathcal{F}(f))$ requires the samples of the function $\mathcal{F}(f)$ at $j << n$ zeros of the Laguerre polynomial $p_n(w)$. Moreover, $V_n^m(w,\mathcal{F}(f))$ depends on the additional parameter $1\le m\le n-1$, which in turns can be fruitfully used to reduce possible Gibbs phenomenon. As it is known, the latter affects Lagrange interpolating approximation, especially when the interpolated function presents isolated "pathologies" (peaks, cusps, etc.). In addition, the Lebesgue constants associated to VP polynomials, are uniformly bounded in weighted spaces of continuous functions, whereas those of the Lagrange processes diverge logarithmically at least.

The outline of the paper is as follows. In Section 2 are collected some notations and preliminary results useful to introduce the proposed numerical method. The latter is stated in Section 3, accompanied by the study of the stability and convergence, and error estimates in suitable spaces of functions. Finally, in Section 4, a selection of numerical tests is proposed.

2. Notations and preliminary results

Along all the paper the notation $\mathcal{C}$ will be used several times to denote a positive constant having different values in different formulas. We will write $\mathcal{C}\neq\mathcal{C}(a,b,\ldots)$ in order to say that $\mathcal{C}$ is independent of the parameters $a,b,\ldots$, and $\mathcal{C}=\mathcal{C}(a,b,\ldots)$ to say that $\mathcal{C}$ depends on $a,b,\ldots$. Moreover, if $A,B>0$ are quantities depending on some parameters, we will write $A\sim B$, if there exists an absolute constant $\mathcal{C}>0$, independent on such parameters, such that $\mathcal{C}^{-1}B\le A\le\mathcal{C}B$.

Denote by $\mathbb{P}_m$ the space of all algebraic polynomials of degree at most m.

2.1. **Orthogonal Polynomials.** For $w(x)=e^{-x}x^\alpha,\quad \alpha>-1$, let $\{p_n(w)\}_n$ be the corresponding sequence of orthonormal polynomials with positive leading coefficients, i.e.

$$p_n(w,x)=\gamma_n(w)x^n+\text{ terms of lower degree},\quad \gamma_n(w)>0.$$

Denoted by $\{x_{n,k}(w)\}_{k=1}^n$ the zeros of $p_n(w)$, it is known that [27]

$$\frac{\mathcal{C}}{n}<x_{n,1}(w)<x_{n,2}(w)<\ldots<x_{n,n}(w)<4n+2\alpha-\mathcal{C}n^{\frac{1}{3}},\qquad \mathcal{C}\neq\mathcal{C}(n). \tag{2.2}$$

For any fixed $0<\rho<1$ the node $x_{n,j}$, $j=j(n)$, is defined as

$$x_{n,j}(w)=\min\left\{x_{n,k}(w):x_{n,k}(w)\ge 4n\rho,\quad k=1,2,..,n\right\}. \tag{2.3}$$

As it is known, the zeros of $p_n(w)$ interlace those of $p_{n+1}(w)$, i.e.

$$x_{n+1,k}(w)<x_{n,k}(w)<x_{n+1,k+1}(w),\qquad k=1,2,\ldots,n. \tag{2.4}$$

Moreover, inside the interval $[0, x_{n+1,j_1}(w)]$ where j_1 is defined as

$$x_{n+1,j_1}(w) = \min\{x_{n+1,k}(w) : x_{n+1,k}(w) \geq 4(n+1)\rho, \quad k = 1, 2, .., n+1\}, \tag{2.5}$$

the distance between two consecutive zeros of $p_{n+1}(w)p_n(w)$ can be estimated as [4, Lemma 2.1]

$$x_{n,k}(w) - x_{n+1,k}(w) \geq \mathcal{C}\sqrt{\frac{x_{n+1,k}(w)}{n}}, \quad k = 1, 2, \ldots, j, \tag{2.6}$$

uniformly in $n \in \mathbb{N}$.

Finally, we recall the "truncated" Gauss-Laguerre rule introduced in [18] and based on the first j zeros of $p_n(w)$, j defined in (2.3),

$$\int_0^\infty f(x)w(x)dx = \sum_{k=1}^{j} f(x_{n,k}(w))\lambda_{n,k}(w) + R_m(f), \tag{2.7}$$

where $\{\lambda_{n,k}(w)\}_{k=1}^n$ are the Christoffel numbers w.r.t. w and $R_n(f)$ is the remainder term.

2.2. **Function Spaces.** Introducing the weight $u(x) = e^{-\frac{x}{2}}x^\gamma, \quad \gamma \geq 0$, we consider the space C_u of the functions f continuous in any closed subset of $]0, \infty[$, such that

$$\lim_{x\to+\infty}(fu)(x) = 0, \qquad \text{and, if } \gamma > 0, \text{ also} \qquad \lim_{x\to 0^+}(fu)(x) = 0,$$

endowed with the norm $\|f\|_{C_u} = \sup_{x\geq 0}|f(x)|u(x)$. The error of best approximation of $f \in C_u$ by algebraic polynomials of degree $\leq n$ is defined as

$$E_n(f)_u = \inf_{P\in\mathbb{P}_n}\|(f-P)u\|_\infty.$$

For $s \in \mathbb{N}$, $s \geq 1$, let $W_s(u)$ be the Sobolev-type space

$$W_s(u) = \left\{f \in C_u : f^{(s-1)} \in AC(\mathbb{R}^+), \|f^{(s)}\varphi^s u\|_\infty < \infty\right\}, \qquad \varphi(x) = \sqrt{x},$$

where $AC(\mathbb{R}^+)$ denotes the set of the functions which are absolutely continuous on every closed subset of $\mathbb{R}^+$, equipped with the norm

$$\|f\|_{W_s(u)} = \|f\|_{C_u} + \|f^{(s)}\varphi^s u\|_\infty. \tag{2.8}$$

In order to deal with more refined subspaces of C_u, for any $\lambda \in \mathbb{R}^+$ let $Z_\lambda(u)$ be the Zygmund-type space

$$Z_\lambda(u) = \left\{f \in C_u \ : \ \sup_{t>0}\frac{\Omega^r_\varphi(f,t)_u}{t^\lambda} < +\infty\right\}$$

of parameter $0 < \lambda < r$, $r \in \mathbb{N}$, where

$$\Omega^r_\varphi(f,t)_u = \sup_{0<h\leq t}\|u\Delta^r_{h\varphi}f\|_{I_{rh}}, \quad t > 0$$

is the main part of the $r-$th $\varphi-$modulus of smoothness, $I_{rh} = \left[4r^2h^2, \frac{\mathcal{C}}{h^2}\right]$, being $\mathcal{C}$ a fixed positive constant, and

$$\Delta^r_{h\varphi}f(x) = \sum_{k=0}^{r}(-1)^k\binom{r}{k}f\left(x + h\varphi(x)(r-k)\right),$$

equipped with the norm

$$\|f\|_{Z_\lambda(u)} = \|f\|_{C_u} + \sup_{t>0}\frac{\Omega^r_\varphi(f,t)_u}{t^\lambda}.$$

$E_n(f)_u$ can be estimated in Zygmund and Sobolev subspaces as follows [6, 16]

$$E_n(f)_u \le \mathcal{C}\frac{\|f\|_{W_s(u)}}{\sqrt{n^s}}, \quad \forall f \in W_s(u), \tag{2.9}$$

$$E_n(f)_u \le \frac{\mathcal{C}}{\sqrt{n^\lambda}}\|f\|_{Z_\lambda(u)}, \quad \forall f \in Z_\lambda(u), \tag{2.10}$$

where in both the cases $\mathcal{C} \neq \mathcal{C}(n,f)$.

2.3. **VP filtered approximation.** For a given $n \in \mathbb{N}$ and with $m \in \mathbb{N}$ s.t. $1 \le m \le n-1$, the discrete VP filtered polynomial $V_n^m(w,f)$ approximating a given function $f \in C_u$ is defined as [25]

$$V_n^m(w,f,x) = \sum_{k=1}^{j} f(x_{n,k}(w))\Phi_{n,k}^m(x), \qquad x \ge 0 \tag{2.11}$$

with j defined in (2.3), and the fundamental VP polynomials defined as

$$\Phi_{n,k}^m(x) = \lambda_{n,k}(w) \sum_{i=0}^{n+m-1} \mu_{n,i}^m p_i(w, x_{n,k}(w)) p_i(w,x), \tag{2.12}$$

where $\mu_{n,i}^m$ are called "filter coefficients"

$$\mu_{n,i}^m := \begin{cases} 1 & \text{if} \quad i = 0,\dots,n-m, \\ \dfrac{n+m-i}{2m} & \text{if} \quad n-m+1 \le i \le n+m-1. \end{cases} \tag{2.13}$$

The polynomial $V_n^m(w,f) \in \mathbb{P}_{n+m-1}$ and does not interpolate f.

One of the main features proved in [25] is the boundedness of the map $V_n^m(w) : f \in C_u \to C_u$ under proper assumptions on w and u. This means to deal with a polynomial sequence uniformly convergent to any function $f \in C_u$, behaving as a near–best approximation polynomial sequence. This property similarly holds in $[-1,1]$ for filtered de la Vallée Poussin polynomials w.r.t. Jacobi polynomials, introduced and studied in [28].

Theorem 2.1 ([25]). *For any $f \in C_u$, under the assumption*

$$\max\left\{\frac{\alpha}{2} - \frac{1}{4},\ 0\right\} < \gamma < \min\left\{\frac{\alpha}{2} + \frac{7}{6},\ \alpha + 1\right\} \tag{2.14}$$

then, fixing $\theta \in (0,1)$ and choosing $m = \lfloor n\theta \rfloor$, the map $V_n^m(w) : C_u \to C_u$ is uniformly bounded w.r.t. n, i.e.

$$\|V_n^m(w,f)\|_{C_u} \le \mathcal{C}\|f\|_{C_u}, \quad \forall f \in C_u, \qquad \mathcal{C} \neq \mathcal{C}(n,m,f). \tag{2.15}$$

Moreover, with $0 < \rho < 1$ fixed to define the index j in (2.3),

$$\|(f - V_n^m(w,f))\|_{C_u} \le \mathcal{C}\left(E_q(f)_u + e^{-An}\|f\|_{C_u}\right), \quad q = \min\left\{n-m,\ \left\lfloor n\frac{\rho}{(1+\rho)}\right\rfloor\right\}, \tag{2.16}$$

with the positive constants $\mathcal{C}, A$ independent of n, m, f.

We point out that Theorem 2.1 has been proved in [25], under more general relationships between n and m.

2.4. **Truncated Lagrange interpolation.** With j defined in (2.3), in [17] it was introduced the truncated Lagrange polynomial $L^*_{n+1}(w,f)$ defined as

$$L^*_{n+1}(w,f,x) := \sum_{k=1}^{j} f(x_{n,k}(w))\ell_{n,k}(x), \tag{2.17}$$

where

$$\ell_{n,k}(x) = \frac{p_n(w,x)}{p_n'(x_k)(x-x_k)}\frac{4n-x}{4n-x_k}, \qquad k=1,2,\dots,j, \tag{2.18}$$

are fundamental Lagrange polynomials based on the zeros of $p_n(w,x)(4n-x)$. $L^*_{n+1}(w,f)$ interpolates the function at the first j zeros of $p_n(w)$ and vanishes at the remaining nodal points $x_{n,j+1}(w),\dots,x_{n,n}(w),4n$. In particular, for $\rho = 1$ $L^*_{n+1}(w,f)$ coincides with the Lagrange polynomial $L_{n+1}(w,f)$, interpolating f at all the zeros of $p_n(w,x)(4n-x)$. It is known that the norm of the operator $L^*_{n+1}(w) : f \in C_u \to C_u$, i.e. the weighted Lebesgue constant

$$\|L^*_{n+1}(w)\|_{C_u} = \sup_{\|fu\|=1}\|L^*_{n+1}(w,f)u\| = \sup_{x\geq 0}\sum_{k=1}^{j}|\ell_{n,k}(x)|\frac{u(x)}{u(x_{n,k}(w))}, \tag{2.19}$$

as $n\to\infty$ diverge at least as $\log n$. To be more precise, the following result holds

Theorem 2.2 ([17]). *Let $w(x)=e^{-x}x^\alpha$, $\alpha>-1$ and $u(x)=e^{-\frac{x}{2}}x^\gamma$, $\gamma\geq 0$. Under the assumption*

$$\min\left(0,\frac{\alpha}{2}+\frac{1}{4}\right)\leq\gamma\leq\frac{\alpha}{2}+\frac{5}{4}, \tag{2.20}$$

we have

$$\|L^*_{n+1}(w,f)\|_{C_u}\leq\mathcal{C}\|f\|_{C_u}\log n, \quad \forall f\in C_u, \qquad \mathcal{C}\neq\mathcal{C}(n,f). \tag{2.21}$$

Remark 2.1. *We point out that in* [19] *it was proved that*

$$\|L_{n+1}(w,f)\|_{C_u}\leq\mathcal{C}\|f\|_{C_u}\log n, \quad \forall f\in C_u, \qquad \mathcal{C}\neq\mathcal{C}(n,f), \tag{2.22}$$

if and only if the assumption (2.20) *holds.*

3. The method

Let us start from the relation

$$\mathcal{H}(f,t)=\mathcal{F}(f,t)+f(t)\mathcal{H}(\mathbf{1},t), \quad \mathcal{F}(f,t)=\int_0^\infty\frac{f(x)-f(t)}{x-t}w(x)dx, \tag{3.23}$$

and assume from now on $\alpha<1$, since in the case $\alpha\geq 1$ we deal equivalently with $\widetilde{\mathcal{H}}(g,t):=\int_0^\infty\frac{g(x)}{x-t}\tilde{w}(x)dx$, $g(x):=f(x)x^{[\alpha]}$, $\tilde{w}(x)=e^{-x}x^{\alpha-[\alpha]}$. Now, taking into account that $\mathcal{H}(\mathbf{1},t)$ can be computed by [11, p. 1086, 9.213]

$$\mathcal{H}(\mathbf{1},t)=\begin{cases}-e^{-t}\mathrm{Ei}(t), & \alpha=0\\ -\pi t^\alpha e^{-t}\cot((1+\alpha)\pi)+\Gamma(\alpha){}_1\mathrm{F}_1(1,1-\alpha,-t), & \alpha\neq 0,\end{cases} \tag{3.24}$$

where $\mathrm{Ei}(t)$ and ${}_1\mathrm{F}_1(a,b,x)$ are the exponential integral function and the Confluent Hypergeometric function, respectively, we focus on the approximation of $\mathcal{F}(f)$. To this end, we recall a result proved in [24], which relates the smoothness of $\mathcal{F}(f)$ to that of f.

Lemma 3.1. *For any $f \in Z_{\lambda+1}(u)$, under the assumption $0 \le \gamma < \alpha + \frac{1}{4}$, the function $\mathcal{F}(f) \in Z_\lambda(u)$, and*

$$E_n(\mathcal{F}(f))_u \le \mathcal{C}\frac{\|f\|_{Z_{\lambda+1}(u)}}{\sqrt{n^\lambda}}, \quad \mathcal{C} \ne \mathcal{C}(n,f). \tag{3.25}$$

Belonging $\mathcal{F}(f)$ to a subspace of C_u allows to approximate $\mathcal{F}(f)$ by the sequence of VP polynomials defined in (2.11), i.e. to consider

$$\mathcal{F}(f,t) \sim V_n^m(w,\mathcal{F}(f),t) = \sum_{k=1}^{j} \Phi_{n,k}^m(t)\mathcal{F}(f,x_{n,k}(w)). \tag{3.26}$$

By Lemma 3.1, and Theorem 2.1 combined with estimate (2.10), under the assumption

$$\max\left\{\frac{\alpha}{2}-\frac{1}{4},\,0\right\} \le \gamma < \alpha + \frac{1}{4},$$

$\mathcal{F}(f)$ can be uniformly approximated by $V_n^m(w,\mathcal{F}(f))$, and the error is

$$\|\mathcal{F}(f) - V_n^m(w,\mathcal{F}(f))\|_{C_u} \le \mathcal{C}\frac{\|f\|_{Z_{\lambda+1}(u)}}{\sqrt{n^\lambda}}, \quad \forall f \in Z_{\lambda+1}(u). \tag{3.27}$$

However, the computational problem in constructing (3.26) is the lack of the samples $\{\mathcal{F}(f,x_{n,k}(w))\}_{k=1}^j$, unknown in the general case. To overcome this problem, the integrals $\mathcal{F}(f,x_{n,k}(w))$, $k=1,2,\dots,j$ are approximated by the $(n+1)$-th truncated Gauss-Laguerre rules w.r.t. the weight w, i.e.,

$$\mathcal{F}(f,x_{n,k}(w)) \sim \sum_{i=1}^{j_1} \lambda_{n+1,i}(w)\frac{f(x_{n+1,i}(w)) - f(x_{n,k}(w))}{x_{n+1,i}(w) - x_{n,k}(w)}, \quad k=1,\dots,j,$$

being for every fixed $\rho \in (0,1)$ the index j_1 defined in (2.5). Note that possible numerical cancellation arising in case t is "too close" to any Gauss-Laguerre nodes is avoided, since the zeros of $p_n(w)$ are far enough from the Gaussian nodes $x_{n+1,k}(w)$ in view of (2.6). Now we prove that these further approximations $\mathcal{F}(f,x_{n,k}(w)) \sim \mathcal{F}_{n+1}(f,x_{n,k}(w))$, induce errors of the same orders as $\|\mathcal{F}(f) - V_n^m(w,\mathcal{F}(f))\|_{C_u}$. This is stated in the next lemma.

Lemma 3.2. *For any $f \in Z_{\lambda+1}(u)$, under the assumption $0 \le \gamma < \alpha + \frac{1}{4}$, the following error estimate holds true*

$$\|\mathcal{F}(f) - \mathcal{F}_{n+1}(f)\|_{C_u} \le \mathcal{C}\,\frac{\|f\|_{Z_{\lambda+1}(u)}}{\sqrt{n^\lambda}}, \quad \mathcal{C} \ne \mathcal{C}(n,f). \tag{3.28}$$

Proof. First we recall that under the assumption $0 \le \gamma < \alpha + \frac{1}{4}$, for any $f \in Z_{\lambda+1}(u)$ in [24, Lemmas 5.5, 5.7] there were proved $\mathcal{F}_{n+1}(f) \in Z_{\lambda+1}(u)$ and

$$E_n(\mathcal{F}_n(f))_u \le \mathcal{C}\frac{\|f\|_{Z_{\lambda+1}(u)}}{\sqrt{n^\lambda}}. \tag{3.29}$$

As a consequence, for any $P_n \in \mathbb{P}_n$

$$\|\mathcal{F}(f) - \mathcal{F}_n(f)\|_{C_u} \le \mathcal{C}\,(E_n(\mathcal{F}(f))_u + E_n(\mathcal{F}_n(f))_u)$$

and in view of estimates (3.25) and (3.29), (3.28) follows. □

In conclusion, we approximate the function $\mathcal{F}(f)$ by the sequence $\{V_n^m(w,\mathcal{F}_{n+1}(f))\}_n$, i.e.,

$$\mathcal{F}(f,t) = \Sigma_n(\mathcal{F},t) + e_{n,m}(f,t),, \tag{3.30}$$

being

$$\Sigma_n(f,t) := \sum_{k=1}^{j} \Phi_{n,k}^m(t)\mathcal{F}_{n+1}(f, x_{n,k}(w)) = \sum_{k=1}^{j} \Phi_{n,k}^m(t) \sum_{i=1}^{j_1} \lambda_{n+1,i}(w) \frac{f(x_{n+1,i}(w)) - f(x_{n,k}(w))}{x_{n+1,i}(w) - x_{n,k}(w)}.$$

Next Theorem states conditions under which formula (3.30) is stable and convergent

Theorem 3.3. *For any $f \in Z_{\lambda+1}(u),\ \lambda > 0$, under the assumption*

$$\max\left(0, \frac{\alpha}{2} - \frac{1}{4}\right) \le \gamma < \alpha + \frac{1}{4}, \tag{3.31}$$

$$\|\Sigma_n(f)\|_{C_u} \le \mathcal{C}\|f\|_{Z_{\lambda+1}(u)}, \tag{3.32}$$

and

$$\|e_{n,m}(f)\|_{C_u} \le \mathcal{C}\frac{\|f\|_{Z_{\lambda+1}(u)}}{\sqrt{n^\lambda}}, \tag{3.33}$$

$\mathcal{C} \ne \mathcal{C}(n, f)$.

Proof. First we prove (3.32). Using $\Sigma_n(f,t) = V_n^m(w, \mathcal{F}_{n+1}(f), t)$, by Theorem 2.1, under the assumption (3.31),

$$\|\Sigma_n(f)\|_{C_u} \le \mathcal{C}\|\mathcal{F}_{n+1}(f)\|_{C_u}$$

and by Lemma 3.2 and (3.25), (3.32) follows. To estimate (3.33), start from

$$\begin{aligned} |e_{n,m}(f,t)|u(t) &= |\mathcal{F}(f,t) - V_n^m(w, \mathcal{F}_{n+1}(f), t)|u(t) \\ &\le |\mathcal{F}(f,t) - \mathcal{F}_{n+1}(f,t)|u(t) \\ &+ |\mathcal{F}_{n+1}(f,t) - V_n^m(w, \mathcal{F}_{n+1}(f), t)|u(t) \\ &=: A_1(t) + A_2(t). \end{aligned} \tag{3.34}$$

Under the assumption $f \in Z_{\lambda+1}(u)$ by Lemma 3.2

$$A_1(t) \le \mathcal{C}\frac{\|f\|_{Z_{\lambda+1}(u)}}{\sqrt{n^\lambda}}, \tag{3.35}$$

and by Theorem 2.1 combined with estimate (3.29), we get

$$A_2(t) \le \mathcal{C}\ E_q(\mathcal{F}_{n+1}(f))_u \le \mathcal{C}\frac{\|f\|_{Z_{\lambda+1}(u)}}{\sqrt{n^\lambda}}, \tag{3.36}$$

and (3.33) follows combining (3.35),(3.36) with (3.34) □

3.1. **Comparison between VP-method and L-method.** As previously said, in [24] the function $\mathcal{F}(f,t)$ has been approximated by using truncated Lagrange polynomials interpolating $\mathcal{F}(f,t)$ and based on Laguerre zeros. To be more precise, denoted by $w^+(x) = e^{-x}x^{\alpha+1}$, $w^-(x) = e^{-x}x^{\alpha-1}$ in the case $\alpha > 0$, the following work-scheme has been considered:

$$\mathcal{F}(f,t) \sim \begin{cases} L_{n+1,1}^*(w^+, \mathcal{F}_{n+1}(f), t) & -\frac{1}{4} < \alpha \le 0 \\ L_{n+2}^*(w^-, \mathcal{F}_n(f), t), & \alpha > 0, \end{cases} \tag{3.37}$$

where $\mathcal{F}_{n+1}(f,t) = \sum_{i=1}^{j} \lambda_{n+1,i}(w)\frac{f(x_{n+1,i}(w))-f(t)}{x_{n+1,i}(w)-t}$, $L_{n+1,1}^*(w^+, \mathcal{F}_{n+1}(f), x)$ is the truncated Lagrange polynomial based on the knots $\{x_{n,k}(w^+)\}_{k=1}^n \cup \{4n\} \cup \{t_1\}$, with $t_1 = \frac{x_{n,1}(w^+)}{2}$, and

$L^*_{n+2}(w^-,\mathcal{F}_n(f),t)$ is the truncated polynomial based on the knots $\{x_{n+1,k}(w^-)\}_{k=1}^n \cup \{4n\}$. It was necessary introduce two different paths, in order to consider interpolation processes having Lebesgue constants behaving always as $\log n$, for any choice of α,γ satisfying (3.31). The VP-method, unlike the L-method, is simpler to construct, since involves only one approximant, without distinguishing two cases, whatever are the values of α and γ satisfying (3.31).

About the rate of convergence, the L-method results a little bit slower than the VP-method, due to the presence of the extra factor $\log n$ (see [24, Theorems 3.2-3.3]. In conclusion from the theoretical and computational point of view, the VP-method represents a simpler strategy to obtain a little bit faster convergence.

4. Numerical Examples

We have tested the VP-method and compared the results with those taken by using the L-method on some test functions. Here we go to propose a selection of three examples which seem to be more exhaustive to highlight the performance of the VP-method in comparison with the L-method. In each tests we have considered the approximation only of the function $\mathcal{F}(f)$, this being the main topic we are dealing with. We precise that:

- $$e^{VP}_{n,m}(\mathcal{F},t) = |V^m_n(w,\mathcal{F}_{n+1}(f),t) - \mathcal{F}(f,t)|u(t),$$
  $$e^{Lag}_{n}(\mathcal{F},t) = |L^*_{n+1}(\mathcal{F}_{n+1}(f),t) - \mathcal{F}(f,t)|u(t),$$
  are the weighted pointwise errors related to the approximation of $\mathcal{F}(f)$ only.
- $$\|e^{VP}_{n,m}(\mathcal{F})\| = \max_{t\in Y} e^{VP}_{n,m}(\mathcal{F},t),$$
  $$\|e^{Lag}_{n}(\mathcal{F})\| = \max_{t\in Y} e^{Lag}_{n}(\mathcal{F},t),$$
  are the maximum weighted errors on Y, where Y is a sufficiently large mesh of equispaced points in the range $(0,a)$ with $a>0$ sufficiently large.
- The parameter $\theta\in(0,1)$ defining $m=\lfloor n\theta\rfloor$ in $V^m_n(w,\mathcal{F}_{n+1}(f),t)$, has been selected as that giving the minimal absolute error $e^{VP}_{n,m}(\mathcal{F},t)$.
- The exact values, always unknown, have been computed for $n=2048,\ m=n/2$.
- All the computations have been performed in double-machine precision ($eps\sim 2.22044e-16$).
- In each test we have selected two values of $t>0$ providing the pointwise absolute errors $|e^{VP}_{n,m}(\mathcal{F},t)|u(t)$ (first column), the values of n and θ in the first and second columns, respectively. The errors $|e^{Lag}_{n}(\mathcal{F},t)|u(t)$ are reported in the fifth column, while the third column contains the number j of functions evaluations in both the VP-rule and the L-rule. Moreover, in each tests are given also the maximum absolute errors taken over proper ranges of t.
- Some graphs are stated to highlight the benefits offered by the VP-method, by suitably modulating the parameter m to reduce pointwise errors, especially in case f presents isolated "pathologies" (peaks, cusps, etc.), i.e. reducing Gibbs phenomenon, which affects Lagrange interpolating polynomials not only around the localized "pathological" point, but also along subinterval "far" from the point itself.

Example 4.1.

$$\mathcal{F}(f,t) = \int_0^\infty \frac{f(x)-f(t)}{x-t}e^{-x}x^{0.6}dx, \quad f(x)=\frac{1}{100+10(x-3)^2},\ \alpha=0.6.$$

According to the conditions stated for both the VP-method and L-method, we take the parameter $\gamma = 0.05$. *In Tables 1, are reported the results related to the pointwise approximation for* $t = 3$, *and* $t = 10$. *The approximate values are in this case*

$$\mathcal{F}(f,3)u(3) \sim 2.0516e-04, \quad \mathcal{F}(f,10)u(10) \sim -5.0389e-06.$$

In this case $f(x) \in Z_\lambda(u),\ \forall \lambda > 0$, *and presents a peak for* $x = 3$. *As Table 1 shows, better results are attained on average by VP-method, and the machine precision is catched for some* n.

n	θ	j	$\|e_{n,m}^{VP}(\mathcal{F},t)\|u(t)$	$\|e_n^{Lag}(\mathcal{F},t)\|u(t)$
20	1.0e-01	19	1.00e-07	9.23e-08
50	1.0e-01	32	3.52e-09	2.20e-09
150	3.0e-01	56	1.47e-14	1.35e-12
250	1.0e-01	73	6.62e-15	6.02e-15
350	2.0e-01	87	3.36e-17	1.07e-16

n	θ	j	$\|e_{n,m}^{VP}(\mathcal{F},t)\|u(t)$	$\|e_n^{Lag}(\mathcal{F},t)\|u(t)$
20	5.0e-01	19	1.12e-08	3.23e-08
50	3.0e-01	32	2.18e-11	1.43e-09
150	1.0e-01	56	1.09e-13	2.47e-13
250	2.0e-01	73	1.30e-16	4.84e-16
350	1.0e-01	87	1.65e-18	1.25e-17

TABLE 1. Ex.1: $t = 3$ (up), $t = 10$ (down)

In Table 2 are given the maximum absolute errors attained for increasing values of n *in* $[0, 10]$, *and a moderate better performance of the VP-method w.r.t. the L-method is confirmed.*

n	$\|e_{n,m}^{VP}(\mathcal{F})u\|$	$\|e_n^{Lag}(\mathcal{F})u\|$
20	6.66e-07	6.27e-07
50	6.98e-09	1.87e-08
150	1.98e-12	1.02e-11
250	8.11e-15	1.49e-14
350	1.04e-15	2.76e-15

TABLE 2. Ex.1: maximum errors in $[0, 10]$

We conclude proposing the graph of the pointwise absolute errors attained for $n = 150$, *choosing the "optimal"* θ *for any point* t *(Fig. 1), and as expected, and the pointwise errors by the VP-method are better than those attained by the L-method. In addition, we have produced in Fig. 2 also the graph of the pointwise absolute errors for* $\theta = 0.1$, *to highlight that also for* θ *fixed, the previous trend is confirmed.*

Example 4.2.

$$\mathcal{F}(f,t) = \int_0^\infty \frac{f(x)-f(t)}{x-t}\frac{e^{-x}}{x^{\frac{1}{8}}}dx, \quad f(x) = \frac{e^{x/4}}{(1+x^2)^4},\ \alpha = -1/8,\ \gamma = 0.5.$$

In this test $f \in Z_\lambda(u), \forall \lambda > 0$, *and grows exponentially as* $x \to +\infty$. *In Table 3 are reported the pointwise errors for* $t = 1$ *and* $t = 15$. *The approximate values are*

$$\mathcal{F}(f,1)u(1) \sim -3.9662e-01, \quad \mathcal{F}(f,15)u(15) \sim -7.0825e-05.$$

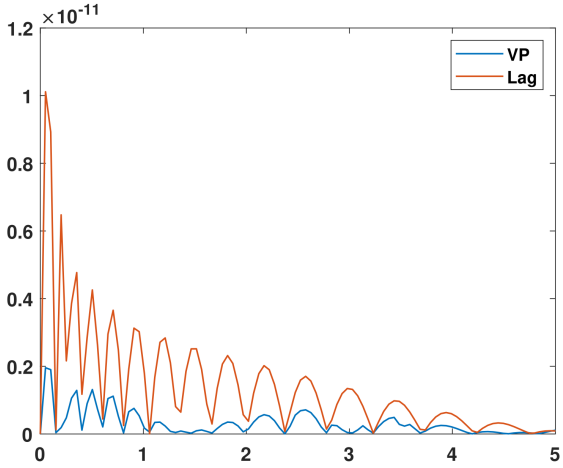

FIGURE 1. Ex. 1: pointwise absolute errors for $n = 150$, θ optimal

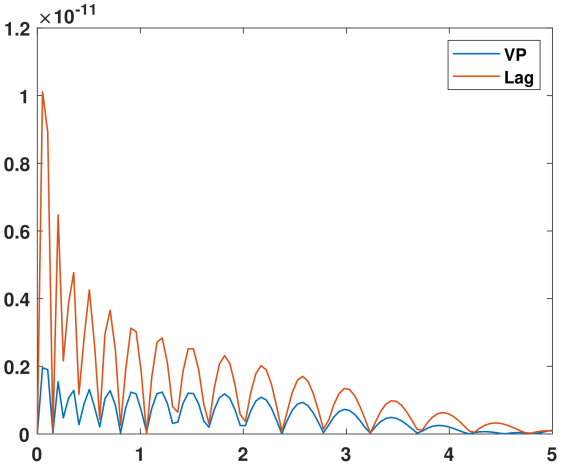

FIGURE 2. Ex. 1: pointwise absolute errors for $n = 150$, $\theta = 0.1$

In Table 4 are given the maximum absolute errors attained for increasing values of n in $[0, 10]$, and a moderate better performance of the VP-method w.r.t. the L-method is confirmed.

Example 4.3.

$$\mathcal{F}(f,t) = \int_0^\infty \frac{f(x) - f(t)}{x - t} e^{-x} dx, \quad f(x) = |x-1|^{1.5}|x-1.5|^{1.9}\ \alpha = 0,\ \gamma = 0.$$

The approximate values for $t = 1$ and $t = 1.5$ are

$$\mathcal{F}(f,1)u(1) \sim 5.6531e-02, \quad \mathcal{F}(f,1.5)u(1.5) \sim 2.4085e-01.$$

n	θ	j	$\|e_{n,m}^{VP}(\mathcal{F},t)\|u(t)$	$\|e_{n}^{Lag}(\mathcal{F},t)\|u(t)$
50	3.0e-01	34	2.20e-05	1.41e-04
150	5.0e-01	61	4.38e-07	7.81e-07
250	2.0e-01	79	4.46e-09	7.36e-09
350	1.0e-01	93	2.67e-10	3.03e-10
450	1.0e-01	106	1.51e-11	1.42e-11
550	1.0e-01	117	8.56e-13	7.58e-13
650	1.0e-01	127	4.38e-13	3.56e-13

n	θ	j	$\|e_{n,m}^{VP}(\mathcal{F},t)\|u(t)$	$\|e_{n}^{Lag}(\mathcal{F},t)\|u(t)$
50	5.0e-01	34	1.92e-05	7.87e-05
150	1.0e-01	61	3.69e-08	1.64e-07
250	2.0e-01	79	9.14e-10	3.30e-09
350	1.0e-01	93	1.05e-11	1.02e-11
450	1.0e-01	106	2.93e-12	1.81e-12
550	1.0e-01	117	1.56e-14	3.78e-14
650	2.0e-01	127	1.92e-14	2.03e-13

TABLE 3. Ex.2: $t = 1$ (up), $t = 15$ (down)

n	$\|e_{n,m}^{VP}(\mathcal{F})u\|$	$\|e_{n}^{Lag}(\mathcal{F})u\|$
50	4.17e-04	6.8490e-04
150	2.64e-06	2.5247e-06
250	1.82e-08	1.27e-08
350	5.34e-10	6.18e-10
450	3.19e-11	3.06e-11
550	2.16e-12	2.08e-12
650	1.40e-12	2.46e-12

TABLE 4. Ex.2: maximum errors in $[0, 10]$

The graph of the function $\mathcal{F}(f,t)u(t)$, in a range including the critical points 1 and 1.5 is shown in Figure 3. In Table 6 are given the maximum absolute errors attained for increasing values of n in $[0, 10]$.

We conclude with the pointwise absolute errors for $n = 200$, in the case of θ chosen "optimal" for each t (Figure 4), and for θ fixed, namely $\theta = 0.5$ (Figure 5).

CONCLUSIONS

We have proposed a method to approximate the Hilbert transform with a Laguerre weight. It employs filtered VP approximation of the function $\mathcal{F}(f)$, and improves a previous method based on the interpolation of the same function by truncated Lagrange polynomials. Indeed, w.r.t. to this, the new method converges a little bit faster. Moreover, while the Lagrange based method requires two different approaches, according to $\alpha > 0$ or not, the proposed rule does not. The algorithm, easier to implement, essentially requires zeros and weights of the Gauss-Laguerre rule, efficiently computable by the Golub-Welsh algorithm. Moreover, differently from the modified Gauss-Laguerre rule [8], we use always the same samples of the density function f at the Laguerre zeros, whatever are the values of t for which to compute $\mathcal{F}(f), t)$.

n	θ	j	$\lvert e_{n,m}^{VP}(\mathcal{F},t)\rvert u(t)$	$\lvert e_{n}^{Lag}(\mathcal{F},t)\rvert u(t)$
50	*9.00e-01*	*41*	*7.21e-04*	*3.76e-03*
100	*8.00e-01*	*60*	*2.87e-04*	*1.44e-03*
200	*1.00e-01*	*86*	*1.10e-03*	*1.06e-03*
400	*9.00e-01*	*122*	*4.16e-04*	*5.16e-04*
800	*1.00e-01*	*173*	*1.63e-04*	*1.51e-04*
1000	*9.00e-01*	*194*	*1.21e-04*	*1.55e-04*

n	θ	j	$\lvert e_{n,m}^{VP}(\mathcal{F},t)\rvert u(t)$	$\lvert e_{n}^{Lag}(\mathcal{F},t)\rvert u(t)$
50	*1.00e-01*	*41*	*2.41e-03*	*2.28e-03*
100	*8.00e-01*	*60*	*2.10e-05*	*4.86e-04*
200	*7.00e-01*	*86*	*6.85e-05*	*3.13e-04*
400	*6.00e-01*	*122*	*6.83e-05*	*9.85e-05*
800	*4.00e-01*	*173*	*2.75e-06*	*6.14e-05*
1000	*2.00e-01*	*194*	*4.74e-07*	*4.90e-06*

TABLE 5. Ex.3: $t = 1$ (up), $t = 1.5$ (down)

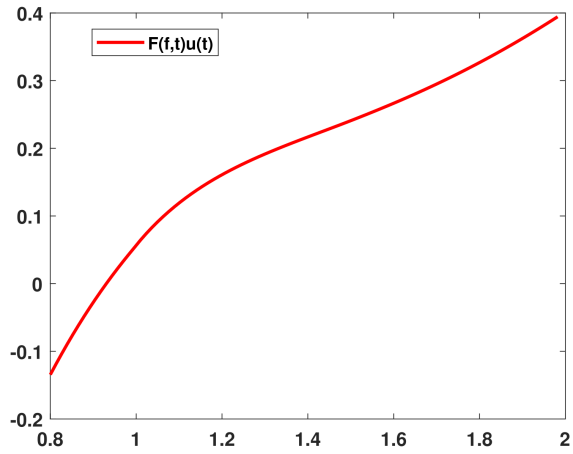

FIGURE 3. Graph of $\mathcal{F}(f,t)u(t),\ t \in [0.8, 2.1]$

n	$\lVert e_{n,m}^{VP}(\mathcal{F})u\rVert$	$\lVert e_{n}^{Lag}(\mathcal{F})u\rVert$
50	*2.6824e-03*	*6.4905e-03*
100	*6.9861e-04*	*2.6261e-03*
200	*2.3962e-03*	*2.3353e-03*
400	*1.0617e-03*	*1.0656e-03*
800	*7.7203e-04*	*7.5605e-04*

TABLE 6. Ex.3: maximum errors in $[0, 10]$

None recurrence relation is required as in product integration type rules [26]. In addition, due to the presence of the localizing parameter $0 < m < n$, oscillations and overshoots around

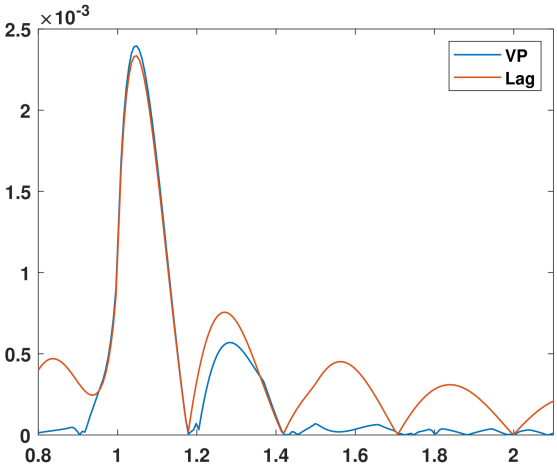

FIGURE 4. Ex. 3: pointwise absolute errors for $n = 200$, θ optimal

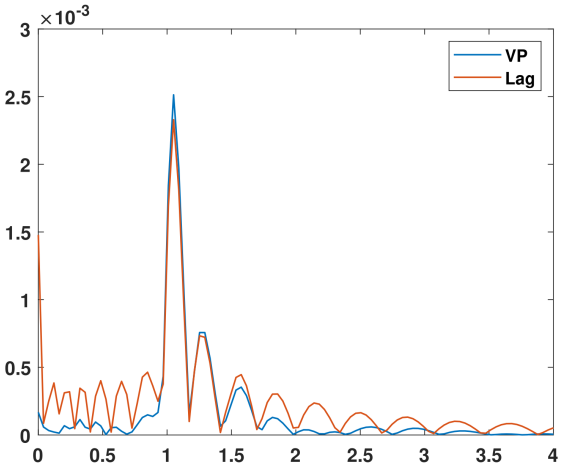

FIGURE 5. Ex. 3: pointwise absolute errors for $n = 200$, $\theta = 0.5$

"pathological" points of the function to be approximated, more present in Lagrange interpolation, are reduced.

Acknowledgments. The author is grateful to the anonymous referees for their valuable comments. The research has been supported by PRIN 2022 PNRR project no. P20229RMLB financed by the European Union - NextGeneration EU and the Italian Ministry of University and Research (MUR).

Memberships. The author is member of the INdAM-GNCS Research Group, TAA-UMI Research Group, RITA "Research ITalian network on Approximation" and ANA&A SIMAI group.

Conflict of interest The author has no conflicts of interest to declare relevant to this article's content.

REFERENCES

[1] B. Bialecki, P. Keast: *A sinc quadrature subroutine for Cauchy principal value integrals*, J. Comput. Appl. Math., **112** (1-2) (1999), 3–20.

[2] G. Criscuolo, G. Mastroianni: *Convergenza di formule Gaussiane per il calcolo delle derivate di integrali a valor principale secondo Cauchy*, Calcolo, **24** (2) (1987), 179–192.

[3] S.B. Damelin, K. Diethelm: *Boundedness and uniform numerical approximation of the weighted Hilbert transform on the real line*, Numer. Funct. Anal. Optim., **22** (1-2) (2001), 13–54.

[4] M. C. De Bonis, B. Della Vecchia and G. Mastroianni: *Approximation of the Hilbert Transform on the real semiaxis using Laguerre zeros*, Jour. of Comput. and Appl. Math., **140** (1-2) (2002), 209–229.

[5] M. C. De Bonis, B. Della Vecchia and G. Mastroianni: *Approximation of the Hilbert Transform on the real semiaxis using Laguerre zeros*, J. Comput. Appl. Math., **140** (2002), 209–229.

[6] M. C. De Bonis, G. Mastroianni and M. Viggiano: *K-functionals, moduli of smoothness and weighted best approximation on the semiaxis*, Functions, Series, Operators, Proceedings of the Alexits Memorial Conference, Budapest, (1999).

[7] M. C. De Bonis, D. Occorsio: *On the simultaneous approximation of a Hilbert transform and its derivatives on the real semiaxis*, Appl. Numer. Math., **114** (2017), 132–153.

[8] M. C. De Bonis, D. Occorsio: *Error bounds for a Gauss-type quadrature rule to evaluate hypersingular integrals*, Filomat, **32** (7) (2018), 2525–2543.

[9] K. Diethelm: *Uniform convergence of optimal order quadrature rules for Cauchy principal value integrals*, J. Comput. Appl. Math., **56** (3) (1994), 321–329.

[10] F. Filbir, D. Occorsio and W. Themistoclakis: *Approximation of Finite Hilbert and Hadamard Transforms by Using Equally Spaced Nodes*, Mathematics, **8** (4) (2020), Article ID: 542.

[11] I. S. Gradshteyn, I.M. Ryzhik: *Table of Integrals, Series, and Products*, Alan Jeffrey, Fifth ed., Academic Press, Inc. Boston, MA (1994).

[12] T. Hasegawa, T. Torii: *An automatic quadrature for Cauchy principal value integrals*, Math. Comp., **56** (194) (1991), 741–754.

[13] F. King: *Hilbert Transforms I & II*, Cambridge University Press: Cambridge UK (2009).

[14] M. L. Krasnov, A. I. Kiselev and G. L. Makarenko: *Integral Equations*, Eds. MIR, Moscow (1983).

[15] I. K. Lifanov, L.N. Poltavskii and G. M. Vainikko: *Hypersingular Integral Equations and their Applications*, Chapman & Hall CRC 2003.

[16] G. Mastroianni: *Polynomial inequalities, functional spaces and best approximation on the real semiaxis with Laguerre weights*, Electron. Trans. Numer. Anal., **14** (2002), 142–151.

[17] G. Mastroianni, G.V. Milovanovič: *Some numerical methods for second kind Fredholm integral equation on the real semiaxis*, IMA J. Numer. Anal., **29** (4) (2009), 1046–1066.

[18] G. Mastroianni, G. Monegato: *Truncated quadrature rules over* $(0, \infty)$ *and Nyström type methods*, SIAM Jour. Num. Anal., **41** (5) (2003), 1870–1892.

[19] G. Mastroianni, D. Occorsio: *Lagrange interpolation at Laguerre zeros in some weighted uniform spaces*, Acta Math. Hungar., **91** (1-2) (2001), 27–52.

[20] S. G. Mikhlin, S. Prössdorf: *Singular Integral Operator*, Springer-Verlag, Berlin, Heidelberg, New York, Tokyo (1986).

[21] G. Monegato: *The Numerical Evaluation of One-Dimensional Cauchy Principal Value Integrals*, Computing, **29** (1982), 337–354,

[22] I. Notarangelo: *Approximation of the Hilbert transform on the real line using Freud weights*, Proceedings of the International Conference "Approximation & Computation", dedicated to the $60-$th anniversary of G. Milovanovič, Niš August 25–29, 2008.

[23] D. Occorsio, M. G. Russo and W. Themistoclakis, *Some numerical applications of generalized Bernstein operators*, Constr. Math. Anal., **4** (2) (2021), 186–214.

[24] D. Occorsio: *A method to evaluate the Hilbert transform on* $(0, +\infty)$, Applied Mathematics and Computation, **217** (12) (2011), 5667–5679.

[25] D. Occorsio, W. Themistoclakis: *De la Vallée Poussin filtered polynomial approximation on the half line*, Appl. Math. Comput., **207** (2025), 569–584.

[26] D. Occorsio, W. Themistoclakis: *Approximation of the Hilbert transform on the half-line*, Appl. Numer. Math., **205** (2024), 101–119.

[27] G. Szegö: *Orthogonal Polynomials*, American Mathematical Society, Providence, RI, 4th Ed. (1975).

[28] W. Themistoclakis: *Uniform approximation on* $[-1, 1]$ *via discrete de la Vallée Poussin means*, Numer. Algor., **60** (2012), 593–612.

DONATELLA OCCORSIO
UNIVERSITY OF BASILICATA
DEPARTMENT OF BASIC AND APPLIED SCIENCES,
VIALE DELL'ATENEO LUCANO, 10, 85100, POTENZA, ITALY
ORCID: 0000-0001-9446-4452
Email address: donatella.occorsio@unibas.it

CONSTRUCTIVE MATHEMATICAL ANALYSIS
7 (2024), No. SI, pp. 129-141
http://dergipark.org.tr/en/pub/cma
ISSN 2651 - 2939

Research Article

Completeness theorems related to BVPs satisfying the Lopatinskii condition for higher order elliptic equations

ALBERTO CIALDEA* AND FLAVIA LANZARA

To Paolo Emilio Ricci on the occasion of his 80th birthday

ABSTRACT. In this paper, we consider a linear elliptic operator E with real constant coefficients of order $2m$ in two independent variables without lower order terms. For this equation, we consider linear BVPs in which the boundary operators $T_1, \dots, T_m$ are of order m and satisfy the Lopatinskii-Shapiro condition with respect to E. We prove boundary completeness properties for the system $\{(T_1\omega_k, \dots, T_m\omega_k)\}$, where $\{\omega_k\}$ is a system of polynomial solutions of the equation $Eu = 0$.

Keywords: Completeness theorems, Lopatinskii condition, elliptic equations of higher order, partial differential equations with constant coefficients.

2020 Mathematics Subject Classification: 35J40, 35E99, 30B60.

1. INTRODUCTION

The problem of the completeness of particular sequences of solutions of a PDE on the boundary of a domain has a long history. The prototype of such results is the theorem which states that harmonic polynomials are complete in $L^p(\partial\Omega)$ $(1 \leqslant p < \infty)$ or in $C^0(\partial\Omega)$, where Ω is a bounded domain in $\mathbb{R}^n$ and $\mathbb{R}^n \setminus \Omega$ is connected. This result has been proved by Fichera [5]. Since then, many other results have been obtained. They are related to different BVPs for several PDEs, including some systems. We refer to [4, Section 2] for an introduction to the subject and a quite updated bibliography. Here we mention that there are numerical methods that are founded on the boundary completeness properties of certain sequences of solutions of a given PDE (see [8, p.36–37]).

In the present paper, we deal with a linear elliptic operator E with real constant coefficients of order $2m$ in two independent variables without lower order terms. For this equation, we consider the BVP in a bounded domain $\Omega \subset \mathbb{R}^2$ in which the boundary conditions are given by m linear differential operators $T_1, \dots, T_m$ of order m. We assume that the operators T_j satisfy the Lopatinskii-Shapiro condition with respect to E and that $\mathbb{R}^2 \setminus \Omega$ is connected.

The aim of this paper is to prove that the system $\{(T_1\omega_k, \dots, T_m\omega_k)\}$, where $\{\omega_k\}$ is a system of polynomial solutions of the equation $Eu = 0$, is complete in the subspace of $[L^p(\partial\Omega)]^m$ constituted by the vectors which satisfy the compatibility conditions of the BVP: $Eu = 0$ in Ω, $T_j u = \psi_j$ on $\partial\Omega$ $(j = 1, \dots, m)$. We also prove a similar and more delicate result in the uniform norm. The BVP $Eu = 0$ in Ω, $T_j u = 0$ on $\partial\Omega$ $(j = 1, \dots, m)$ was considered by Paolo Emilio Ricci in his paper [13]. There Ricci developed a theory of the simple layer potential

Received: 29.08.2024; Accepted: 13.11.2024; Published Online: 16.12.2024
*Corresponding author: Alberto Cialdea; alberto.cialdea@unibas.it
DOI: 10.33205/cma.1540457

for such BVP, mainly using results from complex analysis related to singular integral systems. Our results hinge on Ricci's paper. Later BVPs with higher order boundary conditions were considered in [10]. The present paper could probably be extended to these more general BVPs, using the results contained in [11, 12]. We plan to investigate this topic in future work.

The present paper is organized as follows. In Section 2, after some preliminaries, we recall some of the results obtained by Ricci. Section 3 is devoted to the completeness of the system $\{(T_1\omega_k, \dots, T_m\omega_k)\}$ in L^p norm. The completeness in C^0 norm is proved in Section 4.

2. Ricci's results

Let us consider an elliptic operator of order $2m$

$$E = \sum_{k=0}^{2m} a_k \frac{\partial^{2m}}{\partial x^{2m-k}\partial y^k}$$

a_k being real coefficients. The ellipticity condition we assume is

$$\sum_{k=0}^{2m} a_k \xi^{2m-k}\eta^k \neq 0, \quad \forall\,(\xi,\eta) \in \mathbb{R}^2 \setminus \{(0,0)\}\,.$$

Let Ω be a bounded domain in $\mathbb{R}^2$ and denote its boundary by Σ, which is supposed to be $C^{1,h}$ $(0 < h \leqslant 1)$. Let us consider the following BVP

$$\begin{cases} Eu = 0 & \text{in } \Omega \\ T_j u = \psi_j & \text{on } \Sigma \quad (j = 1, \dots, m), \end{cases} \tag{2.1}$$

where the T_j are m boundary operators of order m. This means that we can write

$$T_j = \sum_{h=0}^{m} b_h^j(z) \frac{\partial^m}{\partial x^{m-h}\partial y^h} + \widetilde{T}_j\,,$$

$$\widetilde{T}_j = \sum_{s=0}^{m-1} \sum_{i=0}^{m-1-s} b_{i,m-1-s}^j(z) \frac{\partial^{m-1-s}}{\partial x^{m-1-s-i}\partial y^i},$$

where $z = x + iy$. We assume that all the functions b_h^j and $b_{i,m-1-s}^j$ belong to $H(\Sigma)$, the space of real valued Hölder continuous functions defined on Σ.

Let us denote by $L(w)$ the characteristic polynomial of E

$$L(w) = \sum_{k=0}^{2m} a_k w^{2m-k}$$

and by $L_j(w,z)$ the characteristic polynomial of the boundary operator T_j, i.e.

$$L_j(w,z) = \sum_{h=0}^{m} b_h^j(z)\, w^{m-h} \quad (j = 1, 2, \dots, m).$$

Let us consider also the polynomial

$$L^{(-)}(w) = (w - w_1)^{\nu_1} \cdots (w - w_p)^{\nu_p},$$

where $w_1, \dots, w_p$ are the zeros of polynomial L with negative imaginary part ($w_i \neq w_j$ if $i \neq j$, $\nu_1 + \cdots + \nu_p = m$).

We recall that the operators T_j satisfy the Lopatinskii condition with respect to E if, for any $z \in \Sigma$, there are no complex constants $c_1, \dots, c_m$ such that the polynomial $L^{(-)}(w)$ divides the polynomial

$$\sum_{j=1}^{m} c_j \, L_j(w, z) \, .$$

From now on, we assume that this condition is satisfied.

Let Γ be a rectifiable Jordan curve in the complex w-plane enclosing the zeros of $L(w)$ in the lower half-plane and oriented in the positive direction. Agmon [1, p.189–190] showed that the function

$$\mathcal{P}(z-\zeta) = \mathbb{R}\mathrm{e}\left\{ \frac{-1}{2\pi^2(2m-2)!} \int_{+\Gamma} \frac{[(x-\xi)w + (y-\eta)]^{2m-2} \log[(x-\xi)w + (y-\eta)]}{L(w)} dw \right\},$$

$(z = x + iy, \zeta = \xi + i\eta)$, where some fixed determination of the logarithm has been chosen, is a fundamental solution of the operator E.

In [7], Fichera gave the concept of simple layer potential for a class of linear elliptic operators of higher order in two independent variables. In the case of the operator E, it is given by

$$u(z) = \sum_{k=0}^{m-1} \int_{\Sigma} \varphi_k(\zeta) \frac{\partial^{m-1}}{\partial \xi^{m-1-k} \partial \eta^k} \mathcal{P}(z-\zeta) ds_\zeta \, ,$$

the functions φ_k being real valued. It is clear that this definition extends the classical one related to the Laplace operator

$$u(z) = \frac{1}{2\pi} \int_{\Sigma} \varphi(\zeta) \, \log|z-\zeta| \, ds_\zeta \, . \tag{2.2}$$

The following jump formula holds (see [7, p. 65–66], [13, p. 7])

$$\begin{aligned} &\lim_{z \to z_0^+} \int_{\Sigma} \varphi(\zeta) \frac{\partial^{2m-1}}{\partial x^{2m-1-l} \partial y^l} \mathcal{P}(z-\zeta) ds_\zeta \\ &= -\varphi(z_0) \frac{1}{2\pi} \mathbb{I}\mathrm{m} \int_{+\Gamma} \frac{w^{2m-1-l}}{L(w)\,(\dot{x}_0 w + \dot{y}_0)} dw \\ &-\frac{1}{2\pi^2} \mathbb{R}\mathrm{e} \int_{\Sigma} \varphi(\zeta) ds_\zeta \int_{+\Gamma} \frac{w^{2m-1-l}}{L(w)\,[(x_0-\xi)\,w + (y_0-\eta)]} dw \, , \ (0 \leqslant l \leqslant 2m-1). \end{aligned} \tag{2.3}$$

Here $z_0 \in \Sigma$ and $z \to z_0$ from the interior of Ω and the dot denotes the derivative with respect to the arc length on Σ. In [13] these formulas have been proved for any $z_0 \in \Sigma$ assuming the Hölder continuity of the density φ, but they are still valid a.e. on Σ if $\varphi \in L^1(\Sigma)$ (see, e.g., [3]). Similarly one can prove that

$$\begin{aligned} &\lim_{z \to z_0^-} \int_{\Sigma} \varphi(\zeta) \frac{\partial^{2m-1}}{\partial x^{2m-1-l} \partial y^l} \mathcal{P}(z-\zeta) ds_\zeta \\ &= \varphi(z_0) \frac{1}{2\pi} \mathbb{I}\mathrm{m} \int_{+\Gamma} \frac{w^{2m-1-l}}{L(w)\,(\dot{x}_0 w + \dot{y}_0)} dw \\ &-\frac{1}{2\pi^2} \mathbb{R}\mathrm{e} \int_{\Sigma} \varphi(\zeta) ds_\zeta \int_{+\Gamma} \frac{w^{2m-1-l}}{L(w)\,[(x_0-\xi)\,w + (y_0-\eta)]} dw \, , \ (0 \leqslant l \leqslant 2m-1), \end{aligned} \tag{2.4}$$

where $z \to z_0$ from the exterior of Ω.

Using jump formulas (2.3), Ricci [13] showed that, given the functions $\psi_j \in H(\Sigma)$ $(j = 1, \dots, m)$, there exists a solution of BVP (2.1) in the form of a simple layer potential (2.2) if and only if there exists a solution of the following singular integral system on the boundary

$$
\begin{aligned}
&-\sum_{k=1}^{m}\sum_{h=0}^{m}\frac{1}{2\pi}\,b_h^j(z)\,\varphi_k(z)\,\mathbb{I}\mathrm{m}\int_{+\Gamma}\frac{w^{2m-1-h-k}}{L(w)\,(\dot{x}w+\dot{y})}dw\\
&-\sum_{k=1}^{m}\sum_{h=0}^{m}\frac{1}{2\pi^2}\,b_h^j(z)\,\mathbb{R}\mathrm{e}\int_{\Sigma}\varphi_k(\zeta)\,ds_\zeta\int_{+\Gamma}\frac{w^{2m-1-h-k}}{L(w)\,[(x-\xi)\,w+(y-\eta)]}dw\\
&+\sum_{k=1}^{m}\sum_{s=0}^{m-1}\sum_{i=0}^{m-1-s}b_{i,m-1-s}^j(z)\int_{\Sigma}\varphi_k(\zeta)\,\frac{\partial^{2m-2-s}}{\partial x^{2m-2-s-i-k}\partial y^{i+k}}\mathcal{P}(z-\zeta)ds_\zeta\\
&=(-1)^{m-1}\psi_j(z)\,,\quad j=1,\dots,m\,.
\end{aligned}
\tag{2.5}
$$

In [13] it is also proved that this singular integral system can be written in the canonical form

$$
\begin{aligned}
&A(z)\Phi(z)+\frac{1}{\pi i}B(z)\int_{+\Sigma}\frac{\Phi(\zeta)}{\zeta-z}d\zeta+\int_{+\Sigma}M(z,\zeta)\Phi(\zeta)d\zeta\\
&=(-1)^{m-1}2\pi\,\Psi(z)\,,\quad z\in\Sigma\,.
\end{aligned}
\tag{2.6}
$$

Here Ψ and Φ are the vectors

$$
\Psi(z)=\begin{pmatrix}\psi_1(z)\\ \psi_2(z)\\ \vdots\\ \psi_m(z)\end{pmatrix},\quad \Phi(z)=\begin{pmatrix}\varphi_0(z)\\ \varphi_1(z)\\ \vdots\\ \varphi_{m-1}(z)\end{pmatrix}
$$

and

$$
A(z)=\{A_{jk}(z)\};\quad B(z)=\{B_{jk}(z)\};\quad M(z,\zeta)=\{M_{jk}(z,\zeta)\},
$$

where

$$
\begin{aligned}
A_{jk}(z)&=-\,\mathbb{I}\mathrm{m}\int_{+\Gamma}\frac{L_j(w,z)\,w^{m-1-k}}{L(w)\,(\dot{x}w+\dot{y})}dw,\\
B_{jk}(z)&=i\,\mathbb{R}\mathrm{e}\int_{+\Gamma}\frac{L_j(w,z)\,w^{m-1-k}}{L(w)\,(\dot{x}w+\dot{y})}dw
\end{aligned}
\tag{2.7}
$$

and $M_{jk}(z,\zeta)$ are weakly singular kernels.

Ricci [13] proved the following result:

Theorem 2.1. *The singular integral system* (2.6) *is regular (i.e.* $\det(A+B)\neq 0;\ \det(A-B)\neq 0$*) if and only if the BVP* (2.1) *satisfies the Lopatinskii condition.*

By (2.7) we get

$$
\begin{aligned}
A+B&=\left\{i\int_{+\Gamma}\frac{L_j(w,z)\,w^{m-1-k}}{L(w)\,(\dot{x}w+\dot{y})}dw\right\},\\
A-B&=\left\{\overline{i\int_{+\Gamma}\frac{L_j(w,z)\,w^{m-1-k}}{L(w)\,(\dot{x}w+\dot{y})}dw}\right\},
\end{aligned}
$$

from which it follows that system (2.6) is of regular type if and only if the function

$$
\delta_0(z)=\det\left\{\int_{+\Gamma}\frac{L_j(w,z)\,w^{m-1-k}}{L(w)\,(\dot{x}w+\dot{y})}dw\right\}
$$

never vanishes on Σ ([13, p.14]).

It is well known (see, e.g., [14]) that if a singular system is of regular type, then the associated homogeneous system has a finite number of eigensolutions and there exists a solution of the system if and only if the data satisfies a finite number of compatibility conditions. More precisely, there exists a complex valued solution of the system (2.6) if and only if the given vector Ψ is such that

$$\int_{+\Sigma} \Psi\, X\, d\zeta = 0$$

for any (complex valued) eigensolution X of the homogeneous adjoint system

$$A'(z)X(z) - \frac{1}{\pi i}B'(z)\int_{+\Sigma}\frac{X(\zeta)}{\zeta - z}d\zeta + \int_{+\Sigma} N(\zeta, z)X(\zeta)d\zeta = 0\,, \quad z \in \Sigma\,. \tag{2.8}$$

Here A' and B' are the transposed matrices of A and B, respectively, and

$$N(\zeta, z) = M'(\zeta, z) - \frac{1}{\pi i}\frac{B'(\zeta) - B'(z)}{\zeta - z}$$

$M'(\zeta, z)$ being the transposed matrix of $M(\zeta, z)$ (see [13, p.12–13]).

We remark that, if we denote by $K\Phi$ and $K'X$ the left hand side of (2.6) and (2.8) respectively, we have

$$\int_{+\Sigma} X\, K\Phi\, d\zeta = \int_{+\Sigma} \Phi\, K'X\, d\zeta \tag{2.9}$$

for any (complex valued) Hölder continuous vector Φ, X (see [13, p.13]).

3. Completeness theorems in L^p norm

From now on, we assume that $\mathbb{R}^2 \setminus \Omega$ is connected.

Let us denote by $\{\omega_k\}$ ($k \in \mathbb{N}$) a complete system of polynomial solutions of the equation $Eu = 0$. This means that any polynomial solution of the equation $Eu = 0$ can be written as a finite linear combination of elements of $\{\omega_k\}$. A method for the explicit construction of the system $\{\omega_k\}$ is given in [2].

Let us denote by $X_1, \ldots, X_s$ a base of the eigenspace related to the equation (2.8). It is well known that these vectors are Hölder continuous.

Let $1 \leqslant p < \infty$ and

$$\Lambda^p = \left\{ G = (g_1, \ldots, g_m) \in [L^p(\Sigma)]^m \;\middle|\; \int_{+\Sigma} G\, X_h\, d\zeta = 0,\ h = 1, \ldots, s \right\}.$$

We remark that $(g_1, \ldots, g_m)$ are real valued functions.

Let us denote by $K^* : [L^q(\Sigma)]^m \to [L^q(\Sigma)]^m$ ($q = p/(p-1)$) the operator defined by

$$\int_{\Sigma} G\, K^* F\, ds = \int_{\Sigma} F\, KG\, ds\,.$$

Recalling (2.9), we have

$$\begin{aligned}\int_{\Sigma} F\, KG\, ds &= \int_{+\Sigma} F\, KG\dot{\bar{\zeta}}\, d\zeta \\ &= \int_{+\Sigma} G\, K'_z(\dot{\bar{z}}F)\, d\zeta = \int_{\Sigma} G\, K'_z(\dot{\bar{z}}F)\, \dot{\zeta}\, ds\end{aligned}$$

and then $K^*F = \dot{\zeta}\, K'_z(\dot{\bar{z}}F)$. This shows that $\dot{\zeta}X_1, \ldots, \dot{\zeta}X_s$ are (complex valued) eigensolutions of the equation $K^*F = 0$. Since the operator K^* maps real vectors to real vectors, we have

that $\mathbb{R}\mathrm{e}(\dot\zeta X_j)$ and $\mathbb{I}\mathrm{m}(\dot\zeta X_j)$ are (not necessarily linearly independent) real eigensolutions of the equation $K^*\Xi = 0$ and that the kernel $\mathrm{Ker}(K^*)$ is spanned by

$$\{\mathbb{R}\mathrm{e}(\dot\zeta X_1), \mathbb{I}\mathrm{m}(\dot\zeta X_1), \dots, \mathbb{R}\mathrm{e}(\dot\zeta X_s), \mathbb{I}\mathrm{m}(\dot\zeta X_s)\}.$$

We note that Λ^p is the annihilator of the kernel of K^*:

$$\Lambda^p = {}^{\perp}\mathrm{Ker}(K^*)\,. \tag{3.10}$$

This follows from the remark that if $G \in \Lambda^p$, we have

$$0 = \int_{+\Sigma} G\, X_h\, d\zeta = \int_\Sigma G\, X_h\, \dot\zeta\, ds = \int_\Sigma G\, \mathbb{R}\mathrm{e}(\dot\zeta X_h)\, ds + i \int_\Sigma G\, \mathbb{I}\mathrm{m}(\dot\zeta X_h)\, ds$$

and then

$$\int_\Sigma G\, \mathbb{R}\mathrm{e}(\dot\zeta X_h)\, ds = \int_\Sigma G\, \mathbb{I}\mathrm{m}(\dot\zeta X_h)\, ds = 0 \quad (h = 1, \dots, s).$$

We remark that K^* has the following expression

$$\begin{aligned} K_k^* F(z) = &- \sum_{j=1}^m \sum_{h=0}^m \frac{1}{2\pi}\, b_h^j(z)\, F_j(z)\, \mathbb{I}\mathrm{m} \int_{+\Gamma} \frac{w^{2m-1-h-k}}{L(w)\,(\dot x w + \dot y)} dw \\ &+ \sum_{j=1}^m \sum_{h=0}^m \frac{1}{2\pi^2}\, \mathbb{R}\mathrm{e} \int_\Sigma b_h^j(\zeta)\, F_j(\zeta)\, ds_\zeta \int_{+\Gamma} \frac{w^{2m-1-h-k}}{L(w)\,[(x-\xi)\,w + (y-\eta)]} dw \\ &+ \sum_{j=1}^m \sum_{s=0}^{m-1} \sum_{i=0}^{m-1-s} \int_\Sigma b_{i,m-1-s}^j(\zeta)\, F_j(\zeta)\, \frac{\partial^{2m-2-s}}{\partial\xi^{2m-2-s-i-k}\partial\eta^{i+k}} \mathcal{P}(z-\zeta) ds_\zeta\,. \end{aligned} \tag{3.11}$$

Note that we have also used the property $\mathcal{P}(z-\zeta) = \mathcal{P}(\zeta - z)$ (see [1, p.189]).

Let us consider the system $\{T\omega_k\} = \{(T_1\omega_k, \dots, T_m\omega_k)\}$. It is clear that it is contained in Λ^p. We aim to show that it is complete in Λ^p. Let us begin with a couple of lemmas.

Lemma 3.1. *Let*

$$p_{k,s}(z,\zeta) = p_{k,s}(x,y,\xi,\eta) = \int_{+\Gamma} \frac{(\xi w + \eta)^k (xw + y)^s}{L(w)}\, dw\,, \tag{3.12}$$

where $k \in \mathbb{N}$, $s \in \mathbb{Z}$. The function $p_{k,s}$ is homogeneous of degree $k+s$. For any fixed $z \in \mathbb{C}$, $p_{k,s}$ is a homogeneous polynomial of degree k in ξ, η and is a solution of the equation $E_\zeta p_{k,s} = 0$. For any fixed $\zeta \in \mathbb{C}$, $p_{k,s}$ is a homogeneous function (a homogeneous polynomial, if $s \geqslant 0$) of degree s in x, y and is a solution of the equation $E_z p_{k,s} = 0$.

Proof. Clearly $p_{k,s}(\lambda x, \lambda y, \lambda\xi, \lambda\eta) = \lambda^{k+s} p_{k,s}(x,y,\xi,\eta)$ ($\lambda > 0$). It is obvious that, for any fixed $z \in \mathbb{C}$, $p_{k,s}$ is a homogeneous polynomial of degree k in ξ, η. Therefore, if $k \leqslant 2m-1$, it satisfies the equation $E_\zeta p_{k,s} = 0$. Let $k \geqslant 2m$. We have

$$\begin{aligned} E_\zeta p_{k,s} &= \sum_{h=0}^{2m} a_h \frac{\partial^{2m}}{\partial\xi^{2m-h}\partial\eta^h} \int_{+\Gamma} \frac{(\xi w + \eta)^k (xw+y)^s}{L(w)}\, dw \\ &= \sum_{h=0}^{2m} a_h\, k(k-1)\cdots(k-2m+1) \int_{+\Gamma} \frac{(\xi w + \eta)^{k-2m} (xw+y)^s w^{2m-h}}{L(w)}\, dw \\ &= k(k-1)\cdots(k-2m+1) \int_{+\Gamma} (\xi w + \eta)^{k-2m} (xw+y)^s\, dw\,. \end{aligned}$$

The holomorphy of $(\xi\cdot + \eta)^{k-2m}(x\cdot + y)^s$ in the interior of Γ gives the result.

A similar argument works for a fixed ζ. □

Lemma 3.2. *There exists $R > 0$ such that, for any $|z| > R$, we have*

$$\mathcal{P}(z-\zeta) = q_0(z,\zeta) + \frac{1}{2\pi^2(2m-2)!}\sum_{h=1}^{\infty}\sum_{j=0}^{2m-2}\binom{2m-2}{j}\frac{(-1)^j}{h}\,\mathbb{R}\mathrm{e}\,p_{j+h,2m-2-j-h}(z,\zeta) \tag{3.13}$$

uniformly for ζ varying on Σ, where q_0 is, for any fixed $z \in \mathbb{C}$, a polynomial of degree at most $2m-2$ in ξ, η (and then satisfies $E_\zeta q_0 = 0$). The series (3.13) can be differentiated with respect to ξ, η term by term and the differentiated series converge uniformly for ζ varying on Σ.

Proof. We first prove that there exists $R > 0$ such that

$$\left|\frac{\xi w+\eta}{xw+y}\right| < 1 \tag{3.14}$$

for any $|z| > R$, $\zeta \in \Sigma$, $w \in \Gamma$. Let us consider the function

$$\psi(u,v,\vartheta) = \sqrt{(u\cos\vartheta + \sin\vartheta)^2 + v^2\cos^2\vartheta}$$

and set

$$m = \min_{\substack{\vartheta\in[0,2\pi]\\ u+iv\in\Gamma}} \psi(u,v,\vartheta), \qquad M = \max_{\substack{\vartheta\in[0,2\pi]\\ u+iv\in\Gamma}} \psi(u,v,\vartheta).$$

It is easy to see that $m > 0$. Then we can write

$$\left|\frac{\xi w+\eta}{xw+y}\right| \leqslant \frac{M}{m}\,\frac{|\zeta|}{|z|}\,.$$

Choosing

$$R \geqslant \frac{M}{m}\max_{\zeta\in\Sigma}|\zeta|\,,$$

we have that (3.14) is satisfied for any $|z| > R$. If $|z| > R$ and $\zeta \in \Sigma$, $w \in \Gamma$, we have

$$\begin{aligned}\log[(x-\xi)w + (y-\eta)] &= \log[(xw+y) - (\xi w+\eta)]\\ &= \log\left[(xw+y)\left(1-\frac{\xi w+\eta}{xw+y}\right)\right]\\ &= \log(xw+y) + \log\left(1-\frac{\xi w+\eta}{xw+y}\right),\end{aligned}$$

where we take the principal determination of $\log\left(1-\frac{\xi w+\eta}{xw+y}\right)$ and the determination of $\log(xw+y)$ is chosen so that this formula holds. Therefore, fixed $|z| > R$,

$$\log[(x-\xi)w + (y-\eta)] = \log(xw+y) - \sum_{h=1}^{\infty}\frac{1}{h}\left(\frac{\xi w+\eta}{xw+y}\right)^h$$

where, thanks to (3.14), the series uniformly converges for $\zeta \in \Sigma$, $w \in \Gamma$. Then

$$\begin{aligned}
&\int_{+\Gamma} \frac{[(x-\xi)w+(y-\eta)]^{2m-2}\log[(x-\xi)w+(y-\eta)]}{L(w)}dw \\
&= \int_{+\Gamma} \frac{[(x-\xi)w+(y-\eta)]^{2m-2}\log(xw+y)}{L(w)}dw \\
&- \sum_{h=1}^{\infty}\frac{1}{h}\int_{+\Gamma}\frac{[(x-\xi)w+(y-\eta)]^{2m-2}}{L(w)}\left(\frac{\xi w+\eta}{xw+y}\right)^h dw \\
&= \int_{+\Gamma} \frac{[(x-\xi)w+(y-\eta)]^{2m-2}\log(xw+y)}{L(w)}dw \\
&- \sum_{h=1}^{\infty}\sum_{j=0}^{2m-2}\binom{2m-2}{j}\frac{(-1)^j}{h}\int_{+\Gamma}\frac{(\xi w+\eta)^{j+h}(xw+y)^{2m-2-j-h}}{L(w)}\,dw\,.
\end{aligned}$$

We have then proved (3.13), where

$$q_0(z,\zeta) = -\,\mathbb{R}\mathrm{e}\,\frac{1}{2\pi^2(2m-2)!}\int_{+\Gamma}\frac{[(x-\xi)w+(y-\eta)]^{2m-2}\log(xw+y)}{L(w)}dw\,,$$

which is clearly a polynomial in ξ, η of degree at most $2m-2$.

In the same manner, we can see the uniform convergence of differentiated series. □

Theorem 3.2. *The system $\{T\omega_k\}$ is complete in Λ^p $(1 \leqslant p < \infty)$.*

Proof. We have to show that, if a functional $\Theta \in ([L^p(\Sigma)]^m)^*$ vanishes on $\{T\omega_k\}$, i.e. if

$$\langle \Theta, T\omega_k\rangle = 0, \quad \forall\, k \in \mathbb{N}\,,$$

then it vanishes on Λ^p:

$$\langle \Theta, G\rangle = 0, \quad \forall\, G \in \Lambda^p.$$

Let $1 < p < \infty$ and suppose that $\Theta = (\Theta_1, \dots, \Theta_m) \in [L^q(\Sigma)]^m$ is such that

$$\int_\Sigma \Theta\, T\omega_k\, ds = 0, \quad \forall\, k \in \mathbb{N}. \tag{3.15}$$

Let us denote by $\omega_{k,1}, \dots, \omega_{k,\nu_k}$ a basis of the (real) linear span generated by all the homogeneous real polynomials of degree k satisfying the equation $Eu = 0$ (see [2, p.34–35]). Since for any $z \in \mathbb{C}$, the polynomials (3.12) are homogeneous and satisfy the equation $Eu = 0$, Lemma 3.2 shows that there exist real functions $c_{k,j}(z)$ such that, for any $|z| > R$,

$$\mathcal{P}(z-\zeta) = \sum_{k=0}^{\infty}\sum_{j=1}^{\nu_k} c_{k,j}(z)\,\omega_{k,j}(\zeta)$$

uniformly for $\zeta \in \Sigma$. The same holds for differentiated series. Then, for any $|z| > R$, we can write

$$\int_\Sigma \Theta(\zeta)\, T_\zeta \mathcal{P}(z-\zeta)\, ds_\zeta = \sum_{k=0}^{\infty}\sum_{j=1}^{\nu_k} c_{k,j}(z)\int_\Sigma \Theta(\zeta)\, T\omega_{k,j}(\zeta)\, ds_\zeta\,.$$

In view of (3.15), we have

$$u(z) = 0$$

for any $|z| > R$, where

$$u(z) = \int_\Sigma \Theta(\zeta)\, T_\zeta \mathcal{P}(z-\zeta)\, ds_\zeta\,.$$

The function u being analytic in $\mathbb{C}\setminus\Sigma$, we find

$$u(z)=0,\quad \forall\, z\in\mathbb{C}\setminus\overline{\Omega}.$$

Then we can write

$$\sum_{j=1}^{m}\sum_{h=0}^{m}\int_{\Sigma}\Theta_j(\zeta)\,b_h^j(\zeta)\,\frac{\partial^m}{\partial\xi^{m-h}\partial\eta^h}\mathcal{P}(z-\zeta)ds_\zeta$$
$$+\sum_{j=1}^{m}\int_{\Sigma}\Theta_j(\zeta)\,\widetilde{T}_{j,\zeta}\mathcal{P}(z-\zeta)ds_\zeta=0$$

for any $z\in\mathbb{C}\setminus\overline{\Omega}$. This implies

$$\sum_{j=1}^{m}\sum_{h=0}^{m}\int_{\Sigma}\Theta_j(\zeta)\,b_h^j(\zeta)\,\frac{\partial^{m-1}}{\partial x^{m-1-k}\partial y^k}\frac{\partial^m}{\partial\xi^{m-h}\partial\eta^h}\mathcal{P}(z-\zeta)ds_\zeta$$
$$+\sum_{j=1}^{m}\int_{\Sigma}\Theta_j(\zeta)\,\widetilde{T}_{j,\zeta}\frac{\partial^{m-1}}{\partial x^{m-1-k}\partial y^k}\mathcal{P}(z-\zeta)ds_\zeta=0,\quad k=0,\dots,m-1$$

for any $z\in\mathbb{C}\setminus\overline{\Omega}$, i.e.

$$(-1)^m\sum_{j=1}^{m}\sum_{h=0}^{m}\int_{\Sigma}\Theta_j(\zeta)\,b_h^j(\zeta)\,\frac{\partial^{2m-1}}{\partial x^{2m-1-h-k}\partial y^{h+k}}\mathcal{P}(z-\zeta)ds_\zeta$$
$$+\sum_{j=1}^{m}\sum_{s=0}^{m-1}\sum_{i=0}^{m-1-s}\int_{\Sigma}\Theta_j(\zeta)\,b_{i,m-1-s}^j(\zeta)\frac{\partial^{m-1-s}}{\partial\xi^{m-1-s-i}\partial\eta^i}\frac{\partial^{m-1}}{\partial x^{m-1-k}\partial y^k}\mathcal{P}(z-\zeta)ds_\zeta$$
$$=0,\qquad k=0,...,m-1$$

for any $z\in\mathbb{C}\setminus\overline{\Omega}$. Applying (2.4), we get

$$-\sum_{j=1}^{m}\sum_{h=0}^{m}\frac{1}{2\pi}\Theta_j(z)\,b_h^j(z)\,\mathbb{I}\mathrm{m}\int_{+\Gamma}\frac{w^{2m-1-h-k}}{L(w)\,(\dot{x}w+\dot{y})}dw$$
$$+\sum_{j=1}^{m}\sum_{h=0}^{m}\frac{1}{2\pi^2}\,\mathbb{R}\mathrm{e}\int_{\Sigma}\Theta_j(\zeta)\,b_h^j(\zeta)\,ds_\zeta\int_{+\Gamma}\frac{w^{2m-1-h-k}}{L(w)\,[(x-\xi)\,w+(y-\eta)]}dw$$
$$+\sum_{j=1}^{m}\sum_{s=0}^{m-1}\sum_{i=0}^{m-1-s}\int_{\Sigma}\Theta_j(\zeta)\,b_{i,m-1-s}^j(\zeta)\frac{\partial^{2m-2-s}}{\partial\xi^{2m-2-s-i-k}\partial\eta^{i+k}}\mathcal{P}(z-\zeta)ds_\zeta=0,$$

$k=0,...,m-1$, a.e. on Σ. Comparing this formula with (3.11), we see that this system coincides with $K^*\Theta=0$, i.e. Θ belongs to $\mathrm{Ker}(K^*)$. Recalling (3.10) we have

$$\int_{\Sigma}\Theta\,G\,ds=0$$

for any $G\in\Lambda^p$. This completes the proof when $1<p<\infty$.

If $p=1$, we observe that if $\Theta\in[L^\infty(\Sigma)]^m$, then $\Theta\in[L^s(\Sigma)]^m$ for any $s>1$. Then we can repeat the proof. □

4. Completeness theorems in C^0 norm

In this section, we prove that the completeness property obtained in the previous section is also valid in the uniform norm. Namely, we want to prove the completeness in the space

$$\Lambda^0 = \left\{ G = (g_1, \dots, g_m) \in [C^0(\Sigma)]^m \;\Big|\; \int_{+\Sigma} G\, X_h \, d\zeta = 0,\ h = 1, \dots, s \right\}.$$

Theorem 4.3. *The system $\{T\omega_k\}$ is complete in Λ^0.*

Proof. We have to show that, if a functional in $\Theta \in ([C^0(\Sigma)]^m)^*$ vanishes on $\{T\omega_k\}$, i.e. if

$$\langle \Theta, T\omega_k \rangle = 0, \quad \forall\, k \in \mathbb{N}\,, \tag{4.16}$$

then it vanishes on Λ^0:

$$\langle \Theta, G \rangle = 0, \quad \forall\, G \in \Lambda^0.$$

It is well known that a functional $\Theta \in ([C^0(\Sigma)]^m)^*$ can be represented as $\Theta = (\mu^1, \dots, \mu^m)$, where μ^j are Borel measures defined on Σ. Therefore conditions (4.16) can be written as

$$\sum_{j=1}^{m} \int_\Sigma T_j \omega_k \, d\mu^j = 0, \quad \forall\, k \in \mathbb{N}\,. \tag{4.17}$$

The same arguments used in the first part of the proof of Theorem 3.2 lead to

$$\sum_{j=1}^{m} \int_\Sigma T_{j,\zeta} \mathcal{P}(z-\zeta)\, d\mu^j_\zeta = 0$$

for any $z \in \mathbb{C} \setminus \overline{\Omega}$. This implies

$$\begin{aligned} &\sum_{j=1}^{m} \sum_{h=0}^{m} \int_\Sigma b^j_h(\zeta)\, \frac{\partial^{m-1}}{\partial x^{m-1-k} \partial y^k} \frac{\partial^m}{\partial \xi^{m-h} \partial \eta^h} \mathcal{P}(z-\zeta)\, d\mu^j_\zeta \\ &+ \sum_{j=1}^{m} \int_\Sigma \widetilde{T}_{j,\zeta} \frac{\partial^{m-1}}{\partial x^{m-1-k} \partial y^k} \mathcal{P}(z-\zeta)\, d\mu^j_\zeta = 0, \quad k = 0, \dots, m-1 \end{aligned}$$

for any $z \in \mathbb{C} \setminus \overline{\Omega}$, i.e.

$$\begin{aligned} &(-1)^{m-1} \sum_{j=1}^{m} \sum_{h=0}^{m} \int_\Sigma b^j_h(\zeta)\, \frac{\partial^{2m-1}}{\partial \xi^{2m-1-h-k} \partial \eta^{h+k}} \mathcal{P}(z-\zeta)\, d\mu^j_\zeta \\ &+ \sum_{j=1}^{m} \sum_{s=0}^{m-1} \sum_{i=0}^{m-1-s} \int_\Sigma b^j_{i,m-1-s}(\zeta) \frac{\partial^{m-1-s}}{\partial \xi^{m-1-s-i} \partial \eta^i} \frac{\partial^{m-1}}{\partial x^{m-1-k} \partial y^k} \mathcal{P}(z-\zeta)\, d\mu^j_\zeta \\ &= 0, \qquad k = 0, \dots, m-1 \end{aligned}$$

for any $z \in \mathbb{C} \setminus \overline{\Omega}$. Let us introduce a family of "parallel curves" Σ_ϱ. Let us denote by $\tau(z)$ a unit vector of class $C^1(\Sigma)$ such that $\tau(z) \cdot \nu(z) \geqslant \beta_0 > 0$, ν being the exterior unit normal to Σ. We can choose $\varrho > 0$ in such a way that the curve Σ_ϱ defined by $z_\varrho = z + \varrho\tau(z)$, $z \in \Sigma$, is the boundary of a domain containing Ω (contained in Ω) if $0 < \varrho \leqslant \varrho_0$ (if $-\varrho_0 \leqslant \varrho < 0$). One can prove that if $\Sigma \in C^1$ such a vector does exist (see [9, p.273–275]). For $0 < \varrho \leqslant \varrho_0$ and for any

$f_k \in H(\Sigma)$ $(k = 0, \dots, m-1)$, we may write

$$\sum_{k=0}^{m-1} \int_{\Sigma_\varrho} f_k(z_\varrho) \Bigg[\sum_{j=1}^{m} \sum_{h=0}^{m} \int_\Sigma b_h^j(\zeta) \frac{\partial^{2m-1}}{\partial \xi^{2m-1-h-k} \partial \eta^{h+k}} \mathcal{P}(z_\varrho - \zeta)\, d\mu_\zeta^j + \sum_{j=1}^{m} \sum_{s=0}^{m-1} \sum_{i=0}^{m-1-s} \int_\Sigma b_{i,m-1-s}^j(\zeta) \frac{\partial^{2m-2-s}}{\partial \xi^{2m-2-s-i-k} \partial \eta^{i+k}} \mathcal{P}(z - \zeta)\, d\mu_\zeta^j \Bigg] ds_{z_\varrho} = 0. \tag{4.18}$$

Due to the weak singularity of the kernel, we have that

$$\lim_{\varrho \to 0^+} \int_{\Sigma_\varrho} f_k(z_\varrho)\, ds_{z_\varrho} \int_\Sigma b_{i,m-1-s}^j(\zeta) \frac{\partial^{2m-2-s}}{\partial \xi^{2m-2-s-i-k} \partial \eta^{i+k}} \mathcal{P}(z - \zeta)\, d\mu_\zeta^j = \int_\Sigma b_{i,m-1-s}^j(\zeta)\, d\mu_\zeta^j \int_\Sigma f_k(z) \frac{\partial^{2m-2-s}}{\partial \xi^{2m-2-s-i-k} \partial \eta^{i+k}} \mathcal{P}(z - \zeta)\, ds_z\,.$$

Concerning the first term in (4.18), we may write

$$\int_{\Sigma_\varrho} f_k(z_\varrho)\, ds_{z_\varrho} \int_\Sigma b_h^j(\zeta) \frac{\partial^{2m-1}}{\partial \xi^{2m-1-h-k} \partial \eta^{h+k}} \mathcal{P}(z_\varrho - \zeta)\, d\mu_\zeta^j = \int_\Sigma b_h^j(\zeta)\, d\mu_\zeta^j \int_{\Sigma_\varrho} f_k(z_\varrho) \frac{\partial^{2m-1}}{\partial \xi^{2m-1-h-k} \partial \eta^{h+k}} \mathcal{P}(z_\varrho - \zeta) ds_{z_\varrho}$$

and

$$\begin{aligned} &\int_{\Sigma_\varrho} f_k(z_\varrho) \frac{\partial^{2m-1}}{\partial \xi^{2m-1-h-k} \partial \eta^{h+k}} \mathcal{P}(z_\varrho - \zeta)\, ds_{z_\varrho} \\ &= \int_{\Sigma_\varrho} f_k(z_\varrho) \frac{\partial^{2m-1}}{\partial \xi^{2m-1-h-k} \partial \eta^{h+k}} \mathcal{P}(z_\varrho - \zeta)\, ds_{z_\varrho} \\ &- \int_\Sigma f_k(z) \frac{\partial^{2m-1}}{\partial \xi^{2m-1-h-k} \partial \eta^{h+k}} \mathcal{P}(z - \zeta_{-\varrho})\, ds_z \\ &+ \int_\Sigma f_k(z) \frac{\partial^{2m-1}}{\partial \xi^{2m-1-h-k} \partial \eta^{h+k}} \mathcal{P}(z - \zeta_{-\varrho})\, ds_z. \end{aligned}$$

By means of the results proved in [6] (see also [3, p.58–60]) and recalling (2.3), we see that

$$\lim_{\varrho \to 0^+} \Bigg(\int_{\Sigma_\varrho} f_k(z_\varrho) \frac{\partial^{2m-1}}{\partial \xi^{2m-1-h-k} \partial \eta^{h+k}} \mathcal{P}(z_\varrho - \zeta) ds_{z_\varrho} - \int_\Sigma f_k(z) \frac{\partial^{2m-1}}{\partial \xi^{2m-1-h-k} \partial \eta^{h+k}} \mathcal{P}(z - \zeta_{-\varrho})\, ds_z \Bigg) = 0$$

and

$$\begin{aligned} &\lim_{\varrho \to 0^+} \int_\Sigma f_k(z) \frac{\partial^{2m-1}}{\partial \xi^{2m-1-h-k} \partial \eta^{h+k}} \mathcal{P}(z - \zeta_{-\varrho})\, ds_z \\ &= \lim_{\varrho \to 0^+} \int_\Sigma f_k(z) \frac{\partial^{2m-1}}{\partial \xi^{2m-1-h-k} \partial \eta^{h+k}} \mathcal{P}(\zeta_{-\varrho} - z)\, ds_z \\ &= -\, f_k(\zeta)\, \frac{1}{2\pi}\, \mathbb{I}\mathrm{m} \int_{+\Gamma} \frac{w^{2m-1-h-k}}{L(w)\, (\dot\xi w + \dot\eta)} dw \\ &- \frac{1}{2\pi^2}\, \mathbb{R}\mathrm{e} \int_\Sigma f_k(z)\, ds_z \int_{+\Gamma} \frac{w^{2m-1-h-k}}{L(w)\, [(\xi - x)\, w + (\eta - y)]} dw \end{aligned}$$

uniformly for ζ varying on Σ. So, letting $\varrho \to 0^+$ in (4.18) and keeping in mind (2.5), we get

$$\sum_{j=1}^{m} \int_{\Sigma} K_j f \, d\mu^j = 0 \tag{4.19}$$

for any $f = (f_0, \dots, f_{m-1}) \in [H(\Sigma)]^m$. Thanks to Theorem 2.1 the operator K can be reduced on the left (and on the right). This means that there exists a singular integral operator S of the form

$$Sg(z) = C(z)g(z) + \frac{1}{\pi i} D(z) \int_{+\Sigma} \frac{g(\zeta)}{\zeta - z} d\zeta$$

such that

$$KSg(z) = g(z) + \int_{+\Sigma} R(z,\zeta)\, g(\zeta) d\zeta,$$

where $R(z,\zeta) = \{R_{jk}(z,\zeta)\}$ is a kernel with a weak singularity. Taking $f = Sg$ in (4.19), we find

$$\sum_{j=1}^{m} \int_{\Sigma} K_j \, Sg \, d\mu^j = 0\,, \quad \forall\, g \in [H(\Sigma)]^m,$$

i.e.,

$$\sum_{j=1}^{m} \int_{\Sigma} g_j \, d\mu^j + \sum_{j,k=1}^{m} \int_{\Sigma} d\mu_z^j \int_{+\Sigma} R_{jk}(z,\zeta)\, g_k(\zeta) d\zeta = 0\,, \quad \forall\, g \in [H(\Sigma)]^m.$$

By Tonelli and Fubini's theorems, we get

$$\sum_{j=1}^{m} \int_{\Sigma} g_j \, d\mu^j = - \sum_{j,k=1}^{m} \int_{+\Sigma} g_k(\zeta) d\zeta \int_{\Sigma} R_{jk}(z,\zeta)\, d\mu_z^j\,, \quad \forall\, g \in [H(\Sigma)]^m.$$

This shows that μ^j are absolutely continuous measures and their Radon Nykodym derivatives with respect to the one-dimensional Lebesgue measure on Σ belong to $L^r(\Sigma)$ for some $r > 1$. In other words, there exist $\Theta^j \in L^r(\Sigma)$ $(r > 1)$ such that

$$d\mu^j = \Theta^j ds \quad (\Theta^j \in L^r(\Sigma)).$$

Conditions (4.17) become

$$\sum_{j=1}^{m} \int_{\Sigma} T_j \omega_k \, \Theta^j ds = 0, \quad \forall\, k \in \mathbb{N}\,.$$

But this coincides with (3.15) and the result follows from what we have proved in Theorem 3.2. □

ACKNOWLEDGEMENT.

A. Cialdea is member of Gruppo Nazionale per l'Analisi Matematica, la Probabilità e le loro Applicazioni (GNAMPA) of the Istituto Nazionale di Alta Matematica (INdAM). A. Cialdea and F. Lanzara acknowledge the support from the project "Perturbation problems and asymptotics for elliptic differential equations: variational and potential theoretic methods" funded by the European Union - Next Generation EU and by MUR "Progetti di Ricerca di Rilevante Interesse Nazionale" (PRIN) Bando 2022 grant 2022SENJZ3.

REFERENCES

[1] S. Agmon: *Multiple layer potentials and the Dirichlet problem for higher order elliptic equations in the plane I*, Comm. Pure Appl. Math., **10** (1957), 179–239.

[2] A. Cialdea: *Teoremi di completezza connessi con equazioni ellittiche di ordine superiore in due variabili in un campo con contorno angoloso,* Rend. Circ. Mat. Palermo (2), **35** (1) (1986), 32–49.

[3] A. Cialdea: *A general theory of hypersurface potentials,* Ann. Mat. Pura Appl., **168** (1995), 37–61.

[4] A. Cialdea: *Completeness theorems on the boundary in thermoelasticity,* In: Analysis as a life, Trends Math. Birkhäuser/Springer, Cham, (2019), 93–115.

[5] G. Fichera: *Teoremi di completezza sulla frontiera di un dominio per taluni sistemi di funzioni,* Ann. Mat. Pura Appl., **27** (1948), 1–28.

[6] G. Fichera: *Approssimazione uniforme delle funzioni olomorfe mediante funzioni razionali aventi poli semplici prefissati I & II*, Atti Accad. Naz. Lincei Rend. Cl. Sci. Fis. Mat. Nat., **27** (1959), 193–201, 317–323.

[7] G. Fichera: *Linear elliptic equations of higher order in two independent variables and singular integral equations, with applications to anistropic inhomogeneous elasticity*, In: R.E. Langer (ed.), Partial differential equations and continuum mechanics, Univ. Wisconsin Press, Madison, WI, (1960), 55–80.

[8] G. Fichera: *The problem of the completeness of systems of particular solutions of partial differential equations*, In: Numerical mathematics (Sympos., Inst. Appl. Math., Univ. Hamburg, Hamburg, 1979), Internat. Ser. Numer. Math., vol. 49. Birkhäuser, Basel-Boston, Mass., (1979), 25–41.

[9] G. Fichera, L. De Vito: *Funzioni analitiche di una variabile complessa*, Terza edizione, Libreria Eredi Virgilio Veschi, Rome (1967).

[10] G. Fichera, P. E. Ricci: *The single layer potential approach in the theory of boundary value problems for elliptic equations*, In: Function theoretic methods for partial differential equations (Proc. Internat. Sympos., Darmstadt, 1976), Lecture Notes in Math., vol. Vol. 561. Springer, Berlin-New York, (1976), 39–50.

[11] F. Lanzara: *A representation theorem for solutions of higher order strongly elliptic systems*, In: A. Cialdea (ed.), Homage to Gaetano Fichera, Quad. Mat., vol. 7. Dept. Math., Seconda Univ. Napoli, Caserta, (2000), 233–271.

[12] F. Lanzara: *On BVPs for strongly elliptic systems with higher order boundary conditions*, Georgian Math. J., **14** (1) (2007), 145–167.

[13] P. E. Ricci: *Sui potenziali di semplice strato per le equazioni ellittiche di ordine superiore in due variabili*, Rend. Mat. (6), **7** (1974), 1–39.

[14] N. P. Vekua: *Systems of singular integral equations*, P. Noordhoff Ltd., Groningen (1967).

ALBERTO CIALDEA
UNIVERSITY OF BASILICATA
DEPARTMENT OF MATHEMATICS, COMPUTER SCIENCES AND ECONOMICS
V.LE DELL'ATENEO LUCANO, 10, 85100 POTENZA, ITALY
ORCID: 0000-0002-0009-5957
Email address: alberto.cialdea@unibas.it

FLAVIA LANZARA
SAPIENZA UNIVERSITY OF ROME
DEPARTMENT OF MATHEMATICS "GUIDO CASTELNUOVO"
PIAZZALE ALDO MORO 5, 00185 ROME, ITALY
ORCID: 0000-0002-2052-4202
Email address: flavia.lanzara@uniroma1.it

CONSTRUCTIVE MATHEMATICAL ANALYSIS
7 (2024), No. SI, pp. 142-153
http://dergipark.org.tr/en/pub/cma
ISSN 2651 - 2939

Research Article

A review of radial kernel methods for the resolution of Fredholm integral equations of the second kind

Dedicated to Professor Paolo Emilio Ricci, on occasion of his 80th birthday, with respect and friendship.

ROBERTO CAVORETTO, ALESSANDRA DE ROSSI, AND DOMENICO MEZZANOTTE*

ABSTRACT. The paper presents an overview of the existing literature concerning radial kernel meshfree methods for the numerical treatment of second-kind Fredholm integral equations. More in detail, it briefly recalls radial basis function (RBF) interpolation and cubature to properly describe numerical methods for two-dimensional linear Fredholm equations. The RBF approach allows us to consider the case when the involved functions are not known analytically, but only as vectors of scattered data samples. The described methods do not require any underlying mesh and hence are also independent on the geometry of the domain.

Keywords: Radial basis functions, Fredholm integral equations, meshfree methods, scattered data.

2020 Mathematics Subject Classification: 65D12, 45B05, 65R20.

1. INTRODUCTION

A huge variety of problems arising in mathematical physics, engineering and mechanics can be described by Fredholm integral equations. Some examples are the rendering equation [31, 32] that generalizes a great variety of known rendering algorithms for computer graphics, and Love's equation [35] that arises in the electrostatic problem of a circular plate condenser in an unbounded perfect fluid. Furthermore, solving a related Fredholm equation is the key in broadband dielectric spectroscopy [45] to study molecular dynamics in complex systems such as glass-forming liquids and liquid crystalline materials, the image deblurring problem [30], the diffraction theory [41] and the study of microtearing modes [18] as an explanation for the anomalous electron thermal transport in tokamak experiments. Many numerical procedures to approximate the solution of Fredholm integral equations, such as projection and iterated projection methods, Nyström methods [14, 3, 29, 36, 38], discrete Galerkin methods [4] and Monte Carlo methods [19, 17] are widely available in the current literature. However, most of these methods are based on piecewise approximating polynomials or rely on zeros of orthogonal polynomials. Hence, to guarantee accurate results, they require that all the involved functions should be known in their analytical form or, at least, sampled at the zeros of orthogonal polynomials. Another possible approach is to consider the case where the involved functions are only known as samples over grids of equally spaced points. This research topic has been approached during the last twenty years and led to the development of some numerical methods based on the generalized Bernstein operator [39, 40] and the constrained mock-Chebyshev operator [16], respectively. Nonetheless, it is a common occurrence that in real-life applications the available data are scattered and, consequently, all the previous accurate methods are not

Received: 26.08.2024; Accepted: 01.12.2024; Published Online: 16.12.2024
*Corresponding author: Domenico Mezzanotte; domenico.mezzanotte@unito.it
DOI: 10.33205/cma.1538581

applicable. In this context, meshless methods, in particular those based on radial basis function (RBF) interpolation [6, 47], are an adequate tool to tackle this problem. RBF interpolation has been extensively studied also to develop methods for the numerical treatment of partial differential equations (PDEs) [20, 21, 8] or cubature formulae to approximate integrals starting from scattered data [9, 12, 46]. It is worth noting that a huge variety of RBFs are scaled in terms of a shape parameter and the task of finding the optimal one to increase the accuracy of the interpolation is still a key topic in the literature [10, 23, 27, 37]. Other approaches can involve the use of variably scaled kernels [5, 43] or the construction of stable bases like RBF-QR [24, 26], Hilbert-Schmidt SVD [13, 22], WSVD [7, 15], and greedy algorithms for the convergence of RBF approximants [48]. More recently, meshless methods based on machine learning have emerged as a novel approach for the numerical treatment of integral equations, offering data-driven techniques that complement traditional strategies [28, 49].

This paper aims to collect recent results about the employment of RBF interpolation in the context of the numerical treatment of Fredholm integral equations of the second kind, focusing on the bivariate case in particular. To our knowledge, the literature about this topic is fragmentary and not so wide. So we decided to gather all the known information about it, intending to work on it in the future. We consider the following two-dimensional Fredholm integral equation of the second kind

$$f(x,y) - \mu \int_\Omega k(x,y,s,t) f(s,t) ds dt = g(x,y), \quad (x,y) \in \Omega, \tag{1.1}$$

where $\Omega \subseteq \mathbb{R}^2$ is a bi-dimensional bounded domain, f is the unknown solution, g is the right-hand side term, k is the kernel and μ is a non-zero real parameter.

The paper is structured as follows. Section 2 recalls some basic definitions and properties about radial basis functions, while Section 3 is devoted to a RBF cubature rule for scattered data. In Section 4, the available methods for the numerical treatment of Fredholm integral equations are described. Finally, Section 5 concludes the paper.

2. Radial basis functions

Suppose that we are given a compact domain $\Omega \subset \mathbb{R}^2$, a set $X = \{P_1, \dots, P_N\} \subset \Omega$, of scattered data $P_i = (x_i, y_i)$, $i = 1, \dots, N$, and the corresponding data (or function) value set $F = \{f_1, \dots, f_N\} \subset \mathbb{R}$ that is obtained by possibly sampling any (unknown) function $f : \Omega \to \mathbb{R}$.

Let $\kappa : \Omega \times \Omega \to \mathbb{R}$ be a given radial kernel. Starting from κ, we may define a RBF $\phi : \mathbb{R}_+ \to \mathbb{R}$ that is strictly conditionally positive definite (SCPD) of order m by setting

$$\kappa(P, P_i) = \phi_i(P) = \phi(\|P - P_i\|_2) = \phi(r), \tag{2.2}$$

we can find a unique interpolating function $\psi : \Omega \to \mathbb{R}$ of the form

$$\begin{aligned} \psi(P) &= \sum_{i=1}^{N} c_i \kappa(P, P_i) + \sum_{i=N+1}^{N+M} c_i \pi_{i-N}(P) \\ &= \sum_{i=1}^{N} c_i \phi_i(P) + \sum_{i=N+1}^{N+M} c_i \pi_{i-N}(P), \end{aligned} \tag{2.3}$$

where $\{\pi_k\}_{k=1}^{M}$ generate a basis for the $M = \binom{m+1}{m-1}$-dimensional linear space $\mathbb{P}^2_{m-1}$ of bivariate real valued polynomials of total degree less than or equal to $m-1$, and $\|\cdot\|_2$ is the Euclidean norm. The coefficients $c_1, \dots, c_{N+M}$ are determined by enforcing the interpolation conditions

$$\psi(P_i) = f_i, \qquad i = 1, \dots, N.$$

Since these conditions lead to a system of N linear equations in the $N+M$ unknowns c_i, one usually adds the M additional conditions

$$\sum_{i=1}^{N} c_i \pi_k(P_i) = 0, \qquad k = 1, \dots, M,$$

to ensure a unique solution. Moreover, from theory it is known that a SCPD function of order 0 is strictly positive definite (SPD), and so in this case the polynomial part in (2.3) is omitted. Solving the interpolation problem for a SCPD function ϕ of order m leads to a symmetric linear system

$$\mathcal{A}\mathbf{c} = \mathbf{b}, \tag{2.4}$$

where

$$\mathcal{A} = \begin{bmatrix} A & Q \\ Q^T & O \end{bmatrix}, \qquad \mathbf{b} = \begin{bmatrix} \mathbf{f} \\ \mathbf{0} \end{bmatrix}.$$

The interpolation matrix $\mathcal{A}$ in (2.4) has entries

$$A_{ij} = \phi(\|P_i - P_j\|_2), \qquad Q_{ik} = \pi_k(P_i), \qquad i,j = 1, \dots, N, \ k = 1, \dots, M,$$

and O is a $M \times M$ zero matrix. Moreover, $\mathbf{c} = [c_1, \dots, c_{N+M}]^T$, $\mathbf{f} = [f_1, \dots, f_N]^T$ and $\mathbf{0}$ is a zero vector of length M. Note that for a SPD RBF ϕ the matrix reduces to $\mathcal{A} = A$, and hence the polynomial part vanishes. Recalling that every SCPD kernel has an associated normalized PD kernel [44], from now on we confine our treatise to the case of SPD kernels.

In the literature, many kernels are dependent on a shape parameter $\epsilon > 0$ such that, by recalling (2.2), it is

$$\kappa_\epsilon(P, P_i) = \phi_\epsilon(\|P - P_i\|_2) = \phi_\epsilon(r) = \phi(\epsilon r).$$

In what follows, to simplify the notation, we refer to $\phi_\epsilon(\|P - P_i\|_2)$ as $\phi_{\epsilon,i}(P)$, $\forall\, P, P_i \in \Omega$, omitting the subscript ϵ when clear from context.

RBF	$\phi_\epsilon(r)$	SCPD order
Gaussian C^∞ (GA)	$e^{-\epsilon^2 r^2}$	0
Inverse quadratic C^∞ (IQ)	$(1+\epsilon^2 r^2)^{-1}$	0
Inverse Multiquadric C^∞ (IMQ)	$(1+\epsilon^2 r^2)^{-1/2}$	0
Multiquadric C^∞ (MQ)	$(1+\epsilon^2 r^2)^{1/2}$	1
Wendland C^2 (W2)	$\max(1-\epsilon r, 0)^4(4\epsilon r + 1)$	0
Wendland C^4 (W4)	$\max(1-\epsilon r, 0)^6(35\epsilon^2 r^2 + 18\epsilon r + 3)$	0
Matérn C^0 (M0)	$e^{-\epsilon r}$	0
Matérn C^2 (M2)	$e^{-\epsilon r}(\epsilon r + 1)$	0

TABLE 1. Some examples of well-known RBFs depending on a shape parameter.

3. A CUBATURE RULE ON SCATTERED DATA

A key role in the numerical treatment of integral equations of the type (1.1) is played by the cubature rule used to approximate the integral operator

$$(\mathcal{I}f)(x,y) = \int_\Omega k(x,y,s,t) f(s,t) ds dt. \tag{3.5}$$

A cubature rule for integrals of the type

$$\int_\Omega h(P)dP,$$

where $h(P)$ is an integrable function, can be obtained by replacing the function h with its RBF interpolant (2.3), i.e.

$$\int_\Omega h(P)dP \approx \int_\Omega \psi(P)dP = \sum_{i=1}^{N} c_i \int_\Omega \phi_i(P)dP + \sum_{i=N+1}^{N+M} c_i \int_\Omega \pi_{i-N}(P)dP. \tag{3.6}$$

Denoting by

$$\mathbf{I} = \left[\int_\Omega \phi_1(P)dP, \ldots, \int_\Omega \phi_N(P)dP, \int_\Omega \pi_1(P)dP, \ldots, \int_\Omega \pi_M(P)dP\right]^T,$$

the moment vector and by $< \cdot, \cdot >$ the scalar product in $\mathbb{R}^2$, we have

$$\int_\Omega h(P)dP \approx \int_\Omega \psi(P)dP =< \mathbf{c}, \mathbf{I} >=< \mathcal{A}^{-1}\mathbf{b}, \mathbf{I} >=< \mathbf{f}, \mathbf{w} >= \sum_{i=1}^{N} w_i f_i. \tag{3.7}$$

In fact, by symmetry of the matrix $\mathcal{A}$ and noting that $\mathcal{A}\mathbf{w} = \mathbf{I}$, the cubature formula (3.6) can be easily rewritten in the usual form of a weighted sum of the sampled values.

By employing the cubature rule (3.7), the integral operator (3.5) is approximated as follows:

$$(\mathcal{I}f)(x, y) \approx \sum_{i=1}^{N} w_i k(x, y, x_i, y_i) f(x_i, y_i). \tag{3.8}$$

The accuracy of the rule can be improved by choosing the optimal RBF shape parameter. For a comprehensive study of the influence of the shape parameter scaling on the accuracy of the RBF interpolation the reader can refer to [34] and the references therein.

A technique to estimate the optimal shape parameter is the *leave one out cross validation* (LOOCV) method. The strategy underlying this algorithm is to minimize a cost function that collects the errors for a sequence of partial fits to the data. More in detail, the data are split into two sets:

- a *training set* of $N - 1$ data to obtain a "partial" interpolation;
- a *validation set* with the remaining data to compute the error.

After iterating this procedure N times (one for each given data), the cost function uses the so-obtained vector of error estimates to determine the optimal shape parameter. More details about the RBF moments computation and the LOOCV method can be found in [12, 11, 42].

4. Methods for Fredholm integral equations

4.1. **Method 1.** The discrete collocation method introduced in [2] assumes that the unknown solution of the Fredholm integral equation (1.1) is approximated by

$$\widetilde{f}(x, y) = \sum_{j=1}^{N} c_j \phi_j(x, y),$$

and hence consider the equation

$$R(x, y) = \widetilde{f}(x, y) - \mu \int_\Omega k(x, y, s, t)\widetilde{f}(s, t)dsdt - g(x, y),$$

where $R(x,y)$ is the residual of the RBF approximation. Then, collocating at the points $(x_i,y_i) \in X \subset \Omega$ and requiring that

$$R(x_i,y_i) = 0, \quad \forall\, i = 1,\dots,N,$$

the following system is obtained

$$\sum_{j=1}^{N} \left[\phi_j(x_i,y_i) - \mu \int_\Omega k(x_i,y_i,s,t)\phi_j(s,t)dsdt \right] c_j = g(x_i,y_i), \quad i = 1,\dots,N. \tag{4.9}$$

To approximate the integrals in (4.9), the authors in [2] introduce a composite Gauss-Legendre cubature rule in the case the domain Ω is of the type

$$\Omega = \{(x,y) \in \mathbb{R}^2 \ : \ a \le x \le b, \ \alpha(x) \le y \le \beta(x)\}, \tag{4.10}$$

with $a,b \in \mathbb{R}$ and α, β continuous functions of x. They also consider the case when Ω is union of domains of the type (4.10).

The rule is achieved recalling that for any function $h(x,y)$ continuous on Ω of the type (4.10), we have

$$\int_\Omega h(x,y)dxdy = \int_a^b \int_{\alpha(x)}^{\beta(x)} h(x,y)dxdy = \int_a^b H(x)dx,$$

with

$$H(x) = \int_{\alpha(x)}^{\beta(x)} h(x,y)dy.$$

Hence, applying a composite m_N-point Gauss-Legendre quadrature rule first to the integral $H(x)$ and then to the integral $\int_a^b H(x)dx$ (both conveniently shifted into the interval $[-1,1]$), we get

$$\int_\Omega k(x,y,s,t)\phi_j(s,t)dsdt \approx \mathcal{G}_{m_N}^M(x,y),$$

$$\mathcal{G}_{m_N}^M(x,y) := \frac{1}{2M} \sum_{h=1}^{M} \sum_{k=1}^{m_N} w_k \frac{\Delta t(\theta_k^h)}{2} \sum_{\ell=1}^{M} \sum_{\iota=1}^{m_N} w_\iota k(x,y,\theta_k^h,\eta_\iota^\ell)\phi_j(\theta_k^h,\eta_\iota^\ell),$$

where

$$\begin{aligned} \Delta t(s) &= \frac{\beta(s)-\alpha(s)}{M}, \\ \theta_k^h &= \frac{1}{M}\left[\frac{z_k+2h-1}{2}\right], \quad h = 1,\dots,M, \quad k = 1,\dots,m_N, \\ \eta_\iota^\ell &= \frac{1}{M}\left[\frac{z_\iota+2\ell-1}{2}\right], \quad \ell = 1,\dots,M, \quad \iota = 1,\dots,m_N, \end{aligned} \tag{4.11}$$

M is the number of subintervals employed and $\{z_k,w_k\}_{k=1}^{m_N}$ are the zeros and weights of the m_N-point Gauss-Legendre rule, respectively.

Finally, the linear system is

$$\sum_{j=1}^{N} \left[\phi_j(x_i,y_i) - \mu \mathcal{G}_{m_N}^M(x_i,y_i) \right] c_j = g(x_i,y_i), \quad i = 1,\dots,N. \tag{4.12}$$

4.2. **Method 2.** The spectral meshless radial point interpolation (SMRPI) method has been proposed as a combination of meshless methods and spectral collocation techniques. More specifically, the point interpolation method with the help of RBFs is used to construct shape functions Φ_i so that

$$\Phi_i(P_j) = \begin{cases} 1, & i = j, \\ 0, & i \neq j, \end{cases} \quad i, j = 1, \dots, n. \tag{4.13}$$

Moreover, the shape functions satisfy the following partition of the unity property

$$\sum_{i=1}^{n} \Phi_i(P) = 1. \tag{4.14}$$

In [25], the authors assume to work only with SPD RBFs. Hence, the function f at a point of interest $P \in \Omega$ is expressed in the form

$$f(P) \approx \psi(P) = \sum_{i=1}^{n} c_i \phi_i(P). \tag{4.15}$$

The idea is that here the coefficients c_i are determined taking into consideration a support domain for the point of interest that includes $n < N$ nodes of Ω. More precisely, the coefficients are determined by solving a linear system of the type (2.4), obtained by requiring that equation (4.15) is satisfied at the n nodes surrounding the point of interest P in the support domain. Note that the support domain $D_P \subset \Omega$ is usually a disk of radius r_P and centred at the considered point of interest P.

Consequently, we have the following linear system

$$A_n \mathbf{c}_n = \mathbf{f}_n,$$

with $\mathbf{c}_n = [c_1, \dots, c_n]^T$ and $\mathbf{f}_n = [f_1, \dots, f_n]^T$ and

$$A_n = \begin{pmatrix} \phi_1(P_1) & \phi_1(P_2) & \dots & \phi_1(P_n) \\ \phi_2(P_1) & \phi_2(P_2) & \dots & \phi_2(P_n) \\ \vdots & \vdots & \ddots & \vdots \\ \phi_n(P_1) & \phi_n(P_2) & \dots & \phi_n(P_n) \end{pmatrix}.$$

Since A_n is a symmetric positive definite matrix, it follows that

$$\mathbf{c}_n = A_n^{-1} \mathbf{f}_n. \tag{4.16}$$

Setting $\mathbf{r}(P) = [\phi_1(P), \dots, \phi_n(P)]^T$, equation (4.15) can be rewritten as

$$f(P) \approx \mathbf{r}^T(P)\mathbf{c}.$$

By (4.16), we have

$$\psi(P) = \mathbf{r}^T(P) A_n^{-1} \mathbf{f}_n = \mathbf{\Phi}^T(P) \mathbf{f}_n = \sum_{i=1}^{n} f_i \Phi_i(P), \tag{4.17}$$

being $\mathbf{\Phi}^T(P) = \mathbf{r}^T(P) A_n^{-1} = [\Phi_1(P), \dots, \Phi_n(P)]$. The n functions in the vector $\mathbf{\Phi}(P)$ are called the radial point interpolation method (RPIM) *shape functions* corresponding to the nodal displacements and satisfy the properties (4.13) and (4.14).

Remark 4.1. *We point out that the number n of nodes included in the support domain D_P clearly depends on the point of interest P. When necessary, to underline this dependence we write it as n_P. Moreover, we can rewrite the RPIM approximation of f as follows*

$$\psi(P) = \sum_{j=1}^{N} f_j \Phi_j(P),$$

noting that for any

$$P_j \in D_P^c := \{P_j \ : \ P_j \notin D_P\}$$

we have $\Phi_j(P) = 0$.

The SMRPI method is constructed by replacing the unknown solution $f(x,y)$ in (1.1) with its RPIM approximation

$$\psi(x,y) = \sum_{j=1}^{N} f_j \Phi_j(x,y). \tag{4.18}$$

This leads to

$$\sum_{j=1}^{N} \Phi_j(x,y) f_j - \mu \sum_{j=1}^{N} f_j \int_\Omega k(x,y,s,t)\Phi_j(s,t)dsdt = g(x,y).$$

By Remark 4.1, the above integral can be rewritten as follows

$$\sum_{j=1}^{N} \Phi_j(x,y) f_j - \mu \sum_{j=1}^{N} f_j \int_{D_{P_j}} k(x,y,s,t)\Phi_j(s,t)dsdt = g(x,y), \tag{4.19}$$

where D_{P_j} is the support domain of the point $P_j = (x_j, y_j)$. Collocating equation (4.19) at the points of $X \subset \Omega$, we obtain the following system of order N

$$\sum_{j=1}^{N} \left[\Phi_j(x_i,y_i) - \mu G(x_i,y_i)\right] f_j = g(x_i,y_i), \quad i = 1,\dots,N.$$

Approximating the integral by a suitable Gaussian cubature rule

$$G_j(x_i,y_i) \approx \int_{D_{P_j}} k(x_i,y_i,s,t)\Phi_j(s,t)dsdt, \quad i = 1,\dots,N, \tag{4.20}$$

and recalling the Kronecker delta property (4.13), we finally obtain the linear system

$$\sum_{j=1}^{N} \left[\delta_{ij} - \mu G_j(x_i,y_i)\right] f_j = g(x_i,y_i), \quad i = 1,\dots,N, \tag{4.21}$$

that can also be written in the following matrix form

$$(\mathbf{I} - \mu\mathbf{G})\mathbf{f} = \mathbf{g},$$

where $\mathbf{I}$ is the identity matrix of order N, the square matrix $\mathbf{G}$ has entries $G_j(x_i,y_i)$, $i,j = 1,\dots,N$, $\mathbf{g} = [g_1,\dots,g_N]^T$ with $g_i = g(x_i,y_i)$, $i = 1,\dots,N$, and $\mathbf{f} = [f_1,\dots,f_N]^T$ with $f_i = fx_i,y_i)$, $i = 1,\dots,N$.

4.3. **Method 3.** The method introduced in [1] is based on hybrid kernels. A *hybrid kernel* is a combination of radial kernels, usually one infinitely smooth depending on a shape parameter along with one of finite smoothness that is shape-parameter-free, in order to combine their benefits and reduce the respective drawbacks. It is known that infinitely smooth kernels generally have a high order of convergence while their stability usually decreases by decreasing the shape parameter and increasing the number of points. Conversely, kernels of finite smoothness often provide lower accuracy and convergence order but better stability in the computations.

RBF	$\phi(r)$
Thin Plate Spline (TPS)	$r^2 \log r$
Cubic (CU)	r^3
Polyharmonic (P7)	r^7

TABLE 2. Some examples of shape-parameter-free RBFs.

A family of hybrid radial kernels (HRKs) is constructed as follows:

$$\Psi_{\epsilon,i}(P) = \phi_{\epsilon,i}(P) + \rho\phi_i(P), \qquad i = 1, \dots, N, \tag{4.22}$$

where $\phi_{\epsilon,i}$ is an infinitely smooth radial kernel with shape parameter ϵ, ϕ_i is a piecewise smooth shape-parameter-free radial kernel and $\rho \in \mathbb{R}$ is the HRK weight parameter. The shape parameter ϵ and the weight parameter ρ control the accuracy and the stability of the HRK interpolation of the function f that is given by

$$\widetilde{\psi}(P) = \sum_{i=1}^{N} \tilde{c}_i \Psi_{\epsilon,i}(P) + \sum_{i=N+1}^{N+M} \tilde{c}_i \pi_{i-N}(P). \tag{4.23}$$

The coefficients $\tilde{c}_1, \dots, \tilde{c}_{N+M}$ are also in this case determined by enforcing the interpolation conditions

$$\widetilde{\psi}(P_i) = f_i, \qquad i = 1, \dots, N,$$

and the M additional conditions

$$\sum_{i=1}^{N} \tilde{c}_i \pi_k(P_i) = 0, \qquad k = 1, \dots, M,$$

with the polynomial part in (4.23) omitted if dealing with SPD hybrid radial kernels. Consequently, we obtain the following symmetric linear system

$$\mathcal{H}\tilde{\mathbf{c}} = \mathbf{b}, \tag{4.24}$$

where

$$\mathcal{H} = \begin{bmatrix} H & Q \\ Q^T & O \end{bmatrix}, \qquad \mathbf{b} = \begin{bmatrix} \mathbf{f} \\ \mathbf{0} \end{bmatrix}.$$

with

$$H_{ij} = \Psi_{\epsilon,i}(P_j), \qquad Q_{ik} = \pi_k(P_i), \qquad i, j = 1, \dots, N, \ k = 1, \dots, M,$$

$\tilde{\mathbf{c}} = [\tilde{c}_1, \dots, \tilde{c}_{N+M}]^T$ the HRK coefficient vector and $\mathbf{f} = [f_1, \dots, f_N]^T$ the scattered data vector. We recall that for a SPD HRK $\Psi_{\epsilon,i}$ the matrix in (4.24) reduces to $\mathcal{H} = H$.

The HRK method is constructed by replacing the unknown solution $f(x, y)$ in (1.1) with its HRK approximation

$$\widetilde{\psi}(x, y) = \sum_{i=1}^{N} \tilde{c}_i \Psi_{\epsilon,i}(x, y)$$

in the case of SPD hybrid kernels obtaining

$$\sum_{j=1}^{N}\left[\Psi_{\epsilon,j}(x,y)-\mu\int_{\Omega}k(x,y,s,t)\Psi_{\epsilon,j}(s,t)dsdt\right]\tilde{c}_j=g(x,y).$$

By collocating the previous equation at the points $(x_i,y_i)\in X\subset\Omega$, we get the following system:

$$\sum_{j=1}^{N}\left[\Psi_{\epsilon,j}(x_i,y_i)-\mu\int_{\Omega}k(x_i,y_i,s,t)\Psi_{\epsilon,j}(s,t)dsdt\right]\tilde{c}_j=g(x_i,y_i),\quad i=1,\ldots,N. \tag{4.25}$$

To approximate the integrals in (4.25), the authors in [1] apply the composite Gauss-Legendre cubature rule that we have recalled in Subsection 4.1

$$\int_{\Omega}k(x,y,s,t)\Psi_{\epsilon,j}(s,t)dsdt\approx\widetilde{\mathcal{G}}^{M}_{m_N}(x,y),$$

$$\widetilde{\mathcal{G}}^{M}_{m_N}(x,y):=\frac{1}{2M}\sum_{h=1}^{M}\sum_{k=1}^{m_N}w_k\frac{\Delta t(\theta^h_k)}{2}\sum_{\ell=1}^{M}\sum_{\iota=1}^{m_N}w_\iota k(x,y,\theta^h_k,\eta^\ell_\iota)\Psi_{\epsilon,j}(\theta^h_k,\eta^\ell_\iota),$$

with $\Delta t(s)$, θ^h_k and η^ℓ_ι defined as in (4.11). Hence, the following linear system is finally obtained

$$\sum_{j=1}^{N}\left[\Psi_{\epsilon,j}(x_i,y_i)-\mu\widetilde{\mathcal{G}}^{M}_{m_N}(x_i,y_i)\right]\tilde{c}_j=g(x_i,y_i),\quad i=1,\ldots,N.$$

Regarding the search for the optimal parameter values of the hybrid kernels, the authors in [1] present a global particle swarm optimization (PSO) method. PSO is a robust algorithm introduced by Kennedy and Eberhart [33] that uses swarm intelligence for solving optimization problems. A swarm in the PSO algorithm comprises a group of particles navigating the problem's search-space, with each particle assigned a fitness value that represents a potential solution to the optimization problem at hand. Key advantages of PSO include its straightforward implementation, information sharing, mutual cooperation among particles, memory utilization, fast convergence, and low computational complexity. However, the conventional PSO algorithm is susceptible to premature convergence and can easily become trapped in local optima. To address these limitations, the authors in [1] introduced some modifications to the standard PSO algorithm to enhance its performance and the reader can refer to their article for further details about it.

4.4. **Advantages and drawbacks.** The three methods presented in this review paper all rely on RBFs and, consequently, face similar challenges, particularly in selecting an optimal shape parameter. At first glance, the hybrid kernel method might seem preferable, as it combines the strengths of two different RBFs: one dependent on a shape parameter and another that is shape-parameter-free. However, this introduces a new challenge: optimizing both the shape parameter and the weight parameter, ρ, which balances the contributions of the two RBFs. While algorithms such as LOOCV and PSO can optimize both parameters, the computational effort increases because these algorithms must now handle two parameters instead of one. In contrast, the SMRPI method is more computationally expensive due to the construction of the shape functions Φ_i, as described in (4.17), whereas the discrete collocation method is the simplest to implement. Regarding the cubature rule used to approximate the integral in (1.1), all three methods rely on Gaussian-type rules. Despite these differences, it is important to note that all three methods are reliable and exhibit comparable performance as far as we know.

5. Conclusions and future research

In this paper, we reviewed three methods for the numerical treatment of Fredholm integral equations of the second kind using RBFs. The described methods are meshless, independent of the geometry of the domain, and reduce the problem to solving a linear system of algebraic equations. To our knowledge, this research topic has not yet been fully explored. Our future goal is to further engage in this field by introducing Nyström-type methods, which, as far as we know, have not yet been considered. Additionally, we plan to carry out a comparison with the methods discussed in this review paper, providing multiple numerical examples. This work could help strengthen the connections between RBF interpolation and the theory of integral equations.

Acknowledgements

The authors are grateful to the anonymous reviewers for carefully reading the manuscript and for their precise and helpful suggestions that allowed to improve the work.

This work has been supported by the INdAM Research group GNCS as part of the GNCS-INdAM 2024 project "Metodi kernel e polinomiali per l'approssimazione e l'integrazione: teoria e software applicativo". It has been also supported by the Spoke 1 "FutureHPC & BigData" of ICSC - Centro Nazionale di Ricerca in High-Performance Computing, Big Data and Quantum Computing, funded by European Union - NextGenerationEU. Moreover, the work has been supported by the Fondazione CRT, project 2022 "Modelli matematici e algoritmi predittivi di intelligenza artificiale per la mobilità sostenibile". This research has been accomplished within the RITA "Research ITalian network on Approximation", the UMI Group TAA "Approximation Theory and Applications", and the SIMAI Activity Group ANA&A "Numerical and Analytical Approximation of Data and Functions with Applications".

References

[1] T. Akbari, M. Esmaeilbeigi and D. Moazami: *A stable meshless numerical scheme using hybrid kernels to solve linear Fredholm integral equations of the second kind and its applications*, Math. Comput. Simulation, **220** (2024), 1–28.

[2] P. Assari, H. Adibi and M. Dehghan: *A numerical method for solving linear integral equations of the second kind on the non-rectangular domains based on the meshless method*, Appl. Math. Model., **37** (22) (2013), 9269–9294.

[3] K. E. Atkinson: *The Numerical Solution of Integral Equations of the second kind*, Cambridge Monographs on Applied and Computational Mathematics, Cambridge University Press (1997).

[4] K. E. Atkinson, F. Potra: *The discrete Galerkin method for linear integral equations*, IMA J. Numer. Anal., **9** (1989), 385–403.

[5] M. Bozzini, L. Lenarduzzi, M. Rossini and R. Schaback: *Interpolation with variably scaled kernels*, IMA J. Numer. Anal., **35** (2015), 199–219.

[6] M. D. Buhmann: *Radial Basis Functions: Theory and Implementation*, Cambridge Monogr. Appl. Comput. Math., vol. 12, Cambridge Univ. Press, Cambridge (2003).

[7] R. Cavoretto, S. De Marchi, A. De Rossi, E. Perracchione and G. Santin: *Partition of unity interpolation using stable kernel-based techniques*, Appl. Numer. Math., **116** (2017), 95–107.

[8] R. Cavoretto, A. De Rossi: *A two-stage adaptive scheme based on RBF collocation for solving elliptic PDEs*, Comput. Math. Appl., **79** (11) (2020), 3206–3222.

[9] R. Cavoretto, A. De Rossi, F. Dell'Accio, F. Di Tommaso, N. Siar, A. Sommariva and M. Vianello: *Numerical cubature on scattered data by adaptive interpolation*, J. Comput. Appl. Math., **444** (2024), 115793.

[10] R. Cavoretto, A. De Rossi and S. Lancellotti: *Bayesian approach for radial kernel parameter tuning*, J. Comput. Appl. Math., **441** (2024), Article ID: 115716.

[11] R. Cavoretto, A. De Rossi, M. S. Mukhametzhanov and Y. D. Sergeyev: *On the search of the shape parameter in radial basis functions using univariate global optimization methods*, J. Global Optim., **79** (2021), 305–327.

[12] R. Cavoretto, A. De Rossi, A. Sommariva and M. Vianello: *RBFCUB: A numerical package for near-optimal meshless cubature on general polygons*, Appl. Math. Lett., **125** (2022), Article ID: 107704.

[13] R. Cavoretto, G. E. Fasshauer and M. McCourt: *An introduction to the Hilbert-Schmidt SVD using iterated Brownian bridge kernels*, Numer. Algor., **68** (2015), 393–422.
[14] M. C. De Bonis, G. Mastroianni: *Projection methods and condition numbers in uniform norm for Fredholm and Cauchy singular integral equations*, SIAM J. Numer. Anal., **44** (4) (2006), 1351–1374.
[15] S. De Marchi, G. Santin: *A new stable basis for radial basis function interpolation*, J. Comput. Appl. Math., **253** (2013), 1–13.
[16] F. Dell'Accio, D. Mezzanotte, F. Nudo and D. Occorsio: *Numerical approximation of Fredholm integral equation by the constrained mock-Chebyshev least squares operator*, J. Comput. Appl. Math., **447** (2024), 115886.
[17] A. Doucet, A. M. Johansen and V. B. Tadić: *On solving integral equations using Markov chain Monte Carlo methods*, Appl. Math. Comput., **216** (2010), 2869–2880.
[18] R. Farengo, Y. C. Lee and P. N. Guzdar: *An electromagnetic integral equation: application to microtearing modes*, Phys. Fluids, **26** (1983), 3515–3523.
[19] R. Farnoosh, M. Ebrahimi: *Monte Carlo method for solving Fredholm integral equations of the second kind*, Appl. Math. Comput., **195** (1) (2008), 309–315.
[20] G. E. Fasshauer: *Meshfree Approximation Methods with MATLAB*, Interdisciplinary Mathematical Sciences, Vol. 6, World Scientific Publishing Co., Singapore (2007).
[21] G. E. Fasshauer, M. J. McCourt: *Kernel-based Approximation Methods using MATLAB*, Interdisciplinary Mathematical Sciences, Vol. 19, World Scientific Publishing Co., Singapore (2015).
[22] G. E. Fasshauer, M. J. McCourt: *Stable evaluation of Gaussian radial basis function interpolants*, SIAM J. Sci. Comput., **34** (2012), A737–A762.
[23] G. E. Fasshauer, J. G. Zhang: *On choosing "optimal" shape parameters for RBF approximation*, Numer. Algorithms, **45** (2007), 345–368.
[24] B. Fornberg, E. Larsson and N. Flyer: *Stable computations with Gaussian radial basis functions*, SIAM J. Sci. Comput., **33** (2011), 869–892.
[25] H. Fatahi, J. Saberi-Nadjafi and E. Shivanian: *A new spectral meshless radial point interpolation (SMRPI) method for the two-dimensional Fredholm integral equations on general domains with error analysis*, J. Comput. Appl. Math., **294** (2016), 196–209.
[26] B. Fornberg, C. Piret: *A stable algorithm for flat radial basis functions on a sphere*, SIAM J. Sci. Comput., **30** (2007), 60–80.
[27] B. Fornberg, J. Zuev: *The Runge phenomenon and spatially variable shape parameters in RBF interpolation*, Comput. Math. Appl., **54** (2007), 379–398.
[28] Y. Guan, T. Fang, D. Zhang and C. Jin: *Solving Fredholm Integral Equations Using Deep Learning*, Int. J. Appl. Comput. Math., **8** (2022), Article ID: 87.
[29] G. Han, R. Wang: *Richardson extrapolation of iterated discrete Galerkin solution for two-dimensional Fredholm integral equations*, J. Comput. Appl. Math., **139** (1) (2002), 49–63.
[30] P. C. Hansen, T. K. Jensen: *Large-scale methods in image deblurring*, Lect. Notes. Comput. Sci., **4699** (2007), 24–35.
[31] J. T. Kajiya: *The rendering equation*, Proceedings of the 13th annual conference on Computer Graphics and Interactive Techniques (SIGGRAPH '86), ACM Press, New York (USA) (1986), 143–150.
[32] A. Keller: *Instant radiosity*, Proceedings of the 24th Annual Conference on Computer Graphics and Interactive Techniques (SIGGRAPH '97), ACM Press, New York (USA) (1997), 49–56.
[33] J. Kennedy, R. Eberhart: *Particle swarm optimization*. Proceedings of IEEE International Conference on Neural Networks, **4** (1995), 1942–1948.
[34] E. Larsson, R. Schaback: *Scaling of radial basis functions*, IMA J. Numer. Analysis, **44** (2) (2024), 1130–1152.
[35] P. A. Martin, L. Farina: *Radiation of water waves by a heaving submerged horizontal disc*, J. Fluid. Mech., **337** (1997), 365–379.
[36] D. Mezzanotte, D. Occorsio and M. G. Russo: *Combining Nyström Methods for a Fast Solution of Fredholm Integral Equations of the Second Kind*, Mathematics, **9** (2021), 2652.
[37] A. Noorizadegan, C.-S. Chen, R. Cavoretto and A. De Rossi: *Efficient truncated randomized SVD for mesh-free kernel methods*, Comput. Math. Appl., **164** (2024), 12–20.
[38] D. Occorsio, M. G. Russo: *Numerical methods for Fredholm integral equations on the square*, Appl. Math. Comput., **218** (2011), 2318–2333.
[39] D. Occorsio, M. G. Russo: *Nyström Methods for Fredholm Integral Equations Using Equispaced Points*, Filomat, **28** (1) (2014), 49–63.
[40] D. Occorsio, M. G. Russo and W. Themistocklakis: *Some numerical applications of generalized Bernstein operators*, Constr. Math. Anal., **4** (2) (2021), 186–214.
[41] J. Radlow: *A two-dimensional singular integral equation of diffraction theory*, Bull. Am. Math. Soc., **70** (1964), 596–599.
[42] S. Rippa: *An algorithm for selecting a good value for the parameter c in radial basis function interpolation*, Adv. Comput. Math., **11** (1999), 193–210.

[43] M. Rossini: *Variably scaled kernels: an overview*, Dolomites Res. Notes Approx., **15** (2022), 61–72.
[44] R. Schaback: *Native Hilbert spaces for radial basis functions I*, New Developments in Approximation Theory. ISNM International Series of Numerical Mathematics, vol 132. Birkhäuser, Basel (1999).
[45] H. Schäfer, E. Sternin, R. Stannarius, M. Arndt, and F. Kremer: *Novel Approach to the Analysis of Broadband Dielectric Spectra*, Phys. Rev. Lett., **76** (1996), 2177–2180.
[46] A. Sommariva, M. Vianello: *Numerical Cubature on Scattered Data by Radial Basis Functions*, Computing, **76** (2006), 295–310.
[47] H. Wendland: *Scattered Data Approximation*, Cambridge Monogr. Appl. Comput. Math., vol. 17, Cambridge Univ. Press, Cambridge (2005).
[48] T. Wenzel, G. Santin and B. Haasdonk: *Analysis of Target Data-Dependent Greedy Kernel Algorithms: Convergence Rates for $f-$, $f \cdot P-$ and $f/P-$Greedy*, Constr. Approx., **57** (2023), 45–74.
[49] E. Zappala, A. H. d. O. Fonseca, J. O. Caro, A. H. Moberly, M. J. Higley, J. Cardin and D. van Dijk: *Learning integral operators via neural integral equations*, Nat. Mach. Intell., **6** (2024), 1046–1062.

ROBERTO CAVORETTO
UNIVERSITY OF TURIN
DEPARTMENT OF MATHEMATICS "GIUSEPPE PEANO"
VIA CARLO ALBERTO 10, 10123, TURIN, ITALY
ORCID: 0000-0001-6076-4115
Email address: roberto.cavoretto@unito.it

ALESSANDRA DE ROSSI
UNIVERSITY OF TURIN
DEPARTMENT OF MATHEMATICS "GIUSEPPE PEANO"
VIA CARLO ALBERTO 10, 10123, TURIN, ITALY
ORCID: 0000-0003-1285-3820
Email address: alessandra.derossi@unito.it

DOMENICO MEZZANOTTE
UNIVERSITY OF TURIN
DEPARTMENT OF MATHEMATICS "GIUSEPPE PEANO"
VIA CARLO ALBERTO 10, 10123, TURIN, ITALY
ORCID: 0000-0001-5154-6538
Email address: domenico.mezzanotte@unito.it